

SYNTHESIS AND CHARACTERISATION OF
THERMOTROPIC LIQUID CRYSTALLINE
POLYESTERS

A THESIS SUBMITTED TO
SHIVAJI UNIVERSITY, KOLHAPUR
FOR THE DEGREE OF
DOCTOR OF PHILOSOPHY
IN CHEMISTRY
UNDER THE FACULTY OF SCIENCE

BY
MR. N. N. CHAVAN

UNDER THE GUIDANCE OF
DR. S. PONRATHNAM
NATIONAL CHEMICAL LABORATORY
PUNE 411008 [INDIA]
DECEMBER 1992

CONTENTS

	Page No.
<i>ACKNOWLEDGEMENTS</i>	(i)
<i>DECLARATION</i>	(iii)
<i>CERTIFICATE</i>	(iv)
<i>LIST OF FIGURES</i>	(v)
<i>LIST OF TABLES</i>	(x)
1. INTRODUCTION	1
1.1 HISTORICAL BACKGROUND AND NOMENCLATURE	1
1.2 DESCRIPTION OF THE MESOPHASES	2
1.2.1 LIQUID CRYSTALS	2
1.2.2 PLASTIC CRYSTALS	4
1.2.3 CONDIS CRYSTALS	4
1.3 REQUIREMENTS FOR LIQUID CRYSTALLINITY	5
1.3.1 THE MESOGEN	6
1.4 TYPES OF LIQUID CRYSTALS	7
1.4.1 THERMOTROPIC LIQUID CRYSTALS	7
1.4.2 LYOTROPIC LIQUID CRYSTALS	20
1.5 CHARACTERISTICS OF LIQUID CRYSTALS	23
1.6 POLYMERIC LIQUID CRYSTALS	25
1.7 THERMOTROPIC LIQUID CRYSTALLINE POLYMERS	27
1.8 STRUCTURE-PROPERTY RELATIONSHIPS	32

1.8.1	EFFECT OF MESOGENIC STRUCTURE	33
1.8.2	NUMBER OF RINGS IN THE MESOGEN	33
1.8.3	NATURE OF TERMINAL SUBSTITUENT	36
1.8.4	INTRAMESOGENIC LINKS	36
1.8.5	FLEXIBLE SPACER	38
1.8.6	POLYETHYLENE OXIDE [PEO] SPACER	44
1.8.7	RING SUBSTITUTION	44
1.8.8	KINKS	49
1.8.9	CRANK-SHAFT MONOMERS	49
1.8.10	ANISODIAMETRIC BRIDGING GROUP	50
1.9	POLYMER SYNTHESIS	51
1.9.1	ACID CHLORIDE ROUTE	52
1.9.2	SOLUTION POLYCONDENSATION	53
1.9.3	INTERFACIAL POLYCONDENSATION	53
1.10	THE PRESENT WORK	54
2.	EXPERIMENTAL	56
2.1	REAGENTS AND CHEMICALS	56
2.2	REACTION INTERMEDIATES	61
2.3	SYNTHESIS OF POLYESTERS	70
3.	PHYSICO-CHEMICAL CHARACTERISATIONS	81
3.1	MORPHOLOGICAL CHARACTERISATION	81
3.1.1	POLARISING MICROSCOPY	81
3.1.2	X-RAY DIFFRACTOMETRY	83
3.2	THERMAL CHARACTERISATION	86
3.2.1	DIFFERENTIAL SCANNING CALORIMETRY	86

3.2.2	TRANSITIONS IN LCPs	87
3.2.3	SOLIDIFICATION PROCESSES	93
3.2.4	T-T-T CONCEPT	95
3.2.5	KINETICS OF CRYSTALLISATION	100
3.2.6	MECHANISM OF CRYSTALLISATION	106
3.3	DSC ANALYSIS	107
3.3.1	THERMODYNAMIC PARAMETERS	107
3.3.2	ISOTHERMAL CRYSTALLISATION KINETICS	108
3.3.3	NON-ISOTHERMAL CRYSTALLISATION KINETICS	111
4.	RESULTS AND DISCUSSION	112
4.1	POLYESTERS OF BHBOB MESOGEN	113
4.1.1	GENERAL PROPERTIES	114
4.1.2	THERMODYNAMICS OF LC STATES	114
4.1.3	CONCLUSION	123
4.2	POLYESTERS OF BHBOMB MESOGEN	123
4.2.1	SUBSTITUTION EFFECTS	124
4.2.2	GENERAL PROPERTIES	125
4.2.3	THERMODYNAMICS OF LC STATES	129
4.2.4	CONCLUSION	134
4.3	POLYESTERS OF BHBOCB MESOGEN	134
4.3.1	SUBSTITUTION EFFECTS	135
4.3.2	GENERAL PROPERTIES	136
4.3.3	THERMODYNAMICS OF LC STATES	139
4.3.4	CONCLUSION	145
4.4	CO-, TER-, TETRAPOLYESTERS OF BHBOB MESOGEN	145

4.4.1	COPOLYESTERS OF BHBOB MESOGEN	147
4.4.2	TER-, TETRAPOLYESTERS OF BHBOB MESOGEN	158
4.4.3	CONCLUSION	161
4.5	ISOTHERMAL CRYSTALLISATION	161
4.5.1	POLYESTERS INVESTIGATED	162
4.5.2	LOW TEMPERATURE REGIME	163
4.5.3	HIGH TEMPERATURE REGIME	197
4.5.4	STRUCTURAL EFFECTS	198
4.5.5	AVRAMI EXPONENT	198
4.5.6	CONCLUSION	200
4.6	NON-ISOTHERMAL CRYSTALLISATION	200
4.6.1	POLYESTERS INVESTIGATED	201
4.6.2	EFFECT OF FLEXIBLE SPACER	207
4.6.3	EFFECT OF SUBSTITUTION	238
4.6.4	CONCLUSION	240
5.	REFERENCES	241

• ACKNOWLEDGEMENTS

I would like to express my deep sense of gratitude to Dr. S. Ponrathnam for his professional guidance and encouragement.

I wish to place on record my sincere thanks to Dr. C.R. Rajan for his continuous professional and personal help during the course of this investigation.

Many of my friends and colleagues have assisted me in this work and I must thank them all. In particular, I thank Dr. A.K. Rath, Dr. R.S. Ghadage, Dr. R.V. Bahulekar, Mr. J. Mathew, Mr. Milind Sonpatki, Mr. Kuber and Mr. A.S. Jadhav of National Chemical Laboratory. All of them have left an indelible mark in this dissertation.

My greatest debt is to my wife Neelam for her great patience with me and for keeping a cheerful spirit around while I pursued this research late into the night on weekdays, weekends and on holidays.

I remember my late father, who had taken tremendous efforts for my educational career. He has been a great source of inspiration in my life.

I am indebted to Dr. S. Sivaram, Head, Polymer Chemistry Division, National Chemical Laboratory and Dr. S.S. Mahajan for their steadfast support during the course of this investigation.

(ii)

I would like to thank to Shivaji University, Kolhapur for permitting me to register for Ph.D. programme. My thanks are due to Dr. R.A. Mashelkar, Director, National Chemical Laboratory, for enabling me to conduct the Ph.D. research work at National Chemical Laboratory and to submit the thesis to Shivaji University, Kolhapur.

A handwritten signature in black ink, appearing to read 'N.N. Chavan', is written above a horizontal line.

[N.N. Chavan]

DECLARATION


I hereby declare that the thesis entitled

**"SYNTHESIS AND CHARACTERISATION OF
THERMOTROPIC LIQUID CRYSTALLINE
POLYESTERS"**

completed and written by me has not previously formed the basis for the award of any Degree or Deploma or other similar title of this or any other University or examining body.

Place : Pune 411008

Date : December 30, 1992


Research Student

CERTIFICATE

I hereby certify that the thesis entitled

**"SYNTHESIS AND CHARACTERISATION OF
THERMOTROPIC LIQUID CRYSTALLINE
POLYESTERS"**

which is being submitted herewith for the award of the Degree of Doctor of Philosophy in Chemistry of Shivaji University, Kolhapur is the result of the original research work completed by Shri N. N. Chavan under my supervision and guidance and to the best of my knowledge and belief the work embodied in this thesis has not formed earlier basis of award of any Degree or similar title of this or any other University or examining body.

Place : Pune 411008

Date : December 30, 1992

S. Venkateshram

Research Guide.

वैज्ञानिक

SCIENTIST

राष्ट्रीय रासायनिक प्रयोगशाला
National Chemical Laboratory

पुणे/PUNE-411 008.

• LIST OF FIGURES

FIGURE No.	CAPTION	PAGE No.
1	Schematic diagram of the relationship between the three limiting phases (double out line) and the six mesophases. The top five mesophases are solids. The bottom four phases show increasing mobility.	3
2	Classification of liquid crystal structures.	8
3	Molecular orientation in several liquid crystal phases.	10
4	Schematic diagram of Smectic A structure.	14
5	Schematic diagram of Smectic C structure.	14
6	Schematic diagram of Smectic B structure.	14
7	Schematic diagram of Smectic D structure.	15
8	Schematic diagram of Smectic E structure. •	15
9	Illustration of the three basic curvature deformations of the Nematic liquid crystals: Splay, twist and bend. The force constants opposing these strains are denoted K_{11} (splay), K_{22} (twist) and K_{33} (bend).	19
10	Schematic diagram of a Nematic phase.	19
11	Schematic diagram of Cholesteric phase showing pitch P and displacement angle θ .	21
12	The Cholesteric liquid-crystal structure. The director (arrow) phase traces but a helical path within the medium.	22
13	Schematic diagram of molecular arrangements in lyotropic form (a) lamellar, (b) cylindrical and (c) spherical forms.	24
14	Schematic diagram of main chain and side chain LCP structures.	28
15	General structures of main chain and side chain LCPs.	29
16	Dependance of the melting point (T_m) and the isotropisation temperature (T_i) on the number of methylene units.	42

17	Extended chain structures of thermotropic polyesters with different number of methylene units.	43
18	General reaction scheme for the synthesis of aliphatic diacid chloride.	63
19	General reaction scheme for the synthesis of rigid diols.	66
20	General reaction scheme for the synthesis of polyesters.	72
21	A typical X-ray diffraction pattern.	85
22	Thermal transition behaviour in LCPs.	89
23	DSC thermograms for a PET/30 HBA copolyester showing the influence of thermal history on the phase behaviour.	89
24	DSC thermogram of a semiflexible LCP showing peak structuring.	91
25	Odd-even relationship for isotropic transitional entropy in some semiflexible LCPs.	91
26	Temperature dependence of the nucleation rate (\dot{N}), the growth rate (\dot{G}) and transformation rate (\dot{X}).	98
27	Time-Temperature-Transformation diagram for Nylon 66.	98
28	Typical Avrami plots of the increase in volume fraction crystallinity as a function of time for Avrami exponents "n" from 1 to 6.	102
29	Textures of polyester PE-207 at (a) 271.0°C, (b) 260.0°C, (c) 229.5°C, (d) 192.0°C, (e) 130°C and (f) 115.8°C.	117
30	DSC thermograms of BHBOMB homopolyesters [first heating cycle].	130
31	DSC thermograms of BHBOMB homopolyesters [second heating cycle].	131
32	Textures of polyester PE-307 at (a) 192.4°C, (b) 187.7°C and (c) 134.8°C.	137
33	DSC thermograms of BHBOCB homopolyesters [first heating cycle].	140
34	DSC thermograms of BHBOCB homopolyesters [second heating cycle].	141
35	A set of DSC heating traces in different time periods of isothermal experiments for copolyester PE-203 ($T_c = 191^\circ\text{C}$).	164

36	A set of DSC heating traces in different time periods of isothermal experiments for copolyester PE-203 ($T_c = 194^\circ\text{C}$).	165
37	A set of DSC heating traces in different time periods of isothermal experiments for copolyester PE-203 ($T_c = 198^\circ\text{C}$).	166
38	A set of DSC heating traces in different time periods of isothermal experiments for copolyester PE-203 ($T_c = 202^\circ\text{C}$).	167
39	The plot of ΔH versus $\log t$ for polyester PE-203.	168
40	The plot of ΔH^{-1} versus $\log t^{-1}$ for polyester PE-203.	169
41	A set of DSC heating traces in different time periods of isothermal experiments for copolyester PE-103 ($T_c = 110^\circ\text{C}$).	170
42	A set of DSC heating traces in different time periods of isothermal experiments for copolyester PE-103 ($T_c = 125^\circ\text{C}$).	171
43	A set of DSC heating traces in different time periods of isothermal experiments for copolyester PE-103 ($T_c = 131^\circ\text{C}$).	172
44	A set of DSC heating traces in different time periods of isothermal experiments for copolyester PE-103 ($T_c = 140^\circ\text{C}$).	173
45	The plot of ΔH versus $\log t$ for polyester PE-103.	174
46	The plot of ΔH^{-1} versus $\log t^{-1}$ for polyester PE-103.	175
47	A set of DSC heating traces in different time periods of isothermal experiments for copolyester PE-303 ($T_c = 108^\circ\text{C}$).	176
48	A set of DSC heating traces in different time periods of isothermal experiments for copolyester PE-303 ($T_c = 113^\circ\text{C}$).	177
49	A set of DSC heating traces in different time periods of isothermal experiments for copolyester PE-303 ($T_c = 118^\circ\text{C}$).	178
50	A set of DSC heating traces in different time periods of isothermal experiments for copolyester PE-303 ($T_c = 125^\circ\text{C}$).	179
51	The plot of ΔH versus $\log t$ for polyester PE-303.	180
52	The plot of ΔH^{-1} versus $\log t^{-1}$ for polyester PE-303.	181
53	A set of DSC heating traces in different time periods of isothermal experiments for copolyester PE-107 ($T_c = 143^\circ\text{C}$).	182
54	A set of DSC heating traces in different time periods of isothermal experiments for copolyester PE-107 ($T_c = 148^\circ\text{C}$).	183

55	A set of DSC heating traces in different time periods of isothermal experiments for copolyester PE-107 ($T_c = 153^\circ\text{C}$).	184
56	A set of DSC heating traces in different time periods of isothermal experiments for copolyester PE-107 ($T_c = 160^\circ\text{C}$).	185
57	The plot of ΔH versus $\log t$ for polyester PE-107.	186
58	The plot of ΔH^{-1} versus $\log t^{-1}$ for polyester PE-107.	187
59	A set of DSC cooling traces from the Nematic state at different cooling rates (a) for homopolyester PE-101.	208
60	Relationships between α (fraction crystallized) and <i>temperature</i> for homopolyester PE-101.	209
61	Plots of $\log [(-\ln (1-\alpha))]$ versus $\log a$ for homopolyester PE-101.	210
62	A portion of the T-T-T plot for homopolyester PE-101.	211
63	A set of DSC cooling traces from the Nematic state at different cooling rates (a) for homopolyester PE-102.	212
64	Relationships between α (fraction crystallized) and <i>temperature</i> for homopolyester PE-102.	213
65	Plots of $\log [(-\ln (1-\alpha))]$ versus $\log a$ for homopolyester PE-102.	214
66	A portion of the T-T-T plot for homopolyester PE-102.	215
67	A set of DSC cooling traces from the Nematic state at different cooling rates (a) for homopolyester PE-105.	216
68	Relationships between α (fraction crystallized) and <i>temperature</i> for homopolyester PE-105.	217
69	Plots of $\log [(-\ln (1-\alpha))]$ versus $\log a$ for homopolyester PE-105.	218
70	A portion of the T-T-T plot for homopolyester PE-105.	219
71	A set of DSC cooling traces from the Nematic state at different cooling rates (a) for homopolyester PE-106.	220
72	Relationships between α (fraction crystallized) and <i>temperature</i> for homopolyester PE-106.	221
73	Plots of $\log [(-\ln (1-\alpha))]$ versus $\log a$ for homopolyester PE-106.	222
74	A portion of the T-T-T plot for homopolyester PE-106.	223
75	A set of DSC thermograms of the dynamic cooling crystallization of homopolyester PE-107.	224

76	Relationships between α (fraction crystallized) and <i>temperature</i> for homopolyester PE-107.	225
77	Plots of $\log[-\ln(1-\alpha)]$ versus $\log a$ for homopolyester PE-107.	226
78	A portion of the T-T-T plot for homopolyester PE-107.	227
79	A set of DSC cooling traces from the Nematic state at different cooling rates (a) for homopolyester PE-203.	228
80	Relationships between α (fraction crystallized) and <i>temperature</i> for homopolyester PE-203.	229
81	Plots of $\log[-\ln(1-\alpha)]$ versus $\log a$ for homopolyester PE-203.	230
82	A portion of the T-T-T plot for homopolyester PE-203.	231
83	A set of DSC cooling traces from the Nematic state at different cooling rates (a) for homopolyester PE-303.	232
84	Relationships between α (fraction crystallized) and <i>temperature</i> for homopolyester PE-303.	233
85	Plots of $\log[-\ln(1-\alpha)]$ versus $\log a$ for homopolyester PE-303.	234
86	A portion of the T-T-T plot for homopolyester PE-303.	235
87	Nature of packing of flexible spacer relative to mesogen ratio less or greater than one.	236

• LIST OF TABLES

TABLE No.	CAPTION	PAGE No.
1	Some examples of nematic liquid crystals	17
2	General structures of main chain liquid crystalline polymers	30
3	Dependence of thermal transitions in thermotropic polyesters on number and type of aromatic rings in the mesogenic structure	34
4	Dependence of nematic to isotropic transitions in liquid crystals based on p-substituted-benzylidene amino-4-methoxy-biphenyls on terminal substituent	37
5	Dependence of thermal transitions in liquid crystalline polymers on intramesogenic link (IML) type	39
6	Dependence of thermal transitions in trimesogenic liquid crystalline polyesters on direction of ester intramesogenic (IML) link	40
7	Dependence of thermal transitions in liquid crystalline polymers on substitution pattern on aromatic nucleus	46
8	Dependence of thermal transitions in liquid crystalline polyesters on substitution pattern on aromatic nucleus	47
9	Synthesis of polyesters of Bis-[4-hydroxy benzoyl oxy]-1,4-benzene [BHBOB] (unsubstituted trimesogenic diol) and aliphatic diacid chlorides, with odd and even number of methylene units, by solution polycondensation	74
10	Synthesis of copolyesters of differing compositions from Bis-[4-hydroxy benzoyl oxy]-1,4-benzene [BHBOB] (unsubstituted trimesogenic diol) and two aliphatic diacid chlorides, with even number of methylene units, by solution polycondensation	75

11	Synthesis of copolyesters from Bis-[4-hydroxy benzoyl oxy]-1,4-benzene [BHBOB] (unsubstituted trimesogenic diol) and three different aliphatic diacid chlorides, with even number of methylene units, by solution polycondensation	76
12	Synthesis of copolyesters from Bis-[4-hydroxy benzoyl oxy]-1,4-benzene [BHBOB] (unsubstituted trimesogenic diol) and four aliphatic diacid chlorides, with even number of methylene units, by solution polycondensation	77
13	Synthesis of copolyesters from Bis-[4-hydroxy benzoyl oxy]-1,4-benzene [BHBOB] (unsubstituted trimesogenic diol) and two different aliphatic diacid chlorides, with odd number of methylene units, by solution polycondensation	77
14	Synthesis of polyesters with Bis-[4-hydroxy benzoyl oxy]-1,4-benzene [BHBOB] (unsubstituted trimesogenic diol) and aliphatic diacid chlorides, with odd and even number of methylene units, by interfacial polycondensation	78
15	Synthesis of polyesters with Bis-[4-hydroxy benzoyl oxy]-2-methyl-1,4-benzene [BHBOMB] (methyl substituted trimesogenic diol) and aliphatic diacid chlorides, with odd and even number of methylene units, by interfacial polycondensation	79
16	Synthesis of polyesters from Bis-[4-hydroxy benzoyl oxy]-2-chloro-1,4-benzene [BHBOCB] (chloro substituted trimesogenic diol) and aliphatic diacid chlorides, with odd and even number of methylene units, by interfacial polycondensation	80
17	Type of nucleation and growth with respect to Avrami exponent "n"	104
18	Temperatures selected for studying isothermal crystallisation kinetics	109
19	Solution polycondensation [BHBOB], transition temperatures and thermodynamic data of BHBOB homopolyesters: effect of flexible spacer	115
20	Interfacial polycondensation [BHBOB], transition temperatures and thermodynamic data of BHBOB homopolyesters: effect of flexible spacer	116
21	First heating cycle [BHBOMB], transition temperatures and thermodynamic data of BHBOMB homopolyesters: effect of flexible spacer	126
22	Second heating cycle [BHBOMB], transition temperatures and thermodynamic data of BHBOMB homopolyesters: effect of flexible spacer	127

23	First heating cycle [BHBOCB], transition temperatures and thermodynamic data of BHBOCB homopolyesters: effect of flexible spacer	142
24	Second heating cycle [BHBOCB], transition temperatures and thermodynamic data of BHBOCB homopolyesters: effect of flexible spacer	143
25	Transition temperatures and thermodynamic data of BHBOB homo- and copolyesters: effect of structural randomisation with flexible spacers of even number of methylene units-1	148
26	Transition temperatures and thermodynamic data of BHBOB homo- and copolyesters: effect of structural randomisation with flexible spacers of even number of methylene units-2	149
27	Transition temperatures and thermodynamic data of BHBOB copolyesters: effect of structural randomisation with flexible spacers of odd number of methylene units	152
28	Transition temperatures and thermodynamic data of BHBOB homo-, co- and terpolyesters: similar averaged flexible spacer length from different aliphatic diacid chlorides-1	154
29	Transition temperatures and thermodynamic data of BHBOB homo-, co-, ter- and tetrapolyesters: similar averaged flexible spacer length from different aliphatic diacids-2	157
30	Transition temperatures and thermodynamic data of BHBOB ter- and tetrapolyesters: effect of structural with even methylene units	159
31	Isothermal crystallisation of polyester PE-203 at 191°C	189
32	Isothermal crystallisation of polyester PE-203 at 194°C	189
33	Isothermal crystallisation of polyester PE-203 at 198°C	190
34	Isothermal crystallisation of polyester PE-203 at 202°C	190
35	Isothermal crystallisation of polyester PE-103 at 110°C	191
36	Isothermal crystallisation of polyester PE-103 at 125°C	191
37	Isothermal crystallisation of polyester PE-103 at 131°C	192
38	Isothermal crystallisation of polyester PE-103 at 140°C	192

39	Isothermal crystallisation of polyester PE-303 at 108°C	193
40	Isothermal crystallisation of polyester PE-303 at 113°C	193
41	Isothermal crystallisation of polyester PE-303 at 118°C	194
42	Isothermal crystallisation of polyester PE-303 at 125°C	194
43	Isothermal crystallisation of polyester PE-107 at 143°C	195
44	Isothermal crystallisation of polyester PE-107 at 148°C	195
45	Isothermal crystallisation of polyester PE-107 at 153°C	196
46	Isothermal crystallisation of polyester PE-107 at 160°C	196
47	Non-isothermal crystallisation of polyester PE-101 at different cooling rates	203
48	Non-isothermal crystallisation of polyester PE-102 at different cooling rates	203
49	Non-isothermal crystallisation of polyester PE-105 at different cooling rates	204
50	Non-isothermal crystallisation of polyester PE-106 at different cooling rates	204
51	Non-isothermal crystallisation of polyester PE-107 at different cooling rates	205
52	Non-isothermal crystallisation of polyester PE-203 at different cooling rates	205
53	Non-isothermal crystallisation of polyester PE-303 at different cooling rates	206
54	Avrami exponent "n" observed in non-isothermal crystallisation of polyesters	206

CHAPTER 1

INTRODUCTION

INTRODUCTION

1.1 HISTORICAL BACKGROUND AND NOMENCLATURE

Liquid crystals were first observed in 1888 by Austrian botanist Reinitzer. He noted the occurrence of two melting points for cholesteryl benzoate^{1,2} at 145°C [cloudy] and 179°C [clear]. Shortly thereafter Lehmann showed that the cloudy intermediate phase contained areas that seemed to have a crystal like molecular structure. He suggested the name "liquid crystal" for this phase and, in spite of many subsequent argument about nomenclature, the name has struck.³⁻⁷

Liquid-crystal research reached a peak during the early 1930's. In addition to an exponential growth in number of experiments, which threw up many new liquid crystals, the field had attracted such eminent theoreticians as W.H. Bragg, Louis de Brogli and Max Born. In spite of this flurry of activity, interest waned for next 30 years apparently from the general feeling among physicists that all important problems in the field had been solved and only minor difficulties remained. As a result many modern workers are only vaguely aware that ambiguous melting points can be attributed to something other than impurities in the substance being tested.

Early this century, G. Friedel investigated liquid crystalline phases by optical microscopy and concluded that the substances are neither perfect crystals nor perfect liquids. He proposed the more logical term "mesomorphs" or "mesoforms", since the properties are intermediate between very well defined phases.⁸ Other names proposed for the mesomorphic state are discussed by Rinne.⁸

Liquid crystals are highly anisotropic fluids that exist between the boundaries of the solids and the conventional isotropic liquid phase. The phase is a result of a long-range orientational ordering among constituent molecules that occur within

certain ranges of temperature in the melts and solutions of many organic compounds. The ordering is sufficient to impart some solid like properties on the fluid but the forces of attraction usually are not strong enough to prevent flow. In those cases, where liquid-crystalline substances are substantially solid in the terms of flow, there are other fluid aspects to its physical state. This dualism of physical properties is expressed in the term "liquid crystal". Liquid-crystals are in thermodynamic equilibrium over wide temperature ranges and undergo well defined phase changes.

1.2 DESCRIPTION OF THE MESOPHASES

The various types of mesophases have usually been treated separately, and rarely did researchers review more than one mesophase at a time. One of the few descriptions of liquid and plastic crystals was given by Smith.⁸ There are three major types of mesophase order, namely:

- 1) Liquid crystals,
- 2) Plastic crystals and
- 3) Condis crystals.

Schematic diagram of the relationship between the three limiting phases (double outline) and the six mesophases are represented in Figure 1.

1.2.1 Liquid crystals

First, it is possible to keep to orientational order, but lose positional order. The "positionally disordered" crystals or "orientationally ordered" liquids are widely known as liquid crystals.⁹ The name liquid crystal was given because of obvious liquid-like flow of these materials. Now it is too late to try to change the nomenclature, especially when the possible new names would be cumbersome.⁸

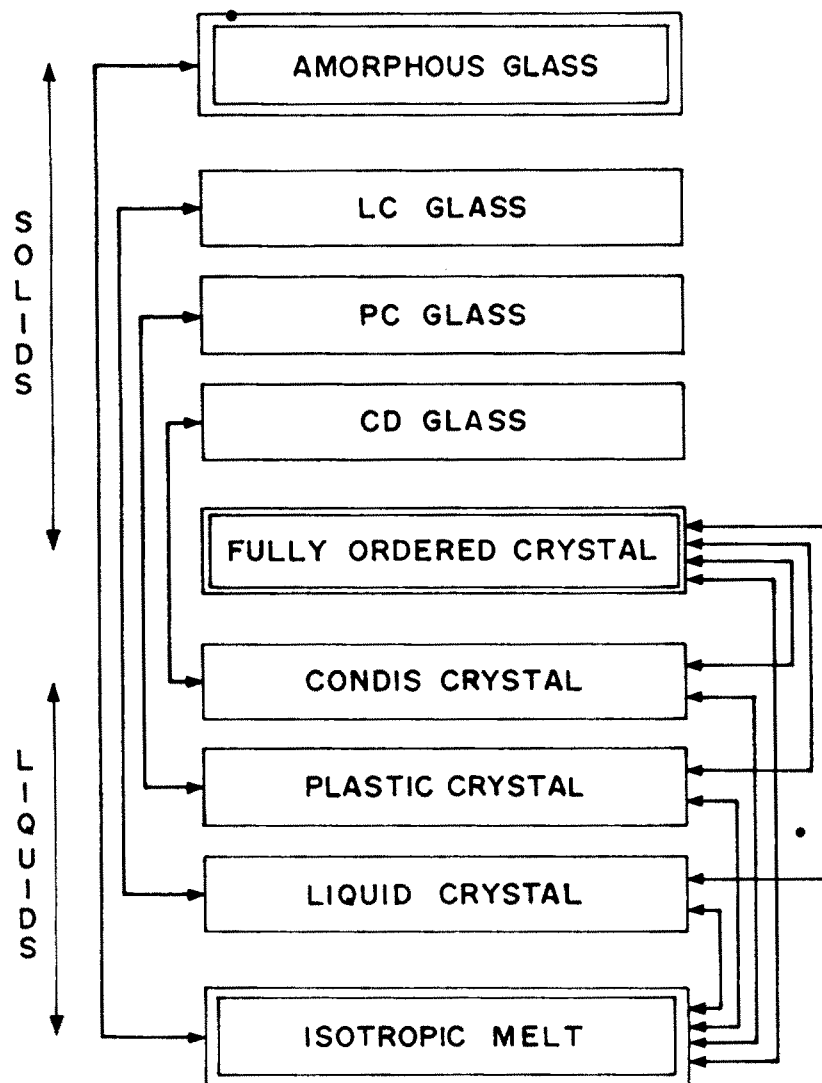


FIG. 1 SCHEMATIC DIAGRAM OF THE RELATIONSHIP BETWEEN THE THREE LIMITING PHASES (DOUBLE OUT LINE) AND THE SIX MESOPHASES. THE TOP FIVE MESOPHASES ARE SOLIDS. THE BOTTOM FOUR PHASES SHOW INCREASING MOBILITY.

1.2.2 Plastic crystals

These group of materials form a mesophase which shows "orientational disorder" but "positional order". These materials are widely known as plastic crystals,¹⁰ because of the ease of deformation of such crystals. Again, this name is well accepted and much less cumbersome than "orientationally disordered" crystals.

1.2.3 Condis crystals

This group of mesophase materials representing the "conformationally disordered" crystals are called condis crystals. The physical properties of condis crystals, which maintain the positional and orientational order, change in much too subtle a way from the fully ordered crystals for a common property to be attached to their name. The difference between the three mesophases crystals are largely based on the geometry of the molecules. The molecules of liquid crystals always have a rigid, mesogenic group which is rod- or disc-like and causes a high activation energy to rotational reorientation.¹ In contrast, the molecules of plastic crystals, are compact and globular^{1,8} and their reorientation is not opposed by a high activation energy barrier. The condis crystals, in turn, consist of flexible molecules which can undergo relatively easily hindered rotation to change conformation without losing positional or orientational order. In general, at the temperature below the respective glass transition one can thus have three further mesophases. Besides the "normal" amorphous glasses there are:

- 1) Positionally disordered glass [LC-glass]
- 2) Orientationally disordered glass [PC-glass]
- 3) Conformationally disordered glass [CD-glass].

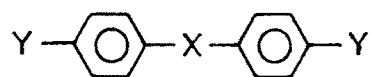
1.3 REQUIREMENTS FOR LIQUID CRYSTALLINITY

Friedel suggested a nomenclature to classify the liquid crystalline state. Solution of rod-like entities in a normally isotropic solvent often form liquid crystal phases at sufficiently high solute concentration. These anisotropic solution mesophases are lyotropic liquid crystals. The other, thermotropic liquid crystals, display the liquid crystallinity on heating. The rod-like entities in lyotropic systems are usually quite long compared to typical thermotropic liquid crystal "mesogens". Their axial ratios, i.e., length-to-diameter ratio are greater than 6.7.⁹ Axial ratios of the materials showing thermotropic liquid crystals phases are usually between 4-8.

The structural requirements discussed in a later section relate to thermotropic liquid crystals only. In general, certain molecular features are essential to generate liquid crystallinity. The molecules of liquid crystals possess some common geometric features, not withstanding the diversity in chemical structures such as anils, azos, azoxies, cholesteric esters etc.

The geometric and polar requirements have been well established through extensive research involving synthesis and optical characterisation. The axial ratios of the molecule should be large. The compound should have geometric asymmetry and molecular rigidity along its molecular axis. Aromatic structure and double bond increase rigidity. In addition, molecular interactions such as dipole-dipole, ion-dipole, induced dipole, and possibly hydrogen bonding play an important role. The presence of strongly polar and/or strongly polarisable groups on the molecular axis and weakly polar terminal groups enhance stability of the liquid crystalline state. The differently polarisable groups present on the molecule induce non-uniformity in cohesive forces between the elongated [rod-like] molecules.^{9,11,12}

The molecular architecture common to most liquid crystalline compounds is presented below:



It consists of two or more planer ring systems, such as, 1,4-phenylene/2,6-naphthalene/trans-[1,4-cyclohexyl] linked together with central group [X] and appropriate terminal group [Y]. The central group may be symmetric or asymmetric. The central or terminal groups determine the attractive forces between the molecules. The variation in cohesive forces is important for the molecules to display different liquid crystalline mesophases. These mesophases are discussed in Section 1.4.

1.3.1 The Mesogen

The term "mesogen" is assigned to the section of a molecule which is indeed responsible for the formation of or capable of liquid crystalline state. It comprises, in general, rigid segments and non-oscillating linear linking functional groups. A mesogen must consist of at least two rigid units made up of aromatic/cycloaliphatic rings and functional group which do not disturb the coplanarity of the aromatic rings. The cylindrical mesogens are classified on the basis of length to diameter usually "axial ratio" and on the basis of number of rigid units. The term "diad" and "triad" refer to mesogens with two and three rigid aromatic units respectively.

Flory developed theories which predict that rod like molecules with an axial ratio between 3.0 and 6.4 are capable of displaying thermal transition from the liquid crystalline state to isotropic state¹³ prior to degradation. The compounds with large axial ratios melt at too high temperature to generate liquid crystalline state. They either pass directly into isotropic state or decompose prior to melting. In these systems,

liquid crystalline state can only be obtained by dissolution in a suitable solvent.

Mesogenic moiety may be classified into two categories: amphiphilic and non-amphiphilic.¹⁴ Subsequently, one can distinguish whether the mesogenic moiety forms a part of the polymer main chain or is attached to the side chain. The whole system can be lyotropic or thermotropic depending upon whether the mesophase is observed by variation of solvent content or temperature.

Non-amphiphilic monomer units are characterised by their rigid, rod like molecular structure typical of low molecular weight liquid crystals. If these monomer units are joined to form the main chain, the polymer backbone itself becomes rigid and rod-like. The rod-like structure causes anisotropic packing of macromolecules, as predicted theoretically by Flory.¹³ For some mesogenic polymers, however, it is not always necessary for the monomer units to be rigid. Chain rigidity can be caused by the secondary structure of the polymer, as exemplified by the cellulose derivatives and polyglutamates.

1.4 TYPES OF LIQUID CRYSTALS

Liquid crystals are broadly divided into two types named as thermotropic and lyotropic. Classification of liquid crystals are presented in Figure 2.

1.4.1 Thermotropic Liquid Crystals

Friedel classified thermotropic liquid crystals into three different types on the basis of optical observations. These are:

- 1.4.1.1 Smectic phases,
- 1.4.1.2 Nematic phase and
- 1.4.1.3 Cholesteric phase.

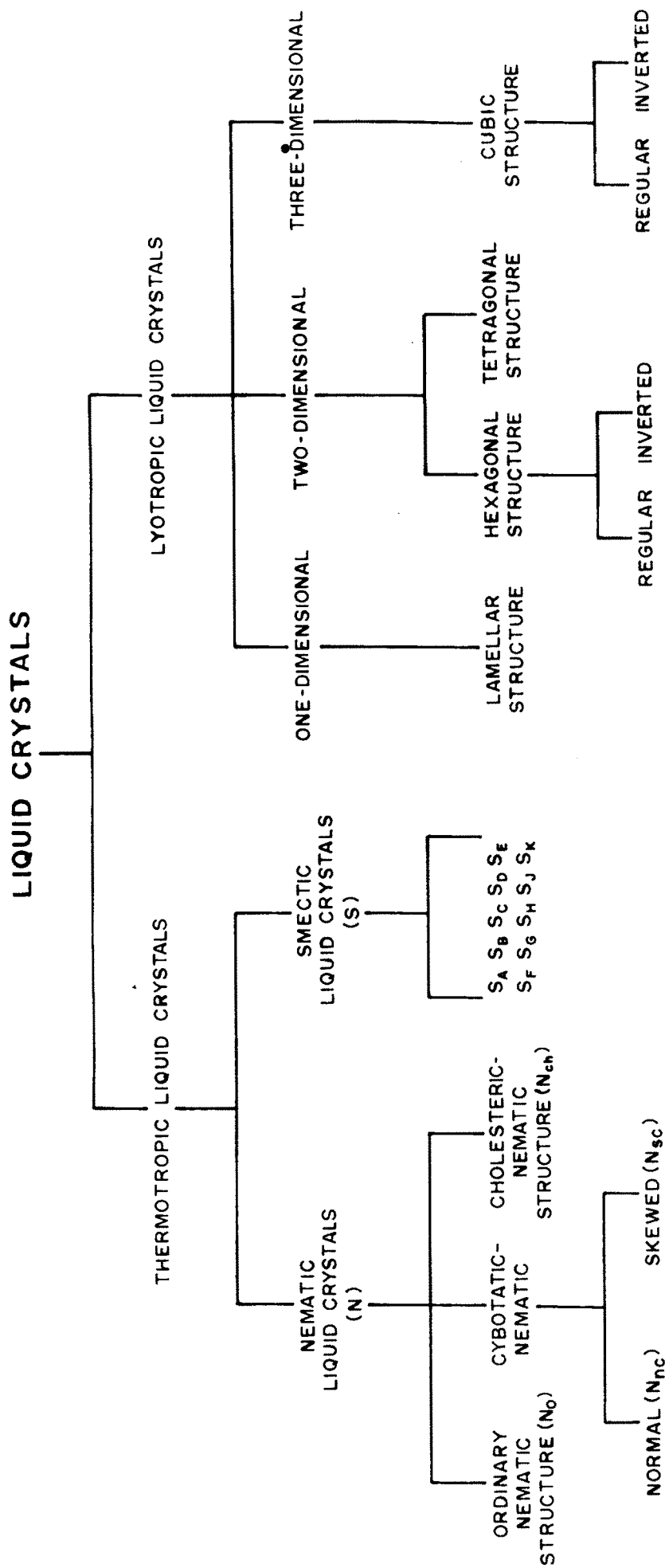


FIG. 2 CLASSIFICATION OF LIQUID CRYSTAL STRUCTURES.

If the cohesion between the molecules within a layer is stronger than that between molecular layers, crystals break down on the heating to generate lamellar arrangement of molecules having well defined layer spacings. The mesophases thus formed are called "smectics" and are usually characterised by high viscosity and characteristics of low angle X-ray patterns from which the thickness of the strata can be determined. Further heating decreases the level of cohesion between molecules within a stratum and at certain temperature the molecules would acquire an additional degree of translational freedom, which may rise to rather poorly organised smectic phase, such as smectic A, or a nematic phase. In "nematic" mesophase, a large scale disappearance of positional order takes place. The unidirectional orientational order is preserved. However on still further heating, the orientational cohesion of molecules breaks down with the appearance of isotropic fluid phase. Such passages on heating, initially from one mesophase to another and finally from the mesophase to an isotropic liquid, all are first order transitions which can be observed by differential scanning calorimetry. If a nematic arrangement of molecules has chiral centres, of a certain sign, the nematic arrays become twisted generating a helical arrangement to the molecular plane. The pitch of the helix depends on the optical power of the chiral group. Such twisted nematic phases are called "cholesteric" phases. The molecular orientation in different liquid crystal phases is presented in Figure 3.

1.4.1.1 Smectic Phases

Smectic liquid crystals are distinguished not only by a parallelism of molecular long axis but by a layering of the centres of gravity in two-dimensional planes or sheets. Smectic layering is similar to that in soap films. These are deviations from planarity and the planes may be bent. Mobility within the smectic layers may be high, although in some cases the centres of gravity are structured.

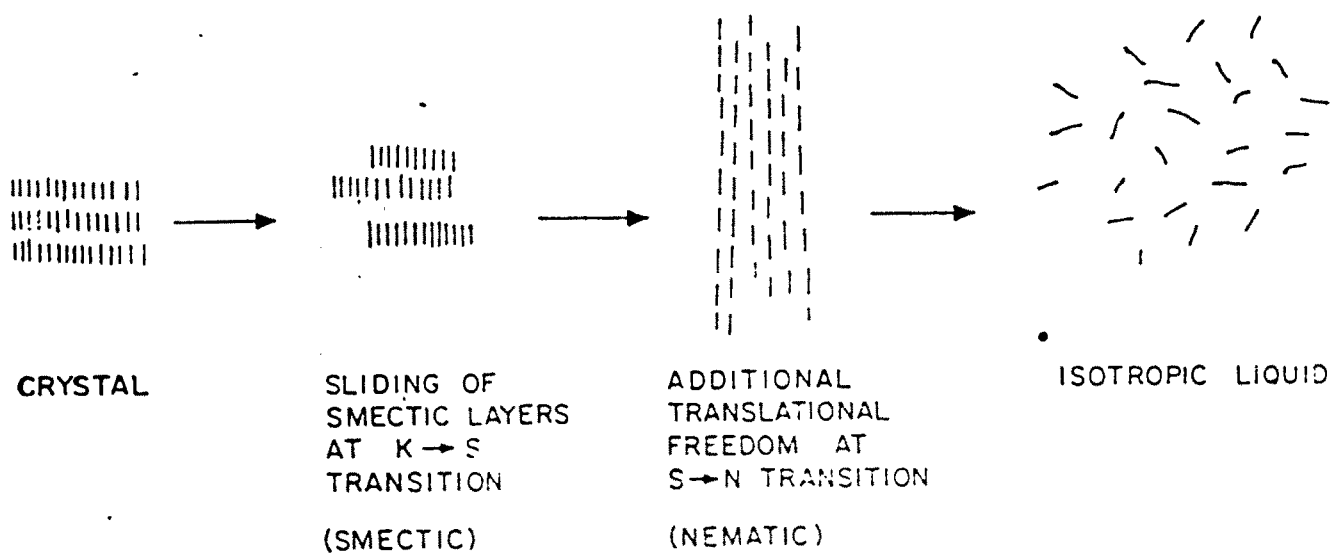


FIG. 3 MOLECULAR ORIENTATION IN SEVERAL LIQUID CRYSTAL PHASES.

The molecules in some smectic phases may translationally move along their long axis in and out of the layers. This involves either single or a column of molecules.^{14,15} Correlations between different smectic layers are also possible. When little or no interplanar rotational or translational coupling exists, fluidity of the liquid crystals is maintained, because the layers may glide past one another with relative ease. Large scale movement in any direction other than tangential to the layer surfaces is difficult. Smectic mesophases, therefore, are typically quite viscous and are most solid-like among the liquid crystal modifications. Strong interlayer coupling would generate a three dimensional array with greatly restricted mobility. It is questionable whether such smectic phases are liquid-crystals or soft solids. There is certainly a difference in term of the scale of the molecular correlation. The liquid crystal is coupled over a finite range.

Polarised light microscopy studies reveal that phase is optically similar to a three dimensional crystal such as quartz. The velocity of light transmitted perpendicular to the layers is less than that transmitted parallel to the layers. Such structures, in which light travels at a lower velocity along the long axes of the molecules, are considered optically positive.

Systematic study of smectic liquid crystals were undertaken by Sackmann, Arnold, Demus et al.¹⁶ and classified on the basis of miscibility. Two phases are of the same type if both are miscible in all proportions. Phases are also identified on the basis of X-ray diffraction patterns and microscopic textures. Smectic crystals are divided into ten types. These are S-A, S-B, S-C, S-D, S-E, S-F, S-G, S-H, S-J, and S-K.

1.4.1.1.1 Smectic A •

This is the least ordered of all smectic structures. The molecules are arranged in equally spaced layers which may be measured by X-ray diffraction. The long axes of the molecules generally are perpendicular to the layer plane. The centres of gravity are randomly dispersed. There is considerable freedom of translational motion, and rotation about the long axes is relatively unrestricted. The phase is optically uniaxial and frequently shows pseudo-isotropic or homeotropic textures under polarised microscope. Tilted smectic A phase, with layer thickness less than molecular length, is optically uniaxial. There is no long range order in the direction of tilt.¹⁷⁻¹⁹ A schematic representation of a smectic A structure is shown in Figure 4.

1.4.1.1.2 Smectic C

The smectic C structure is similar to smectic A except that the molecules in the layers are tilted at a uniform angle with respect to the normal and the structure is optically biaxial. The molecules within a smectic C layer are disorganised positionally and move about freely. The layers are flexible and easily slide past one another. In some smectic C modifications the tilt angle varies significantly with temperature, while in others it remains fairly constant.^{20,21} A schematic presentation of smectic C structure is shown in Figure 5.

1.4.1.1.3 Smectic B and Smectic H

Smectic B and H phases differ from the A and C phases respectively in that an ordered arrangement of the molecules is obtained in the layers rather a disordered one. X-ray photographs of monodomains of smectic B liquid crystal indicate a hexagonal arrangement of molecules in planes that are perpendicular to the long axis. The ordered arrangement within layers makes B and H phases much more rigid than A

and C phases. It seems that the smectic B phase is a soft solid with three-dimensional ordering of finite range.^{22,23} The latter property qualifies these substances as liquid crystals. A schematic presentation of smectic B structure is shown in Figure 6.

1.4.1.1.4 Smectic D

This phase is intermediate between smectic A and smectic C and has been the subject of considerable discussion.^{9,24,25} The structured arrangement is a cubic lattice. The sites are occupied by multimolecular spherical units [micelles]. The structure of smectic D is optically isotropic.²⁵ A schematic presentation of smectic D structure is shown in Figure 7.

1.4.1.1.5 Smectic E

X-ray diffraction pattern reported for smectic E reveals highly ordered structure without hexagonal lattice. Molecules are aligned perpendicular to the layers.²⁵ The structure generates a mosaic texture and is optically uniaxial. Tilted smectic E phase designated smectic E_f is also possible. A schematic presentation of smectic E structure is shown in Figure 8.

1.4.1.1.6 Smectic F

Smectic F phase is very similar to Smectic C. In fact, at the present time there is little clarity as to what the major difference between the two are. The difference, if any, is that tilt of molecules with respect to the layer is greater in smectic F. The arrangement of molecules in this phase is pseudo-hexagonal.²⁶

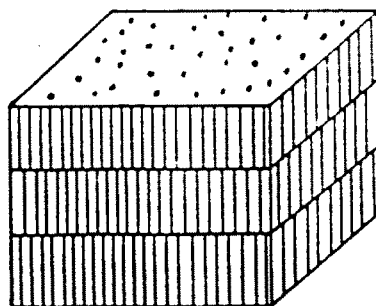


FIG. 4 SCHEMATIC DIAGRAM OF SMECTIC A STRUCTURE.

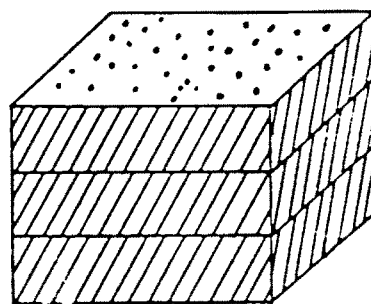


FIG. 5 SCHEMATIC DIAGRAM OF SMECTIC C STRUCTURE.

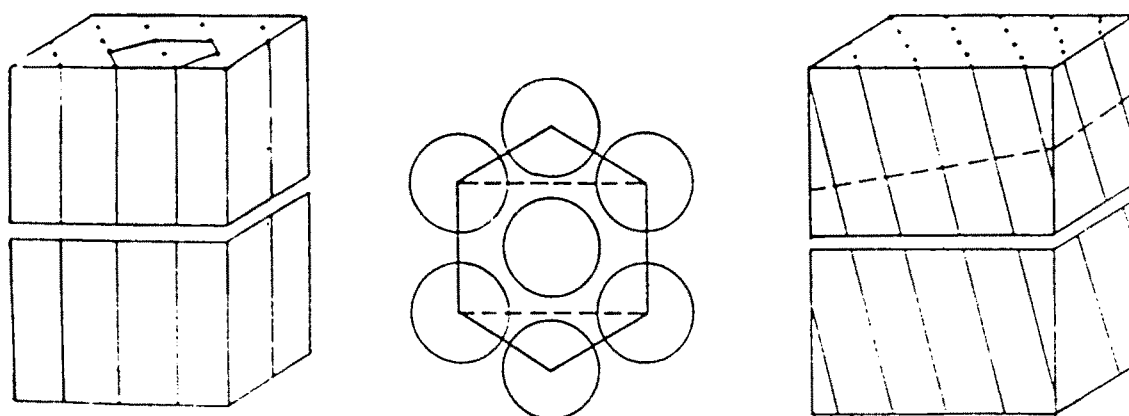


FIG. 6 SCHEMATIC DIAGRAM OF SMECTIC B STRUCTURE.

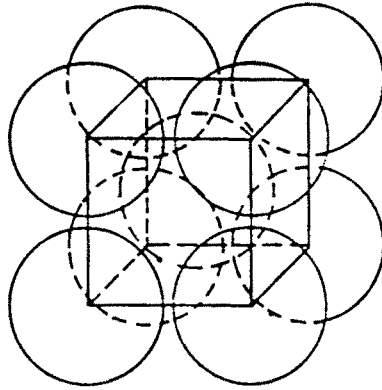


FIG. 7 SCHEMATIC DIAGRAM OF SMECTIC D STRUCTURE.

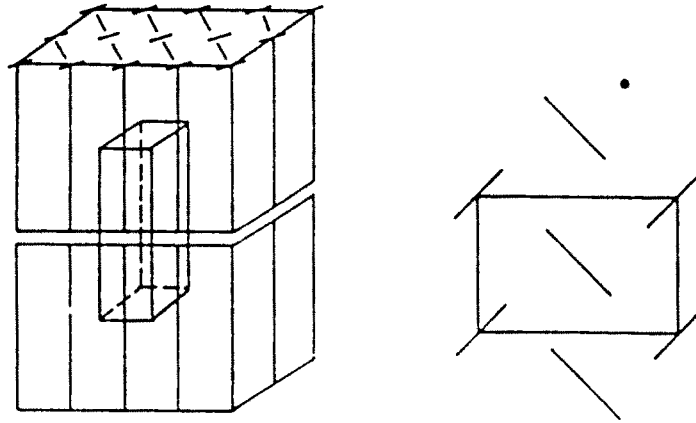


FIG. 8 SCHEMATIC DIAGRAM OF SMECTIC E STRUCTURE.

1.4.1.1.7 Smectic G •

The smectic G phase has an ordered arrangement of molecules within the layer. The molecules appear to be tilted. Three dimensional lattice probably exists within the layers. X-ray photographs of monodomains of smectic B liquid crystals indicate a hexagonal arrangement of molecules in planes that are perpendicular to long axes.

1.4.1.1.8 Smectic H

The arrangement of molecules in the smectic H phases are hexagonal. Molecular disposition of the molecules are tilted.

1.4.1.2 Nematic Phase

Nematic phase consists of microscopic threadlike structures.^{27,28} Structures displaying typical nematic phase are presented in Table 1. Nematic is less ordered than smectic.²⁹ Molecules are arranged with their long axis parallel. This phase does not separate into layers. Nematic phase is also optically positive.

The spontaneous alignment along the long axis or orientation process generates highly birefringent material with dissimilar refractive indices for polarised light along and perpendicular to the optical path. The most common textures observed under polarised microscope is the schlieren or threaded texture. Specific heat, compressibility and thermal volume expansion in nematics are similar to those in normal liquids. Thermal energy causes fluctuations in the orientations of nematic molecules about the director. These fluctuations moderate the refractive index of the material on a microscopic level and lead to strong light scattering. This gives the nematic mesophase a cloudy, turbid appearance even at rest. A bright, satin like texture is observed, when

TABLE 1

Some examples of nematic liquid crystals

STRUCTURE	NAME	LC RANGE °C
$\text{CH}_3\text{O}-\text{C}_6\text{H}_4-\text{CH}=\text{N}-\text{C}_6\text{H}_4-\text{C}_4\text{H}_9$	MBBA	21-47
$\text{CH}_3\text{O}-\text{C}_6\text{H}_4-\text{N}(\text{O})=\text{N}-\text{C}_6\text{H}_4-\text{OCH}_3$	PAA	117-137
$n\text{C}_6\text{H}_{15}-\text{C}_6\text{H}_4-\text{C}_6\text{H}_4-\text{CN}$	PHCBP	14-28
$\text{CH}_3-\text{O}-\text{C}_6\text{H}_4-\text{O}-\text{C}(=\text{O})-\text{C}_6\text{H}_4-\text{C}_6\text{H}_4-\text{C}(=\text{O})-\text{O}-\text{C}_6\text{H}_4-\text{OCH}_3$	DMPTCHDC	143-242
$-\text{C}_6\text{H}_4-\text{C}_6\text{H}_4-\text{C}_6\text{H}_4-\text{C}_6\text{H}_4-\text{C}_6\text{H}_4-$	PQP	401-445

MBBA = p-methoxy benzylidene-p'-n-butyl aniline; PAA = p-azoxy anisole; PHCBP = p-n-hexyl-p'-cyano-biphenyl; DMPTCHDC = di-4-methoxy phenyl-trans-1,4-cyclohexane dicarboxylate; PQP = p-quinquephenyl

nematic liquid crystals are viewed between crossed polarisers with characteristic dark thread at lines of optical discontinuity. In thinner films, a schlieren texture, with a point like singularities, may be observed.

Orientation of nematic liquid crystals may be achieved easily in electric or magnetic fields.³⁰ Depending on the sign of the electric anisotropy $\Delta E = [E_{\parallel} - E_{\perp}]$ of the material, nematics orient parallel [$\Delta E > 0$] or the perpendicular [$\Delta E < 0$] to the applied field direction. Typically, only a few volts are required for distortion to occur. The diamagnetic anisotropy $\Delta Y = [\Delta Y_{\parallel} - \Delta Y_{\perp}]$ usually is positive, there by permitting parallel magnetic field alignment. Molecules of nematic liquid crystal also are aligned in flow field³¹⁻³³ which result in a viscosity lower than that of isotropic liquid. The rod shaped molecules easily stream past one another in the oriented condition. Flow may be impeded if an electric or magnetic field is applied counter to the flow orientation. The viscosity then becomes an anisotropic property.

All distortions of the nematic phase may be decomposed into three basic curvatures of the molecular director, shown in Figure 9. Liquid crystals are unusual fluids in that such elastic curvatures may be sustained. Molecules of true liquid would immediately reorient to flow out of an imposed mechanical shear. The force constants of imaginary physical springs resisting the motions [K_{11} , K_{22} , K_{33} respectively] are very weak, i.e., about 10^{-10} N [10^{-10} dyne], make the material exceedingly sensitive and easy to perturb. Illustrations of the three basic curvature deformations of the nematic liquid crystal opposing these strains are denoted K_{11} (splay), K_{22} (twist) and K_{33} (bend). These are represented in Figure 9. Schematic diagram of a nematic phase is presented in Figure 10.

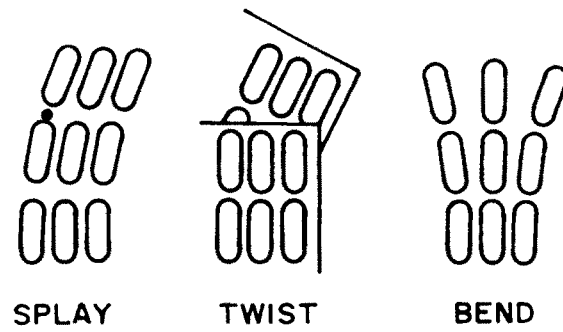


FIG. 9 ILLUSTRATION OF THE THREE BASIC CURVATURE DEFORMATIONS OF THE NEMATIC LIQUID CRYSTALS: SPLAY, TWIST AND BEND. THE FORCE CONSTANTS OPPOSING THESE STRAINS ARE DENOTED K_{11} (SPLAY), K_{22} (TWIST) AND K_{33} (BEND).

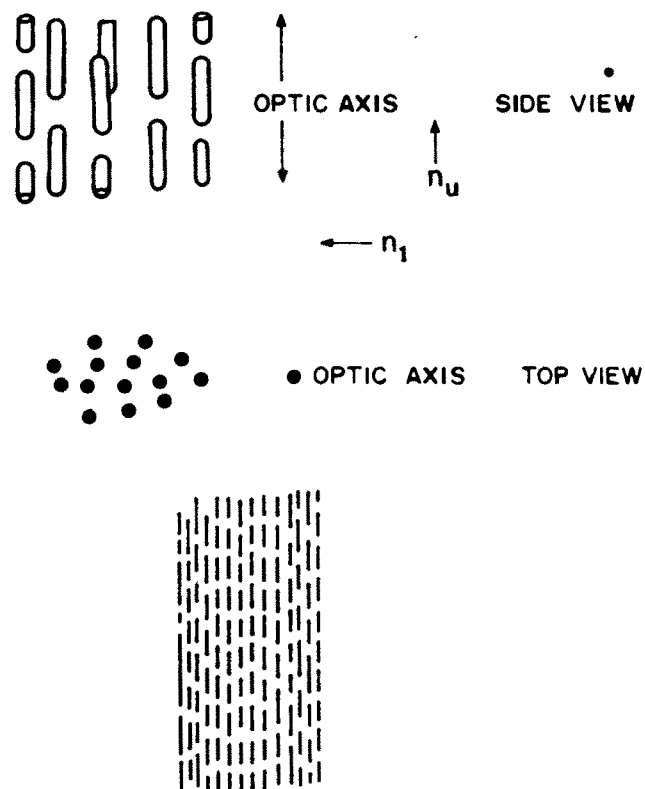


FIG. 10 SCHEMATIC DIAGRAM OF A NEMATIC PHASE.

1.4.1.3 Cholesteric Phase

The third thermotropic liquid crystal, the cholesteric phase³⁴, is termed so since a large number of derivatives of cholesterol exhibit this phase. Many properties of this phase resemble those of nematic phase. As in smectic phase, molecules are arranged in layers. Within each layer, parallel alignment of molecules is more reminiscent of the nematic phase. However, each layer is systematically twisted with respect to the previous one. The molecular layer are very thin. The long axes of the molecules are aligned parallel to the plane of layers. The individual molecules are essentially flat, with the substituent in the chiral centre projecting upward from the plane of each molecule. This unusual configuration causes the direction of the long axes of the molecules in each layer to be displaced slightly from the corresponding direction in adjacent layers. This displacement is cumulative through successive layers, so that the over-all displacement traces out a helical path.³⁵ The distance for a 360° turn is called the pitch. Cholesteric mesophase can also be obtained by mixing a nematic liquid crystal with a miscible optically active compound. Cholesteric liquid crystals are miscible with nematic liquid crystals and the thermodynamic properties are very much similar. This phase displays batonnet texture under polarised light.³⁶ Schematic diagram of cholesteric phase showing pitch P and displacement angle Q is represented in Figure 11. The director (arrow) traces out a helical path within the medium as represented in Figure 12.

1.4.2 Lyotropic Liquid Crystals

Lyotropic liquid crystals, which arise from the action of a solvent, are multi-component mixtures. Frequently, none of the components in a lyotropic liquid crystal phase is individually mesomorphic. Under isothermal condition, the concentration of

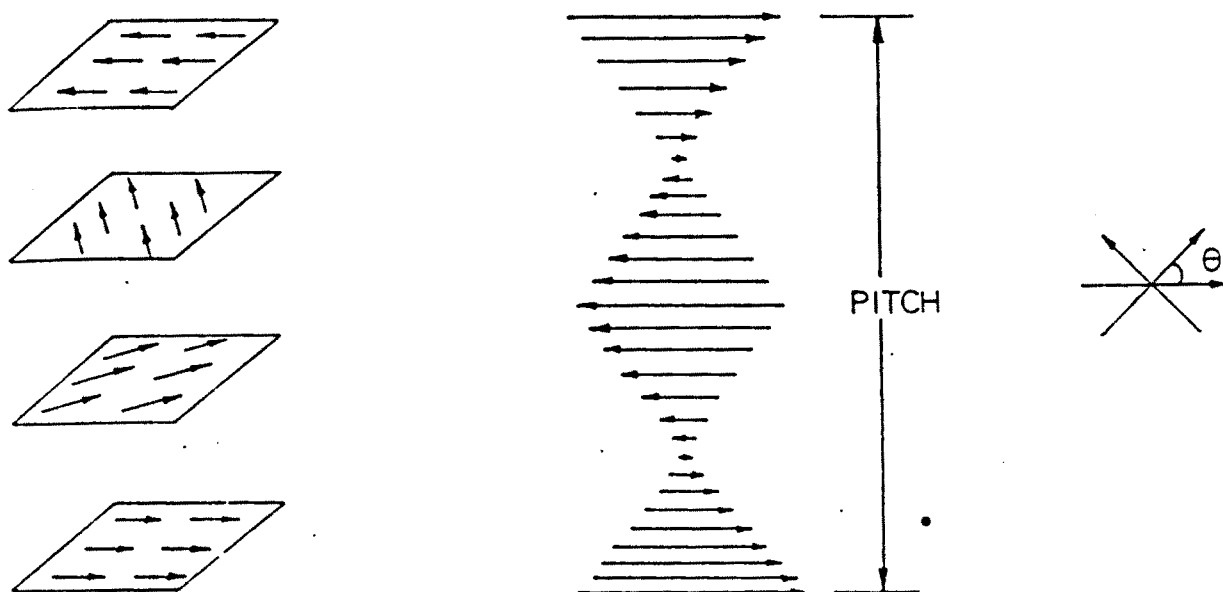


FIG. 11 SCHEMATIC DIAGRAM OF CHOLESTERIC PHASE
SHOWING PITCH P AND DISPLACEMENT ANGLE θ .

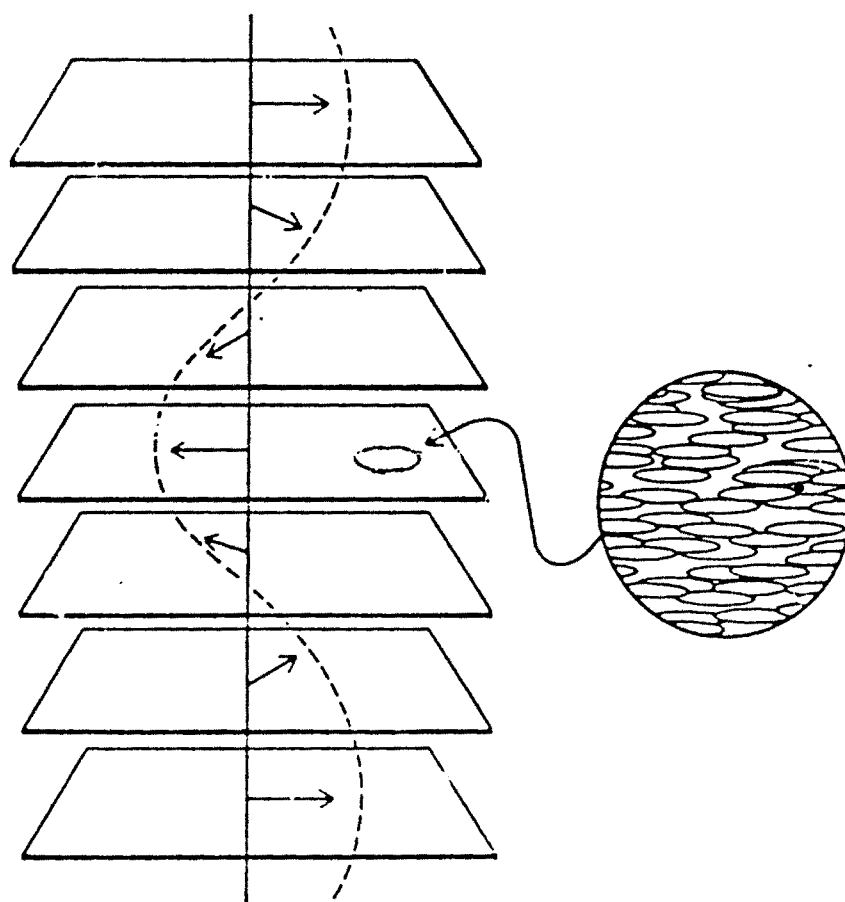


FIG. 12 THE CHOLESTERIC LIQUID-CRYSTAL STRUCTURE.
THE DIRECTOR (ARROW) PHASE TRACES BUT A
HELICAL PATH WITHIN THE MEDIUM.

the anisotropic component determines the degree of order present. Lyotropic liquid crystal is destroyed or converted into an isotropic fluid at sufficiently high temperatures. In principle, the dissolved substance must be amphiphilic. Soaps, Lipids and some dyes in an aqueous medium may serve as examples of such systems. The molecular complexes are arranged in the solvent medium can exhibit lamellar, cylindrical or spherical mesomorphic states. These forms are represented schematically in Figure 13.

1.5 CHARACTERISTICS OF LIQUID CRYSTALS

The orientation order in nematic liquid crystalline state is intermediate to that observed in crystalline solids and in normal liquids. The extent of orientation is represented by the order parameter "S" as defined by the expression:

$$S = \frac{1}{2} \langle 3 \cos^2 \theta \rangle - \frac{1}{2} \quad [1]$$

Where θ is angle between the molecular axis and the preferred direction while $\langle \rangle$ indicates an average value. The order parameter varies between zero for an isotropic liquid and one for a perfect solid. The order parameter near the clearing point is generally 0.3 to 0.4 but at lower temperature may become as high as 0.8 for nematic mesophase.

A number of liquid crystals exhibit both smectic and nematic mesophases. Compounds forming only one of them are named smectogenic or nematogenic. The temperature at which phase change occurs is known as the transition temperature. Transition temperatures are usually recognised on the basis of the phases involved in a transition, such as crystal-smectic, crystal-nematic, smectic-nematic and nematic or smectic-isotropic temperatures. The temperature for the phase change from a mesophase to an isotropic liquid is often called clearing temperature $[T_c]$. Thermotropic

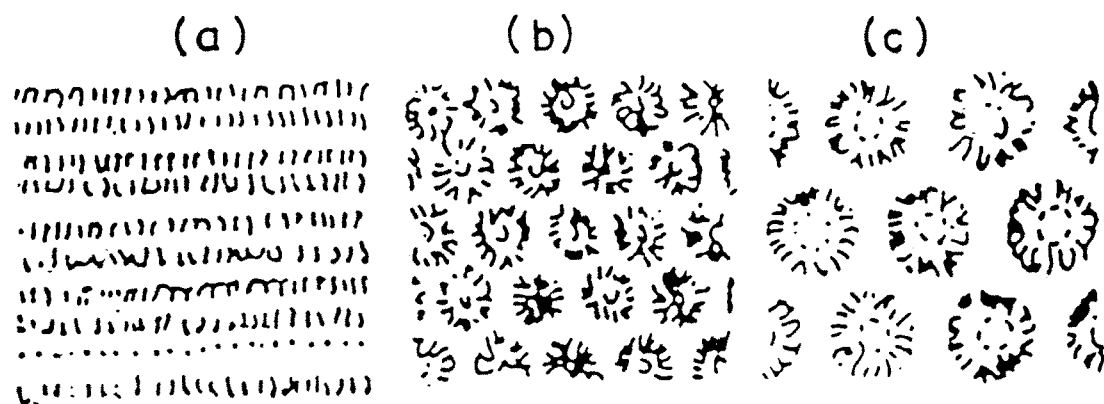


FIG. 13 SCHEMATIC DIAGRAM OF MOLECULAR ARRANGEMENTS IN LYOTROPIC FORM (a) LAMELLAR, (b) CYLINDRICAL AND (c) SPHERICAL FORMS.

liquid crystals, on heating, undergo a sequence of characteristic phase changes at the transition temperatures, and the three dimensional geometric organisation of the molecules generally collapses. This gradual breakdown of the molecular organisation is obviously related to the asymmetric nature of intermolecular attractive forces operating between sides, planes and terminal groups of the molecules. When the forces operating along the three axes of molecules are identical, the three dimensional crystalline arrangement will naturally collapse at the same temperature to form a normal liquid without displaying mesophases in between. It is, therefore, essential that these three intermolecular forces be not identical and also be strong enough to maintain partially ordered molecular organisation against thermal vibrations. Systems are known in which mesomorphic states are not formed during heating cycle but are only observed on cooling from the isotropic melt. These are termed monotropic. Mesophases are termed "enantiotropic" when they are observed in heating as well as in cooling cycles.^{37,38}

1.6 POLYMERIC LIQUID CRYSTALS

Liquid crystal polymers, or LCPs, are made of rigid rod like ordered molecules that maintain a crystalline order even on melting.³⁹⁻⁴⁸ They are classified into two types. First is thermotropic and second one is lyotropic. Lyotropic materials can be processed only from solution. Thermotropic materials can be melt processed.

KEVLAR is a well known first generation of liquid crystalline polymer.⁶⁷⁻⁷² This lyotropic system is infusible. The capabilities as high strength fibre can be harnessed only by part wet/part dry jet spinning from its solution in concentrated sulphuric acid. Composites can be made by reinforcing with thermoset and thermoplastic resins.

The second generation liquid crystalline polymers are thermotropic liquid crystals.⁴⁸⁻⁶⁶ These are melt processible and have intrinsic bone-flesh character suitable for in situ generation of composites. The first thermotropic LCP commercially introduced was **XYDAR** in 1984, by **DART and KRAFT**. It is based on 4-hydroxy benzoic acid, biphenol, and terephthalic acid. High temperature performance is its outstanding property. **CELANESE** commercialised a family of LCP called **VECTRA** in 1985, which are based on 4-hydroxy benzoic acid and 6-hydroxy-2-naphthoic acid. Both **XYDAR** and **VECTRA** resins are thermotropic and have nematic structures, which gives one dimensional parallel order to the molecules and high melt strength, coupled with extremely low melt viscosity.

Thermotropic LCP resins have, (a) extremely high strength and modulus for thermoplastic resins, (b) high impact strength for resins with such high temperature capability, (c) excellent chemical resistance, even at elevated temperature, (d) excellent dimensional stability, including an extremely low coefficient of thermal expansion and low moisture absorption and (e) outstanding processibility, especially in thin sections and as intricate components.

In addition to their excellent dielectric and arc resistance properties, LCPs are outstandingly resistant to radiation, hydrolysis and weathering and have self-extinguishing characteristics. LCPs have excellent dimensional stability that is superior to other high-performance engineering plastics, thermoset epoxy and ceramics. LCPs retain a high percentage of their room temperature toughness at temperatures of -27°C and below, while maintaining high strength and modulus. The tensile strength of LCP compounds actually increases at reduced thickness because of orientation effects. They

show virtually zero shrinkage and stability over a wide temperature range, their as-molded and in-use precision-tolerance can be much narrower than for competing resins.

Mesophase forming polymers are divided into main-chain and side-chain systems.⁴⁹ Polymers with mesogenic moiety as an integral part of backbone are termed as "main-chain liquid-crystalline polymers".⁴⁹ When mesogenic moiety is introduced in the side-chain or as a pendant the system is known as "side-chain liquid-crystalline polymers".⁷³⁻⁷⁵ A spacer is used to dissociate the disorder of the main-chain from the greater order of the mesogenic groups and to decouple the motion of the mesogenic moiety from those of the polymer backbone. Schematic diagram of liquid Crystalline polymers with mesogenic units in the main chain and side chain are presented in Figure 14.

Flexible spacers have also been extensively used to separate mesogenic groups placed in the main-chain from each other. The backbone flexibility achieved by this approach has the effect of markedly improving solubility and lowering transition temperatures in contrast to those of the rigid rod polymers.⁴⁴

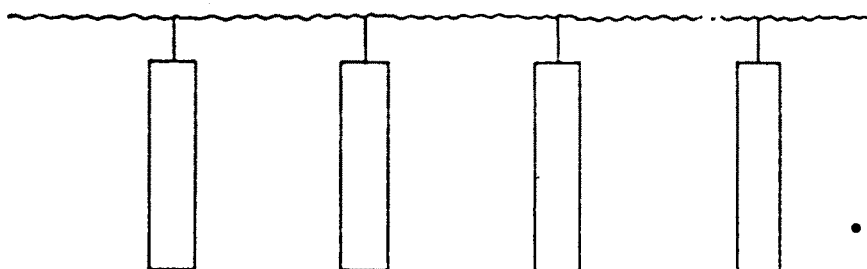
1.7 THERMOTROPIC LIQUID CRYSTALLINE POLYMERS

Thermotropic liquid crystalline polymers have received considerable attention in the recent past.^{49,74,76-80} The chemical units useful for thermotropic LCPs formation are generally those already exemplified in Table 2. Structures of a few wholly aromatic thermotropic copolymers are shown in Figure 15. However, these units in homopolymer form give rise to crystalline polymers with melting points above their decomposition temperatures. The problem of polymer design is to reduce the melting temperature in order to obtain LC phase at a temperature below that of decomposition.

a) MAIN CHAIN LCPs



b) SIDE CHAIN LCPs



 ← MESOGEN

 ← FLEXIBLE SPACER

FIG. 14 SCHEMATIC DIAGRAM OF MAIN CHAIN AND SIDE CHAIN LCP STRUCTURES.

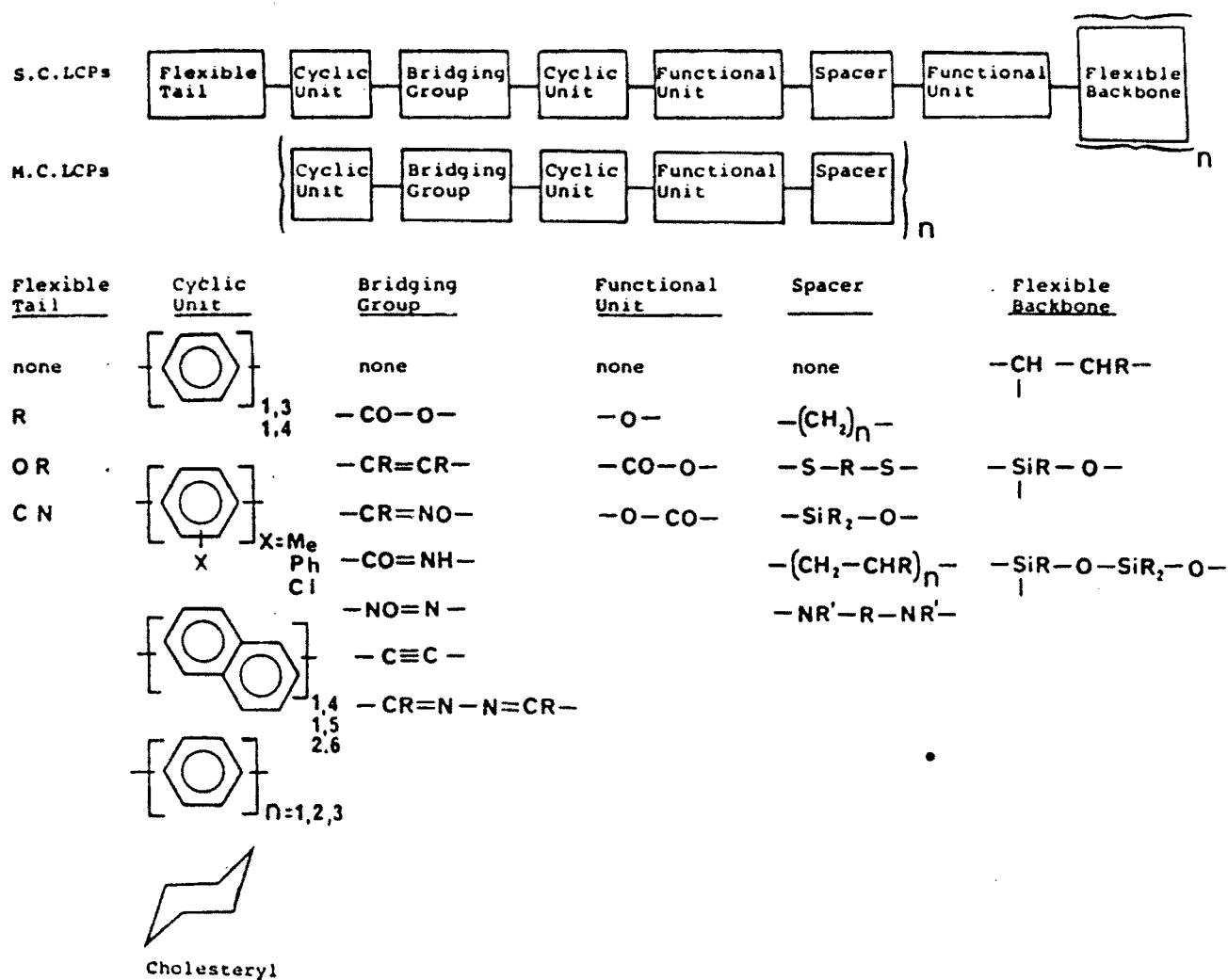
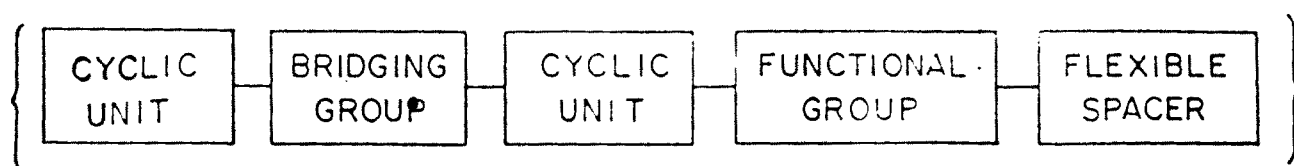

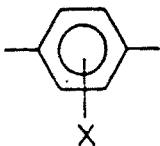
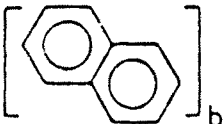
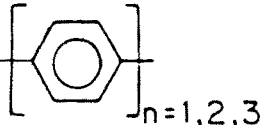

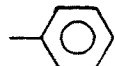


FIG. 15 GENERAL STRUCTURES OF MAIN CHAIN AND SIDE CHAIN LCPS.



CYCLIC UNIT	BRIDGING GROUP	FUNCTIONAL GROUP	FLEXIBLE SPACER
	none	none	none
	-CO-O-	-O-	$\text{-(CH}_2\text{)}_n\text{-}$
	-CR=CR-	-CO-O-	$\text{-(CH}_2\text{-CHR)}_n\text{-}$
	-CR=NO-	-O-CO-	$\text{-(CH}_2\text{-CH-O)}_n\text{-}$
	-CO=NH-		-SiR ₂ -O-
	-NO=N-		
	-C≡C-		
	-CR=N-N=CR-		
			

X = CH₃, , Cl

a = 1,3 or 1,4 disubstituted benzene ring

b = 1,4 or 1,5 or 2,6 disubstituted naphthalene ring

TABLE-2: GENERAL STRUCTURES OF MAIN CHAIN LCPs

Thermotropic systems are more usually based on polymers that contain ester groups or other linking units free from hydrogen bonds. Even without the inter-chain association caused by amide groups, considerable disruption of main-chain order is necessary to depress crystallinity. Thus, poly[4-oxybenzoyl], poly[4-phenylene terephthalate] and poly[4'-phenylene naphthalene-2,6-dicarboxylate] melt at temperature of 610°C,⁸¹ 596°C and 577°C respectively.⁸² These temperatures are too high for formation of a stable nematic melt. Considerable research efforts have focused on structural modification to generate melt processible mesomorphic polymers suitable for conventional processing equipments.

A variety of approaches have been made to reduce the crystal perfection and the crystal lattice energy with the objective of the melting temperature ranges of rigid rod polymers and to generate liquid crystallinity at suitable lower temperature. These include: (1) use of non-rigid group [flexible spacer] in the main chain to reduce the axial ratio of the mesogen,⁵¹ (2) placement of substituents on the mesogenic group to disturb regularity of the repeating unit,⁵² (3) use of non-linear cycloaliphatic comonomers [kinks],⁸³ (4) incorporating crank-shaft monomers⁸⁴ and (5) copolymerisation of mesogens.⁵³ Random placements of repeat units can lower the transition temperatures still further.⁵⁴

The three flexible spacers used predominantly are polymethylene,^{41,85-88} polyethylene oxide,^{43,55,89} and polysiloxane segments.⁹⁰ Liquid crystalline polymers with alkyl, alkoxy, halo, nitro, phenyl, cycloalkyl or cyano substituted on 1,4-phenylene ring are reported in literature.^{57,58,91,92} 1,4-Phenylene or 2,6-naphthalene based LCPs were extensively studied and discussed. Homopolymers based on these aromatic moieties are crystalline and non-melting. The melting ranges are reduced by incorporating 1,3-phenylene, 2,5- or 1,4-naphthalene rings in the polymer chain.^{45,93-96}

Modification to rigid rod systems by incorporating flexible spacer to reduce transition temperature affects the mechanical behaviour due to dilution and randomisation of directional vectors associated with the mesogens. Copolymerisation of 1,4-benzene/2,6-naphthalene moieties with slight loading of either 1,4-benzene/2,5-naphthalene units in the main chain result in thermotropic LCPs without much compromise of the mechanical performance of linear rigid homopolymer.⁹⁷ Thermotropic LCPs generally compromise non hydrogen bonding groups e.g., esters as central linking units.

The monomers most frequently used in the synthesis of LC polyesters are listed in Table 2. The generalised skeleton structure of a main chain LCP is represented in Figure 15. The central linking unit must ensure that the linearity of the rigid unit is maintained. Aromatic ring should be separated by odd number of chemical bonds. It is "1" for biphenyls, "3" for esters, azo, azoxy, azomethine, amide group and "5" for alazines.⁹⁸

1.8 STRUCTURE-PROPERTY RELATIONSHIPS

The liquid crystalline transition temperatures change markedly when molecular structure is varied widely within a group of suitable compounds. The type and the number of liquid crystalline states may be different. In such cases, it is difficult to relate the observed changes in liquid crystalline behaviour to the numerous molecular parameters that have been altered. For this reason, it is profitable to examine the effects of making relatively small changes in the molecular structure of one particular type of liquid crystalline compound, while retaining a greater part of the molecular skeleton unaltered.

The thermal behaviour, especially the transition temperature, is probably the most discussed property in the study of thermotropic liquid crystalline polymers. The thermal transitions are related to structural parameters such as the nature of aromatic rings, central link units, substitution on mesogen, the flexible spacer type and the number of carbon atoms in the flexible spacer. Polyesters have been investigated extensively since these can be synthesised by low temperature polycondensation and high temperature melt transesterification reactions from easily available or already synthesised monomers.⁴⁸ The structure-property relationship discussed under the following three subsections are pertinent to LC polyesters. These are: (1) effect of mesogenic structure, (2) effect of flexible spacer and (3) copolymerisation.

1.8.1 Effect of Mesogenic Structure

Factors related to mesogenic structure which affect the thermal behaviour of mesomorphic polymers are: (1) number of the rings in the mesogen, (2) intra-mesogenic link and (3) substitution on the mesogen.

1.8.2 Number of Rings in the Mesogen

Transition temperatures of mesomorphic polymers are enhanced by an increase in number of aromatic rings in the main chain, as seen from data presented in Table 3. However, the presence of large number of aromatic rings would result in non-melting polymers.¹⁰⁰ Crystal-mesomorphic, mesomorphic-isotropic transition temperatures and temperature range over which mesophase is stable⁴³ are higher for polymer. This is attributed to the additional aromatic ring in the polymer, which increases the length and hence axial ratio of the mesogen. Similar trend is observed in the thermal characteristics⁵¹ of polyesters I-3 and I-4. Transition temperatures of these polyesters are

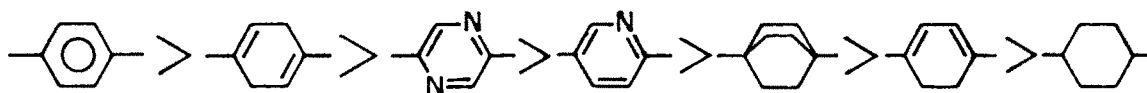
TABLE 3

Dependence of thermal transitions in thermotropic polyesters on number and type of aromatic rings in the mesogenic structure

POLYMER No.	STRUCTURE	TRANS. TEMP. °C
I-1	$-\text{C}-\text{C}_6\text{H}_4-\text{C}_6\text{H}_4-\overset{\text{O}}{\parallel}{\text{C}}-\text{O}-[\text{CH}_2]_{10}-\text{O}-$	C 154 LC 160 I
I-2	$-\overset{\text{O}}{\parallel}{\text{C}}-\text{C}_6\text{H}_4-\text{C}_6\text{H}_4-\text{C}_6\text{H}_4-\overset{\text{O}}{\parallel}{\text{C}}-\text{O}-[\text{CH}_2]_{10}-\text{C}-$	C 256 LC 311 I
I-3	$-\text{O}-\text{C}_6\text{H}_4-\text{O}-\overset{\text{O}}{\parallel}{\text{C}}-\text{C}_6\text{H}_4-\text{O}-\overset{\text{O}}{\parallel}{\text{C}}-[\text{CH}_2]_{10}-\overset{\text{O}}{\parallel}{\text{C}}-$	C 237 LC 294 I
I-4	$-\text{O}-\text{C}_6\text{H}_4-\text{O}-\overset{\text{O}}{\parallel}{\text{C}}-\text{C}_6\text{H}_4-\overset{\text{O}}{\parallel}{\text{C}}-\text{O}-\text{C}_6\text{H}_4-\overset{\text{O}}{\parallel}{\text{C}}-\text{C}-[\text{CH}_2]_{10}-\overset{\text{O}}{\parallel}{\text{C}}-$	C 236 LC 265 I

presented in Table 3. Polymer I-3 has only one intramesogenic link. The diad mesogenic ester shows directional sense.⁴⁹ The thermal behaviour of polymer I-3 is related to the manner in which the flexible spacer $-\text{[CH}_2\text{]}_{10}\text{-}$ is linked.⁵⁷

As discussed in the Section 1.5, the mesomorphic properties like mesophase transition behaviour and mesophase thermal stability are affected by the intermolecular attractive forces. The nature of central ring changes mesophase stability and transition temperature of mesomorphic compounds. In low molecular weight liquid crystals this trend in transition temperature is related to the central ring as:¹⁰¹⁻¹⁰³



The central ring can be differentiated into three major groups: (a) aromatic, (b) unsaturated cyclic and (c) cycloaliphatic. Incorporation of hetero atoms in aromatic ring reduces the mesophase transition temperature. In case of diene ring systems, location of double bond plays a significant role in mesophase stability. The non-planar 1,3-cyclohexadiene ring makes it harder for the molecules to pack into a regular structure and results in lower mesophase transition temperature. The greater packing efficiency of bridged bicyclo compounds results in thermally stable mesophases. Thus, the thermal stability of mesomorphic compound with unsaturated cyclic central ring is intermediate between those with aromatic and cycloaliphatic central rings. Rings other than 1,4-benzene and 2,6-naphthalene may completely destroy liquid crystallinity by disturbing molecular linearity.⁵⁹

1.8.3 Nature of Terminal Substituent

Transition temperature of low molecular mass liquid crystals have been studied systematically¹⁰⁴ relative to the variation in the nature of substituent in para position. A representative data is presented in Table 4. Substituents may be arranged to give orders of group efficiency in promoting liquid crystalline properties.

A simplified group efficiency order published by Dave and Dewar^{105,106} is:

Nematic: $\text{NO}_2 > \text{MeO} > \text{NMe}_2 > \text{Me} > \text{Cl} > \text{Br} > \text{H}$

Smectics: $\text{Br} > \text{Cl} > \text{F} > \text{NMe}_2 > \text{Me} > \text{H} > \text{NO}_2 > \text{MeO}$

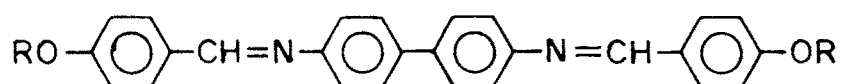
Four factors need to be considered nematic-isotropic transition while examining with respect to chain. These are: (1) The layer molecules will be less readily rotated out of the ordered state. (2) The overall polarisability increases with each added methylene unit. (3) The frequency with which readily polarisable aromatic parts of the molecules lie next to one another in the fluid nematic melt will decrease. The residual lateral attractions will tend to decrease. (4) Each methylene unit would force apart the polarisable centres in the molecules, and decrease the residual terminal attractions. (1) and (2) would increase the nematic-isotropic transitions temperatures, while (3) and (4) would decrease it.

1.8.4 Intramesogenic Links

The intramesogenic links are the group of atoms that connect two aromatic rings of the mesogen. The type and linking direction in unsymmetrical intramesogenic links of the mesogen have a pronounced effect on the thermal behaviour of mesogenic polymers. The extensively investigated intramesogenic links units are: (a) azo, (b)

TABLE 4

Dependence of nematic to isotropic transitions in liquid crystals based on 4-p-substituted-benzylidene amino-4-methoxy-biphenyls on terminal substituent



SUBSTITUENT	TRANS. TEMP., °C	SUBSTITUENT	TRANS. TEMP., °C
H	176	F	265.5
Me	279	Cl	295
MeO	318	Br	294.5
Γ -PrO	296	NO ₂	308
neo-PnO	274	NMe ₂	293.5
s-PrO	256	NHCOCH ₃	345

Me = methyl; Pr = propyl; Pn = pentyl;

azoxy, (c) ethene or substituted ethene, (d) azomethine or substituted azomethine, (e) substituted or unsubstituted alazine and (g) ester. A few selective examples of polyesters with different intramesogenic link units are listed in Table 5.^{43,107-110}

Polyesters I-5 to I-8 are of the rigid rod-flexible spacer type and polymers and decamethylene spacer with diad mesogenic group. A change in intramesogenic link alters the thermal behaviour of the polymers. The unit is altogether absent in polymer I-5. Additional factor in ester linkage is the direction during linking of two rings together. This can be either head to tail [random] or head to head [ordered] sequences. The random arrangement in polymer I-9 generates non-mesomorphic character where as ordered arrangement in polymer I-10 generates monotropic nematic behaviour. Thus, structure randomisation affects the crystal packing efficiency dramatically, resulting in either non-mesomorphic or poorly defined mesophases.

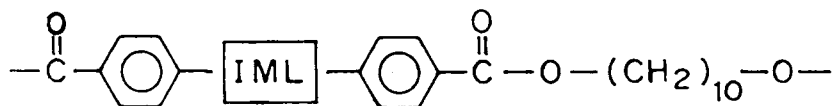
Similar observations are recorded for liquid crystalline polyesters with triad mesogens and decamethylene flexible spacer are presented in Table 6. The polymer I-13 appears to form smectic phase and polymer I-16 showed poorly defined smectic phase. In polymer I-13 and I-14 as well in polymers I-15 and I-16 the intramesogenic ester units are interchanged. The axial ratios are identical.⁶¹ The difference in these polymers is in the crystal packing efficiency and intermolecular forces due to the interchange of the ester linkages. These factors affect mesophase transition temperatures of polymer I-13 and the clearing temperatures of polymer I-15.

1.8.5 Flexible Spacer

In the early 1970's, Kuhfuss and Jackson¹¹¹ did pioneering work on effect of flexible spacers. Two years later, Roviello and Sirigu¹¹² reported the first academic example. The following salient features were recorded:

TABLE 5

Dependence of thermal transitions in liquid crystalline polymers on intramesogenic link (IML) type



POLYMER No.	INTRAMESOGENIC LINK (IML)	TRANS. TEMP., °C
I-5	NONE	C 154 LC 160 I
I-6	-CH=CH-	C 197 LC 200 I
I-7	-N=N-	C 210 I
I-8	-N=N[O]-	C 200 I
I-9 (random)	-C[O]-O-	No LC
I-10 (ordered)	-C[O]-O-	Monotropic LC
I-11	-C(CH ₃)=CH-	C 200 LC 222 I
I-12	-C(CH ₃)=N-N=C(CH ₃)-	C 217 LC 242 I

Ar = 1,4-phenylene unit

TABLE 6

Dependence of thermal transitions in trimesogenic liquid crystalline polyesters on direction of ester intramesogenic (IML) link



POLYMER	INTRAMESOGENIC LINK (IML)				TRANS. TEMP. °C
	(IML ₁)	(IML ₂)	(IML ₃)	(IML ₄)	
I-13					C 220 S 267 I
I-14					C 230 N 265 I
I-15					C 236 N 265 I
I-16					C 237 N 294 I

Ar = 1,4-phenylene unit

- [1] A decrease in the transition temperatures with increase in spacer length,
- [2] zigzag manner of change in transition temperatures and isotropisation entropy with odd-even number of methylene units and
- [3] A change in the micromolecular packing structure.

The dependence of the melting [T_m], the isotropisation temperature [T_i] of two main chain LCPs with the number of methylene units¹¹³ is shown in Figure 16. In general, polymers with even methylene units have higher T_i and ΔS [entropy change] than those having odd units. However, opposing trends have been reported by Ober et al.^{49,57} The temperature difference between T_i and T_m implies the range of stability of the mesophase. Jackson and Kuhfuss reported that mechanical properties such as tensile strength, flexural properties of injection molded 4,4-[alkylenedioxy]dibenzoic acid polyesters dropped with an increase in methylene units.

Krigbaum et al.¹¹⁴ reported that main chain LCPs with an even number of methylene groups are smectic, while those having an odd number exhibit nematic phase. Ober et al.⁵⁷ observed that main chain LCPs with nine and ten units display a smectic phase on melting, while polymer with lower only nematic phase. In general, the odd-even effect is strongly related to the trans and gauche conformation of the flexible spacer. As a result, it influences the stability of the mesophase.

Krigbaum et al.¹¹⁴ and Abe et al.¹¹⁵ concluded that polymers with an even number of methylene units have high degree of crystallinity and melt to form a highly ordered smectic structure stable over a broader temperature range, while the series with odd number of methylene units are less crystalline and only form a nematic phase. In addition, systems in the even series with mesogens based on biphenyl rings adopt a twisted arrangement represented in Figure 17. As a result, these have a more favourable packing configuration in the crystalline state.

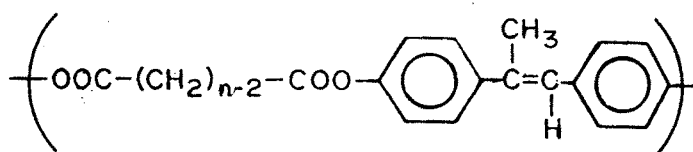
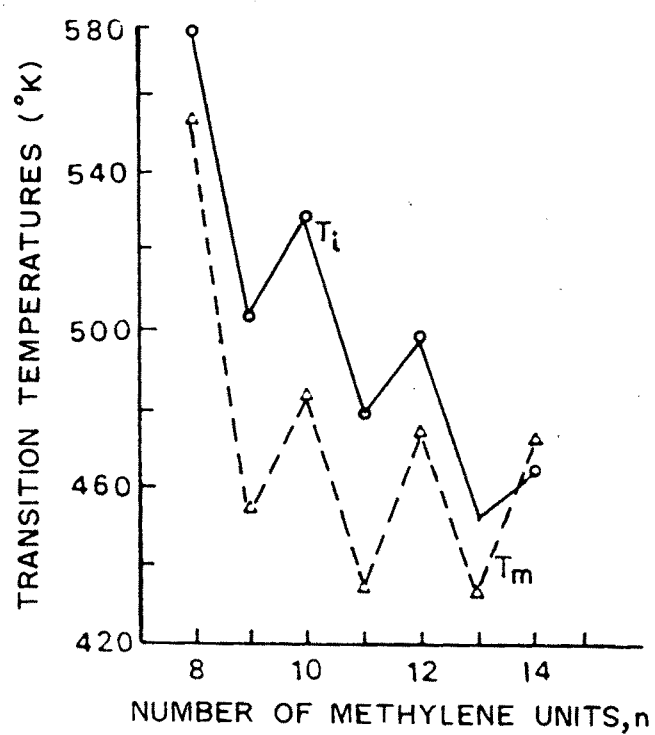


FIG. 16 DEPENDANCE OF THE MELTING POINT (T_m) AND THE ISOTROPISATION TEMPERATURE (T_i) ON THE NUMBER OF METHYLENE UNITS.

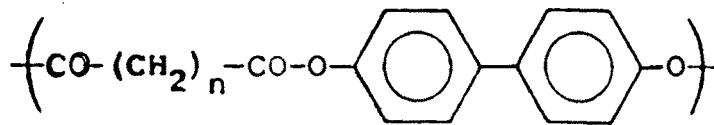
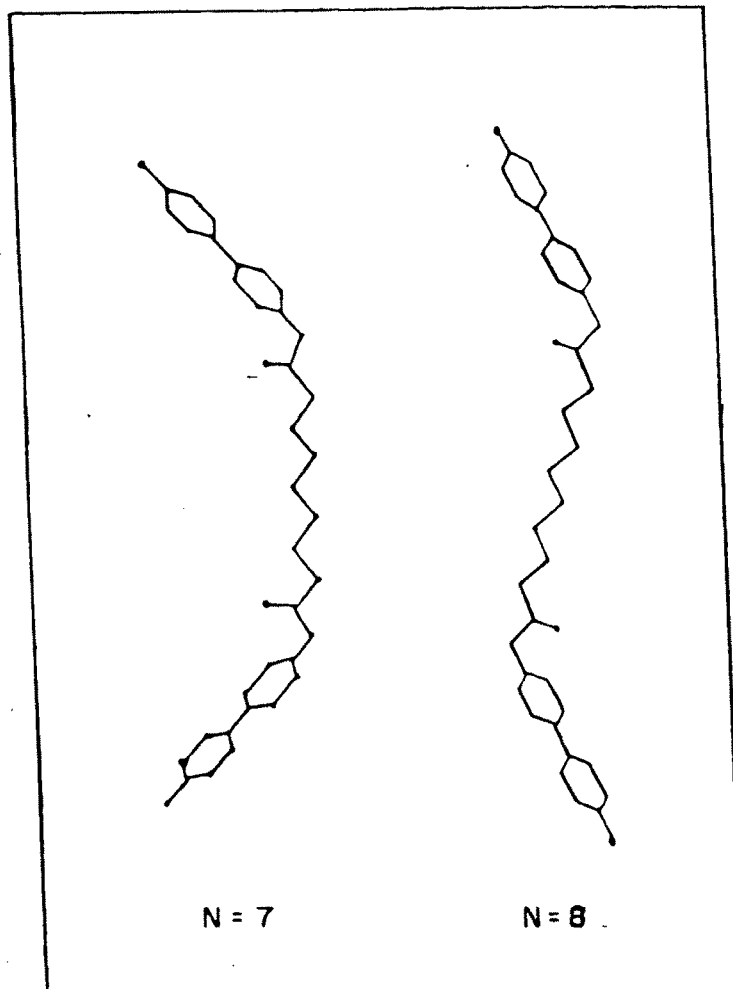


FIG. 17 EXTENDED CHAIN STRUCTURES OF THERMOTROPIC POLYESTERS WITH DIFFERENT NUMBER OF METHYLENE UNITS.

1.8.6. Polyethylene oxide [PEO] Spacer

The polar oxygen atom in polyethylene oxide spacer strengthens lateral intermolecular attractions and promotes the formation of smectic mesophases. The mesophase type changes with the number of PEO units in the flexible spacer.^{43,55,89}



The type of mesophase formed, if any, has been shown to vary with the number of ethylene oxide units in the flexible spacer moiety. Thus, nematic phase is formed with 1,2-ethane diol, a monotropic smectic with diethylene glycol and a smectic with triethylene glycol.

1.8.7 Ring Substitution

Morgan et al.¹¹⁶ and Kalyvas et al.¹¹⁷ synthesised a variety of thermotropic polyazomethines by modifying unmoldable polymer derived from 1,4-phenylene diamine and terephthaldehyde. Substituent type strongly altered the mechanical properties of heat-treated fibres. Thus, growth of LC order and packing of molecular chain during annealing are related to substituent type. Milland and Strazelle¹¹⁸ prepared thermotropic poly [nitriolo-2-methyl-1,4-phenylene nitro methylidene-1,4-phenyl methylidene] [Me-PNPM]. The Mark-Houwkin's constant was 1.15 - 1.20, slightly below that for ideal rigid-rod model. Jackson⁸¹ observed significant reduction in the heat treatment time for fibre in the presence of a phenyl substituent.

Perhaps most experiments in this area were conducted and also summarised by Lenz and coworkers.⁴⁸⁻⁶⁶ In short, an introduction of halogen and alkyl groups into one aromatic ring of a mesogenic unit depresses the glass transition temperature, melting and clearing points. This implies that both the melting point and thermal

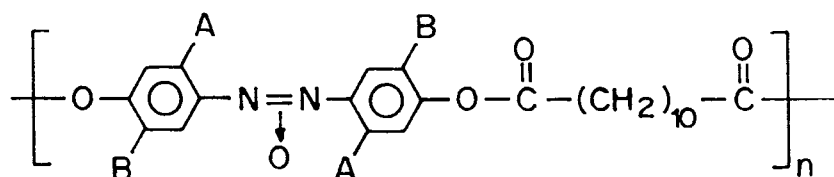
stability of mesophases decrease with an increase in the size of cycloaliphatic substituent. Polymers lose LC order on incorporation of long alkyl ring substituents. Blumstein et al.¹¹⁹ reported that substitution of methyl group in the 2,2'- and 3,3'-positions of the mesogenic core gave soluble polymers. This phenomenon may be caused by the twisting of the molecular structure around the interlinking double bond.¹⁰⁴

Substitution on mesogenic unit increases diameter of the mesogen, and decreases the axial ratio. The orientation of the adjacent mesogen is reduced its packing efficiency is disrupted. The phase transition temperature decreases as a result. Polar substituents enhance dipolar attractions between neighbouring chains, which lead to an increase in transition temperatures. In polymers with mono- or di-substituted mesogenic units the nature and relative position of substituted groups govern the thermal behaviour,¹¹⁹⁻¹²² as seen from Tables 7 and 8. Thus, thermotropic LC polymeric systems with symmetrically disubstituted mesogenic unit [2,5-disubstituted-1,4-phenylene] have higher transition temperatures than monosubstituted analogues. The packing efficiency is enhanced in the presence of symmetric disubstitution.

The diols used in these polymers in Table 7 were 4,4-dihydroxy azoxy benzene [polymer I-17]; 4,4-dihydroxy-3,3-dimethyl azoxy benzene [polymer I-18] and 4,4-dihydroxy-2,2-dimethyl azoxy benzene [polymer I-19]. It is observed that the introduction of substituent into mesogenic units results in depression in both mesophase [T_m] and clearing temperature [T_c] of the polymer. The methyl group positioning are altered in polymers I-18 and I-19. Greater disturbance of coplanarity was observed in polymer I-19.

TABLE 7

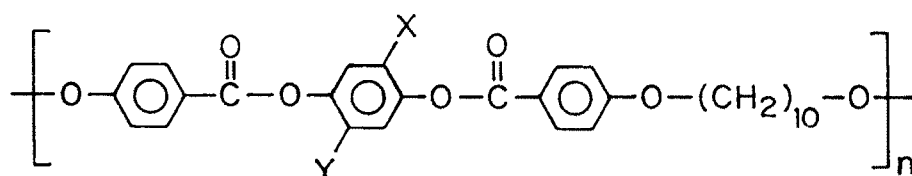
Dependence of thermal transitions in liquid crystalline polymers on substitution pattern on aromatic nucleus



POLYMER No.	A	B	TRANS. TEMP., °C
I-17	H	H	C 216 N 265 I
I-18	H	CH ₃	C 196 N 218 N
I-19	CH ₃	H	C 118 N 163 I

TABLE 8

Dependence of thermal transitions in liquid crystalline polyesters on substitution pattern on aromatic nucleus



POLYMER No.	X	Y	BOND LENGTH $\overset{\circ}{\text{A}}$	T_m °C	T_i °C	ΔT °C
I-20	H	H	1.10 [C-H]	236	297	61
I-21	H	CH ₃	1.53 [C-C]	162	274	112
I-22	H	NO ₂	1.43 [C-N]	161	194	33
I-23	H	Cl	1.70 [C-Cl]	157	279	122
I-24	H	CN	1.53 [C-C]	157	219	62
I-25	H	C ₆ H ₅	1.53 [C-C]	151	168	117
I-26	H	Br	1.85 [C-Br]	146	270	124
I-27	Cl	Cl	1.70 [C-Cl]	200	255	55
I-28	H	OCH ₃	1.36 [C-O]	158	NO	LC

A series of substituted LCPs investigated by Lenz et al.⁵⁵ were based on the structure presented in Table 8. Polar effects were found to be of less importance than steric constraints in governing the thermal behaviour. Substituents X, Y were either halogen atoms or alkyl groups. The transition temperatures are presented in Table 8. The thermal transitions of LCPs from substituted mesogens are affected by the four factors presented in Sections 1.8.7.1 to 1.8.7.3.

1.8.7.1 Bond Length

The phase transition temperatures decreased with an increase in bond distance between mesogenic units and with incorporation of substitution on the unit. This is seen from the data presented in Table 8 above for the different bond lengths that arise from a variance in the substituent attached to the aromatic nucleus.

1.8.7.2 Bulkiness of Substituent Group

A downturn in phase transition temperature is observed with an increase in the Van der waal radii (bulkiness) of the substituent. A look at the Table 8 reveals that a change from methyl (I-21) to cyano group (I-24) decreases the transition temperature by 55°C. This is brought down further by 51°C on substitution with phenyl group (I-25).

1.8.7.3 Polarity of the Substituent

Polar substituents on the mesogenic core increase the attractive forces transverse to the chain. This tends to depress and/or destroy liquid crystallinity. Replacing methyl group in polymer I-21 with methoxy substituent in polymer I-28 (Table 8) destroys the thermotropic character completely.

1.8.8 Kinks

This involves the incorporation of meta-aromatic isomers. This generates a kink and reduces the rigidity of the mesogenic structure and lowers the transition temperature. Cottis¹²³ modified [4-oxybenzoyl] by inserting isophthalic acid [IA] and biphenol [BP] to yield polymers having reasonable processing temperatures. The effect of a meta-isomer has been extensively investigated.^{45,48,81,124} Researchers at Eastmann Kodak partially replaced 4-hydroxy benzoic acid [HBA], hydroquinone [HQ] and terephthalic acid [TA] in LCPs with 3-hydroxy benzoic acid, resorcinol [R] and isophthalic acid [IA] respectively, to generate low melting polyesters. The mechanical properties of injection molded parts decreased with an increase in meta-isomer content. The kink approach changed molecular packing and reduced melt density. Lenz and Jin^{48,63} prepared LCPs using up to 60 percent of resorcinol [R]. This approach, while being very effective in reducing the transition temperature of an LCP, reduces the oxidative resistance¹²³ and hydrolytic stability.¹²⁵

1.8.9 Crank-Shaft Monomers

Using 2,6-functionally disubstituted naphthalene monomers such as 2,6-naphthalene dicarboxylic acids [NDA], 2,6-naphthalene diol [ND] and 6-hydroxy-2-naphthoic acid [HNA] offset the linearity of rigid cores in the main chain. This approach has generated LCPs with relatively lower transition temperatures having excellent mechanical properties.¹²⁵⁻¹²⁷ The HBA/HNA LCP, a typical example of this method, has received a great deal of attention from both thermoplastic industry and the academic world.

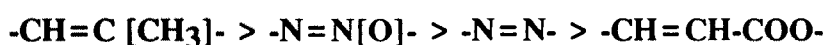
Addition of 6-hydroxy-2-naphthoic acid [HNA] to HBA causes a decrease in the melting point.¹²⁵ X-ray studies of these polymers showed that an increase in HNA

content caused a reduction of the linearity as well as the persistence length of the molecular chain. Due to the non-linearity of the 2,6-naphthalene linkages, the directions of successive oxygen central linkages groups are no longer parallel to the chain axis, but off set from the axis in the range of $+20^\circ\text{C}$.

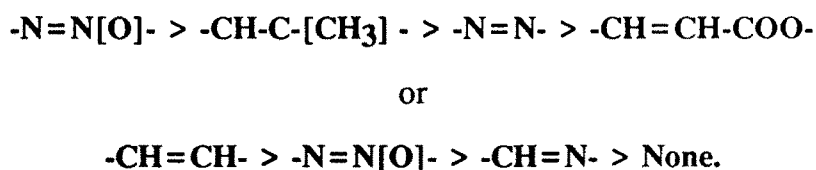
Jackson^{79,81} has thoroughly investigated the LCPs synthesised from 2,6-naphthalene dicarboxylic acid [NDA] and a variety of monomers, such as IA, TA, HBA, m-HBA, HQ, resorcinol and ethylene glycol. His results showed that polymers containing NDA usually have longer relaxation times than those without it, such as HBA/PET. Replacing 2,6-NDA by either 1,4-NDA, 1,4- or 1,5-naphthalene diols [ND] and then polymerising with almost the same monomers still gave polymers which exhibit LC phase. However, LC copolyesters prepared with 2,6-derivatives [2,6-NDA and 2,6-ND] have lower melting points than those synthesised from 1,4- and 1,5-derivatives. This phenomenon arises from the fact that each isomer has a unique repeating unit length. The 2,6-derivative has the longest length and has the greatest difficulty in fitting into an LC lattice.

1.8.10 Anisodiametric Bridging Group

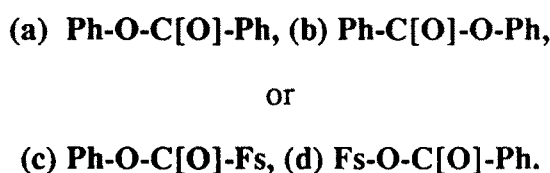
A variety of main chain and side chain LCPs has been developed using this approach.^{49,83,88,119,128-131} LCPs prepared from this approach seem to be better than those from the spacer and kink method because of the thermal and chemical stability of the central bridging units. Chiellini and Galli¹³⁰ studied the structure of chiral LC polyesters. The effectiveness of the central bridging group in extending the mesogenic behaviour followed this order:



The stability of the resulting mesogenic phase in the order¹³⁹:



These orders are in agreement with the trend observed for low molecular weight LCs.¹³¹ Gray reported that ester group has two ways to be associated with phenyl [Ph] groups or flexible spacers [Fs]:



This complicates stability and orientational order. Lenz and his coworkers⁴⁹ investigated the effect and reported that it changes the LC structure as well as the transitional temperatures.

1.9 POLYMER SYNTHESIS

Most LC polymers investigated have been polyesters. The four routes used in the synthesis of LC polyesters are:

- 1] Direct polyesterification,
- 2] Ester exchange/transesterification,
- 3] Self polycondensation, and
- 4] Schotten-Baumann reaction^{48,74,76,108,132,133}

Direct polyesterification of diols with dicarboxylic acids generates polyesters with the elimination of water. The second method of direct polycondensation is through

the formation of diphenyl chlorophosphate-pyridine complex in presence of lithium halide. The complex reacts with diacids to generate polyesters. A number of strategies adopted to synthesise polycondensation products through such complexes are discussed by Higashi et al.¹³⁴⁻¹³⁸ Synthesis of polyesters by high temperature transesterification reactions, suitably catalysed, is well documented and reviewed by R.E. Wilfong.¹³⁹ Polycondensation procedures are applicable only in the case of hydroxy acids. Schotten-Baumann reactions, are performed between carbonyl halides and hydroxy compounds in the presence of an appropriate acid acceptor, are discussed in Section 1.9.1. The reactants must be extremely pure, present stoichiometrically and the viscosity of polymerisation medium should not hinder removal of the side product in order to generate high molecular weight polyesters. Main chain LCPs are synthesized by two strategies. These are: (1) polymerisation of rigid core with appropriate flexible spacer and (2) monomer design by the incorporation of the flexible segment into the rigid core and subsequent polymerisation. Synthesis of such LC copolyesters by (a) acid halide route and (b) transesterification are described in the following Sections.

1.9.1 Acid Chloride Route

This route is divided into low and high temperature polycondensations. The most extensively used halide is chloride. The low temperature polycondensation technique has advantages over high temperature method in the polymerisation of thermally and conformationally unstable reactants. In addition, the polycondensation can be conducted in melt, solution or by interfacial method. In low temperature reactions, a preformed mesogenic core may be reacted to form the polymer or the mesogenic moiety is generated insitu during the polymerisation. The structure obtained by the

former strategy is more ordered. Here, the mesogenic core used is generally in the form of a diol and is reacted with acid chlorides which incorporate the aliphatic flexible spacer moiety.

1.9.2 Solution Polycondensation

In this technique mesogenic diol dissolved in polar aprotic solvent-acid acceptor mixture is added to acid halide dissolved in polar solvent. The reactants are taken in stoichiometric amounts and the reaction is allowed to proceed under inert atmosphere at room temperature or at an elevated temperature.

The experimental parameters which influence the molecular weight of polyesters formed are: (1) reactivity of the monomer, (2) solvent system, (3) monomer purity and stoichiometry, (4) acid acceptor, (5) stirring rate, and (6) reaction temperature.

1.9.3 Interfacial Polycondensation

The reaction is conducted in two miscible liquid phases, of which one is aqueous and the other is organic. Acid halides are taken in the organic phase and diol, acid acceptor and phase transfer catalyst are taken in aqueous phase. The two phases are intimately mixed to induce polycondensation. Important factors governing interfacial polycondensation reaction are:

(a) chemical reaction rate, (b) precipitation rate of polymer, (c) reactant and solvent purity, (d) stirring rate, (e) concentration of monomers in two phases, (f) hydrolysis of acid halides, (g) solution viscosity, (h) interfacial energy barrier, and (i) partition of reactant in the two liquid phases.

1.10 THE PRESENT WORK

This thesis deals with (i) the synthesis of three new series of ordered rigid rod-flexible spacer type thermotropic liquid crystalline polyesters and randomised co-, ter- and tetrapolyesters; (ii) Characterisation of polyesters, co-, ter- and tetrapolyesters for thermal properties using differential scanning calorimetry; (iii) Visual observation of the synthesised polymers for liquid crystalline phase type using hot stage coupled polarising microscopy; (iv) Estimation Degree of crystallinity at room temperature with X-ray diffraction; (v) Inherent and intrinsic viscosities estimations for soluble polyesters and (vi) Crystallisation kinetics of specific polyesters in the isothermal and nonisothermal modes.

Three triad mesogenic diols with ester intramesogenic link were synthesised. The central moiety consisted of hydroquinone or substituted hydroquinone. This was supported on both sides with hydroxy benzoic acid. The syntheses are presented in Sections 2.2.8 to 2.2.10.

The first polyester series consisted of hydroquinone moiety as the central unit of the mesogen. A series of copolyesters were synthesised by coupling the mesogen to aliphatic diacid chlorides having 3, 4, 5, 6, 7, 8 and 10 methylene spacers between the acid chloride groups. The polyesters were synthesised through low temperature solution and interfacial methodologies presented in Sections 2.3.1 and 2.3.2 respectively. Temperatures corresponding to thermal transitions such as crystal-liquid crystal and liquid crystal-isotropisation were estimated in a dynamic mode. The related thermodynamic parameters such as enthalpy and entropy were calculated. The polyesters were evaluated for the phase type (Nematic/Smectic). The transition temperatures,

thermodynamic parameters and phase types were correlated relative to the synthesis methodology and the number of methylene units in the flexible spacer. These results are presented in Section 4.1.

Polyesters constructed from mesogens with unsymmetric nonpolar methyl and polar chloro substituent and aliphatic diacids of varying lengths were then investigated. The specific objective was to determine whether downturn in crystal-liquid crystal and isotropic transitions occur. The relationships of these relative to the structural variables such as spacer length and polarity of the substituent were also investigated. These results are presented in Sections 4.2 and 4.3.

A well documented means to cause a downward shift in the crystal-liquid crystal transition temperature has been structural randomisation through copolymerisation. With this objective, a series of co-, ter- and tetrapolyesters were synthesised from the unsubstituted mesogen and combinations of diacids (odd-odd, even-even methylene units). The thermal behaviour and thermodynamic data were related to structural variables such as length of flexible spacer, mode of randomisation. The results are presented in Section 4.4. Very interesting results emerge, which run counter to the popularly accepted thoughts on this subject.

The inherent high mechanical performance of these systems are harnessed by processing from liquid crystalline melts. Thermal history pathways would dictate the performance. The crystallisation behaviour of polyesters in the isothermal and non-isothermal modes were examined relative to spacer length, liquid crystalline phase type and substitution on the mesogen. Avrami exponents were estimated. Partial Time-Temperature-Transformation profiles were constructed. These results are presented in Section 4.5 and 4.6.

CHAPTER 2

EXPERIMENTAL

EXPERIMENTAL

2.1 REAGENTS AND CHEMICALS

2.1.1 4-Hydroxy benzoic acid

Empirical formula	:	$C_7 H_6 O_3$
Molecular weight	:	138.12
Melting point	:	215-217°C

4-Hydroxy benzoic acid was obtained from M/S Loba Chemie Indo-Austranal Co. [Bombay, India]. It was recrystallised from hot distilled water.

2.1.2 Thionyl chloride

Empirical formula	:	$S O Cl_2$
Molecular weight	:	111.97
Density	:	1.631 gm/mL
Boiling Point	:	79°C

Thionyl chloride was obtained from M/S S.D. Fine Chemicals Pvt. Ltd. [Bombay, India]. This was purified by distillation.

2.1.3 1,4-Benzene diol

Empirical formula	:	$C_6 H_6 O_2$
Molecular weight	:	110.11
Melting point	:	172°C

1,4-Benzene diol [hydroquinone] was obtained from M/S Loba Chemie Indo-Austranal Co. [Bombay, India]. This monomer was recrystallised from acetone and used to synthesise rigid rod trimesogenic diol.

2.1.4 2-Methyl-1,4-benzene diol

Empirical formula	:	C ₇ H ₈ O ₂
Molecular weight	:	124.14
Melting point	:	126-128°C

2-Methyl-1,4-benzene diol [Methyl hydroquinone or toluquinone] obtained from M/S Aldrich Chemical Co. [USA] and was purified by recrystallisation from toluene. This monomer was used to synthesise 1,4-bis-[acetoxy benzoyl oxy]-2-methyl-1,4-benzene [see Section 2.2.9].

2.1.5 2-Chloro-1,4-benzene diol

Empirical formula	:	C ₆ H ₅ Cl O ₂
Molecular weight	:	144.56
Melting point	:	100-102°C

2-Chloro-1,4-benzene diol [chloro hydroquinone] was obtained from M/S Aldrich Chemical Co. [USA]. It was purified by recrystallisation from toluene. This monomer was used for the synthesis of chloro-substituted rigid rod trimesogenic diol [see Section 2.2.10].

2.1.6 Pyridine

Empirical formula	:	C ₅ H ₅ N
Molecular weight	:	79.10
Density	:	0.978 gm/mL
Boiling Point	:	115°C

Pyridine was from M/S S.D. Fine Chemical Pvt. Ltd. [Bombay, India]. It was refluxed over sodium hydroxide pellets and distilled with careful exclusion of moisture. This was used as acid acceptor in the synthesis of polyesters by low temperature solution polymerisation route.

2.1.2 Methanol

Empirical formula	:	$\text{C H}_4 \text{ O}$
Molecular weight	:	32.04
Density	:	0.791 gm/mL
Boiling Point	:	64°C

Commercial grade methanol was distilled as per standard procedure. It was used to isolate polyesters by precipitation.

2.1.2 Toluene

Empirical formula	:	$\text{C}_7 \text{ H}_8$
Molecular weight	:	92.14
Density	:	0.867 gm/mL
Boiling Point	:	110°C

Toluene was obtained from M/S S.D. Fine Chemicals Pvt. Ltd. [Bombay, India] was washed with about fifteen percent of its volume of concentrated sulphuric acid in a stoppered separating funnel. The procedure was repeated till the acid layer was colourless. It was distilled and used for recrystallisation of 2-methyl hydroquinone and 2-chloro hydroquinone.

2.1.9 1,2-Dichloro ethane

Empirical formula	:	$\text{C}_2 \text{ H}_4 \text{ Cl}_2$
Molecular weight	:	98.96
Density	:	1.256 gm/mL
Boiling Point	:	82°C

Commercial grade 1,2-dichloro ethane [DCE] was refluxed over anhydrous phosphorus pentoxide and distilled. DCE was stored over activated 4Å molecular sieves. It was used in the synthesis of rigid rod diols as well as solution and interfacial polyesterifications.

2.1.10 Acetic anhydride

Empirical formula	:	C ₄ H ₆ O ₃
Molecular weight	:	102.09
Density	:	1.082 gm/mL
Boiling Point	:	138-140°C

Acetic anhydride was obtained from M/S S.D. Fine Chemicals Pvt. Ltd. [Bombay, India]. It was purified by distillation and used in the synthesis of 4-acetoxy benzoic acid.

2.1.11 Benzyl triethyl ammonium chloride

Empirical formula	:	C ₁₃ H ₂₂ Cl N
Molecular weight	:	227.78
Melting point	:	185°C [dec.]

Benzyl triethyl ammonium chloride was obtained from Aldrich Chemical Co. [USA]. It was dried in vacuum oven at 80°C for 4 hours. It was used as phase transfer catalyst in the low temperature polyesterifications.

2.1.12 Glutaric acid

Empirical formula	:	C ₅ H ₈ O ₄
Molecular weight	:	132.12
Melting point	:	95-96°C

It was obtained from Aldrich Chemical Co. [USA] and used as received to synthesise glutaryl chloride.

2.1.13 Adipic acid

Empirical formula	:	$C_6 H_{10} O_4$
Molecular weight	:	146.14
Melting point	:	152-154°C

It was obtained from Aldrich Chemical Co. [USA] and used as received to synthesise adipoyl chloride.

2.1.14 Pimelic acid

Empirical formula	:	$C_7 H_{12} O_4$
Molecular weight	:	160.17
Melting point	:	103-105°C

It was obtained from Aldrich Chemical Co. [USA] and used as received to synthesise pimeloyl chloride.

2.1.15 Suberic acid

Empirical formula	:	$C_8 H_{14} O_4$
Molecular weight	:	174.20
Melting point	:	142-144°C

It was obtained from Aldrich Chemical Co. [USA] and used as received to synthesise suberoyl chloride.

2.1.16 Azelaic acid

Empirical formula	:	$C_9 H_{16} O_4$
Molecular weight	:	188.22
Melting point	:	109-111°C

It was obtained from Aldrich Chemical Co. [USA] and used as received to synthesise azeloyl chloride.

2.1.17 Sebacic acid

Empirical formula	:	$C_{10}H_{18}O_4$
Molecular weight	:	202.25
Melting point	:	135-137°C

It was obtained from Aldrich Chemical Co. [USA] and was used as received to synthesise sebacoyl chloride.

2.1.18 1,10-Dodecane dicarboxylic acid

Empirical formula	:	$C_{12}H_{22}O_4$
Molecular weight	:	230.30
Melting point	:	128-130°C

Dodecanedioic acid was obtained from Aldrich Chemical Co. [USA] and was used as received to synthesise 1,10-dodecanedioyl chloride.

2.2 REACTION INTERMEDIATES

2.2.1 Glutaryl chloride

Empirical formula	:	$C_5H_6Cl_2O_2$
Molecular weight	:	169.01
Density	:	1.324 gm/mL
Boiling Point	:	216-218°C

This acid chloride was synthesised by reacting glutaric acid with thionyl chloride under gentle reflux. It was distilled under reduced pressure over nitrogen blanket prior to

use in the synthesis of polyesters and copolyesters with rigid rod trimesogenic diols by low temperature solution and interfacial polyesterifications. General reaction scheme for the synthesis of aliphatic diacid chloride is represented in Figure 18.

2.2.2 Adipoyl chloride

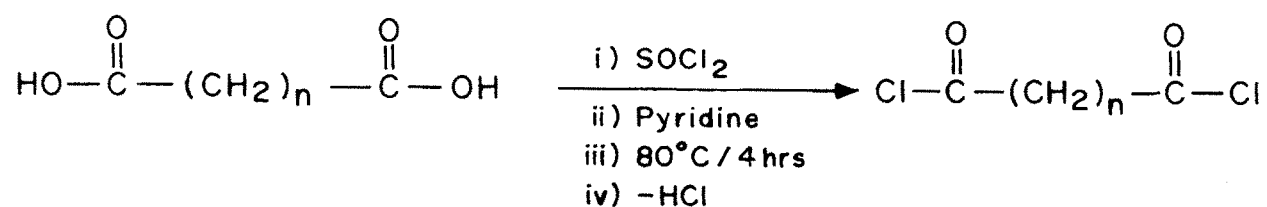
Empirical formula	:	$C_6 H_8 Cl_2 O_2$
Molecular weight	:	183.03
Density	:	1.259 gm/mL
Boiling Point	:	105-107°C/2 torr

Adipoyl chloride was synthesised from adipic acid by refluxing with thionyl chloride. It was purified by distillation under reduced pressure over nitrogen blanket prior to use in the synthesis of polyesters and copolyesters from trimesogenic diols by low temperature solution and interfacial polyesterifications.

2.2.3 Pimeloyl chloride

Empirical formula	:	$C_7 H_{10} Cl_2 O_2$
Molecular weight	:	197.06
Density	:	1.205 gm/mL
Boiling Point	:	113 °C/5 torr

Pimeloyl chloride was synthesised from pimelic acid by refluxing with thionyl chloride. It was purified by distillation under reduced pressure prior to use. This acid chloride was used in the synthesis of polyesters and copolyesters by coupling with trimesogenic diols by low temperature solution and interfacial polyesterifications.



Where, $n = 3$ [Glutaryl chloride]
 $n = 4$ [Adipoyl chloride]
 $n = 5$ [Pimeloyl chloride]
 $n = 6$ [Suberoyl chloride]
 $n = 7$ [Azeloyl chloride]
 $n = 8$ [Sebacoyl chloride] and
 $n = 10$ [Dodecanedioyl chloride]

FIG. 18 GENERAL REACTION SCHEME FOR THE SYNTHESIS OF ALIPHATIC DIACID CHLORIDE.

2.2.4 Suberoyl chloride

Empirical formula	:	$C_8 H_{12} Cl_2 O_2$
Molecular weight	:	211.09
Density	:	1.172 gm/mL
Boiling Point	:	162-163°C/15 torr

Suberoyl chloride was synthesised from suberic acid by refluxing with thionyl chloride. It was purified by distillation under reduced pressure over nitrogen blanket prior to use. This acid chloride was used in the synthesis of polyesters and copolyesters from trimesogenic diols by low temperature solution and interfacial polyesterifications.

2.2.5 Azeloyl chloride

Empirical formula	:	$C_9 H_{14} Cl_2 O_2$
Molecular weight	:	225.12
Density	:	1.143 gm/mL
Boiling Point	:	166°C/18 torr

Azeloyl chloride was synthesised from azelaic acid by refluxing with thionyl chloride. It was purified by distillation under reduced pressure over nitrogen blanket prior to use. This acid chloride was used in the synthesis of polyesters and copolyesters from trimesogenic diols by low temperature solution and interfacial polyesterifications.

2.2.6 Sebacoyl chloride

Empirical formula	:	$C_{10} H_{16} Cl_2 O_2$
Molecular weight	:	239.14
Density	:	1.121 gm/mL
Boiling Point	:	168°C/12 torr

Sebacoyl chloride was synthesised from sebacic acid by refluxing with thionyl chloride. It was purified by distillation under reduced pressure over nitrogen blanket prior to use. This acid chloride was used in the synthesis of polyesters and copolyesters from trimesogenic diols by low temperature solution and interfacial polyesterifications.

2.2.7 1,10-Dodecanedioyl chloride

Empirical formula	:	$C_{12}H_{20}Cl_2O_2$
Molecular weight	:	267.20
Density	:	1.069 gm/mL
Boiling Point	:	140°C/0.5 torr

1,10-Decane dioyl chloride was synthesised from 1,10-decanedicarboxylic acid by refluxing with thionyl chloride. It was purified by distillation under reduced pressure over nitrogen blanket prior to use. It was used in the synthesis of polyesters and copolyesters from trimesogenic diols by low temperature solution and interfacial polyesterifications.

2.2.8 Bis-[4-hydroxy benzoyl oxy]-1,4-benzene [BHBOB]

General reaction scheme for the synthesis of rigid rod diols is presented in Figure 19. The four step synthesis scheme is presented below.

2.2.8.1 4-Acetoxy benzoic acid [4-ACBA]

4-Hydroxy benzoic acid, 13.81 gm [0.1 mole], was taken in a 500 mL beaker. Distilled water, 250 mL, was added and stirred to make an uniform slurry. In another beaker, 4.4 gm of sodium hydroxide [0.11 mole] was dissolved in 50 mL distilled water. This sodium hydroxide solution was added to the slurry and stirred to dissolve 4-hydroxy benzoic acid as the sodium salt. Distilled acetic anhydride, 11 mL [0.11 mole], was then added and stirred for 4 hours at room temperature to obtain a precipitate of 4-acetoxy

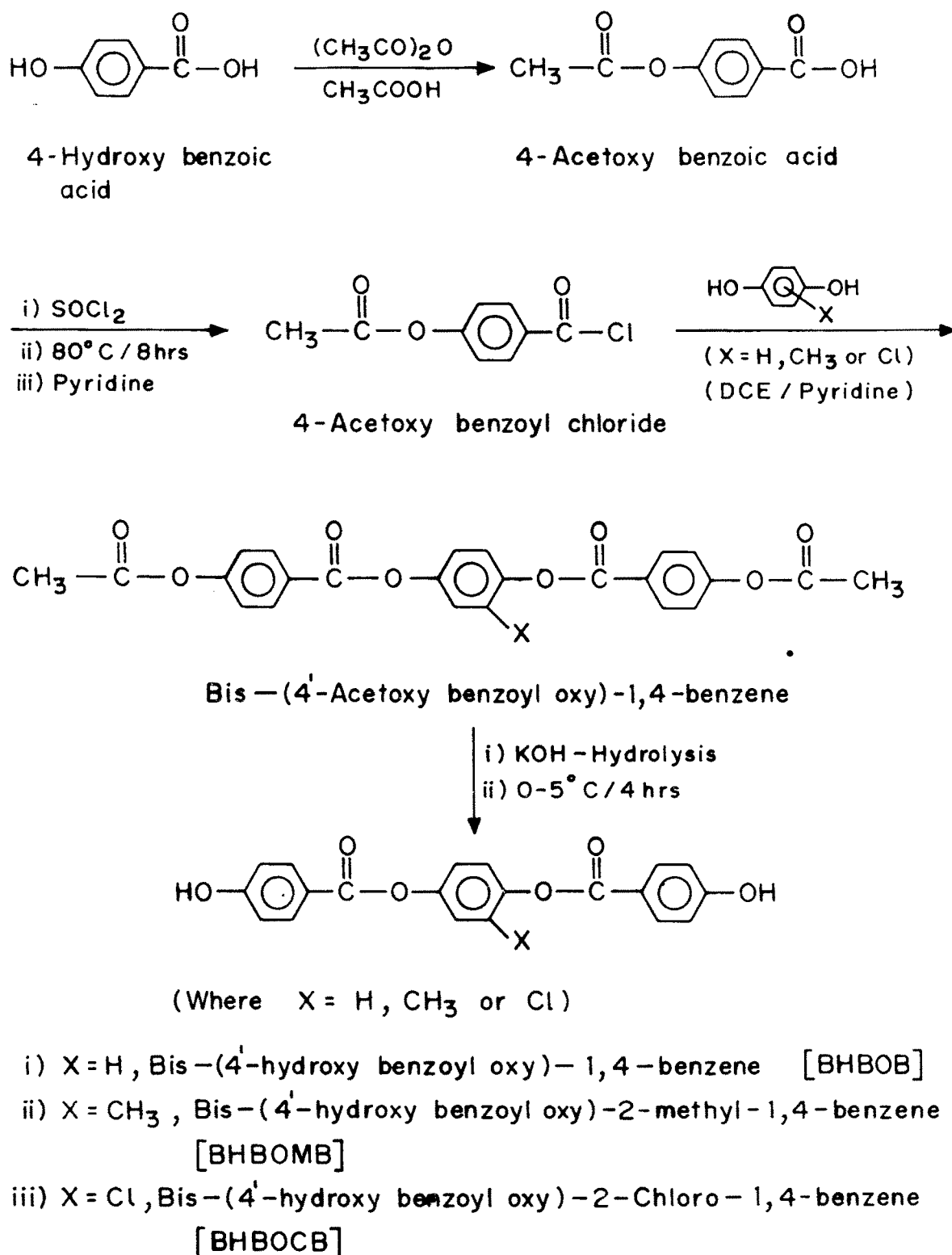


FIG. 19 GENERAL REACTION SCHEME FOR THE SYNTHESIS OF RIGID DIOLS.

benzoic acid. The precipitate was filtered and washed several times with cold dilute hydrochloric acid and distilled water. The crude product was recrystallised from methanol and dried under reduced pressure [1-2 torr] at 80°C for 8 hours. The yield was 75 percent.

Melting point	: 190°C
IR [nujol]	: 1730 cm ⁻¹ [C=O]
¹ H NMR [DMSO-d ₆]	: 8.00 d [d,2H]; 7.30 d [d,2H]; 2.30 d [S,3H] and 10.10 d [S,1H]

2.2.8.2 4-Acetoxy benzoyl chloride

4-Acetoxy benzoic acid, 9.00 gm [0.05 mole], was taken in a single necked 100 mL round bottom flask. Thionyl chloride, 5 mL [0.07 mole] was added dropwise and reaction mixture was refluxed gently for 8 hours. The initially heterogeneous mass homogenised to give a colourless liquid. Excess thionyl chloride was removed by normal distillation. The crude acid chloride was purified by distillation under reduced pressure [1-2 torr] at 130°C. Yield was 90 percent.

Melting point	: 29-30°C
Boiling point	: 132°C
IR [nujol]	: 1780 cm ⁻¹ [COCl]; 1730 cm ⁻¹ [C=O] and 1370 cm ⁻¹ [-CH]
¹ H NMR [CDCl ₃]	: 2.1 d [S,3H]; 7.1 d [d,2H] and 8.0 d [d,2H]

2.2.8.3 Bis-[4-acetoxy benzoyl oxy]-1,4-benzene

A 500 mL three necked round bottom flask was equipped with magnetic stirrer, nitrogen inlet and calcium chloride guard tube. In this reaction flask, 4.4 gm of hydroquinone [0.04 mole], and 25 mL pyridine [0.3 mole] were added and stirred to

dissolve. In another flask, 23.82 gm of 4-acetoxy benzoyl chloride [0.12 mole] and 300 mL of dry 1,2-dichloroethane were taken. The acid chloride solution was added to the hydroquinone solution. This reaction mixture was stirred under nitrogen blanket for 48 hours at room temperature. The reaction mixture was then washed sequentially with 5 percent sodium carbonate solution, 5 percent hydrochloric acid and distilled water. 1,2-Dichloroethane layer was evaporated to dryness on rotavapor. This crude product was recrystallised from chloroform/petroleum ether [60-80] solvent mixture. Filtered the product and dried in vacuum oven at 80°C for 4 hours. Yield was 90 percent.

Melting point	: 186°C
IR [nujol]	: 1730 cm ⁻¹ [C=O]
¹ H NMR [CDCl ₃]	: 2.2 d [S,6H]; 7.1 d [d,8H] and 8.1 d [d,4H]

2.2.8.4 Bis-[4-hydroxy benzoyl oxy]-1,4-benzene [BHBOB]

A single necked 250 mL round bottom flask was equipped with magnetic stirrer and kept in ice bath. In this reaction flask, 1.32 gm of potassium hydroxide [0.02 mole] and 100 mL methanol were taken and stirred up to dissolve. Alcoholic potassium hydroxide solution was cooled to 0-5°C. In reaction flask, 4.34 gm [0.01 mole] of bis-[4-acetoxy benzoyl oxy]-1,4-benzene was added. It was stirred at 0-5°C for 4 hours and then acidified with 4 Normal hydrochloric acid. Methanol was removed under reduced pressure. The crude product was dissolved in 400 mL of ethyl acetate. This solution was washed times with distilled water. Ethyl acetate was distilled off and the solids were extracted with chloroform. Chloroform was distilled off to get purified product. This product was washed with methanol and dried on vacuum oven at 80°C for 4 hours. Yield was 75 percent. The compound was characterised by melting point, IR, NMR and Mass spectra.

Melting point	: 330°C
IR [nujol]	: 3390 cm ⁻¹ [OH] and 1690 cm ⁻¹ [C=O]
¹ H NMR [DMSO-d ₆]	: 10.4 d [s,2H]; 8.0 d [d,4H]; 7.3 d [d,4H] and 6.8 d [d,4H]
M/e	: 350

2.2.9 Bis-[4-hydroxy benzoyl oxy]-2-methyl-1,4-benzene [BHBOMB]

This was synthesised in four steps identical to that presented in Section 2.2.8.1 to 2.2.8.4. The synthesis procedures for 4-Acetoxy benzoic acid, 4-acetoxy benzoyl chloride, bis-[4-acetoxy benzoyl oxy]-2-methyl-1,4-benzene and bis-[4-hydroxy benzoyl oxy]-2-methyl-1,4-benzene were similar and hence not presented. The characterisation of product obtained in the third and fourth steps are presented below.

2.2.9.1 Bis-[4-acetoxy benzoyl oxy]-2-methyl-1,4-benzene

Melting point	: 108°C
IR [nujol]	: 1720 cm ⁻¹ [C=O] and 820 cm ⁻¹ [C-CH ₃]
¹ H NMR [CDCl ₃]	: 2.2 d [s,3H]; 2.3 d [s,6H]; 7.4 d [m,8H] and 8.4 d [dd,3H]

2.2.9.2 Bis-[4-hydroxy benzoyl oxy]-2-methyl-1,4-benzene

Melting point	: 280°C
IR [nujol]	: 3390 cm ⁻¹ [OH]; 1700 cm ⁻¹ [C=O] and 820 cm ⁻¹ [C-CH ₃]
¹ H NMR [DMSO-d ₆]	: 2.2 d [s,3H]; 6.9 d [d,4H]; 7.2 d [s,3H]; 8.0 d [dd,4H] and 10.6 d [s,2H]

2.2.10 Bis-[4-hydroxy benzoyl oxy]-2-chloro-1,4-benzene [BHBOCB]

This was synthesised in four steps identical to that presented in Section 2.2.8.1 to 2.2.8.4. The synthesis procedures for 4-Acetoxy benzoic acid, 4-acetoxy benzoyl chloride, bis-[4-acetoxy benzoyl oxy]-2-chloro-1,4-benzene and bis-[4-hydroxy benzoyl oxy]-2-chloro-1,4-benzene were similar and hence not presented. The characterisation of product obtained in the third and fourth steps are presented below.

2.2.10.1 Bis-[4-acetoxy benzoyl oxy]-2-chloro-1,4-benzene

Melting point	: 181°C
IR [nujol]	: 1740 cm ⁻¹ [C=O] and 760 cm ⁻¹ [C-Cl]
¹ H NMR	: 2.3 d [s,6H]; 7.1 d [m,6H]; 7.3 d [d,1H] and 8.2 d [dd,4H]

2.2.10.2 Bis-[4-hydroxy benzoyl oxy]-2-chloro-1,4-benzene

Melting point	: 296°C
IR [nujol]	: 3400 cm ⁻¹ [OH]; 1760 cm ⁻¹ [C=O] and 740 cm ⁻¹ [C-Cl]
¹ H NMR	: 6.8 d [dd,4H]; 7.3 d [dd,2H]; 7.6 d [d,1H]; 8.0 d [dd,4H] and 10.5 d [s,2H]

2.3 SYNTHESIS OF POLYESTERS

The polyesters were synthesised by low temperature solution and interfacial polycondensation procedures. The standardised solution polycondensation procedure is presented in Section 2.3.1. The procedure adopted for interfacial polycondensation is presented in Section 2.3.2.

2.3.1 Solution Polycondensation

Three necked 250 mL round bottom flask was equipped with magnetic stirrer, nitrogen inlet, and calcium chloride guard tube. Into this reaction flask, 0.004 mole of diols, synthesised as per Sections 2.2.10 to 2.2.12, 0.2 mole [16 mL] of pyridine were taken and stirred to dissolve. In another stoppered flask 0.004 mole of diacid chloride and 25 mL of dry 1,2-dichloroethane were taken. [General reaction scheme for the synthesis of aliphatic diacid chlorides is presented in Fig. 19]. The mixture was stirred at room temperature for 48 hours under nitrogen flow. The reaction mixture was then heated at 60°C for 4 hours with stirring under nitrogen. The reaction mixture was poured into 500 mL methanol to precipitate the polyester. The polyester was filtered and washed with 5 weight percent sodium carbonate solution, 5 percent hydrochloric acid, water and methanol respectively. It was dried under reduced pressure for 4 hours at 80°C. The polyesters and copolyesters synthesised are presented in the results and discussion sections (Chapter 4.1 and 4.2) under specific systems. General reaction scheme for the synthesis of polyesters and copolyesters is represented in Figure 20.

2.3.2 Interfacial Polyesterification

Two necked 100 mL baffled round bottom flask was equipped with mechanical stirrer, dropping funnel and set on ice-bath. In this reaction flask, 0.004 mole of representative unsubstituted or substituted mesogenic diol and 0.008 mole of sodium hydroxide solution were taken and stirred to dissolve. 0.02 gm [0.0001 mole] of benzyl triethyl chloride was added and stirred for 2 minutes. In another stoppered flask, 0.004 mole of acid chloride and 10 mL of dry 1,2-dichloro ethane were taken. The acid chloride solution was added to the solution of mesogenic diol. The reaction mixture was very vigorously stirred [6000-7000 RPM] for 30 minutes at 0-5°C. The polyester or copolyester formed was precipitated by the addition of methanol and filtered. The

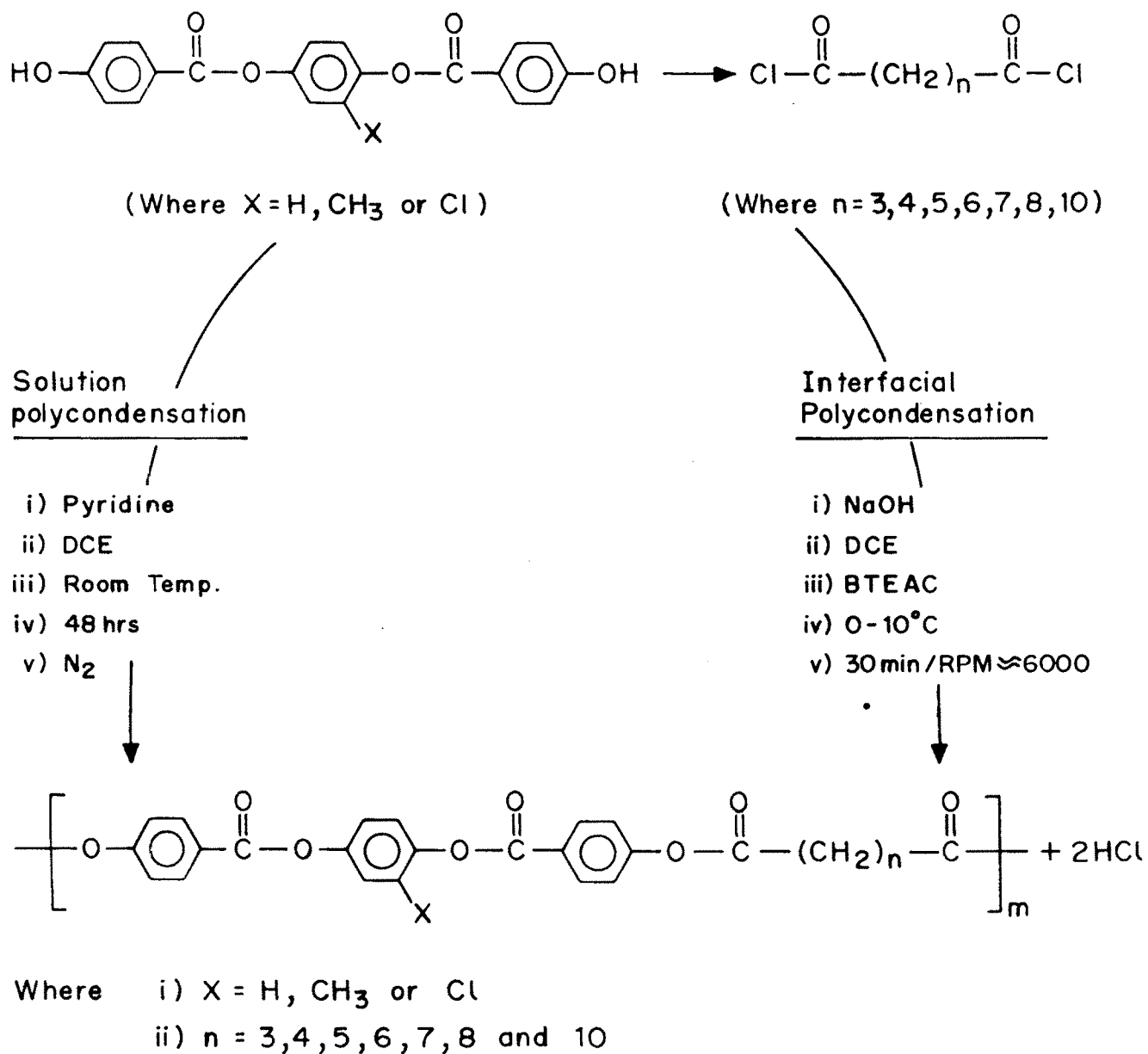


FIG. 20 GENERAL REACTION SCHEME FOR THE SYNTHESIS OF POLYESTERS.

polymer was washed with 5 weight percent sodium carbonate solution, 5 percent hydrochloric acid, water and methanol respectively. It was dried under reduced pressure for 4 hours at 80°C. The synthesis details, such as specific systems and their composition, are presented in the results and discussion sections in Chapter 4.

TABLE - 9

Synthesis of polyesters of Bis-[4-hydroxy benzoyl oxy]-1,4-benzene [BHBOB] (unsubstituted trimesogenic Diol) and aliphatic diacid chlorides, with odd and even number of methylene units, by solution polycondensation.

CODE	BHBOB		ALIPHATIC DIACID CHLORIDE			POLYESTER
	No.	[mole]	[gm]	[name]	[mole]	[gm]
PE-7	0.04	1.4012	Glutaryl	0.04	0.6760	446.39
PE-1	0.04	1.4012	Adipoyl	0.04	0.7321	460.41
PE-6	0.04	1.4012	Pimeloyl	0.04	0.7882	474.44
PE-2	0.04	1.4012	Suberoyl	0.04	0.8443	488.46
PE-3	0.04	1.4012	Azeloyl	0.04	0.9004	502.49
PE-4	0.04	1.4012	Sebacoyl	0.04	0.9565	516.52
PE-5	0.04	1.4012	Dodecane	0.04	1.0687	544.57

^a = m/ru = mole per repeat unit

TABLE - 10

Synthesis of copolyesters of differing compositions from Bis-[4-hydroxy benzoyl oxy]-1,4-benzene^a [BHBOB] (unsubstituted trimesogenic Diol) and two aliphatic diacid chlorides, with even number of methylene units, by solution polycondensation.

CODE	ALIPHATIC DIACID CHLORIDES						COPOLY-ESTER
	No.	[name]	[mole]	[gm]	[name]	[mole]	
PE-15	Adipoyl	0.001	0.1830	Suberoyl	0.003	0.6332	481.45
PE-9	Adipoyl	0.002	0.3661	Suberoyl	0.002	0.4222	474.44
PE-16	Adipoyl	0.003	0.5491	Suberoyl	0.001	0.2111	467.43
PE-17	Adipoyl	0.001	0.1830	Sebacoyl	0.003	0.7174	502.49
PE-10	Adipoyl	0.002	0.3661	Sebacoyl	0.002	0.4783	488.46
PE-18	Adipoyl	0.003	0.5491	Sebacoyl	0.001	0.2391	474.44
PE-19	Adipoyl	0.001	0.1830	Dodecane	0.003	0.8015	523.53
PE-11	Adipoyl	0.002	0.3661	Dodecane	0.002	0.5344	502.49
PE-20	Adipoyl	0.003	0.5491	Dodecane	0.001	0.2672	481.45
PE-21	Suberoyl	0.001	0.2111	Sebacoyl	0.003	0.7174	509.50
PE-12	Suberoyl	0.002	0.4222	Sebacoyl	0.002	0.4783	502.49
PE-22	Suberoyl	0.003	0.6332	Sebacoyl	0.001	0.2391	495.48
PE-23	Suberoyl	0.001	0.2111	Dodecane	0.003	0.8015	530.54
PE-13	Suberoyl	0.002	0.4222	Dodecane	0.002	0.5344	516.52
PE-24	Suberoyl	0.003	0.6332	Dodecane	0.001	0.2672	502.49
PE-25	Sebacoyl	0.001	0.2391	Dodecane	0.003	0.8015	537.56
PE-14	Sebacoyl	0.002	0.4783	Dodecane	0.002	0.5344	530.54
PE-26	Sebacoyl	0.003	0.7174	Dodecane	0.001	0.2672	523.53

^a = 0.04 mole (1.4012 gm) of Bis-[4-hydroxy benzoyl oxy]-1,4-benzene [BHBOB] (Trimesogenic Diol) in all copolyesterifications.

^b = m/ru = mole per repeat unit

TABLE - 11

Synthesis of copolyesters from Bis-[4-hydroxy benzoyl oxy]-1,4-benzene^a [BHBOB] (unsubstituted trimesogenic Diol) and three different aliphatic diacid chlorides, with even number of methylene units, by solution polycondensation.

CODE No.	ALIPHATIC DIACID CHLORIDES						COPOLY- ESTER [m/ru] ^b
	[name] (mole)	[mass] (gm)	[name] (mole)	[mass] (gm)	[name] (mole)	[mass] (gm)	
PE-27	Adipoyl (0.0013)	0.2440	Suberoyl (0.0013)	0.2812	Sebacoyl (0.0013)	0.3188	488.46
PE-28	Adipoyl (0.0013)	0.2440	Suberoyl (0.0013)	0.2812	Dodecane (0.0013)	0.3562	497.82
PE-29	Adipoyl (0.0013)	0.2440	Sebacoyl (0.0013)	0.3188	Dodecane (0.0013)	0.3562	507.17
PE-30	Suberoyl (0.0013)	0.2812	Sebacoyl (0.0013)	0.3188	Dodecane (0.0013)	0.3562	516.52

a = 0.04 mole (1.4012 gm) of Bis-[4-hydroxy benzoyl oxy]-1,4-benzene [BHBOB] (Trimesogenic Diol) in all copolyesterifications.

b = m/ru = mole per repeat unit

TABLE - 12

Synthesis of copolyester from Bis-[4-hydroxy benzoyl oxy]-1,4-benzene [BHBOB] (unsubstituted trimesogenic Diol) and four aliphatic diacid chlorides, with even number of methylene units, by solution polycondensation.

CODE No.	BHBOB		ALIPHATIC DIACID CHLORIDES			POLYESTER [m/ru] ^b
	[mole]	[gm]	[name]	[mole]	[gm]	
PE-31	0.04	1.4012	Adipoyl	0.01	0.1830	502.49
			Suberoyl	0.01	0.2111	
			Sebacoyl	0.01	0.2391	
			Dodecane	0.01	0.2672	

TABLE - 13

Synthesis of copolyesters of Bis-[4-hydroxy benzoyl oxy]-1,4-benzene^a [BHBOB] (unsubstituted trimesogenic Diol) and two different aliphatic diacid chlorides, with odd number of methylene units, by solution polycondensation.

CODE No.	ALIPHATIC DIACID CHLORIDES						COPOLY- ESTER [m/ru] ^b
	[name]	[mole]	[gm]	[name]	[mole]	[gm]	
PE-35	Glutaryl	0.002	0.3380	Azeloyle	0.002	0.4502	474.44
PE-36	Glutaryl	0.001	0.1690	Azeloyle	0.003	0.6753	488.46
PE-51	Glutaryl	0.002	0.3380	Pimeloyle	0.002	0.3941	460.41
PE-52	Pimeloyle	0.002	0.3941	Azeloyle	0.002	0.4502	488.46

^a = 0.04 mole (1.4012 gm) of Bis-[4-hydroxy benzoyl oxy]-1,4-benzene [BHBOB] (Trimesogenic Diol) in all copolyesterifications.

^b = m/ru = mole per repeat unit

TABLE - 14

Synthesis of polyesters with Bis-[4-hydroxy benzoyl oxy]-1,4-benzene [BHBOB] (unsubstituted trimesogenic Diol) and aliphatic diacid chlorides, with odd and even number of methylene units, by interfacial polycondensation.

CODE No.	BHBOB		ALIPHATIC DIACID CHLORIDE			POLYESTER [m/ru] ^a
	[mole]	[gm]	[name]	[mole]	[gm]	
PE-201	0.04	1.4012	Glutaryl	0.04	0.6760	446.39
PE-202	0.04	1.4012	Adipoyl	0.04	0.7321	460.41
PE-203	0.04	1.4012	Pimeloyl	0.04	0.7882	474.44
PE-204	0.04	1.4012	Suberoyl	0.04	0.8443	488.46
PE-205	0.04	1.4012	Azeloyl	0.04	0.9004	502.49
PE-206	0.04	1.4012	Sebacoyl	0.04	0.9565	516.52
PE-207	0.04	1.4012	Dodecane	0.04	1.0687	544.57

^a = m/ru = mole per repeat unit

TABLE - 15

Synthesis of polyesters with Bis-[4-hydroxy benzoyl oxy]-2-methyl-1,4-benzene [BHBOMB] (methyl substituted trimesogenic Diol) and aliphatic diacid chlorides, with odd and even number of methylene units, by interfacial polycondensation.

CODE	BHBOMB		ALIPHATIC DIACID CHLORIDE			POLYESTER
	No.	[mole]	[gm]	[name]	[mole]	[gm]
PE-101	0.04	1.4573	Glutaryl	0.04	0.6760	460.41
PE-102	0.04	1.4573	Adipoyl	0.04	0.7321	474.44
PE-103	0.04	1.4573	Pimeloyl	0.04	0.7882	488.46
PE-104	0.04	1.4573	Suberoyl	0.04	0.8443	502.49
PE-105	0.04	1.4573	Azeloyl	0.04	0.9004	516.52
PE-106	0.04	1.4573	Sebacoyl	0.04	0.9565	530.54
PE-107	0.04	1.4573	Dodecane	0.04	1.0687	558.59

^a = m/ru = mole per repeat unit

TABLE - 16

Synthesis of polyesters from Bis-[4-hydroxy benzoyl oxy]-2-chloro-1,4-benzene [BHBOCB] (chloro substituted trimesogenic Diol) and aliphatic diacid chlorides, with odd and even number of methylene units, by interfacial polycondensation.

CODE	BHBOCB		ALIPHATIC DIACID CHLORIDE			POLYESTER
	No.	[mole]	[gm]	[name]	[mole]	
PE-301	0.04	1.5390	Glutaryl	0.04	0.6760	480.83
PE-302	0.04	1.5390	Adipoyl	0.04	0.7321	494.86
PE-303	0.04	1.5390	Pimeloyl	0.04	0.7882	508.88
PE-304	0.04	1.5390	Suberoyl	0.04	0.8443	522.91
PE-305	0.04	1.5390	Azeloyl	0.04	0.9004	536.94
PE-306	0.04	1.5390	Sebacoyl	0.04	0.9565	550.96
PE-307	0.04	1.5390	Dodecane	0.04	1.0687	579.01

^a = m/ru = mole per repeat unit

CHAPTER 3

PHYSICO-CHEMICAL CHARACTERISATIONS

PHYSICO-CHEMICAL CHARACTERISATIONS

The techniques used frequently in the physico-chemical characterisation of liquid-crystalline polymers may be grouped as under: (1) Morphology, (2) Polarising microscopy, (3) X-ray diffractometry and (4) Thermal analysis.

3.1 MORPHOLOGICAL CHARACTERISATION

Polymer morphology pertains to the study of the arrangement into crystalline and amorphous domains as well as form, structure and organisation of the domains. Morphology of liquid crystalline materials is dependent on thermal history, chemical and physical characteristics as well as processing conditions. Optical microscopy, x-ray diffractometry, birefringence are used to elucidate the morphology. Two techniques used in present investigation, namely optical microscopy and x-ray diffractometry, are discussed below.

Microscopy is the study of fine structure. The study of materials with optical microscopy is well documented.¹⁴⁰⁻¹⁴⁹

3.1.1 Polarising Microscopy

Study of microstructure through interaction of matter with polarised light¹⁵⁰⁻¹⁵³ is widely applied to polymers and liquid crystals.¹⁵³ The common arrangement in polarising microscope is crossed polarisers, with the reaction of polarisers perpendicular to each other, so that field of view will be dark for an isotropic specimen.

Optically anisotropic materials like polymeric liquid crystals appear bright between crossed polarisers. These materials split the light passing through into two plane polarised waves vibrating in planes normal to each other. The transmitted waves have different refractive indices [n_1 and n_2] and velocities. The difference between

the two refractive indices, $\Delta n = [n_1 - n_2]$, is the birefringence. Birefringence is due to the alignment of optical anisotropic elements. Hence, liquid crystallinity can be identified by observing birefringence pattern in the partially ordered liquid crystalline fluid phases between crossed polars. The biphasic [crystalline and isotropic] nature of such materials generate different characteristic liquid crystalline textures.

Birefringence gives a qualitative estimate of the molecular organisation in a specimen which may appear bright coloured under crossed polars. The colour [interference] pattern depends on the retardation, Δn , at constant sample thickness. Polarising microscopy technique is also useful in the determination of thermotropic liquid crystalline phase transition temperatures. The sample, on heating in a programmed manner, displays anisotropic fluidity at a specific temperature and forms characteristic textures. These specific temperatures, termed as crystal-mesophase transition temperatures, are further classified as crystal-smectic, crystal-nematic and crystal-cholesteric transition temperatures on the basis of textures observed under crossed polars. The formation of easily identifiable texture are difficult in polymeric liquid crystals due to high melt viscosities, which retard the molecular alignment process. The change in textures are seen as fronts passing slowly across the field of view. The exact transition temperature from crystalline solid to the mesophasic state are difficult to detect precisely, when the liquid crystalline textures closely resemble those of crystalline solids. The change from mesophase to the isotropic liquid can be very clearly observed since birefringent mesophase textures darken on isotropisation.

A few polymer particles were placed between a glass slide and a glass cover slip. The specimen was heated at a programmed rate using a Koffler hot stage mounted on a polarising microscope. The optical characteristic of the sample were monitored

visually. The temperature at which the sharp crystalline edges tended to shrink and round off while retaining optical anisotropy, under crossed polarised light, was recorded as the liquid crystalline phase transition temperature.

It is important to note that birefringence is an optical property of a representative volume of the polymer, with dimensions at least equaling those of the wave length of light. It is not a molecular property but is proportional to order parameter S. It is not only a measure of orientation but also the constant of proportionality which is not easily determined. In general, the textures exhibited by polymers are identical to those of low molecular weight analogs. Nematic phases exhibit threaded schlieren textures while fan shaped or focal conic textures are typical of smectics. Cholesteric phases show "oily streaks" and parallel disclinations.⁴

3.1.2 X-ray Diffractometry

X-ray diffraction of polymers is reviewed extensively.¹⁵⁴⁻¹⁶³ X-ray diffraction studies are useful in determining the percentage of crystalline and amorphous regions in semicrystalline polymers. Systematic study of the X-ray crystallography of model compounds are necessary to arrive at the crystal structure of the polymer. Selection of model compounds should be on the basis of structure of the repeating unit of polymer chain. Liquid crystalline polymers display crystalline order and the increase in crystallinity generates denser, stiffer and solvent resistant materials.

X-ray diffraction follows Bragg's law given by:

$$n\lambda = 2 d_{hkl} \sin \theta \quad [2]$$

Where λ = wavelength of x-ray diffraction, θ = angle of scattering, d_{hkl} = the spacing between the planes that cause diffraction and n = diffraction order.

X-ray of wavelength 1.542 \AA is suitable for the diffraction studies of organic polymers.¹⁵⁴ This is achieved by the electron bombardment of a copper target in an evacuated tube and the filtration of generated X-ray using a Nickel filter. Generally, the wavelength is held constant and 2θ is varied. The X-ray scans are obtained as a plot of 2θ versus scattered intensity. The intensities are obtained from X-ray counters. The polymer could be in the form of powder, film or fibre. The diffraction could either be amplified and recorded by electron X-ray detectors or be photographed. A typical X-ray diffraction scan indicating crystalline and amorphous scattering is represented in Figure 21.

Several techniques are used to calculate the degree of crystallinity or crystallinity index. The most extensively employed method is the measurement of areas under crystalline and amorphous regions in a X-ray diffraction scan. The degree of crystallinity is calculated from the equation:

$$C_i = [A_c] / [A_c] + [A_a] \quad [3]$$

Where, C_i = degree of crystallinity, A_c = area of crystalline phase and A_a = area of amorphous phase.

Peak integration method can be also be used to evaluate the crystallinity index. The d spacings between different planes are calculated using the relation:

$$d = n \lambda / [2 \sin \theta] \quad [4]$$

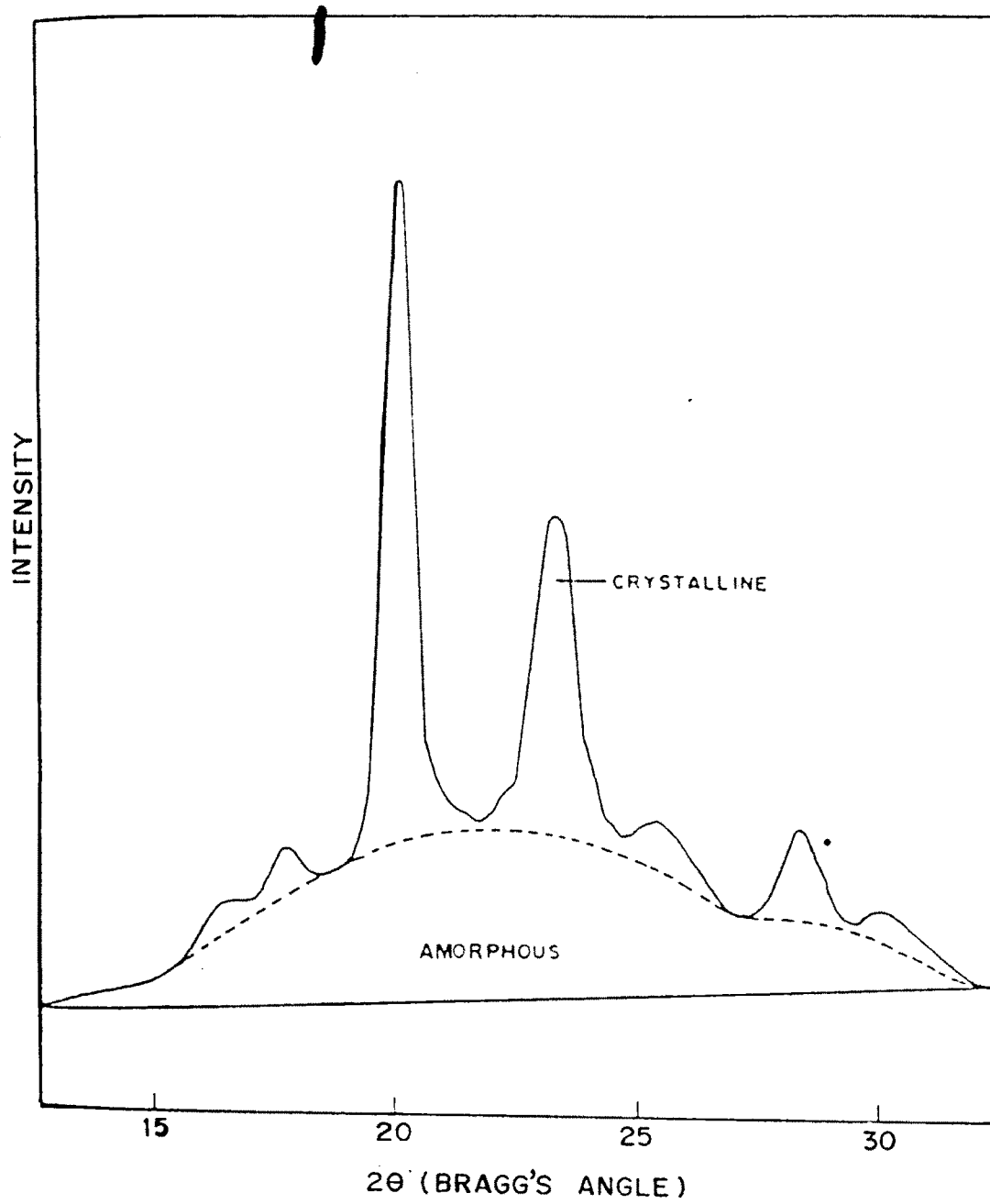


FIG. 21 A TYPICAL X-RAY DIFFRACTION PATTERN.

Where, $\lambda = 1.542 \text{ \AA}$ [Cu K] and $\theta =$ half angle of the Bragg's angle $[2\theta]$.

The wide angle X-ray scattering of copolyesters synthesised in this investigation, in the precipitated state, were obtained at room temperature at a rate of 2000 counts per second [cps] between range of 5 to 40° , on a Philips 1730 X-ray diffractometer using Cu K target and nickel filter. Copolyesters used for the study were in powder form. The crystallinity index was computed.

3.2 THERMAL CHARACTERISATION

Important thermal analysis techniques include thermogravimetric analysis [TGA], differential thermal analysis [DTA], and differential scanning calorimetry [DSC]. The characteristic parameters evaluated in the thermal analysis are: (1) the glass transition temperature, (2) the crystalline melting point for crystalline polymers, (3) phase transition temperature in liquid crystals, (4) thermal stability of polymers and (5) rate of growth of crystals.

3.2.1 Differential Scanning Calorimetry

Differential scanning calorimetry [DSC] is used for the quantitative estimation of: (1) temperatures, enthalpy and entropy changes accompanying first order transitions akin to melting and crystallisation, (2) glass transition temperature $[T_g]$, (3) specific heat change at glass transition, (4) curing as well as (5) kinetics of crystallisation of thermoplastic melt under isothermal/non-isothermal conditions [physical process] and of curing of a thermosetting resins [chemical reaction]. In general, it is not suitable for studying decomposition reactions.

Commercially available DSC units are either power compensation or heat flux type. In power compensation DSC [Perkin-Elmer], the correcting differential electric power required to zero any temperature difference between sample and reference empty crucible, during a thermodynamic transition or a chemical reaction, is measured directly in mW or m cal/sec. as a function of either temperature [non-isothermal] or time [isothermal]. In heat flux DSC [Mettler] the temperature between a sample and a reference is measured as a differential voltage which is then converted by a thermal analysis processor to the actual heat flow.

3.2.2 Transitions in LCPs.

DSC is used extensively in the study of thermotropic LCPs. The technique reveals transition temperatures and gives a measure of thermodynamic parameters of transitions [ΔH and ΔS]. The two limiting states between which liquid crystalline fluid phases can be formed is presented in Figure 22. The first [low-temperature] limiting state is either fully ordered crystal with long three-dimensional order (in crystalline polymers), or glassy state (in amorphous polymers). The second limiting state is completely amorphous isotropic liquid, with only short range order. On heating from a crystalline solid state, liquid crystals lose positional and perhaps conformational order and gain molecular or conformational mobility at the melting temperatures. The crystal to liquid crystal and liquid crystal to isotropic phase transitions are all thermodynamic first order transitions.

The melting process can be approximately characterized by the overall increase in entropy on fusion ΔS_f .¹⁶⁴ Here,

$$\Delta S_f = \Delta S_{\text{positional}} + \Delta S_{\text{orientational}} + \Delta S_{\text{conformational}} \quad [5]$$

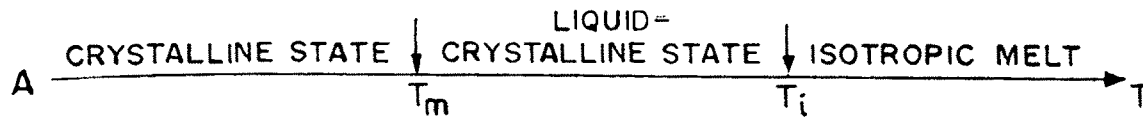
In contrast, the transition is characterised by similar gain in molecular or conformational mobility, observable as increase in heat capacity, without any change in order or entropy.

The melting temperatures of LCPs are markedly affected by the thermal history of the sample [no crystallinity effect]^{49,165} as shown in Figure 23. Thermal treatment alters the size, amount of crystallites and degree of crystal perfection.⁴⁹ The crystalline regions in macromolecules are only 2-10 nm in one dimension. LC domains are much bigger. Frequently, the melting peaks in the DSC thermograms, as shown in Figure 24, are "structured".⁴⁹ The reasons for structuring are: (1) polymorphism in the solid state [solid-solid transitions], (2) successive meltings and recrystallisations of imperfect crystalline regions. Sometimes complex structuring interferes with the interpretation of DSC thermogram.¹⁶⁶ The existence of multiple mesophases in the melt results in two or more LC transitions. In wholly or highly aromatic LCPs complications arise in measurements, since isotropisation at high temperature is followed by decomposition in rapid succession.

The transition to the isotropic phase is largely governed by entropy. It is often close to an equilibrium process¹⁶⁷ as the extent of supercooling is small. Liquid crystalline behaviour is observed in rod or disc shaped molecules. Assuming the rules of Richards¹⁶⁷ and Walden,¹⁶⁸ the entropy of isotropisation may be computed in the range of 15-50 J/[K][mole]. The Figure 24 corresponds to the contribution of molecular size-dependant orientational entropy. Generally, entropy of isotropisation is much smaller. Thus, orientational order is very imperfect on liquid crystalline state.

Wunderlich and Grebowicz¹⁶⁷ compiled data on the transition parameters for a variety liquid crystalline polymers. The magnitudes of ΔS_i , through small, were much

CRYSTALLISABLE POLYMERS



NONCRYSTALLISABLE POLYMERS

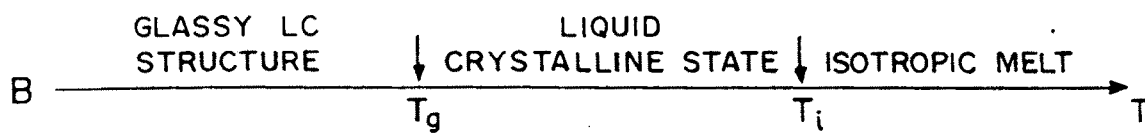


FIG. 22 THERMAL TRANSITION BEHAVIOUR IN LCPS.

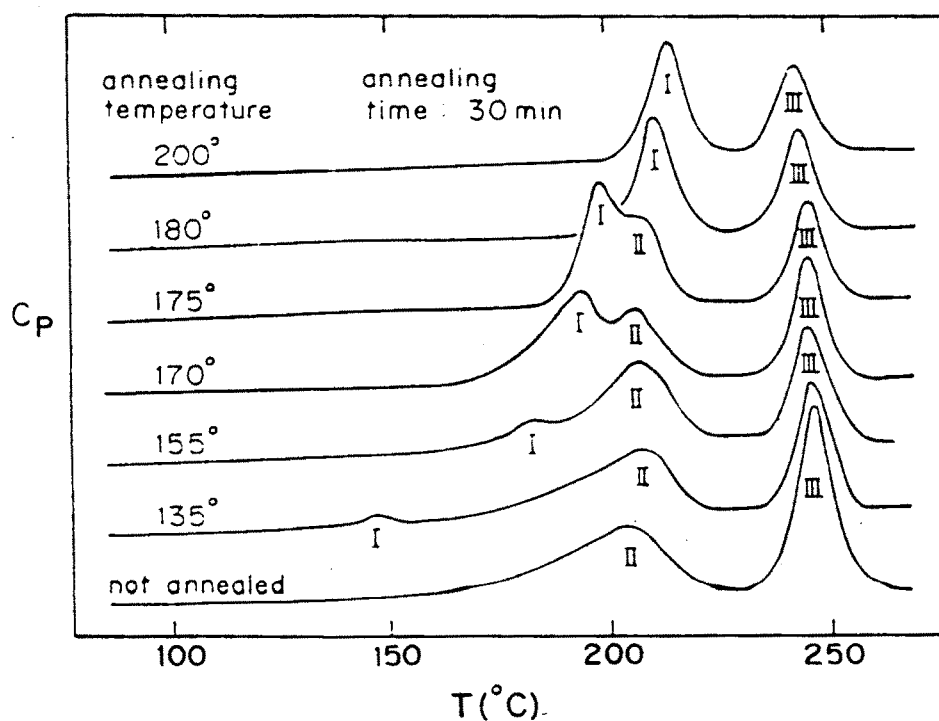


FIG. 23 DSC THERMOGRAMS FOR A PET/30 HBA COPOLYESTER SHOWING THE INFLUENCE OF THERMAL HISTORY ON THE PHASE BEHAVIOUR.

larger than those noted for low molecular weight nematic liquid crystals. Thus, polymeric mesophases are more ordered. A possible explanation proposed is that this results from the mixing between the spacer and mesogenic groups.

An odd-even effect in the entropy of isotropisation is observed with in a homologous series of thermotropic rigid rod-flexible spacer type polymers.¹⁶⁹⁻¹⁷¹ Polymers with even number of atoms in the spacer have higher values ΔS_i than those with odd number of atoms as seen in Figure 25. Similar markedly odd-even alternation have been observed in melting and marginally in isotropic transition temperatures. The spacer type greatly influences ΔS_i which is otherwise insensitive to the type of mesophase.⁴⁹ It is in the range 2-20 J/[K][mole] for polymethylene spacers but is only 1-5 J/[K][mole] for more polar polyoxyethylene spacers, regardless of the mesophase present.¹⁷² In some polymers, with increase in spacer length considerable increase in ΔS_i have been observed without any discernable odd-even effect.¹²² In the nematic state the flexible spacer in these systems is probably in an extended configuration. Such odd-even effects, known for low molecular mass LCs, are rationalised in terms of packing regularity in the crystal lattice. In LCPs, the odd-even effects have been theoretically interpellated in terms of orientational correlation of mesogens.¹¹⁵ In polyesters, with even number of spacer atoms, colinear alignment of mesogen in the nematic phase is one of lowest energy, suggesting a higher nematic order. In systems with odd number of atoms in the spacer, the energy of colinear alignment is higher than that of antiparallel orientation, with inclinations of mesogen exceeding 160 degree. Therefore, low nematic order results. The model predicts that orientational distributions of mesogens would be unaltered by the direction of the ester linkages attached to the flexible spacer.

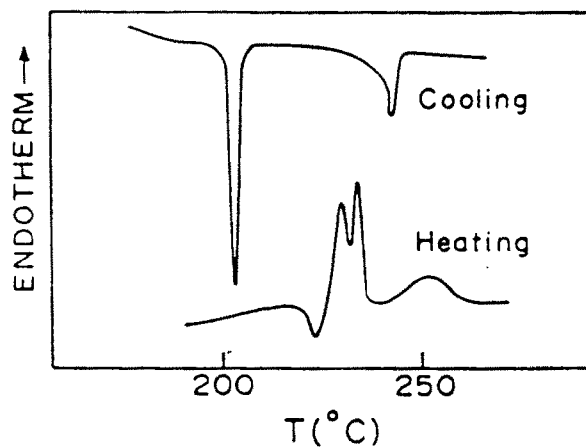


FIG. 24 DSC THERMOGRAM OF A SEMIFLEXIBLE LCP SHOWING PEAK STRUCTURING.

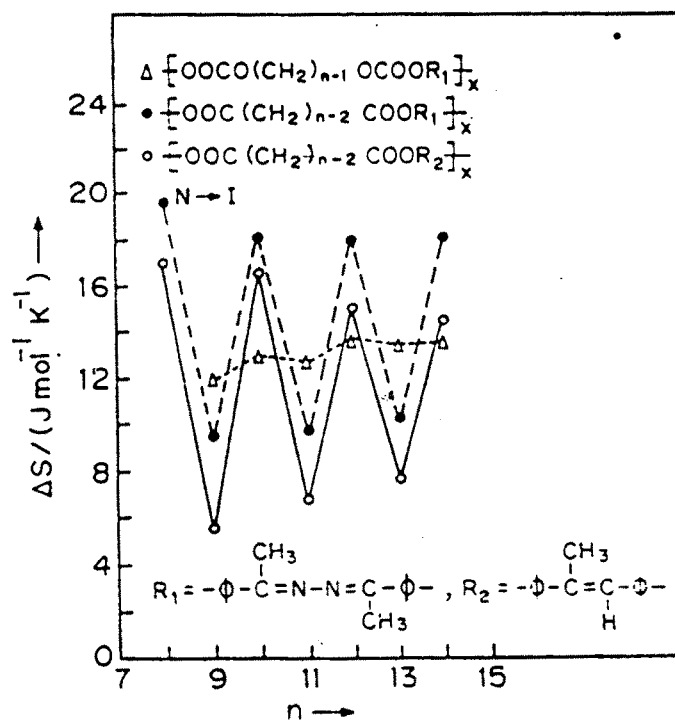


FIG. 25 ODD-EVEN RELATIONSHIP FOR ISOTROPIC TRANSITIONAL ENTROPY IN SOME SEMIFLEXIBLE LCPs.

However, experimentally it is observed that mesophases with -COO-R-O-CO- linkages are less stable compared to -O-CO-R-COO-, wherein -R- is the flexible spacer.⁸⁵ Yoon and Bruckner¹⁷³ developed a theoretical framework to predict the mesophase stability behaviour on the basis of conformational energies of spacers and distributions of chain extensions. The approach provides a firm theoretical basis for predicting mesophase stability. The calculated transitional entropies seem to agree with experimental results.¹⁷⁴ In odd-even case, the theory needs some refinements to improve the accuracy of calculations.

The isotropisation enthalpy in LCs is much smaller [3-5 percent] than the enthalpy of melting.¹⁶⁹ The specific volumes of LCs and isotropic liquids are similar. Thus, molecular interactions are predominantly altered during crystal to liquid crystal transitions. In LCPs, incomplete crystallinity in the solid state, melt history and mesogen type lead to similar enthalpies of melting and isotropisation.¹⁷⁵

In LCPs, melting and isotropisation temperatures increase with molecular weight and reach a plateau at high molecular weight.¹⁷⁶ The molecular weight dependence of isotropisation temperature is greater, as compared to crystal-liquid crystal transition.¹⁷⁷ Discrepancy in transition temperature reported for similar compositions¹⁷⁸ arise from differences in molecular weight and/or non uniform sequence distributions [heterogeneity].

The crystal to liquid transition in semi-flexible LCPs have not been investigated in detail.¹⁶⁷ The enthalpies of crystal to liquid crystal transitions of LCPs are much lower than melt enthalpies in typical polyesters, even when normalised to 100 percent crystallinity.¹⁷⁹ This is due to crystal imperfections. The flexible spacers are poorly organised in the crystal to accommodate the relatively large and rigid mesogenic units.

The crystal to liquid crystal transition involves more of mesogenic segments.¹⁸⁰ The conformational motion in the spacer induces mobility in the mesogens of rigid rod-flexible spacer type liquid crystalline polymers. The glass transition temperature [T_g] is independent of molecular weight. Thus, the T_g increases on shortening of flexible spacer length and polymer show more proclivity towards the formation of lyotropic mesophases. It is generally difficult to quench isotropic melt of LCPs directly to an amorphous glass.¹⁶⁷ Extraordinary quenching techniques may be necessary to baffle the strong drive to equilibrium. However, on heating above T_g , the unstable amorphous solid easily transforms back to mesophase.¹⁸¹ Thus, the flexible spacer greatly influences the thermal and thermodynamic properties of LCPs. It plays a vital role in determining the manner of organisation, degree of cooperativity and the order in the crystalline and liquid crystalline state.

3.2.3 Solidification Processes

During cooling, polymer melt is transferred into solid material. The manner in which solidification may occur is by: (1) Crystallisation, (2) Vitrification.

Crystallisation is the favoured mode of solidification in nature. Many low molecular weight substances like water, mercury, benzene, waxes, copper, citric acid solidify by crystallisation. The atoms in a crystalline solids are arranged in a regular three dimensional array. The repeating units in linear polymers crystallise under suitable conditions into arrangements describable by the crystallographic lattices. Polyethylene is orthorhombic. Isotactic polypropylene is monoclinic and nylon-66 is triclinic.

The large aspect ratio in polymers decreases the rate of crystallisation. Crystallinity varies from 30-90 percent and is never complete.^{182,183} It occurs in two steps involving nucleation followed by crystal growth.¹⁸³ The nucleation of newly formed grains of the solid phase is almost exclusively heterogeneous. Nuclei arising from crystalline catalyst residues are present in the quiescent polymer melts.¹⁸⁴ Sufficient supercooling of melt would lead to thermal or spontaneous nucleation. The number of potential nucleation sites change with time in thermal nucleation. In spontaneous nucleation these do not change with time. The crystal nuclei become active over a narrow time on attaining the crystallisation temperature. The growing morphological unit is a complex entity. The growth kinetics is limited either by the rate of incorporation of molecules in to the developing crystalline phase or by the diffusional transport velocity of the molecules towards the melt-crystal interface. In most cases, the experimental situation is complicated by additional phenomena such as incubation/induction and secondary growth. In a crystal growth process an initial induction [incubation] period, more apparent than real, is followed by accelerated crystallisation. Then a delayed process of crystallisation, called secondary crystallisation, occurs till a pseudo-equilibrium level of crystallinity is reached. The rate of change of crystallinity is extremely small during this secondary growth. Complete crystallinity is, therefore, never accomplished. The level reached is dependent on molecular weight. However, the same value of crystallinity is attained after sufficient lapse in time.

The process of vitrification involves solidification without crystallisation. In thermoplastics, vitrification is observed on rapid cooling of polymer melt. This effectively prevents nucleation and crystal growth. The free volume reduces as temperature drops, while the viscosity increases. The polymer melt solidifies below glass transition temperature, T_g . In essence, vitrified solid is a "supercooled liquid".

!

On solidification polymer melts acquire and retain the shapes of molds and dies used for fabrication. The conditions [time, temperature] of transformation from liquid to solid largely dictate the microstructure and the performance of solidified material. It, therefore, entails considering a crystallisation process and relating it to structural details. A thorough knowledge of the liquid to crystalline solid transformation in polymers can form the basis of structure-property relationships. This is the foundation of any fabrication technology. Such an information on thermotropic LCPs has not been reported in literature.

3.2.4 Time-Temperature-Transformation Concept

Polymer crystallisation process is schematically presented in Figure 26, depicting both nucleation and growth. The solid lines depict the temperature dependence of rates of nucleation [N] and growth [G]. The growth rate initially increases, as a function of temperature, with increasing degree of supercooling [T], but eventually starts to decrease as the thermal energy [RT] falls. Figure 26 also reveals that the nucleation rate attains a maximum rate at an intermediate degree of supercooling. The maximum growth rate occurs usually at a higher temperature than the maximum in nucleation rate.

The overall transformation [crystallisation] rate may be aptly described by a function of growth and nucleation rates:

$$X = F [G, N] \quad [6]$$

Where X is the at which fraction "X" of new crystalline phase increases with time "t".

The "X" curve, shown in Figure 26 as broken line, is similar to G and N curves since the transformation rate is a function of both nucleation and growth rates. Maximum transformation occurs in between the temperatures of maximum growth rate and nucleation rate.

It is often convenient to plot the time taken at various isothermal temperatures for a fixed fraction of transformation X , in the form of a time-temperature-transformation [T-T-T] diagram. This is also called the solidification diagram. It would take a "C" shape, an inverse of "X" curve. The nose of T-T-T diagram corresponds to the minimum time required for a specified fractional crystallisation. The nose temperature is the temperature at which X is maximum. The T-T-T diagram is a familiar concept for studying the phase transformations in metal and alloys.¹⁸⁵ It is a non-equilibrium diagram since transformations occur as a function of time. T-T-T diagrams are frequently used to define thermal history [heat-treatment] paths to obtain a desired microstructure in metals. The diagrams are specific to a particular material composition. Considerable insight into the design of alloys is achieved after exploring the influences of additives on the T-T-T-diagram.

The T-T-T diagrams are contour maps on a time-temperature reference plane. The contour lines are boundaries separating liquid, liquid + solid, and solid regions. These describe zones in which transformation or solidification takes place. Time may be expressed in logarithmic scale. The map allows visualisation of transformations which occur over shorter time spans in an economical production process. Ideally, the diagram should cover the entire temperature range of interest. This range is from below T_g to well above T_m for the processing of thermoplastic. In thermosets it extends well above the final T_g .

T-T-T diagram for nylon-66 are shown¹⁸⁶ in Figure 27. The polymer remains molten for an indefinite period of time when processed above T_m . Crystallisation can occur only between T_m and T_g . The nose of curve [100 seconds, 180°C] represents the shortest time for onset of crystallisation. This time is sufficiently long to possibly quench the polymer into a glassy state. In contrast, for polyethylene the nose point occurs at around at 60°C within a small fraction of a second.¹⁸⁷ This near impossibility to quench polyethylene into a glassy state is ascribed to very high rates of nucleation and crystallisation. Three distinct paths for solidification are shown in Figure 27 by lines 1, 2 and 3.

Line 1: This represents the path of quenching, when the molten mass is cooled from a processing temperature above T_m , at a rate defined by line 1. The specimen would pass directly to the glassy state below the point "a". The polymer would crystallise at an infinitely slow rate if the cooling is discontinued at "a" and the specimen is maintained isothermally for the corresponding time.

Line 2: This represents the path of fast cooling. The polymer is cooled from the processing temperature along the line 2. At this rate of cooling, crystallisation starts at the time and temperature corresponding to the point "b". Crystallisation proceeds between the point b and b'. After the elapse of time corresponding to b, the polymer yield develop a degree of crystallinity [20 percent] characteristic of this cooling path. In this cooling profile the possibility of transformation into a completely glassy state at room temperature does not exist at all. However, the uncrystallised portion of the melt will become glassy below 70°C, the glass transition temperature of nylon 66.

Line 3: This defines the path of the isothermal crystallisation. The polymer is cooled rapidly to temperature T_1 [between 300 and 200°C] and is held isothermally.

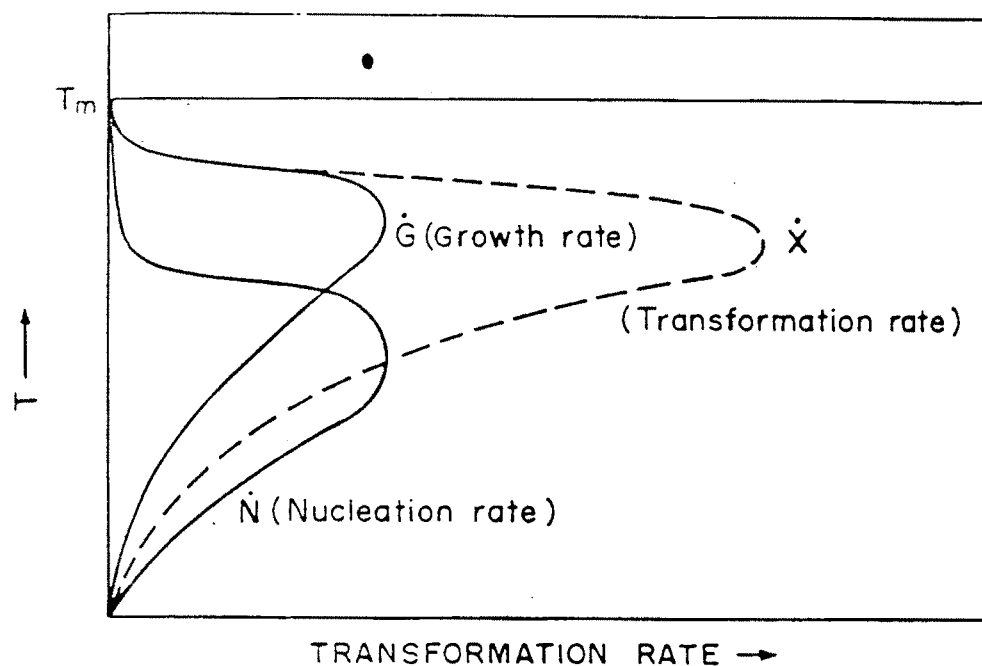


FIG. 26 TEMPERATURE DEPENDENCE OF THE NUCLEATION RATE (\dot{N}), THE GROWTH RATE (\dot{G}) AND TRANSFORMATION RATE (\dot{X}).

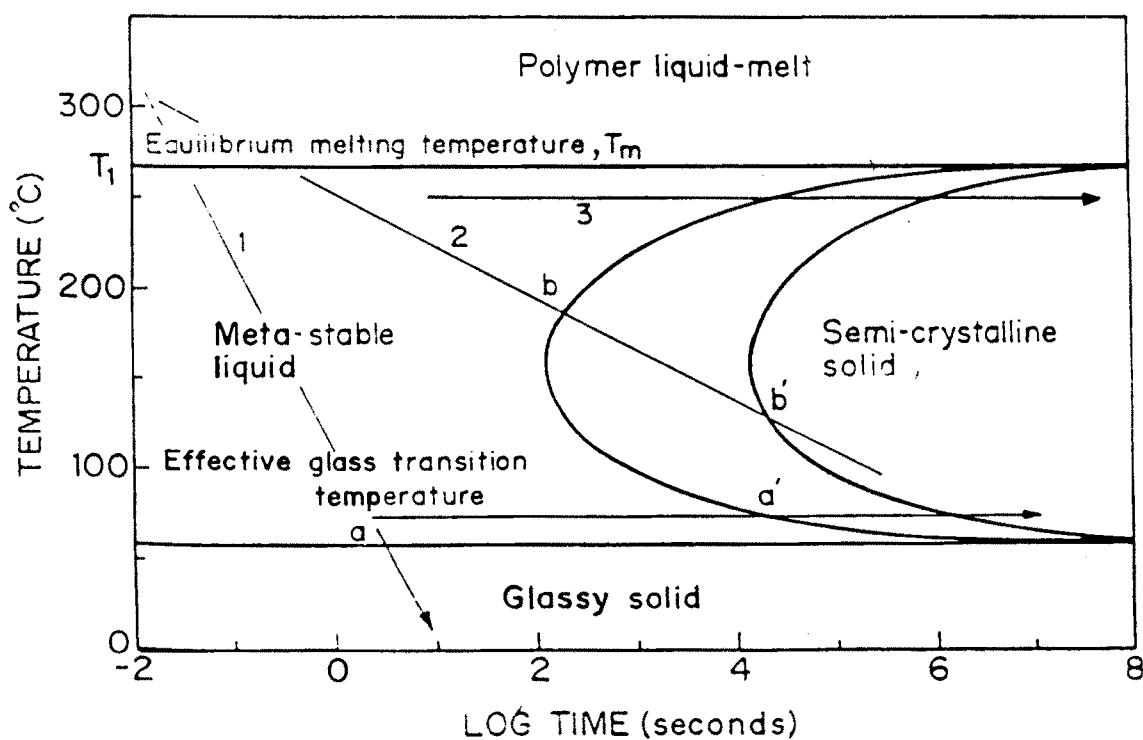


FIG. 27 TIME-TEMPERATURE-TRANSFORMATION DIAGRAM FOR NYLON 66.

Crystallisation will start after a long time lapse, as observable from the diagram. This slow process of crystallisation will lead to the high degree of crystallinity [60 percent] and large microstructure [spherulites]. It must be noted that the line depicting the end of crystallisation does not correspond to 100 percent crystallinity. Apart from the rate of cooling, the degree of crystallinity is influenced by: (1) molecular weight, (2) nature of polymer, especially the chemical composition and structural regularities, (3) presence of additives/impurities. The fold between crystalline lamellae and interfaces between spherulites may account for at least 10 per cent amorphous content.

The T-T-T diagram provides a quantitative framework for understanding and comparing the crystallisation process of thermoplastic materials or the curing process of thermosetting and linearly polymerising materials. Processing conditions can be correlated with crystallisation [or curing] parameters. Such a diagram affords a practical and useful way of finding processing conditions and the course of crystallisation. By selecting a particular set of processing conditions, the crystallisation can be forced to occur along a path, yielding a desired microstructure and a predictable level of performance. T-T-T crystallisation curve can be constructed from DSC thermograms obtained at different cooling rates. Only the upper high temperature section of the C-shaped T-T-T diagrams can be obtained from such non-isothermal scans, by separately joining the start and end of crystallisation. The curve can be completed by coupling the low-temperature regime obtainable from isothermal cooling data. The T-T-T diagram constructed from the non-isothermal cooling data provides immensely valuable information. It is worth noting that crystallisation in all cases of practical importance proceeds under non-isothermal conditions, wherein polymer melt is cooled continuously from the melt temperature to room temperature. Such continuous cooling can be monitored using DSC. Modern injection molding techniques utilize information

provided by T-T-T diagrams. The settings such as mold temperature, mold hold-up time and melt temperature on the injection molding machine can be had from the T-T-T diagrams and be used to obtain a desired microstructure and production rate.

3.2.5 Kinetics of Crystallisation

Some salient features of crystallisation kinetics of LCPs are: (1) It is similar to crystallisation in oriented flexible polymer melts; (2) In the nematic phase, molecules are more mobile than in the corresponding isotropic melt; (3) Heat of fusion is very small and (4) The rigid rod molecules agglomerate into domains for purely geometric reasons.

There are two types of crystallisation kinetics, namely (1) isothermal and (2) non-isothermal.

3.2.5.1 Isothermal Crystallisation

The microscopic, overall crystallisation can be described by an Avrami equation:^{183,188}

$$1 - V_c = \exp[-Kt^n] \quad [7]$$

Where V_c is the volume fraction crystallinity, K is the temperature-dependant kinetic constant, " n " is an Avrami exponent characteristic of crystal nucleation mechanism and geometry of crystal growth, and t is the time. The general mathematical theory was originally developed by Avrami¹⁸⁸ for crystallisation of metals and other low molecular weight substances. The derivations were later simplified by Evans¹⁸⁹ and, with minor modifications, used in the polymer context by Meares¹⁹⁰ and Hay.¹⁹¹

The free growth of crystal proceeds, as described by equation [7], till the first crystals impinge on the another.

$$V_c = G N [vt]^n \quad [8]$$

Where **G** is a geometric factor [which is 4/3 for spheres], **N** is the nucleation density, **v** is the radical growth rate, and "**n**" is normally equal to 3. The growth slows down on impingement.

In the Avrami treatment this impingement is corrected by the Poisson equation.¹⁹² The Avrami equation is derived on the basis of three assumptions. These are: (1) phase transition proceeds under isothermal conditions, (2) nucleation are random and (3) growth rate of a new crystalline phase is dependant on temperature and not on time, or in other words the growth rate is linear. It is also presumed that the transformation occurs entirely by primary crystallisation. Often this assertion is reasonable, since secondary crystallisation sets in only during the final stages of transformation and only a minute fraction of the material remains to be crystallised by this process.

The Avrami exponent "**n**" is related to the conditions of nucleation and growth, and is theoretically between 1 to 4. The exact value depends on the molecular mechanism of nucleation and growth. Avrami equation per Se provides little insight into the molecular organisation of the crystalline regions, structure of the spherulites and so forth. Typical Avrami crystallisation kinetics for various exponents are shown in Figure 28.

The values of "**n**" are usually equal to 3 and 4 respectively for time-dependant nucleation in three dimensional growth. The values of "**n**" decreases by one for two dimensional morphologies. Quite often, fractional exponents are observed due to

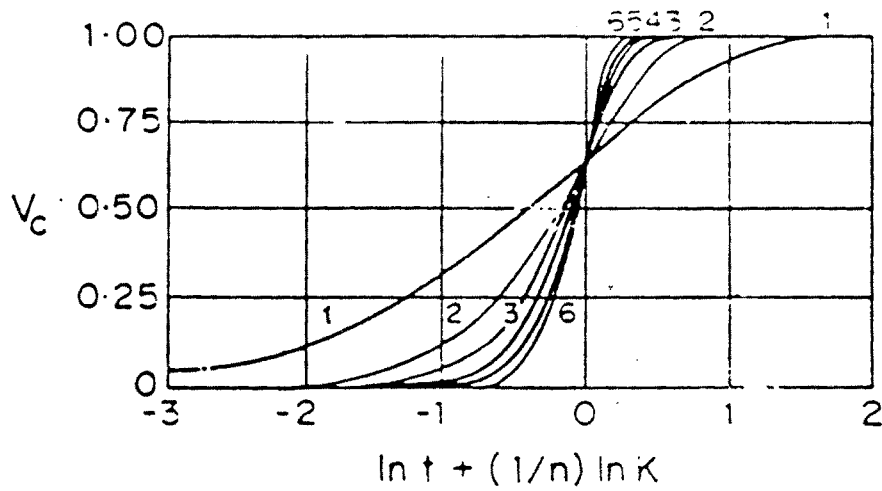


FIG. 28 TYPICAL AVRAMI PLOTS OF THE INCREASE IN VOLUME FRACTION CRYSTALLINITY AS A FUNCTION OF TIME FOR AVRAMI EXPONENTS "n" FROM 1 TO 6.

secondary crystallisation.¹⁸³ The experimental data may also fit two sequential Avrami expressions with different values of "n" when the densities of melt and crystal differ appreciably or when imperfect crystallisations occur. In over 50 flexible semi-crystalline polymers analysed, the exponent is greater than 2.¹⁸³ Exceptions to this are crystallisation of fibrous and drawn samples, which have lower exponent. The Avrami treatment is applicable for oriented rigid macromolecules growing longitudinally, as a two-dimensional growth with all molecules parallel. Thus, the Avrami parameter "n" must be 2 for predetermined nuclei.¹⁹³ The interpretation of Avrami parameter is not unambiguous without a simultaneous knowledge of the microscopic, independently proven mechanism of crystallisation.

Warner and Jaffe¹⁹⁴ used optical microscopy, differential scanning calorimetry [DSC], and wide-angle X-ray scattering [WAXS] to investigate kinetics of liquid crystal transition in wholly aromatic thermotropic copolyesters. Large scale structural rearrangements did not occur on crystallisation. The bulk crystallisation followed Avrami expression with $n=2$, suggesting a sporadic, rod like growth. The Avrami exponent "n" for liquid crystal to crystal transition in rigid rod-flexible spacer type liquid crystalline polyesters was found to be very similar¹⁷⁹ to that in low molecular weight materials. It varied between 3 and 4 over a 40°C wide temperature range, in which the maximum of linear growth was observed. It revealed a spherulitic morphology induced by an instantaneous nucleation. Bhattacharya et al¹⁹⁵ found an Avrami exponent of 1 for another flexible spacer type thermotropic copolyester and suggested an instantaneous rod like growth.

Some disadvantages of isothermal crystallisation kinetics are: (1) Material do not crystallise; (2) It does not release sufficient heat of crystallisation per unit time; (3) It

TABLE 17

Type of nucleation and growth with respect to Avrami exponent " n "¹⁹⁴

n	GROWTH	NUCLEATION
4	Spherulitic	Sporadic
3	Spherulitic	Instantaneous
3	Disc-like	Sporadic
2	Disc-like	Instantaneous
2	Rod-like	Sporadic
1	Rod-like	Instantaneous

shows multiple crystallisation peaks; (4) Thermal response time of the measured system is large compared with the rate of process [The process begins to occur before the system reaches the desired temperature].

3.2.5.2 Non-Isothermal Crystallisation

Practical crystallisation processes proceed under dynamic, non-isothermal conditions. The isothermal measurement is feasible only if thermal response time of measuring module is shorter than the rate of crystallisation.¹⁹⁶ Ozawa¹⁹⁶ modified the isothermal Avrami equation to suit non-isothermal crystallisation behaviour under constant rates of cooling. The assumptions are the same as those in Avrami treatment. The following equation was arrived at:

$$1 - V_c [T] = \exp [-X_c\{T\}/a^n] \quad [9]$$

Where $V_c [T]$ is the volume of crystallinity at temperature " T " and the cooling rate " a ". $X_c\{T\}$ is called the cooling fraction of the crystallisation process, and " n " is similar to the Avrami parameter.

Plots of $\log [-\ln\{1 - V_c [T]\}]$ against $\log a$ yield a series of nearly a parallel straight lines at a number of constant temperatures. The common averaged slope of the lines gives the value of " n " and the intercept furnish the values of cooling function, $X_c \{T\}$, at the respective temperatures.

The assumptions of linear growth rate for polymers in the dynamic crystallisation process may not necessarily be valid because the fold-length of polymer depends on the temperature of crystallisation.¹⁹⁶ The value of " n " varies with crystallisation

temperature. The appropriate modification of the equation is possible only if mechanism for the variation in "n" is established.¹⁹⁶ The effect of slow "secondary" crystallisation on the value of "n" is not appreciable in dynamic non-isothermal crystallisation, since secondary crystallisation becomes slower at lower temperatures. The discrepancy in "n" obtained from isothermal and non-isothermal kinetic studies appears to be due to secondary crystallisation.¹⁹⁶

3.2.6 Mechanism of Crystallisation

Keller¹⁹⁷ proposed chain folding mechanism in polymer crystals. Soon after, a microscopic mechanism of polymer crystal growth was proposed.¹⁹⁸ Understanding of the crystallisation phenomenon has proceeded rapidly. Present efforts to describe the crystal growth phenomenon are mostly based on the activated state theory,¹⁹⁸⁻²⁰² using surface free energy as the main barrier. The very high free energy barrier, of entropic origin, is essential to create step across the perimeter of the lamellae so as to predict chain folded [lamellar] growth. Theories have been proposed based on molecular segregation²⁰³ and continuous growth, due to morphological changes on crystal surfaces.²⁰⁴

The crystalline state of flexible random copolymers, comprising crystallisable "A" and not crystallisable "B" units, lie between two extremes: (1) the crystalline phase is composed entirely of "A" units in metastable equilibrium. The amorphous phase is composed of partly "A" units and partly non-crystallisable "B" units [comonomer exclusion]. (2) The crystalline phase is an intimate solution of "A" and "B" units with "B" units producing defects in the crystalline "A" lattice. Both crystalline and amorphous phases have the same composition [uniform comonomer inclusion].

Faster the growth rate, greater will be the inclusion of "B" counits. A theory has been developed for the crystallisation of flexible random copolymers which predicts melting point depression,²⁰⁵⁻²⁰⁸ crystallisation kinetics,²⁰⁶⁻²⁰⁸ and the amount of non-crystallisable counits incorporated into the crystalline phase.²⁰⁷ Recently,²⁰⁹ an unexpectedly high crystallinity [60 percent] was observed in all aromatic, thermotropic hydroxy benzoic acid-hydroxy naphthoic acid copolyester. It was proposed that the two repeat units co-crystallise in the crystals. The copolymer crystallisation theory of Sanchez and Eby²⁰⁶ has been criticised. It has been suggested, based on the mechanical and dielectric relaxation data,²¹⁰ that the basic crystal structure has rotational disorder due to conformational mobility. The chain packing in the mesophase structure occurs by a matching of order [of monomer units] between adjacent molecules.²¹¹ The mesophase formed during the transition are conformationally disordered crystals ["condis" crystals].²¹²

3.3 DSC ANALYSIS

The thermodynamics of thermal transitions were estimated using a Mettler TA 4000 series instrument. It consisted of a DSC 30 cell coupled to Mettler TC 11 TA processor. Data acquisition was through a PC-AT computer having Mettler QNX operating system and thermal analysis software. The DSC 30 cell was capable of handling samples in the temperature range -170 to 600°C.

3.3.1 Estimation of Thermodynamic Parameters

A definite amount of sample [10-15 mg] was crimped into the sample pan, placed in the DSC 30 cell and heated from 40 to 240°C at the rate of 10°C/minute under constant nitrogen pressure. The phase change etc. were recorded and the thermogram of the heating cycle was obtained. The sample was held for 10 minutes at 240°C to

impart constant thermal history. This constituted the first heating cycle. The sample was cooled from 240 to 40°C at the rate of 10°C/minute. This constituted the first cooling cycle. The thermogram of the cooling cycle were recorded for subsequent analysis. The sample was reheated from 40 to 400°C at the rate of 10°C/minute under constant nitrogen pressure. This constituted the second heating cycle.

3.3.2 Isothermal Crystallisation Kinetics

The specific temperatures chosen for isothermal crystallisation kinetic study were decided up on from the transition temperatures observed during thermal characterisation in dynamic mode, as presented in Section 3.3.1. Two temperatures regimes were selected from non-isothermal dynamic mode. These are named as high temperature crystallisation regime and low temperature crystallisation regime. Two isothermal temperatures were selected in each of these two crystallisation regimes. These temperatures are presented in Table 18. The study was conducted using a series of dynamic and isothermal programmes. The thermograms corresponding to the second heating cycles were recorded and analysed for estimating isothermal crystallisation kinetics for each polyester. The specific analysis profiles for each polyester are presented below.

3.3.2.1 Polyester PE-103

A definite amount of sample was weighed [10-15 mg] into the DSC pan. It was inserted into DSC cell maintained at 40°C and heated to 240°C at the rate of 100°C/minute. The sample was maintained isothermally at 240°C for 5 minutes under nitrogen atmosphere. This constituted the first heating cycle.

TABLE 18

Temperatures selected for studying isothermal crystallisation kinetics

Code No.	Low Temperature Regime, °C	High Temperature Regime, °C
PE-103	110, 125	131, 140
PE-107	143, 148	153, 160
PE-203	191, 194	198, 202
PE-303	108, 113	118, 125

The sample was then cooled from 240°C to isothermal crystallisation temperature [e.g. 110, 125, 131 and 140°C] at the rate of 100°C/minute. This constituted the first cooling cycle. The sample was annealed for different times such as 5, 15, 30, 90, 240 and 660 minutes at the specific isothermal crystallisation temperatures. After the varied annealing times, the sample was cooled to 90°C at the rate of 10°C/minute. This constituted the second cooling cycle. The sample was again reheated from 90 to 220°C at the rate of 10°C/minute. This constituted the second heating cycles.

3.3.2.2 Polyester PE-107

A definite amount of sample was heated from 40 to 230°C at the rate of 100°C/minute. It was held for 5 minutes at 230°C under nitrogen atmosphere. This constituted the first heating cycle.

The sample was then cooled from 230°C to isothermal crystallisation temperature [e.g. 143, 148, 153 and 160°C] at the rate of 100°C/minute. This constituted the first cooling cycle. The sample was annealed at the specific isothermal crystallisation

temperatures for 5, 15, 30, 90, 240 and 660 minutes. After the varied annealing times, the sample was cooled to 90°C at the rate of 10°C/minute. This constituted the second cooling cycle. The sample was reheated from 90 to 230°C at the rate of 10°C/minute. This constituted the second heating cycles.

3.3.2.3 Polyester PE-203

A definite amount of sample was heated from 40 to 245°C at the rate of 100°C/minute. The sample was held for 5 minutes at 245°C under nitrogen atmosphere. This constituted the first heating cycle.

The sample was then cooled from 245°C to isothermal crystallisation temperature [e.g. 191, 194, 198 and 202°C] at the rate of 100°C/minute. This constituted the first cooling cycle. The sample was annealed at the specific isothermal temperatures for 5, 15, 30, 90, 240 and 660 minutes. The sample was then cooled to 90°C at the rate of 10°C/minute. This constituted the second cooling cycle. The sample was reheated from 90 to 275°C at the rate of 10°C/minute. This constituted the second heating cycles.

3.3.2.4 Polyester PE-303

A definite amount of sample was heated from 40 to 225°C at the rate of 100°C/minute. The sample was held for 5 minutes at 225°C under nitrogen atmosphere. This constituted the first heating cycle.

The sample was then cooled from 225°C to isothermal crystallisation temperature [108, 113, 118, 125°C] at the rate of 100°C/minute. This constituted the first cooling cycle. The sample was annealed at the specific isothermal temperatures for 5, 15, 30,

90 and 240 minutes. The sample was then cooled to 50°C at the rate of 10°C/minute. This constituted the second cooling cycle. The sample was reheated from 50 to 225°C at the rate of 10°C/minute. This constituted the second heating cycles.

3.3.3 Non-Isothermal Crystallisation Kinetics

Non-isothermal crystallisation kinetic method is based on the following DSC programmes presented below:

A definite amount of sample [10-15 mg] was weighed into the DSC pan and kept in DSC cell. It was heated from 40 to 240°C at the rate of 100°C/minute under nitrogen atmosphere. The sample was held for 10 minutes at this temperature to completely melt the sample. This constituted the heating cycle. The sample was cooled from 240 to 40°C at different cooling rates. The cooling rates were varied from 3 to 20°C/minute. This constituted the cooling cycle. The thermograms corresponding the cooling cycles were recorded and analysed to estimate the non-isothermal crystallisation kinetics.

CHAPTER 4

RESULTS AND DISCUSSION

RESULTS AND DISCUSSION

In this chapter the results are presented and discussed relative to structural variations. The polyesters based on bis-[4-hydroxy benzoyl oxy]-1,4-benzene, unsubstituted trimesogen, are discussed in Section 4.1. The polyesters synthesised from bis-[4-hydroxy benzoyl oxy]-2-methyl-1,4-benzene, methyl substituted trimesogen, are presented in Section 4.2. The polyesters generated from bis-[4-hydroxy benzoyl oxy]-2-chloro-1,4-benzene, chloro substituted trimesogen, are examined in Section 4.3. The co-, ter- and tetra- polyesters made from bis-[4-hydroxy benzoyl oxy]-1,4-benzene are discussed in Section 4.4. The isothermal crystallisation kinetics are examined in Section 4.5. The non-isothermal crystallisation kinetics are presented in Section 4.6.

The thermotropic liquid crystalline behaviour of polymers is of strong current interest among polymer scientists because of their development into new materials with unique properties.²¹³⁻²¹⁵ A great variety of structures are achievable. Essentially all these can be assigned to one of the two categories. The first class comprises of those which have mesogenic units attached as pendants either directly or through spacers, to a polymer backbone. These are known as side chain liquid crystalline polymers. The second class are those having mesogenic units and rigid or flexible spacers in the backbone. The term "main chain liquid crystalline polymers" is used to describe these structures.

We have been particularly interested in delineating relationships between the structure and liquid crystal properties.²¹⁶ Flexible chain polymers will not exhibit liquid crystalline behaviour, while more rod-like polymers show only lyotropic mesomorphism. Hence, thermotropic mesomorphism is restricted to those significant polymers having intermediate chain extensions. The liquid crystalline phase may be nematic or smectic. De Gennes²¹³ suggested that the incorporation of both rigid and flexible segments into the repeating unit of a polymer chain should afford semi-flexible

polymers exhibiting thermotropic mesomorphism with the ability to control transition temperatures. A number of polymers of this type have been investigated.⁵⁷ Many interesting properties were observed for rigid rod-flexible spacer type polymers. The odd-even dependence of transition temperatures in main chain thermotropic polymers with polymethylene spacers is a matter of importance. This generalises the thermal behaviour of a series of polymers with varying length of spacers.²¹⁷

4.1 POLYESTERS OF BHBOB MESOGEN

The first series of ordered homopolyesters studied comprise of coupling a new unsubstituted trimesogenic diol with a number of aliphatic dicarboxylic acids. This mesogen is bis-[4-hydroxy benzoyl oxy]-1,4-benzene [BHBOB]. The aliphatic diacid chlorides used as flexible spacers were: glutaryl [n=3], adipoyl [n=4], pimeloyl [n=5], suberoyl [n=6], azeloyl [n=7], sebacoyl [n=8] and dodecane dioyl [n=10] chlorides.

The synthesis scheme for bis-[4-hydroxy benzoyl oxy]-1,4-benzene is depicted in Figure 19 and presented in Section 2.2.8. The syntheses of acid chlorides are presented in Sections 2.2.1 to 2.2.7. Polyesterifications of bis-[4-hydroxy benzoyl oxy]-1,4-benzene with the aliphatic acid chlorides were conducted using low temperature solution and interfacial polycondensation methodologies. These are presented in Sections 2.3.1 and 2.3.2 respectively. The polymers synthesised by solution polycondensation were coded as PE-1 to PE-7, where n = 3, 4, 5, 6, 7, 8 and 10 respectively. The polymers synthesised by interfacial polycondensation were coded as PE-201 to PE-207 respectively.

These polymers were not soluble in typical solvents, such as chloroform, carbon tetrachloride, dichloro methane, dichloro ethane, 4-chloro phenol and phenol:tetrachloro ethane (50:50 wt./wt.) mixture used to solubilise rigid rod-flexible spacer type thermotropic liquid crystalline copolyesters. The thermal behaviour were analysed with a Mettler DSC-30 instrument^{*}. Details are presented in Section 3.2.1. A Leitz

Ortholux polarising microscope with a Mettler FP-52 hot stage controlled by a Mettler FP-5 temperature control was used for visual examination of phase changes under dynamic and for textures formed under isothermal conditions. Wide angle X-ray diffractometer was used to determine the degree of crystallinity at room temperature.

4.1.1 General properties

The transition temperatures and thermodynamic properties are presented in Tables 19 and 20. Textures observed with polarising microscope are presented in Figure 29 [$n=10$]. These photographs were taken at 230°C from heating cycle while the six other photographs were taken at 271°, 260°, 229.5°, 192°, 130° and 115.8°C in the cooling cycle.

All polymers formed turbid melts that showed strong stir-opalescence up to the isotropic transition temperature (T_i). Polyesters with longer [$n=10$] flexible spacers, such as PE-5 and PE-207, showed focal conic texture typical of smectic C phase while others showed threaded-schlieren texture ascribable to nematic phase. It has been well established by other investigators that long flexible spacers [$n>8$] tend to crystallise as well as allow higher degrees of freedom to the mesogenic units which permit their alignment into smectic layers.

4.1.2 Thermodynamics of LC States

Thermodynamic data for polymers in this series, synthesised by solution polycondensation method, are presented in Table 19. Similarly, the data for polymers synthesised by interfacial polycondensation are presented in Table 20. The thermal transitions occurred over a broad temperature range. This points to polydispersity in the samples. The polyesters formed during syntheses tended to precipitate out from the solvent. As a result, a wide distribution in molecular weights could not be avoided.

Table - 19

Solution polycondensation [BHBOB]

Transition Temperatures and Thermodynamic Data of BHBOB Homopolyesters:
Effect of Flexible Spacer.

Code	K-N	N-I	ΔT	ΔH	ΔH	ΔS	ΔS	$[\text{CH}_2]_n$	DOC
No.	[°C]	[°C]	[°C]	K-N	N-I	K-N	N-I	n	%
PE-7	197.5	320.8	123.3	3.26	8.30	6.93	13.98	3	50.00
PE-1	207.9	293.1	85.2	3.50	2.67	7.14	4.79	4	64.12
PE-6	187.2	291.1	103.9	8.54	7.74	18.55	14.18	5	70.00
PE-2	203.0	299.8	96.8	5.12	6.16	10.75	10.80	6	60.00
PE-3	169.9	304.8*	135.2*	5.98	10.30	13.51	17.82*	7	56.02
PE-4	176.1	304.6	128.5	4.50	5.82	10.02	10.07	8	62.80
PE-5	201.0 ^a	291.2 ^b	90.2	4.63 ^a	5.83 ^b	9.77 ^a	10.33 ^b	10	65.72

K-N, [°C] = Crystal-Liquid Crystal Transition Temperature; N-I, [°C] = Liquid Crystal-Isotropic Transition Temperature; ΔT , [°C] = Temperature Range of Mesophase Stability; ΔH , K-N and N-I = Enthalpy change in Kilo-Joule/mole of repeat unit (mru); ΔS , K-N and N-I = Entropy change in Joule/(mru)(°K); DOC = Percent Degree of Crystallinity; ^a = Crystal to Smectic Transition; ^b = Smectic to Isotropic Transition; * = Decomposition and Isotropisation occur in parallel.

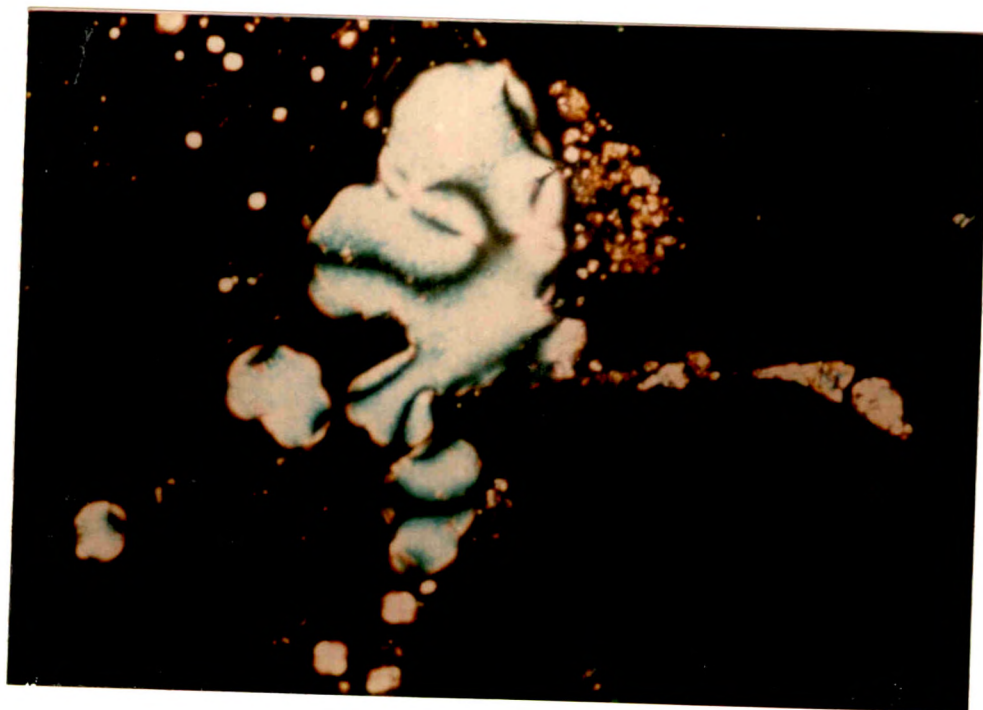
Table - 20

Interfacial polycondensation [BHBOB]

Transition Temperatures and Thermodynamic Data of BHBOB Homopolyesters:
Effect of Flexible Spacer.

Code	K-N	N-I	ΔT	ΔH	ΔH	ΔS	ΔS	$[\text{CH}_2]_n$	DOC
No.	[°C]	[°C]	[°C]	K-N	N-I	K-N	N-I	n	%
PE-201	188.0	297.9	109.9	3.93	5.40	8.52	9.45	3	48.71
PE-202	211.3	319.1	107.8	0.51	8.43	1.06	14.24	4	44.10
PE-203	207.3	299.2	91.9	3.14	6.50	6.54	11.36	5	50.00
PE-204	199.4	301.7	102.3	2.00	6.15	4.24	10.70	6	58.94
PE-205	202.2	286.2	84.0	3.37	4.02	7.09	7.18	7	52.27
PE-206	179.6	284.9	105.3	1.35	3.09	2.98	5.54	8	65.51
PE-207	191.4 ^a	291.2 ^b	99.8	1.74 ^a	31.86 ^b	3.74 ^a	56.46 ^b	10	67.32

K-N, [°C] = Crystal-Liquid Crystal Transition Temperature; N-I, [°C] = Liquid Crystal-Isotropic Transition Temperature; ΔT , [°C] = Temperature Range of Mesophase Stability; ΔH , K-N and N-I = Enthalpy change in Kilo-Joule/mole of repeat unit (mru); ΔS , K-N and N-I = Entropy change in Joule/(mru)(°K); DOC = Percent Degree of Crystallinity; a = Crystal to Smectic Transition; b = Smectic to Isotropic Transition.



(a)



(b)

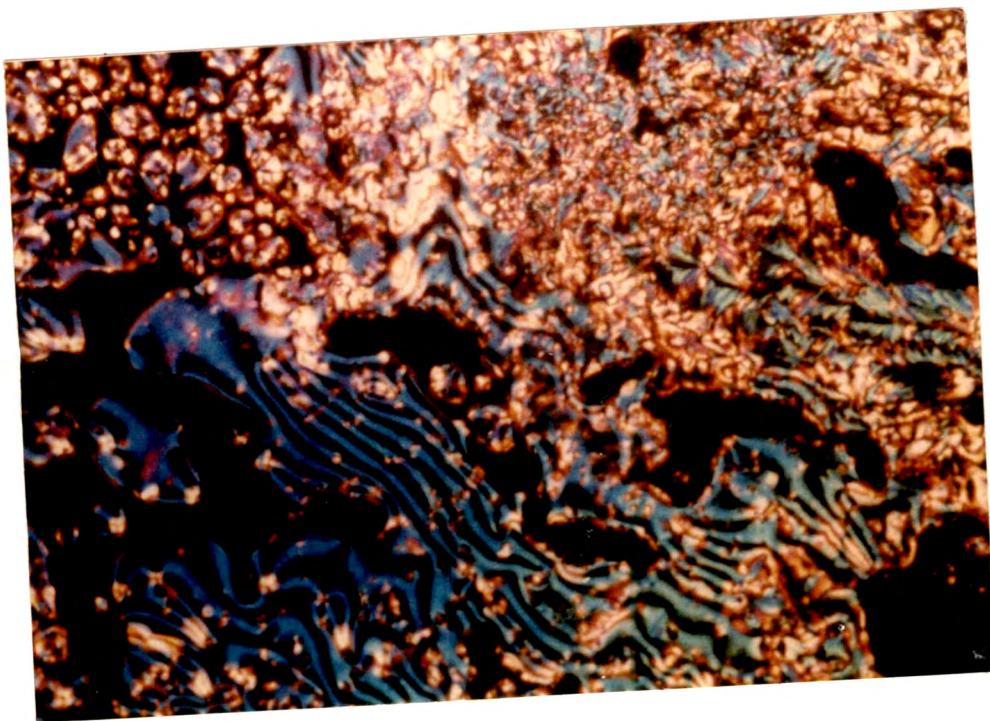
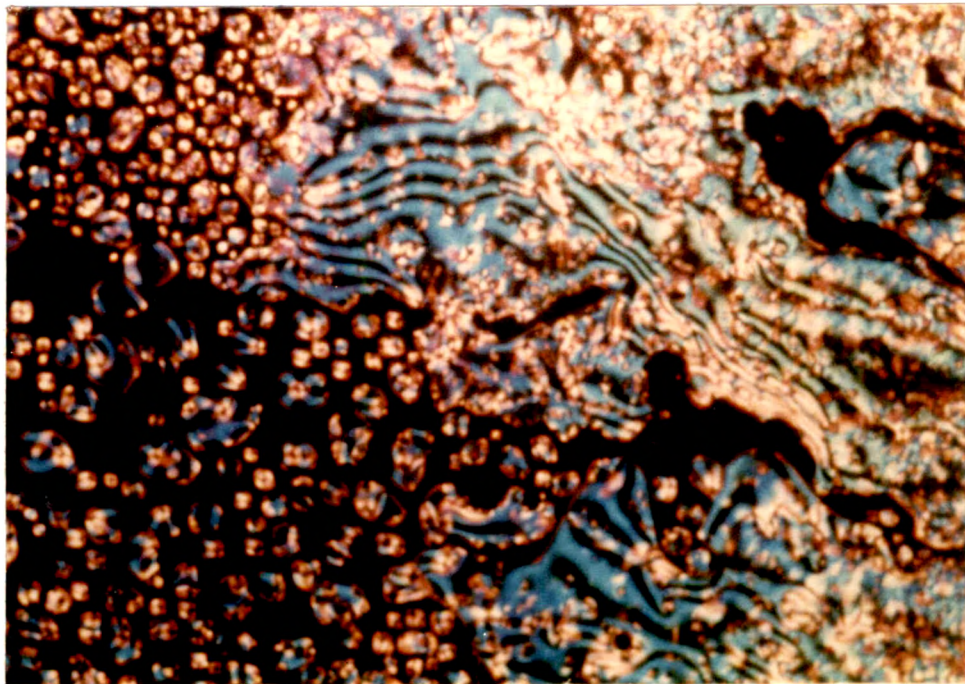
AT

(a) 271.0 °C AND (b) 260.0 °C.

(c)



FIG.29 : TEXTURES OF POLYESTER PE-207 AT
(c) 229.5 °C AND (d) 192.0 °C.



(f)

FIG.29 : TEXTURES OF POLYESTER PE-207 AT
(e) 130.0 °C AND (f) 115.8 °C.

4.1.2.1 Crystal to Liquid Crystal [K-N/K-S] Transition, T_m

Temperatures corresponding to crystal to liquid crystal transition reflect a zigzag change with increase in number of methylene units in the flexible spacer. The transitions occurred at higher temperatures for polyesters with even number of methylene units than those with odd number of units. This arises from a more or less colinear or parallel alignment of mesogenic unit with even number of methylene units. The presence of an odd number of methylene units is known to generate a tilt between adjacent mesogens which disrupts the packing efficiency and causes a downturn in transition temperature.

The transition temperatures decrease with increase in length with both even and odd number of methylene units. This is due to a dilution of the mesogen. In polyesters with decamethylene spacer, synthesised by both solution (PE-5) and interfacial (PE-207) methods, onset of smectic phase shifts the transition to a higher temperature. This is due to additional crystallisation of the longer decamethylene flexible spacer. *W. 2*

4.1.2.2 Liquid Crystal to Isotropic [N-I/S-I] Transition, T_i

Isotropisation temperatures decrease with increase in the length of flexible spacer due to dilution of mesogen. The zigzag effect, with odd-even number of methylene units, is weak. Reduction of isotropisation temperature with increased lengths of odd or even polymethylene spacers is generally due to a congruent increase in the number of possible conformations with the spacer length which distorts the cylindrical shape of the molecules. Polyesters PE-5 and PE-207 [n=10] show higher isotropisation temperature than PE-4 and PE-206 [N=8]. There is no plausible explanation for this observation. The higher T_i in PE-3 [n=7] and PE-4 [n=8] prepared by solution polycondensation is perhaps due to disparity in the molecular weights. These polyesters

may be of higher molecular weights. Also, this may be arise from the superimposed decomposition processes observed in these two polyesters which tend to mask lower enthalpy changes accompanying phase transformations.

See also

4.1.2.3 Mesophase stability, $[\Delta T]$

In polyesters synthesised via solution polycondensation methodology the systems with odd number of methylene units display higher mesophase stability than those with even number of methylene units. This arises from greater depression of crystal-liquid crystal (K-N) transition in the presence of odd number of methylene units while the subsequent liquid crystal-isotropic transition temperatures are only marginally affected. This trend is reversed in the polyesters synthesised by interfacial method. This has been conformed by repeating the syntheses. A more detailed analysis to quantify these results is desirable. This is beyond the scope of this thesis due to instrumental constraints.

The mesophase stability in polyesters synthesised by solution polycondensation decrease with an increase in the length of the flexible spacer. Similar observations have been noted by other researchers as well.⁵¹ This is probably due to an increased rotational as well as translational mobility. The concurrent decompositions accompanying isotropisations in PE-3 [n=7] and PE-4 [n=8] erroneously point to a higher mesophase stability. The odd-even effect in mesophase stability is rather weak in polyesters prepared by interfacial method. However, the mesophase stability is depressed with increasing spacer length.

4.1.2.4 Enthalpy Change for K-N, $[\Delta H_m]$

In polyesters prepared by solution polycondensation method it is difficult to relate very precisely the enthalpy change accompanying crystal to liquid crystal transition

with either odd-even number of methylene units or length of the flexible spacer. Qualitatively, enthalpy values increase with length of the flexible spacer. This probably reflects arrangement of flexible spacer into the organised crystalline array generated by the mesogen at room temperature. In polyesters synthesised by interfacial method the enthalpy change for polyesters with even number of methylene units were significantly lower than those with odd number. This result runs contrary that observed for diad mesogen-flexible spacer type systems²¹⁸ and points to greater order in the liquid crystalline state of polyesters with even number of methylene units.

4.1.2.5 Enthalpy Change for N-I, [ΔH_i]

In polyesters prepared by solution polycondensation ΔH_i values were higher than ΔH_m . This is opposite to that observed with low molecular mass liquid crystals and is due a high degree of order in the liquid crystalline state in polymeric systems. The polyesters synthesised by the two methodologies differ in the odd-even effect relative to published information for diad mesogens. In the series prepared by solution polycondensation, the polyesters with odd number of methylene units display higher enthalpy change than those with even number. This trend is also qualitatively reflected in the polymers prepared by interfacial method. This observation, once again, runs contrary to established literature data. Critical examination of the system using techniques such as high temperature x-ray are probably in order.

4.1.2.6 Entropy Changes, [ΔS_m and ΔS_i]

Entropy change relative to structural variation is not very precise. The ΔS_m seems to increase and points to higher degree of ordering with increasing flexible spacer

length. The ΔS_m for polyesters with odd number of methylene units are higher. The discomfoting observation is the conflicting set of values obtained for ΔS_i by the two synthesis methodologies.

4.1.3 Conclusion

Polyesters with very large mesophasic stability ($> 80^\circ\text{C}$) are generated by incorporating triad-mesogen in a rigid rod-flexible spacer type thermotropic system. There is enough and consistent proof to indicate that thermal properties are also dependent on molecular weight and molecular weight distribution. At lower molecular weights, obtained by solution polycondensation, the mesophase stability is larger for polyesters with odd number of methylene units, while the opposite is true at higher molecular weights. Marked odd-even effects are observable for the crystal-liquid crystal transition. Similar trend for isotropisation is rather weak. Degree of crystallinity decreases with increase in molecular weights. Irrespective of molecular weights and structural variations such as odd-even methylene units, the liquid crystalline state retains a high degree of order. The nematic order shifts to a higher smectic one with the incorporation of a decamethylene spacer.

4.2 POLYESTERS OF BHBOMB MESOGEN

The second ordered homopolyester series studied comprised of coupling a new methyl substituted trimesogenic diol with a number of aliphatic dicarboxylic acids. This mesogen is bis-[4-hydroxy benzoyl oxy]-2-methyl-1,4-benzene [BHBOMB]. The aliphatic diacid chlorides used as flexible spacers were: glutaryl [n=3], adipoyl [n=4], pimeloyl [n=5], suberoyl [n=6], azeloyl [n=7], sebacoyl [n=8] and dodecane dioyl [n=10] chlorides.

The synthesis scheme for bis-[4-hydroxy benzoyl oxy]-2-methyl-1,4-benzene, depicted in Figure 19, are presented in Section 2.2.9. The syntheses of acid chlorides are presented in Sections 2.2.1 to 2.2.7. Polyesterifications of bis-[4-hydroxy benzoyl oxy]-2-methyl-1,4-benzene with the aliphatic acid chlorides were conducted using low temperature interfacial polycondensation methodology. This is presented in Section 2.3.2. The polymers were coded as PE-101 to PE-107 respectively, where $n = 3, 4, 5, 6, 7, 8$ and 10 respectively.

4.2.1 Substitution Effects

The liquid crystalline behaviour of low molecular mass liquid crystals, with substituents on the mesogenic units, have been studied systematically by Gray²¹⁹⁻²²¹ and others.^{222,223} In general, the influence of substitution is complicated by both steric and polar effects. The steric effect, which leads to a less thermally stable mesophase, may involve the following molecular contributions: (1) a broadening of the mesogenic groups by the substituents and, therefore, a decrease in the overall length to diameter (axial or aspect) ratio; (2) a decrease in the coplanarity of adjacent mesogenic moieties due to steric interactions between substituents and (3) a tendency for the substituents to force apart mesogenic groups in neighbouring polymer chains due to spatial requirements. On the other hand, substituents that impart an increased polarisability and stronger dipolar interaction between the mesogenic groups acquire stronger intermolecular attractions. This leads to higher thermal stabilities for both crystalline and liquid crystalline phases and results in higher crystal-liquid crystal and isotropisation (clearing) temperatures.

In thermotropic polymers the substituent effects are of interest since crystal-liquid crystal transition temperature of fully extended rigid rod polymers are extremely high. It is desirable to lower the crystal-liquid crystal temperature for processing from liquid

crystalline melts. It is apparent that this could be accomplished by introducing substituents into the mesogenic units of the polymer.²²² The use of monosubstituted hydroquinones in random copolyesters result in a considerable decrease in the crystal-liquid crystal transition temperatures and permit melt spinning from the liquid crystalline states.⁵⁹

4.2.2 General Properties

The thermal behaviour (thermograms) were analysed with a Mettler DSC-30 instrument. Details of analysis are presented in Section 3.2.1. The polyesters exhibited similar crystal-liquid crystal transitions in the first and second DSC heating cycles. The second heating cycle was undertaken subsequent to imparting a constant thermal history, of one heating/cooling cycle at 10°C/minute in the temperature range of 40-250°C. The data are presented in Tables 21, 22. A Leitz Ortholux polarising microscope with a Mettler FP-52 hot stage, controlled by a Mettler FP-5 temperature control, was used for visual examination of phase changes in dynamic mode and for the textures formed under isothermal conditions. Wide angle X-ray diffractometer was used to determine the degree of crystallinity at room temperature. These polymers were soluble at room temperature in typical chlorinated solvents, such as chloroform, carbon tetrachloride, dichloromethane, dichloroethane, 4-chloro phenol and phenol:tetrachloro ethane (50:50 wt./wt.) mixture used to solubilise rigid rod-flexible spacer type thermotropic liquid crystalline copolyesters. Inherent viscosities, determined with 0.5 weight percent solution in chloroform at 30°C, are presented in Table 22.

The melting endotherms were pleasingly simple (unstructured). Main chain thermotropic liquid crystalline polyesters exhibit complex and some times uninterpretable thermograms for crystal-liquid crystal transitions. Some factors responsible for such complex thermal behaviour are: solid-solid transitions; melting of

Table - 21

First heating cycle [BHBOMB]

Transition Temperatures and Thermodynamic Data of BHBOMB Homopolyesters:

Effect of Flexible Spacer.

Code	K-N	N-I	ΔT	ΔH	ΔH	ΔS	ΔS	$[\text{CH}_2]_n$	DOC
No.	[°C]	[°C]	[°C]	K-N	N-I	K-N	N-I	n	%
PE-101	208.3	355.2	146.9	9.58	0.28	19.20	0.44	3	54.60
PE-102	186.4	349.5	165.1	3.75	-	8.15	-	4	42.93
PE-103	173.3	327.5	154.2	6.55	1.54	14.67	2.57	5	37.15
PE-104	199.1	325.7	126.6	4.07	4.88	8.62	8.14	6	44.44
PE-105	164.3	289.9	124.8	12.35	5.17	28.23	9.18	7	40.60
PE-106	182.8	291.0	108.2	3.02	7.69	6.63	13.64	8	38.60
PE-107	184.6 ^a	274.4 ^b	89.8	5.92 ^a	6.93 ^b	12.94 ^a	12.65 ^b	10	46.15

K-N, [°C] = Crystal-Liquid Crystal Transition Temperature; N-I, [°C] = Liquid Crystal-Isotropic Transition Temperature; ΔT , [°C] = Temperature Range of Mesophase Stability; ΔH , K-N and N-I = Enthalpy change in Kilo-Joule/mole of repeat unit (mru); ΔS , K-N and N-I = Entropy change in Joule/(mru)(°K); DOC = Percent Degree of Crystallinity; a = Crystal to Smectic Transition; b = Smectic to Isotropic Transition.

Table - 22

Second heating cycle [BHBOMB]

Transition Temperatures and Thermodynamic Data of BHBOMB Homopolyesters:

Effect of Flexible Spacer.

Code	K-N	N-I	ΔT	ΔH	ΔH	ΔS	ΔS	$[\text{CH}_2]_n$	IV ^a
No.	[°C]	[°C]	[°C]	K-N	N-I	K-N	N-I	n	
PE-101	210.6	350.3	139.7	4.42	1.24	11.43	1.99	3	0.97
PE-102	186.3	369.5	210.2	3.84	-	8.37	-	4	0.93
PE-103	173.3	351.4	170.1	3.81	1.66	8.54	2.66	5	1.46
PE-104	195.5	349.5	154.0	2.71	7.24	5.79	11.62	6	1.10
PE-105	164.1	311.0	146.9	8.73	5.68	19.97	8.70	7	1.03
PE-106	177.2	312.9	135.7	2.86	6.74	6.36	11.50	8	0.98
PE-107	188.2 ^b	294.6 ^c	106.4	6.31 ^b	8.94 ^c	8.24 ^b	15.75 ^c	10	1.05

K-N, [°C] = Crystal-Liquid Crystal Transition Temperature; N-I, [°C] = Liquid Crystal-Isotropic Transition Temperature; ΔT , [°C] = Temperature Range of Mesophase Stability; ΔH , K-N and N-I = Enthalpy change in Kilo-Joule/mole of repeat unit (mru); ΔS , K-N and N-I = Entropy change in Joule/(mru)(°K); DOC = Percent Degree of Crystallinity; a = Intrinsic viscosity was determined at 30°C in chloroform; b = Crystal to Smectic Transition; c = Smectic to Isotropic Transition; - = Could not estimated or may not be present.

crystals/recrystallisation of new ones; formation, in rapid succession, of more than one liquid crystalline phase; etc. All polyesters exhibited a rather narrow endothermic transition for the mesophase at the isotropisation temperature, which suggests that polydispersity were rather narrow. The polyesters synthesised here were all chemically ordered and soluble in the polymerisation solvent medium. A broadening of isotropic transition would be expected for polydisperse samples, as indeed observed for the polyesters based on unsubstituted trimesogen, wherein insolubility intervened. The peak maxima were chosen to make comparative estimates of structure-thermal property correlations. We were unable to study the transition from the isotropic to the liquid crystal state (deisotropisation process) as the isotropisation in most samples in this series are rapidly followed by decomposition. It is known that deisotropisation in main chain liquid crystalline polyesters exhibits a smaller degree of supercooling. In other words, isotropisation is thermodynamically more of an equilibrium (reversible) process, rather than crystal to liquid crystal transition. The recrystallisation in these polyesters, when cooled at 10°C/minute from 250°C, showed a moderate supercooling of about 50°C.

All polyesters formed turbid melt that showed strong stir-opalescence up to the isotropisation or clearing temperature (T_i). Thin films of the polymer melts were examined on the hot stage of a polarising microscopy for optical textures. Patterns displayed by polyesters other than PE-107 ($n=10$) in the heating mode had the characteristic features pertaining to a nematic mesophase (i.e. threaded-schlieren texture). Polyester PE-107 ($n=10$) displayed focal conic texture typical of a smectic mesophase prior to the isotropic transition. Thus, the longest flexible spacer in this series ($n=10$) allowed the rigid mesogenic unit to align more readily in two-dimensional layers giving rise to a smectic mesophase.

4.2.3 Thermodynamics of LC States

The transition temperatures and thermodynamic data, as determined from DSC first heating thermograms, are summarised in Table 21. Typical thermograms are illustrated in Figures 30 and 31. In thermotropic liquid crystalline polyesters the liquid crystal and isotropic transition temperatures are dependant on molecular weight till a critical value is attained. The polyesters of this series were all soluble and hence it is believed that these had attained sufficiently high molecular weights (see Table 22) to enable a meaningful comparison of the thermal and thermodynamic properties.

Leaving aside first and last polyesters (PE-101 and PE-107) in this series, others display moderate, though not very precise, odd-even fluctuation in the crystal-liquid crystal transition temperatures, T_m , relative to methylene unit length. This odd-even effect seems to suggest that the spacer part of the polymer backbone is largely in its most extended (trans) conformation. In this conformation, even numbered methylene spacers can retain their colinearity with mesogenic parts while the odd numbered methylene spacers can not. It must be mentioned that the odd-even effect in T_m is not universal in homologous LCPs. The off-equilibrium nature of the crystal to liquid crystal transition can mar this odd-even effect to some extent. The non-emergence of a real odd-even effect in T_m (even in the second heating cycle) is obviously attributable to this. The isotropisation temperatures T_i show more of the tendency towards a continual decrease rather than an odd-even fluctuation. Unlike liquid crystal transition, isotropisation is a near equilibrium process. But very often, isomerisation reactions occur at high temperatures with polyesters and risk of concurrent or imminent degradations are not entirely avoidable. The problem of degradation can impair the actual effect in T_i . The odd-even effect in T_i has been observed by some researchers. In the present series, the isotropisation temperature decreased continuously with the spacer length.

→ was degraded (observed)

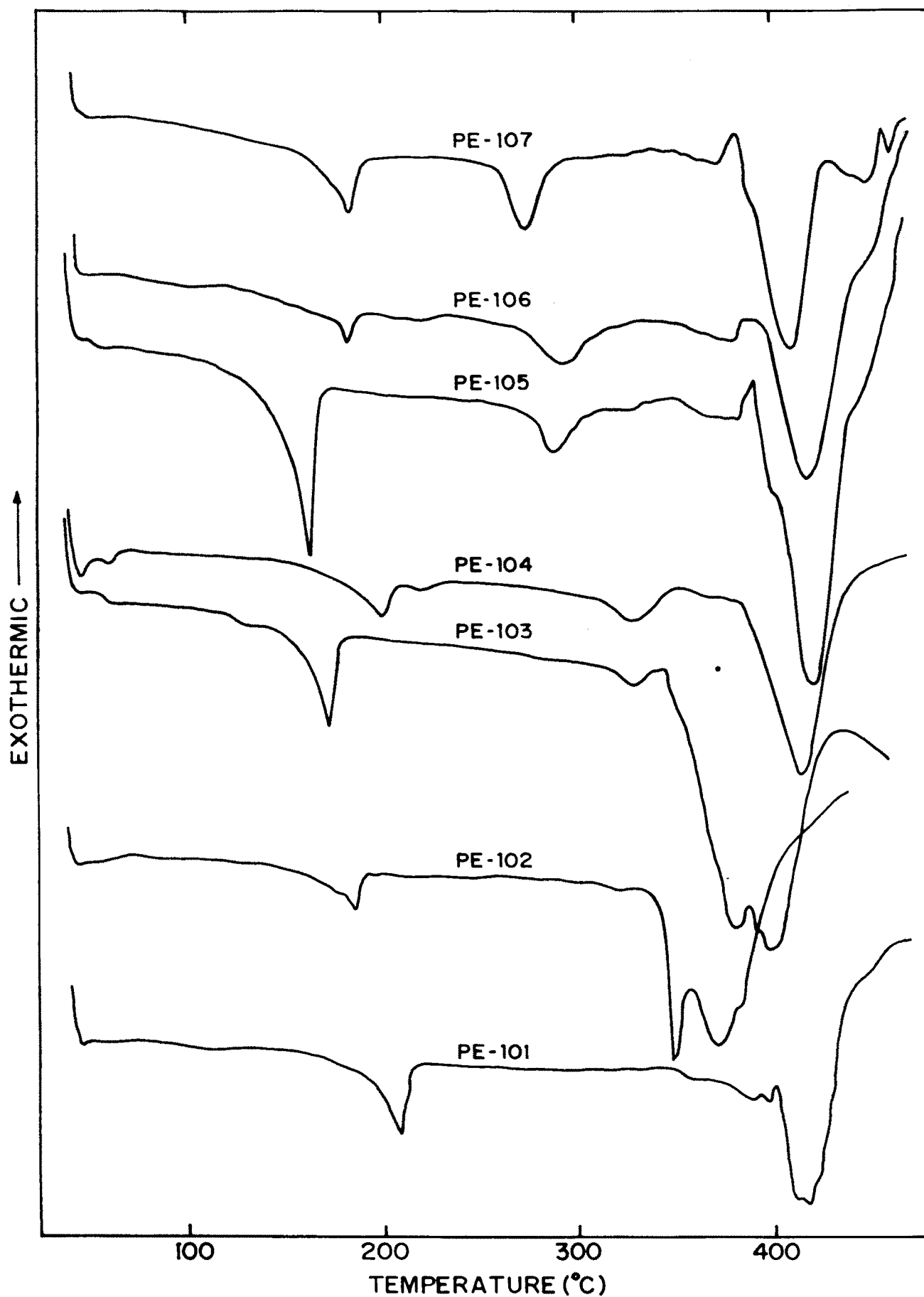


FIG. 30 DSC THERMOGRAMS OF BHBOMB HOMOPOLYESTERS [FIRST HEATING CYCLE].

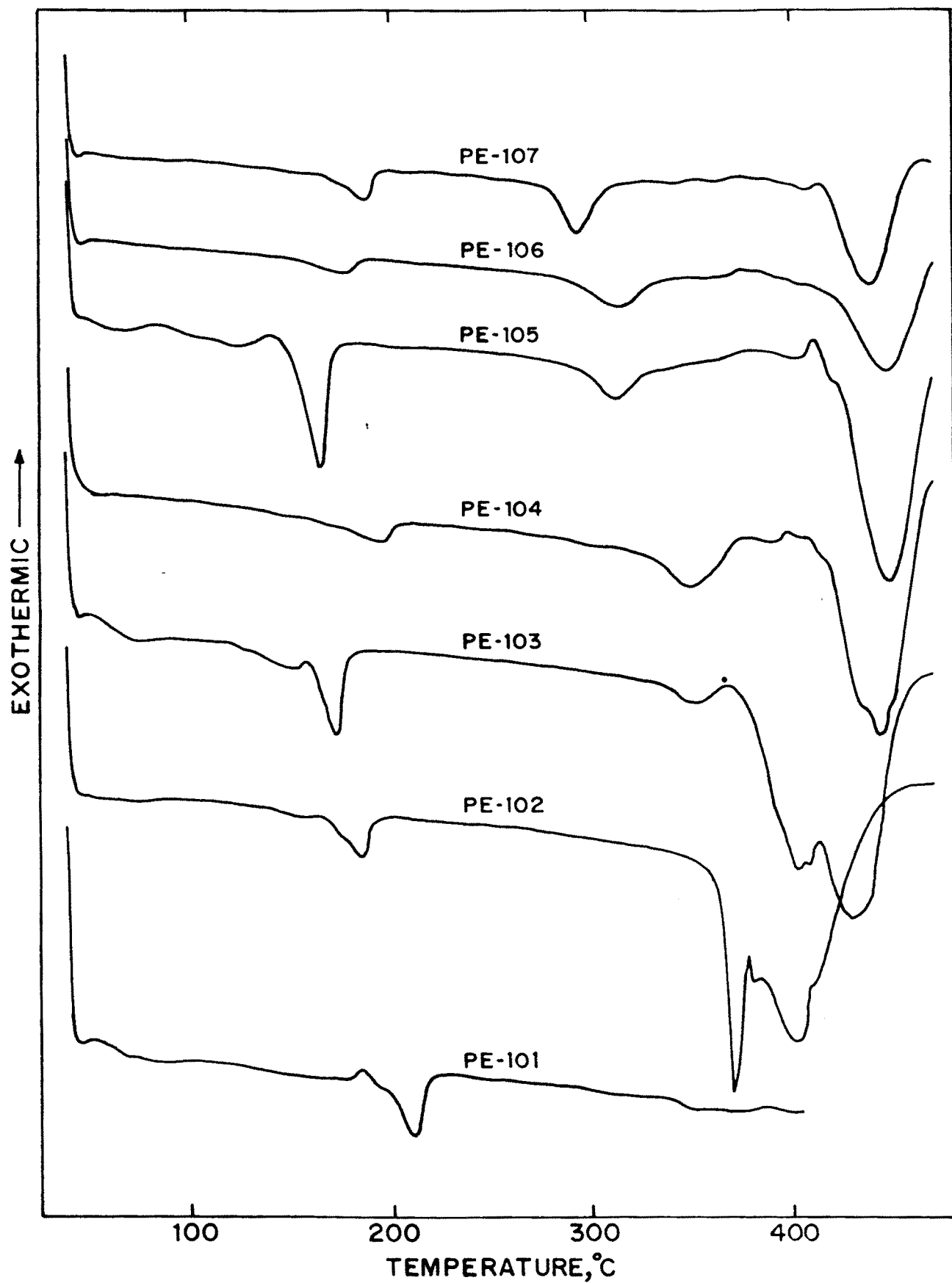


FIG. 31 DSC THERMOGRAMS OF BHBOMB HOMOPOLYESTERS [SECOND HEATING CYCLE].

4.2.3.1 Mesophase stability, $[\Delta T]$

Mesophase stabilities ($\Delta T = T_i - T_m$) of these polyesters show a decrease, although irregularly, with increasing methylene units "n" in flexible spacer. Such narrowing of the nematic phase interval with increasing methylene spacer length ends with the onset of smectic phase at $n=10$. The irregular narrowing of the mesophase interval is rationalised on the basis of the fact that there is no definite trend in T_i and there is some kind of fluctuation in T_m . The mesophase stability of these polyesters were found to be quite high ($> 100^\circ\text{C}$).

4.2.3.2 Enthalpy and Entropy Changes

The enthalpy and entropy change up on transition in the first and second heating cycles of these polymers are represented in Tables 21 and 22. These are plotted in Figures 30 and 31. These data do not show any clear and regular trend (e.g. odd-even effect) for crystal to liquid crystal (K-LC) or for liquid crystal to isotropic (LC-I) transition in either first or second heating cycle. As indicated earlier, the crystal to liquid crystal transition is known to exhibit pronounced off-equilibrium character. The enthalpy and entropy data for $n = 3$ to 10 indicate a variable degree of supercooling of the nematic to crystal (N-K) transition, i.e., a variable degree of crystallinity in the supercooled sample prior to the second heating cycle. In other words, our attempts to maintain a constant thermal history in all these samples had not been successful.

The enthalpy and entropy change for the liquid crystal to isotropic transition (LC-I) are more or less comparable in both first and second heating cycles. For the polyesters discussed here the values of ΔH_{K-LC} and ΔS_{K-LC} observed in both cycles are comparable with those found normally in main chain liquid crystalline polyesters. The degradations in polyesters PE-104 to PE-107 generate some what elevated values of ΔH_{LC-I} and ΔS_{LC-I} . Such elevated values of ΔH_{LC-I} and ΔS_{LC-I} are usually typical

of a transition from highly ordered smectic phase to the isotropic phase. We have seen the presence of a smectic phase in PE-107 and hence the high values of ΔH_{LC-I} and ΔS_{LC-I} are expected in this case, provided the isotropic transition has occurred from the smectic phase. In other polyesters (PE-104 to PE-106), textures corresponding only to nematic phases were observable under hot stage coupled polarising microscopy. The high values of ΔH_{LC-I} and ΔS_{LC-I} point to some conformational ordering in the flexible spacer.

Our conclusion is reinforced when we find that ΔH_{LC-I} and ΔS_{LC-I} increase monotonously for the odd and even series of nematic polyesters. The increase for ΔH_{LC-I} is from 0.27 KJ/mru for $n=3$ to 7.69 KJ/mru for $n=8$ (mru = mole of repeat unit). Similarly, the increase for ΔS_{LC-I} is from 0.44 J/[K][mru] to 13.64 J/[K][mru]. The values quoted are from the data of the first heating cycle. The increases for the odd and even series do not proceed with any uniform, average increment of ΔH_{LC-I} and ΔS_{LC-I} per methylene unit. However, the fact remains that there is significant, but non-uniform extension of the flexible spacer in the nematic phase of polyesters PE-104 to PE-106. The population of trans conformers in nematic phase could not be estimated due to a lack of knowledge about the respective population of trans/gauche conformers in the pretransition state.

4.2.3.3 X-ray Diffraction

Bragg spacings measured for as polymerised samples are collated along with the degree of crystallinity data in Table 21. The degree of crystallinity data from X-ray diffractions are not always in concordance with the values of ΔH_{K-LC} from DSC data. Bragg spacings less than 5\AA , that are seen in all the polyesters, arise mainly from preferred separations in the lateral packing of the polyesters chains. Spacings of 12\AA or higher indicate regularity of packing along the chain. Lateral packing, however, can

allow a regular arrangement of molecules along the chain in spite of the randomness arising out of the positional isomerisation of the unsymmetrical mono substituent on the central unit of the trimesogen. The degree of crystallinity in one case overlooks any such order along the chain because we have not been able to harness any reflection below $\Delta = 5^\circ$ due to instrumental limitations. It is likely that the crystallinity arising out of this order could have contributed to higher values of ΔH_{K-LC} for PE-103 and PE-105 with $n=5$ and $n=7$ respectively.

4.2.4 Conclusion

Soluble polyesters with very large mesophasic stability ($> 100^\circ\text{C}$) are generated by incorporating a methyl substituted triad-mesogen in a rigid rod-flexible spacer type thermotropic system. The endotherms are rather sharp indicating narrow molecular weight distribution. The polyesters display moderate odd-even fluctuations in liquid crystal transition temperatures with increase in flexible spacer length. No such effect is observable for the isotropisation temperatures. Mesophase stability ($\Delta T = T_i - T_m$) decreases irregularly with increasing methylene units. No clear trend is noted for enthalpy and entropy change with respect to spacer length for either crystal to liquid crystal (K-LC) or liquid crystal to isotropic (LC-I) transition due to inability to maintain constant thermal history in all the samples. Interestingly, these values are depressed by the unsymmetrical mono methyl substitution on the mesogenic core and points to greater disorder induced by the substitution.

4.3 POLYESTERS OF BHBOCB MESOGEN

The third series of ordered homopolyesters studied comprise of coupling a new chloro substituted trimesogenic diol with a number of aliphatic dicarboxylic acids. This

mesogen is bis-[4-hydroxy benzoyl oxy]-2-chloro-1,4-benzene [BHBOCB]. The aliphatic diacid chlorides used as flexible spacers were: glutaryl [n=3], adipoyl [n=4], pimeloyl [n=5], suberoyl [n=6], azeloyl [n=7], sebacoyl [n=8] and dodecane dioyl [n=10] chlorides.

The synthesis scheme for bis-[4-hydroxy benzoyl oxy]-2-chloro-1,4-benzene is depicted in Figure 19 and presented in Section 2.2.10. The syntheses of acid chlorides are presented in Sections 2.2.1 to 2.2.7. Polyesterifications of bis-[4-hydroxy benzoyl oxy]-2-chloro-1,4-benzene with the aliphatic acid chlorides were conducted using low temperature interfacial polycondensation methodology. This is presented in Section 2.3.2. The polymers were coded as PE-301 to PE-307 respectively, where n = 3, 4, 5, 6, 7, 8 and 10 respectively.

4.3.1 Substitution Effects

It is desirable to lower the melting temperature for processing. This is accomplished by introducing substituents into mesogenic units of thermotropic polymers. The first description of substituted main chain thermotropic liquid crystalline polymer was by Roviello and Sirigu.¹¹³ The first patent on lowering the melting temperature of main chain thermotropic polymers by substitution is assigned to Kleinschuster et al.,⁹¹ who prepared random copolyesters from chloro, bromo and methyl hydroquinones.

Highly polar substituents (-CN, -NO₂) are known to be very effective in depressing the crystal-liquid crystal transition temperatures. This partially arises from steric effects, which limit the molecular packing efficiency in both crystalline and liquid crystalline states. The Van der Waal radii of chloro, bromo, cyano and nitro substituents are larger than that of methyl groups. However, literature reports indicate that the incorporation of these substituents in random structures result in higher isotropisation

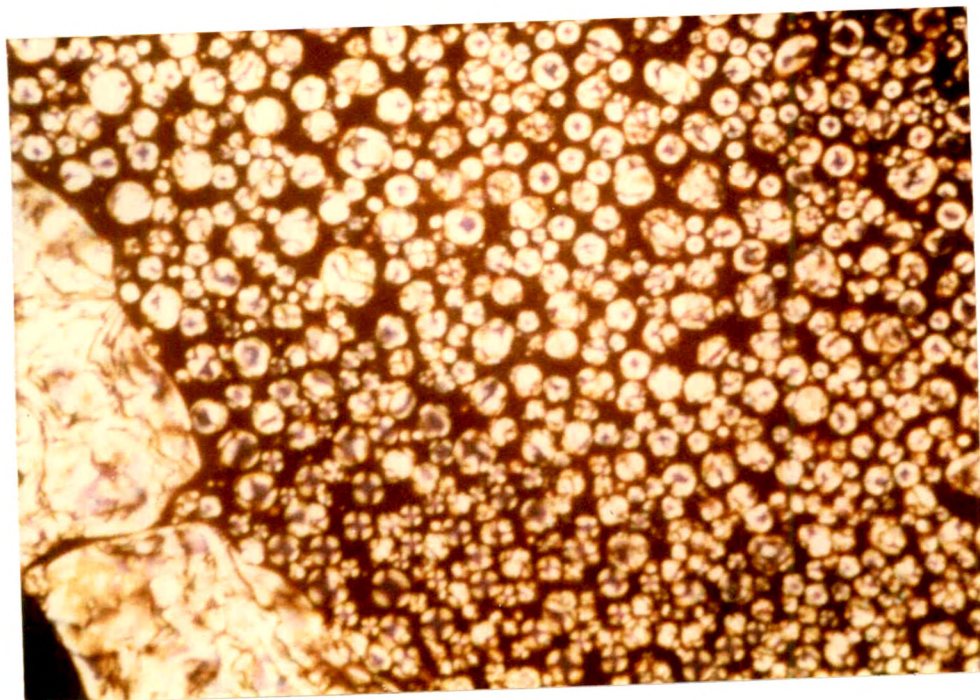
(clearing) temperatures relative to methyl substitution.

4.3.2 General Properties

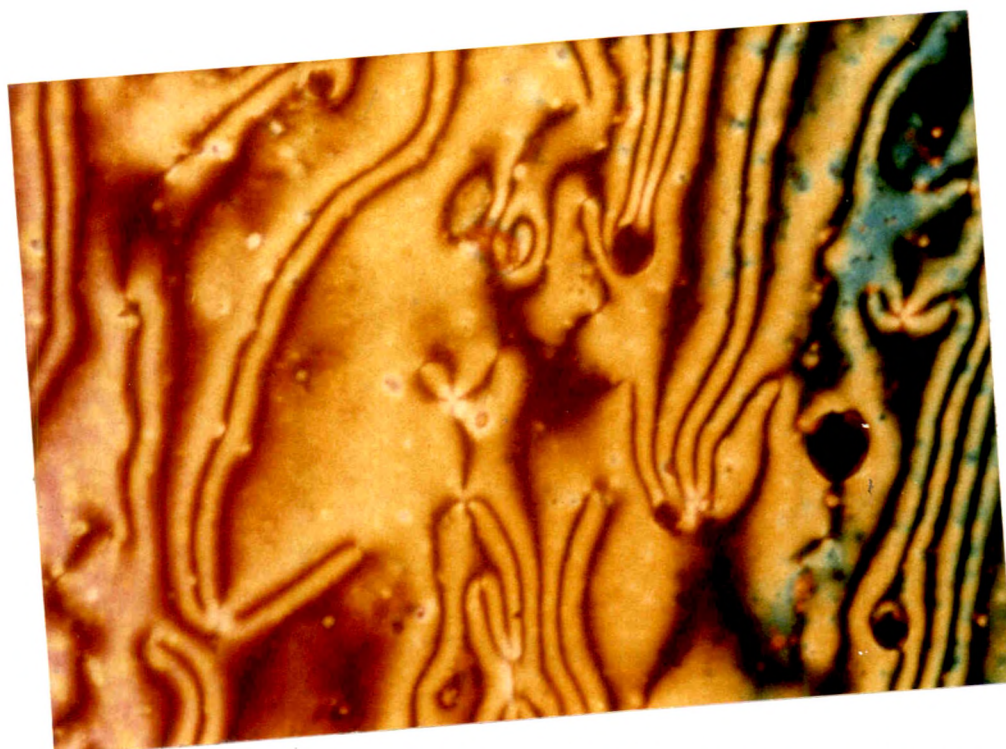
These polyesters were soluble in chlorinated solvents such as chloroform, carbon tetrachloride, dichloromethane, dichloroethane, 4-chloro phenol and phenol:tetrachloro ethane (50:50 wt./wt.) mixture. The inherent viscosities were not estimated. The molecular weights polymers were expected to be similar to those based on methyl substitution since the polycondensation methodology adopted for both series were identical.

The thermal transitions and thermodynamic parameters (thermograms) were estimated with a Mettler DSC-30 instrument. Details are presented in Section 3.2.1. A Leitz Ortholux polarising microscope with a Mettler FP-52 hot stage, coupled to a Mettler FP-5 temperature controller, was used for visual examination of phase changes in dynamic mode and for the textures formed under isothermal conditions. Wide angle X-ray diffractometer was used to determine the degree of crystallinity at room temperature.

All polyesters excepting PE-307 showed nematic textures under polarising microscope. Polyester PE-307 showed focal conic texture representative of smectic phase and did not pass into nematic state before isotropisation. No textures representative of nematic phase was observable on gradual and controlled slow cooling to room temperature, over several hours. Photomicrographs for PE-307 taken at three different temperatures during cooling cycle namely 192.4°, 187.7° and 134.8°C are shown in Figure 32.



(a)



(b)

FIG.32 : TEXTURES OF POLYESTER PE-307 AT
(a) 192.4°C AND (b) 187.7°C .

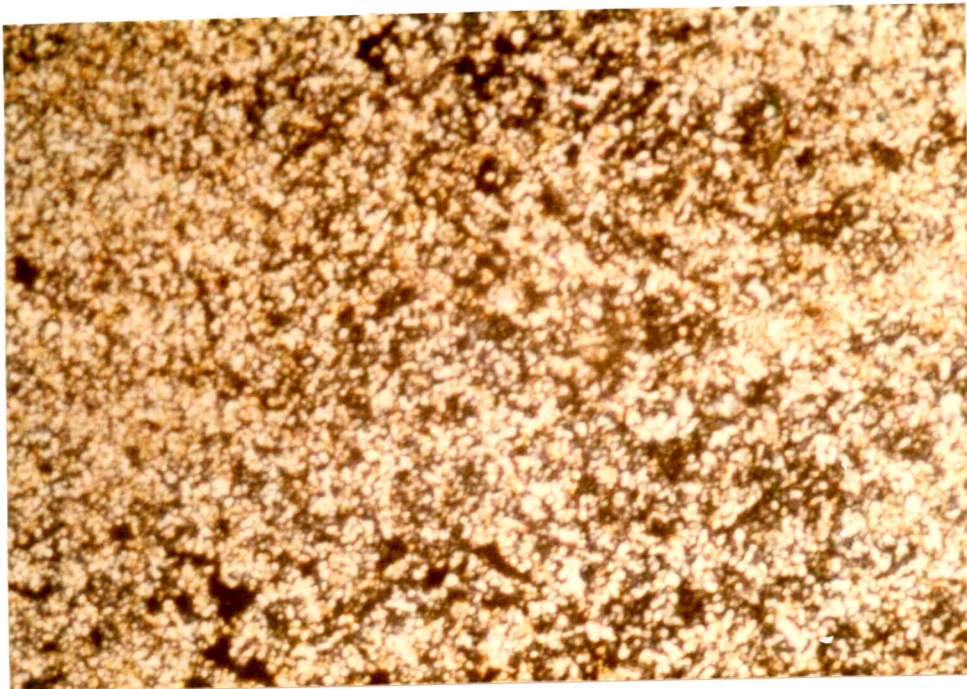


FIG.32 : TEXTURE OF POLYESTER PE-307 AT (c) 134.8 °C.

4.3.3 Thermodynamics of LC States

The DSC thermograms corresponding to the first and second heating cycle of these polyesters are shown in Figures 33 and 34. The odd and even behaviour clearly separate out in polyesters with methylene units from $n=3$ to $n=8$, in respect of the nature of the thermograms they display. The thermograms of polyesters with odd number of methylene units display a sharply peaked liquid crystal transition which is followed almost immediately by a diffuse and broad isotropic transition. In contrast, the liquid crystal transition in the polyesters with even number of methylene units are quite well separated from somewhat narrow isotropic transition, but the liquid crystal transition in this series is always doubly peaked. The latter kind of mesophasic gap has been noted, as a general case, for methyl substituted mesogen series. The temperature corresponding to the second (high temperature) peak is reported as the T_m for the polyesters with even number of methylene units. The "even" polyesters (excepting PE-307) were examined carefully under a polarising microscope in the temperature range corresponding to the doublets. No significant difference in textures was observed. All samples displayed threaded nematic texture under microscope. However, it may be qualitatively stated that viscosity was higher for the low temperature peak, as is to be expected.

The transition temperatures and the thermodynamic values of transition for these polyesters are presented in Tables 23 and 24. Looking at the liquid crystal transition temperatures, it can be stated that the "exaggerated" odd-even effect has been weakly expressed in this homologues series of polyesters. These transitions, when compared to the corresponding polyesters of methyl series, show that the bulkiness of the chloro group tends to separate the chains more, at least in polyesters with n exceeding 4.

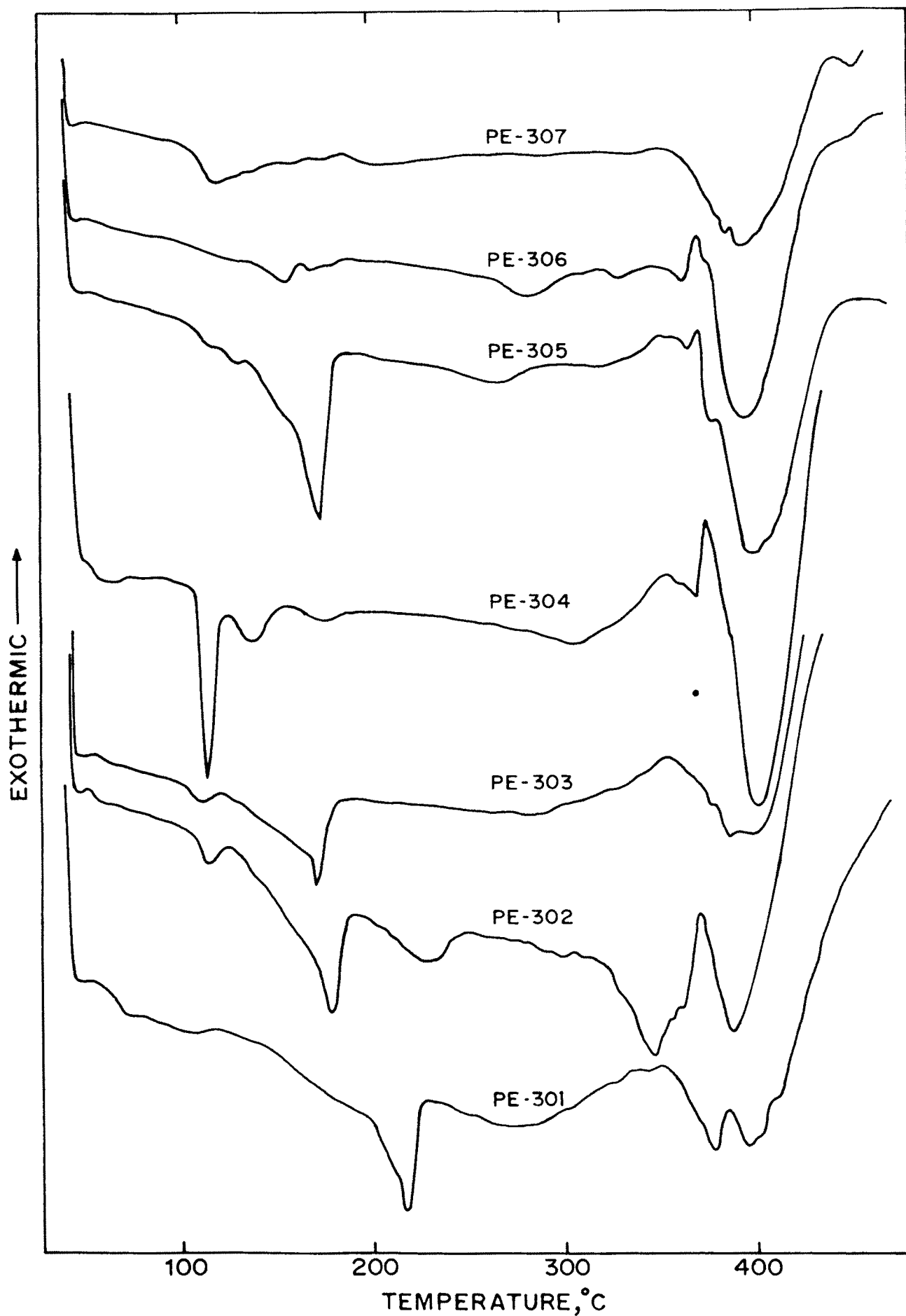


FIG. 33 DSC THERMOGRAMS OF BHBOCB HOMOPOLYESTERS
[FIRST HEATING CYCLE].

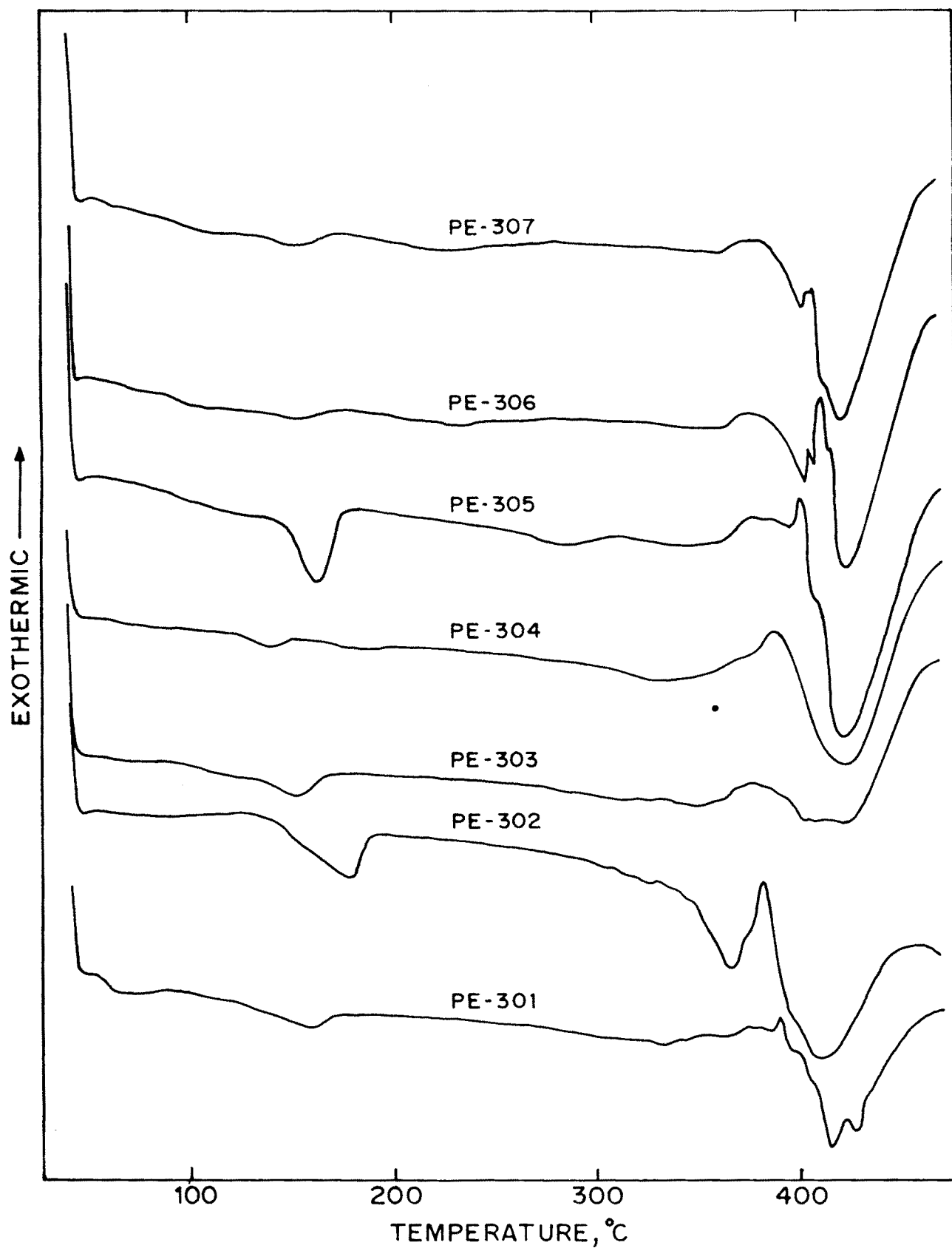


FIG. 34 DSC THERMOGRAMS OF BHBOCB HOMOPOLYESTERS
[SECOND HEATING CYCLE].

Table - 23

First heating cycle [BHBOCB]

**Transition Temperatures and Thermodynamic Data of BHBOCB Homopolyesters:
Effect of Flexible Spacer.**

Code	K-N	N-I	ΔT	ΔH	ΔH	ΔS	ΔS	$[\text{CH}_2]_n$	DOC
No.	[°C]	[°C]	[°C]	K-N	N-I	K-N	N-I	n	%
PE-301	217.5	278.1	60.6	4.52	6.35	9.22	11.52	3	40.81
PE-302	224.9	345.9	121.0	6.88	4.45	13.81	7.19	4	40.00
PE-303	170.0	278.2	108.2	6.62	5.24	14.95	9.50	5	46.07
PE-304	173.6	303.8	130.2	1.68	3.09	3.76	5.36	6	37.50
PE-305	173.2	261.5	88.3	12.30	3.40	27.57	6.36	7	50.00
PE-306	155.2	283.8	128.6	2.65	3.47	6.19	6.24	8	40.42
PE-307	120.4 ^a	204.8 ^b	84.4	3.42 ^a	2.90 ^b	8.70 ^a	6.07 ^b	10	48.13

K-N, [°C] = Crystal-Liquid Crystal Transition Temperature; N-I, [°C] = Liquid Crystal-Isotropic Transition Temperature; ΔT , [°C] = Temperature Range of Mesophase Stability; ΔH , K-N and N-I = Enthalpy change in Kilo-Joule/mole of repeat unit (mru); ΔS , K-N and N-I = Entropy change in Joule/(mru)(°K); DOC = Percent Degree of Crystallinity; a = Crystal to Smectic Transition; b = Smectic to Isotropic Transition.

Table - 24

Second heating cycle [BHBOCB]

**Transition Temperatures and Thermodynamic Data of BHBOCB Homopolyesters:
Effect of Flexible Spacer.**

Code	K-N	N-I	ΔT	ΔH	ΔH	ΔS	ΔS	$[\text{CH}_2]_n$	DOC
No.	[°C]	[°C]	[°C]	K-N	N-I	K-N	N-I	n	%
PE-301	162.9	341.3	178.4	2.12	5.72	4.86	9.32	3	40.81
PE-302	178.8	367.7	188.9	5.88	9.80	13.04	15.30	4	40.00
PE-303	159.6	348.2	188.5	3.10	6.92	7.18	11.15	5	46.07
PE-304	139.6	337.8	198.4	0.73	8.74	1.78	25.85	6	37.50
PE-305	166.0	282.8	116.8	5.37	4.67	12.23	8.41	7	50.00
PE-306	162.8	303.8	141.0	5.06	6.34	11.63	10.63	8	40.42
PE-307	104.3 ^a	227.3 ^b	123.0	0.70 ^a	2.44 ^b	1.85 ^a	4.87 ^b	10	48.13

K-N, [°C] = Crystal-Liquid Crystal Transition Temperature; N-I, [°C] = Liquid Crystal-Isotropic Transition Temperature; ΔT , [°C] = Temperature Range of Mesophase Stability; ΔH , K-N and N-I = Enthalpy change in Kilo-Joule/mole of repeat unit (mru); ΔS , K-N and N-I = Entropy change in Joule/(mru)(°K); DOC = Percent Degree of Crystallinity; a = Crystal to Smectic Transition; b = Smectic to Isotropic Transition.

Recently, Rath and Ponrathnam²²⁴ have observed that the nature of lateral substituent on the mesogen has very marginal influence on T_m in random thermotropic copolyesters.

Ordered copolyesters with a bulkier substituent on the mesogen usually show a greater depression in T_m .⁵³ The attraction due to greater electronegativity of chlorine is outweighed by the steric repulsion in ordered systems and results in a reduced lateral packing of chains. The greater effect of steric repulsion is not easily realised in randomised structures. Unlike the methyl series, the ordered chloro series show some odd fluctuations in isotropic transition temperature, T_i . In general, these temperatures are lower than those in methyl homologues. Partial decomposition during isotropisation and non-equilibrium nature of crystal to liquid crystal or liquid crystal to crystal transitions are the probable reasons for the non-emergence of odd-even effect in a clear cut fashion during isotropic and liquid crystal transitions respectively.

The enthalpy and entropy change for the crystal-liquid crystal and liquid crystal-crystal transitions are of the same magnitude as those presented in literature for other main chain thermotropic liquid crystalline polymers. The values associated with the isotropisation are, however, somewhat on the higher side. Similar high values have been noted in methyl substituted series of polyesters as well (see Tables 21 and 22). The origin of such high values point to some conformational ordering of spacers in the liquid crystalline state.

Unlike methyl substituted polyesters, the chloro series exhibit continually decreasing values of ΔS_{LC-I} for odd and even group of polyesters, with increasing n . What is surprising is the consistently higher values of ΔS for this series. Such high values of ΔS could arise if the liquid crystalline phase undergoing isotropisation is not a purely nematic one but consists of a nematic phase encapsulated in a smectic mesophase.

Detailed investigations are required to ascertain the origin of these higher values for ΔS . We are sure that the problem of degradation did not always inflate the values of ΔS_{LC-I} .

Let us take the odd members of this series of polyesters. Isotropisation occurred at relatively lower temperatures so as not to be tampered by any partial degradation. Unlike "even" members, the transition occurred in a diffuse manner over a wide temperature. The ΔS values are higher. We believe, on the basis of some approximate estimation, that only conformational ordering of the spacer may not lead to such high values unless there is a ordered phase (mixed with usual nematic phase) involved in this transition as well.

4.3.4 Conclusion

Soluble polyesters with very large mesophasic stability ($> 110^{\circ}\text{C}$) are generated by incorporating a chloro substitution on triad-mesogen in a rigid-rod-flexible spacer type ordered thermotropic liquid crystalline system. The polyesters display somewhat complex nematic ordering in the liquid crystalline state. Smectic phase manifests with decamethylene spacer. The odd-even effect is noted in isotropisation temperatures as well as enthalpy and entropy changes accompanying isotropisation. The high enthalpy and entropy change on isotropisation points to conformational ordering in the liquid crystalline state. Unlike in random copolyesters, incorporation of chloro substituent into an ordered polyester structure depresses the isotropisation temperature.

4.4 CO-, TER- AND TETRAPOLYESTERS OF BHBOB MESOGEN

The polymeric structures described herein comprise of unsubstituted triad BHBOB mesogenic diol hooked to two, three or four different aliphatic diacids with varying number of methylene units. These are termed as co-, ter- and tetrapolyesters

respectively. In general, transition temperatures of thermotropic polyesters based on triad mesogens are higher than similar systems arising from diad mesogens due to increased rigidity.¹⁰⁹ The presence of different aliphatic spacers along a single polymer chain is a means to disrupt the packing efficiency and to permit mesomorphic transition to occur at lower temperatures.³⁸ The purpose co-, ter- and tetrapolyesters described in this section is to evaluate whether any downturn in thermal transition temperatures arise and if so the extent to which this occurs relative to structural randomisations and the relative effectiveness of different flexible spacers etc. Homopolyesters discussed in Sections 4.1 to 4.3 consist of ordered array of mesogen and flexible spacers of definite lengths along the polymer chain and are hence termed ordered polyesters while copolyesters are randomised by variations in the sequencing of flexible spacers of differing lengths along the chain. Odd methylene unit flexible spacers cause a shift of 55° between adjacent mesogens. This shift is absent in even methylene spacers. Thus, another objective of the study is to observe, compare and relate the changes in crystal-liquid crystal transition temperatures in random copolyesters to those in the ordered polyesters of similar flexible spacer length.

The synthesis scheme for bis-[4-hydroxy benzoyl oxy]-1,4-benzene is depicted in Figure 19 and is presented in Section 2.2.8. The syntheses of acid chlorides are presented in Sections 2.2.1 to 2.2.7. Synthesis of homo-, co-, ter, and tetrapolyesters of bis-[4-hydroxy benzoyl oxy]-1,4-benzene with the different aliphatic acid chlorides were conducted using low temperature solution polycondensation methodology under inert atmosphere. This is presented in Section 2.3.1.

Inherent viscosities of homo-, co-, tri- and tetrapolyesters could not be determined since these were not soluble in chloroform, carbon tetrachloride, dichloromethane, dichloroethane, 4-chloro phenol, 1-chloro phenol or phenol:tetrachloro ethane (50:50, wt./wt.) mixed solvent. Molecular weights of these homo-, co-, ter- and tetrapolyesters

would be low since the synthesis was by solution polycondensation methodology. Thermal transitions were estimated with Mettler DSC-30 under nitrogen blanket with a heating or cooling rate of 10°C/minute. Second heating cycle was used for characterisation. The temperature corresponding to the endothermic peak maxima was taken as the transition temperature. The ΔH and ΔS values were estimated, based on Indium ($\Delta H_m = 6.8$ cal/gm), from endothermic peak areas and sample mass.

A Leitz ortholux polarising microscope with Mettler FP-52 hot stage was used for visual examination of phase changes. All homo-, co-, ter- and tetrapolyesters formed turbid melts that showed strong stir-opalescence up to isotropisation or clearing temperature, T_i , and displayed threaded schlieren textures typical of nematic phase.

4.4.1 Copolyesters of BHBOB Mesogen

The thermodynamic parameters of copolyesters synthesised from even methylene unit containing flexible spacers are presented in Tables 25 and 26. Similar parameters of copolyesters based on odd number of methylene units are presented in Table 27. These parameters of random copolyesters are compared with those of ordered homopolyesters of similar flexible spacer lengths in Table 28 and 29. Discussions are presented in Sections 4.4.1.1 to 4.4.1.3.

4.4.1.1 Copolyesters from Even Methylene Units

Copolyesters were synthesised from aliphatic diacids with 4, 6, 8 and 10 methylene units. Combinations of these were used in 25/75, 50/50 and 75/25 mole ratios. Thermodynamic parameters of sets of copolyesters prepared from the aliphatic diacid combination with 4/6, 4/8 and 4/10 methylene units are presented (in bold) in Table 25. Similarly, those pertaining to copolyesters from the combinations 6/8, 6/10 and 8/10 methylene units are shown (in bold) in Table 26. The parameters of ordered homopolyesters are incorporated for easy comparison. While exceptions are indeed

Table - 25

Transition Temperatures and Thermodynamic Data of BHBOB Homo- and Copolyesters: Effect of Structural Randomisation with flexible spacers of even number of methylene units - 1

Code No.	K-N [°C]	N-I [°C]	ΔT [°C]	ΔH K-N	ΔH N-I	ΔS K-N	ΔS N-I	$[\text{CH}_2]_n$ n	DOC %
PE-1	207.5	293.1	85.2	3.50	2.67	7.14	4.79	4	60.00
PE-16	187.4	305.7	118.3	4.01	4.76	8.08	8.22	4.5	56.37
PE-9	191.4	289.9	98.5	3.70	2.09	7.96	3.71	5	63.12
PE-15	189.7	281.2	91.5	4.69	6.32	10.09	11.46	5.5	68.73
PE-2	203.0	299.8	96.8	5.12	6.16	10.75	10.80	6	64.12
PE-1	207.5	293.1	85.2	3.50	2.67	7.14	4.79	4	60.00
PE-18	185.7	303.7	118.0	3.55	3.85	7.74	7.07	5	64.22
PE-10	179.2	279.6	100.4	4.83	3.18	10.68	5.75	6	66.27
PE-17	171.8	282.0	110.2	10.04	5.02	22.57	9.03	7	62.62
PE-4	176.1	304.6*	128.5*	4.50	5.82	10.02	10.07	8	62.80
PE-1	207.5	293.1	85.2	3.50	2.67	7.14	4.79	4	60.00
PE-20	191.8	281.7	89.9	4.08	5.54	8.65	8.89	5.5	62.70
PE-11	189.6	285.2	96.2	5.32	6.78	11.30	12.13	7	66.78
PE-19	179.6	273.6	94.0	1.89	7.49	4.18	13.70	8.5	53.64
PE-5	201.0 ^a	291.2 ^b	90.2	4.63 ^a	5.83 ^b	9.77 ^a	10.33 ^b	10	65.72

K-N, [°C] = Crystal-Liquid Crystal Transition Temperature; N-I, [°C] = Liquid Crystal-Isotropic Transition Temperature; ΔT , [°C] = Temperature Range of Mesophase Stability; ΔH , K-N and N-I = Enthalpy change in Kilo-Joule/mole of repeat unit (mru); ΔS , K-N and N-I = Entropy change in Joule/(mru)(°K); DOC = Percent Degree of Crystallinity; **a** = Crystal-Smectic transition temperature in [°C]; **b** = Smectic-Isotropic transition temperature in [°C]; * = Isotropisation and decomposition processes occur in parallel.

Table - 26

Transition Temperatures and Thermodynamic Data of BHBOB Homo- and Copolyesters: Effect of Structural Randomisation with flexible spacers of even number of methylene units - 2

Code No.	K-N [°C]	N-I [°C]	ΔT [°C]	ΔH K-N	ΔH N-I	ΔS K-N	ΔS N-I	$[\text{CH}_2]_n$	DOC %
PE-2	203.0	299.8	96.8	5.12	6.16	10.75	10.80	6	64.12
PE-22	197.8	349.9*	152.8*	2.18	1.64	4.64	2.64	6.5	63.78
PE-12	191.6	305.6	114.0	4.78	8.74	10.25	15.11	7	61.63
PE-21	185.2	299.6	114.4	4.99	10.13	10.89	17.69	7.5	60.43
PE-4	176.1	304.6*	128.5*	4.50	5.82	10.02	10.07	8	62.80
PE-2	203.0	299.8	96.8	5.12	6.16	10.75	10.80	6	64.12
PE-24	199.7	301.8	102.1	4.32	7.03	9.13	12.23	7	68.44
PE-13	191.5	349.8*	158.3*	4.55	9.15	9.79	14.69	8	63.33
PE-23	169.9	269.8	102.2	7.35	13.52	16.54	16.82	9	61.07
PE-5	201.0 ^a	291.2 ^b	90.2	4.63 ^a	5.83 ^b	9.77 ^a	10.33 ^b	10	65.72
PE-4	176.1	304.6*	128.5*	4.50	5.82	10.02	10.07	8	62.80
PE-26	219.5	285.7	66.2	5.14	7.85	11.78	14.07	8.5	61.76
PE-14	167.2	301.7	134.5	5.20	10.61	11.80	17.82	9	60.35
PE-25	209.6	329.8	120.2	5.76	8.44	11.92	14.00	9.5	71.90
PE-5	201.0 ^a	291.2 ^b	90.2	4.63 ^a	5.83 ^b	9.77 ^a	10.33 ^b	10	65.72

K-N, [°C] = Crystal-Liquid Crystal Transition Temperature; N-I, [°C] = Liquid Crystal-Isotropic Transition Temperature; ΔT , [°C] = Temperature Range of Mesophase Stability; ΔH , K-N and N-I = Enthalpy change in Kilo-Joule/mole of repeat unit (mru); ΔS , K-N and N-I = Entropy change in Joule/(mru)(°K); DOC = Percent Degree of Crystallinity; a = Crystal-Smectic transition temperature in [°C]; b = Smectic-Isotropic transition temperature in [°C]; * = Isotropisation and decomposition processes occur in parallel.

seen, structural randomisation due to copolymerisation decreases the crystal-liquid crystal transition temperature in most cases. Similarly, the isotropisation temperatures are also retarded. It becomes somewhat difficult to identify the isotropisation temperature in some copolyesters. This tends to result in higher values, probably due to identifying degradation onset as isotropisation. An important observation was the rather high degree of crystallinity in these copolyesters. Mesogen is able to accommodate these structural variations, even when the number of methylene units in the two spacers used varied widely. This is seen in polyesters PE-11, PE-19 and PE-20 in the 4/10 system presented in Table 25. This high degree of crystallinity could also be concluded from the inability to dissolve in chlorinated solvents. Interestingly, this solubilisation could be easily induced by methyl and chloro substitutions on the mesogen. Additionally, if shifts in degree of crystallinity could be rationalised to mean disruption of packing into a regular three-dimensional crystalline lattice, maximum disruption is not always observable, as anticipated, for 50/50 copolyesters PE-9, PE-10, PE-11, PE-12, PE-13 and PE-14 respectively. However, PE-14, a 50/50 composition of 8/10 methylene spacers (Table 26) has the lowest crystal-liquid crystal transition temperature.

Copolyesterification effect is specifically observed on crystal-liquid crystal transition temperature, T_m and only marginally on clearing (isotropisation) temperature, T_i . Copolyesters synthesised from flexible spacers with 4 and 6 methylene units show a decrease in T_i with increase in average length of the flexible spacer (PE-15 < PE-9 < PE-16). Reduction in clearing temperature with increased spacer length is due to increase in the number of possible conformations for longer spacer which distort the cylindrical shape of the molecules. This observation could be noted in most copolyester sets. Copolyester PE-22, synthesised from flexible spacers with 4 and 8 methylene units (Table 26), shows extremely high T_i . This is probably due to an error

in estimating isotropisation since decomposition is occurring in parallel. Similar interpretation can be made for copolyesters PE-13 and PE-25 as well. Mesophase stability (ΔT) decreases with increase in spacer length. This is purely due to dilution of mesogen. It also reduces the degree of crystallinity. Most copolyesters have higher ΔT than parent ordered homopolyester.

In the copolyesters enthalpy change arising from crystal-liquid crystal transition, ΔH_m , tends to be lower than that observable for the corresponding homopolyesters. Randomisation marginally lowers the packing efficiency and hence degree of crystallinity. The ΔH_m values increase with length of flexible spacer. There are some deviations, as seen from Table 25, which can not be explained from the current set of data on the basis of degree of crystallinity alone. Thus, the ΔH_m value is abnormally for PE-17 while PE-19 shows extremely low value.

As a general trend, enthalpy change on isotropisation, ΔH_i , for most copolyesters are higher. This points to a high degree of order even in melts of these randomised copolyesters. The ΔH_i values tend to increase with the length of the averaged flexible spacer. This is an interesting observation and seems to imply incorporation of the nonmesogenic flexible spacer into the liquid crystalline phase.

4.4.1.2 Copolyesters from Odd Methylene Units

Four copolyesters were synthesised to investigate whether copolymerising two flexible spacers with odd number of methylene would decrease the crystal-liquid crystal transition temperature appreciably. The data is presented in Table 27. As indicated earlier, these flexible spacers tend to tilt the successive mesogenic units by an angle of 55° . Three aliphatic diacids, with 3, 5 and 7 methylene units were used. Though the data is not sufficient enough to make unambiguous observations, it can be stated that crystal-liquid crystal transition temperatures are marginally lowered, temperature

Table - 27

**Transition Temperatures and Thermodynamic Data of BHBOB Copolyesters:
Effect of Structural Randomisation with flexible spacers of odd number of methylene units.**

Code No.	K-N [°C]	N-I [°C]	ΔT [°C]	ΔH K-N	ΔH N-I	ΔS K-N	ΔS N-I	$[\text{CH}_2]_n$	DOC %
PE-7	197.5	320.8	123.3	3.26	5.63	6.93	13.98	3	50.00
PE-35	161.6	295.7	134.1	6.69	3.99	15.40	7.02	5	39.89
PE-36	159.7	307.9	148.2	5.86	5.52	3.52	9.50	6	50.87
PE-3	169.6	304.8*	135.2*	5.98	10.30	13.51	17.82*	7	56.02
PE-7	197.5	320.8	123.3	3.26	5.63	6.93	13.98	3	50.00
PE-51	201.6	327.2*	125.6*	4.18	6.96	8.80	11.14	4	-
PE-6	187.2	291.1	103.9	8.54	7.74	18.55	14.18	5	70.00
PE-6	187.2	291.1	103.9	8.54	7.74	18.55	14.18	5	70.00
PE-52	169.7	279.6	109.9	5.82	5.03	13.14	9.10	6	-
PE-3	169.6	304.8*	135.2*	5.98	10.30	13.51	17.82*	7	56.02

K-N, [°C] = Crystal-Liquid Crystal Transition Temperature; N-I, [°C] = Liquid Crystal-Isotropic Transition Temperature; ΔT , [°C] = Temperature Range of Mesophase Stability; ΔH , K-N and N-I = Enthalpy change in Kilo-Joule/mole of repeat unit (mru); ΔS , K-N and N-I = Entropy change in Joule/(mru)(°K); DOC = Percent Degree of Crystallinity; * = isotropisation and decomposition processes are parallel.

range of mesophase stability are enhanced and degree of crystallinity are decreased. This is also reflected in the enthalpy change on isotropisation. It can be qualitatively stated that odd methylene units do disrupt crystallisation as well as liquid crystallinity more appreciably than flexible spacers with even number of methylene units.

4.4.1.3 Copolyesters With Same Averaged Spacer Length

In this Section randomised copolyesters synthesised from two different aliphatic diacids which result in same values for averaged flexible spacer length are compared with parent ordered homopolyesters of similar spacer lengths. The same averaged values could be generated from combinations of two even or two odd methylene spacer units. This averaged mesogen lengths can also be generated from ter- and tetrapolyesters. The thermodynamic data are presented in Tables 28 and 29 in the order of increasing spacer lengths. The data for parent homopolyesters are also depicted for comparison. We now examine these systems individually on the basis of averaged flexible spacer lengths, the origin of these spacer lengths and relate the observed crystal-liquid crystal transition temperatures to these structural variations, which otherwise globally generate the same averaged repeat structures.

Polymers PE-1 and PE-51, presented in Table 28, have similar repeating structure consisting of 4 methylene units. PE-1 is ordered polyester while PE-51 is a 50/50 copolyester of 3/5 methylene units. The odd number of methylene units in the copolyester would tilt the adjacent mesogens present along the chain. In addition, the induced randomisation should decrease the degree of crystallinity. These two factors ought to work synergistically to depress the crystal-liquid crystal transition temperature. A depression of 6.3°C noted here can only be termed as marginal. The higher isotropisation temperature observed for the copolymer is marred by a concurrent decom-

Table - 28

Transition Temperatures and Thermodynamic Data of BHBOB Homo, Co- and Terpolyesters: Similar Averaged Flexible Spacer Length from Different Aliphatic Diacids - 1

Code No.	K-N [°C]	N-I [°C]	ΔT [°C]	ΔH K-N	ΔH N-I	ΔS K-N	ΔS N-I	$[\text{CH}_2]_n$	DOC %
PE-1	207.9	293.1	85.2	3.00	2.67	7.14	4.79	4	64.12
PE-51	201.6	327.2*	125.6*	4.18	6.96	8.80	11.14	4	-
PE-6	187.2	291.1	103.9	8.54	7.14	18.55	14.18	5	70.00
PE-9	191.4	289.9	98.5	3.70	2.09	7.96	3.71	5	63.12
PE-18	185.7	303.7	118.0	3.55	3.85	7.74	7.07	5	64.22
PE-35	161.6	295.7	134.1	6.69	3.99	15.40	7.02	5	39.89
PE-15	189.7	281.2	91.5	4.69	6.32	10.09	11.46	5.5	68.73
PE-20	191.8	281.7	89.9	4.08	5.54	8.65	8.89	5.5	62.70
PE-2	203.0	299.8	96.8	5.12	6.16	10.75	10.80	6	64.12
PE-10	185.6	289.7	104.1	1.91	0.74	10.53	1.32	6	66.27
PE-36	159.7	307.9	148.2	5.86	5.52	3.52	9.50	6	51.87
PE-52	169.7	279.6	109.9	5.82	5.03	13.14	9.10	6	-
PE-27	157.1	285.7	128.6	6.94	3.90	15.99	6.92	6	61.19

K-N, [°C] = Crystal-Liquid Crystal Transition Temperature; N-I, [°C] = Liquid Crystal-Isotropic Transition Temperature; ΔT , [°C] = Temperature Range of Mesophase Stability; ΔH , K-N and N-I = Enthalpy change in Kilo-Joule/mole of repeat unit (mru); ΔS , K-N and N-I = Entropy change in Joule/(mru)(°K); DOC = Percent Degree of Crystallinity; * = Isotropisation and decomposition processes occur in parallel; - = not observed.

position. Interestingly, the enthalpy change accompanying the crystal-liquid crystal transition for the copolyester is also larger than that noted for the ordered homopolyester.

Copolyesters PE-9, PE-18 and PE-35 with an averaged pentamethylene spacer are compared with ordered homopolyester PE-6 in Table 28. Here, copolyester PE-9 is a 50/50 combination of 4/6 methylene units, Copolyester PE-18 is 75/25 combination of 4/8 while PE-35 is 50/50 combination of 3/7 units. Very interesting set of data emerge for this system. As indicated earlier, the odd pentamethylene unit in homopolyester PE-6 would tilt adjacent mesogens along the chain. In copolyesters PE-9 and PE-18, from even number of methylene units, this tilt between adjacent mesogens would not be present while structural randomisation arising from copolymerisation would disrupt the packing efficiency. In the copolyester based on odd methylene units (PE-35) both tilt and randomisation would be operating along the chain. The effectiveness of these parameters are qualitatively reflected in the crystal-liquid crystal transition temperatures. Generation of an averaged odd number of methylene units through copolymerisation of even number of methylene units in fact increases the transition temperature (PE-9) or decreases only marginally (PE-18). Here, PE-9 is built from combination of 4/6 methylene units, while PE-18 is built from combination of 4/8. When the lengths of the flexible moieties differ appreciably (4/6 versus 4/8), greater disruption in packing probably occurs. However, the degree of crystallinity for these two copolyesters are very similar within experimental errors. Truly amazing is the depression of over 25°C observable for copolyester PE-35 built up from odd number of methylene units. Here, the degree of crystallinity is also depressed considerably. The temperature range of mesophase stability (134°C) is also very large.

Polyesters PE-15 and PE-20 have an averaged flexible spacer length of 5.5. Of these, PE-15 is 25/75 combination of 4/6 methylenes while PE-20 is by 75/25

combination of 4/10. Polyester PE-20 is complicated by the possible onset of smectic phase due to the presence of decamethylene unit along the chain. Polarising microscopic observations revealed texture corresponding to a typical nematic phase, never the less. These two differ only marginally in the transition temperatures and thermodynamic parameters. However, the degree of crystallinity of polyester PE-20, comprising of widely varying spacer lengths, is lower.

Polyesters with an averaged hexamethylene spacer are examined next, in Table 28. Homopolymer PE-2 is compared with copolyesters PE-10 (50/50 of 4/8), PE-36 (25/75 of 3/7) and PE-52 (50/50 of 5/7) as well as terpolymer PE-27 (33/33/33 of 4/6/8). All randomisation procedures (co- and terpolymerisation) depress the crystal-liquid crystal transition temperature. This depression is least when effected with other even methylene units (PE-10), large with odd methylene units (PE-52), more so when the lengths of the odd methylene units differ appreciably (PE-36) and is maximum with terpolymer (PE-27). The temperature range of mesophase stability is largest and simultaneously the degree of liquid crystallinity is lowest with copolymer PE-36, built up from odd number of methylene units. Terpolymerisation of flexible spacers with even number of methylene units depresses the degree of crystallinity only marginally. Quantitative estimates need to be made from high temperature x-ray to establish the molecular origins for the presumably conflicting data for the terpolymer, of greatest depression but without appreciable change in crystallinity.

Data extracted for polyesters with an averaged heptamethylene (7) spacer are presented in Table 29. Homopolymer PE-3 is compared with copolyesters PE-17 (25/75 of 4/8), PE-11 (50/50 of 4/10), PE-12 (50/50 of 6/8), PE-24 (75/25 of 6/10) as well as tetrapolymer PE-31 (25/25/25/25 of 4/6/8/10). Here too the observations are akin to those noted for the odd pentamethylene spacer. All randomisation procedures effected through copolymerisations of even methylene units brought about a

Table - 29

Transition Temperatures and Thermodynamic Data of BHBOB Homo-, Co-, Ter- and Tetrapolyesters: Similar Averaged Flexible Spacer Length from Different Aliphatic Diacids - 2

Code No.	K-N [°C]	N-I [°C]	ΔT [°C]	ΔH K-N	ΔH N-I	ΔS K-N	ΔS N-I	$[\text{CH}_2]_n$ n	DOC %
PE-3	169.6	304.8	135.2	5.98	10.30	13.51	17.82	7	56.02
PE-17	171.8	282.0	110.2	10.04	5.02	22.57	9.03	7	62.62
PE-11	189.6	285.6	96.2	5.32	6.78	11.30	12.13	7	66.78
PE-12	191.6	305.6	114.0	4.78	8.74	10.25	15.11	7	61.63
PE-24	199.7	301.8	102.1	4.32	7.03	9.13	12.23	7	68.44
PE-31	147.4	310.5	154.1	5.92	8.14	14.08	14.16	7	65.65
PE-4	176.1	304.6*	128.5*	4.50	5.82	10.02	10.07	8	62.80
PE-13	191.5	349.8*	158.3*	4.55	9.15	9.79	14.69*	8	63.33
PE-30	171.3	293.7	223.4	16.47	14.46	37.06	25.52	8	63.25
PE-19	179.6	273.6	94.0	1.89	7.49	4.18	13.70	8.5	53.64
PE-26	219.5	285.7	66.2	5.14	7.85	11.78	14.07	8.5	61.76
PE-23	169.9	269.8	102.2	7.35	13.52	16.54	16.82	9	61.07
PE-14	167.2	301.7	134.5	5.20	10.61	11.80	17.82	9	60.35

K-N, [°C] = Crystal-Liquid Crystal Transition Temperature; N-I, [°C] = Liquid Crystal-Isotropic Transition Temperature; ΔT , [°C] = Temperature Range of Mesophase Stability; ΔH , K-N and N-I = Enthalpy change in Kilo-Joule/mole of repeat unit (mru); ΔS , K-N and N-I = Entropy change in Joule/(mru)(°K); DOC = Percent Degree of Crystallinity; * = Isotropisation and decomposition processes occur in parallel.

reversal of that anticipated, judging from literature reports. In fact, with most systems the increase in the crystal-liquid crystal transition temperature are quite appreciable. Depression is, however, effected through tetrapolyesterification with even number of methylene units. The temperature range of mesophase stability for this tetrapolyester (154°C) is probably the highest ever observed for any rigid rod-flexible spacer type thermotropic liquid crystalline polymer. Another exciting observation is the retention of high degree of crystallinity in all random polyesters. The adjacent mesogens in the ordered parent homopolyester with heptamethylene spacer are tilted while in copolyesters with even number of methylene units this is absent. This shift in tilt angle contributes more effectively in depressing crystal-liquid crystal transition temperature than randomisation effected through copolymerisation. This system needs to be probed in greater depth using experimental techniques such as high temperature x-ray and electron microscopy. Data for randomised copolyester systems with an averaged 8, 8.5 and 9 methylene units are also presented in Table 29. The trend noted for these systems are similar to that observed for other spacer lengths.

4.4.2 Ter- and tetrapolyesters of BHBOB Mesogen

The thermodynamic data for tri- and tetrapolyesters prepared from even number of methylene unit (4, 6, 8 and 10) containing aliphatic diacids are presented in Table 30 and compared with the parent ordered homopolyesters. Here, PE-1, PE-2, PE-4 and PE-5 are the ordered homopolyesters; PE-27, PE-28, PE-29 and PE-30 are terpolyesters while PE-31 is tetrapolyester. The terpolyester compositions were as follows: PE-27 comprised of 4/6/8 methylene units in 33/33/33 mole ratio; PE-28 comprised of 4/6/10 methylene units in 33/33/33 mole ratio; PE-29 comprised of 4/8/10 methylene units in 33/33/33 mole ratio and PE-30 comprised of 6/8/10 methylene units in 33/33/33 mole ratio. The composition of the tetrapolyester was based on

Table - 30

Transition Temperatures and Thermodynamic Data of BHBOB Ter- and Tetrapolyesters: Effect of Structural with Even methylene Units

Code No.	K-N [°C]	N-I [°C]	ΔT [°C]	ΔH K-N	ΔH N-I	ΔS K-N	ΔS N-I	$[\text{CH}_2]_n$ n	DOC %
PE-1	207.5	293.1	85.2	3.50	2.67	7.14	4.79	4	60.00
PE-2	203.0	299.8	96.8	5.12	6.16	10.75	10.80	6	64.12
PE-4	176.1	304.6*	128.5*	4.50	5.82	10.02	10.07	8	62.80
PE-5	201.0 ^a	291.2 ^b	90.2	4.63 ^a	5.83 ^b	9.77 ^a	10.33 ^b	10	65.72
PE-27	157.1	285.7	128.6	6.94	3.90	15.99	6.92	6	61.19
PE-28	156.9	277.5	120.6	7.52	4.83	17.38	8.70	6.67	60.22
PE-29	171.3	287.6	116.3	15.22	6.85	34.25	12.21	7.33	59.86
PE-30	171.3	293.7	122.4	16.47	14.46	37.06	25.52	8	63.25
PE-31	147.7	301.5	154.1	5.92	8.14	14.08	14.16	7	65.65

K-N, [°C] = Crystal-Liquid Crystal Transition Temperature; N-I, [°C] = Liquid Crystal-Isotropic Transition Temperature; ΔT , [°C] = Temperature Range of Mesophase Stability; ΔH , K-N and N-I = Enthalpy change in Kilo-Joule/mole of repeat unit (mru); ΔS , K-N and N-I = Entropy change in Joule/(mru)(°K); DOC = Percent Degree of Crystallinity; * = isotropisation and decomposition processes are parallel.

25/25/25/25 mole ratio of 4/6/8/10 methylene units. The averaged spacer lengths are also presented. The transition temperatures in these terpolyesters are compared with that of the parent ordered homopolyesters as well as relative to each other.

The crystal-liquid crystal transition temperatures are depressed by terpolymerisation (relative to ordered homopolyesters). Only a marginal depression in degree of crystallinity and the isotropisation temperature are observed. As a result, the temperature range of mesophase stability is enhanced. A comparison of ΔH_{K-N} and ΔH_{N-I} values in homopolyesters and terpolyesters reveals that the relative order in the liquid crystalline state (degree of liquid crystallinity) of the terpolyesters are lower. Terpolyesters show lower T_m values relative to random copolyesters due to greater randomisation of polymer chain structures. All terpolyesters (PE-27 to PE-30) show higher ΔT than copolyesters as well.

An unusual observation within terpolyesters relative to averaged flexible spacer length is that crystal-liquid crystal transition temperature (T_m) increases with flexible spacer length. Also, terpolyesters seem to show higher isotropisation temperature, T_i , with increasing spacer length. The ΔH_m and ΔS_m values increase for terpolyesters with increase in spacer length. These too point to lower degree of order in the mesophase with increase in spacer length. The lower degree of liquid crystallinity in terpolyesters (relative to ordered homopolyesters) is also revealed in the lower ΔS_i values compared to ΔS_j . The tetrapolyester PE-31, as discussed earlier, displays the highest temperature range of mesophase stability. However, the mesophase of this polyester seems to be highly ordered, as seen from enthalpy and entropy changes accompanying liquid crystalline and isotropic transitions.

4.4.3 Conclusion

Random co-, ter- and tetrapolyesters were synthesised. The thermal properties were examined relative to flexible spacer lengths within these as well as related to ordered polyesters of similar spacer lengths. The features that emerge for these random polyesters vary with the specific system under consideration. Depressions do manifest when the averaged mesogen is an even one. Very interesting and logical enhancements in the crystal-liquid crystal transition temperatures do arise when ordered mesogen with odd number of methylene unit are mimicked by copolyesters originating from combinations of even methylene units. This runs counter to the postulation in literature that copolyesterification is a universal means to depress transition temperatures. An unusually high and reproducible mesophase stability of 154°C is noted for tetrapolyester. Degree of crystallinity for copolyesters arising from even methylene units are also unusually high.

4.5 ISOTHERMAL CRYSTALLISATION

Thermotropic liquid crystalline copolyesters display an anisotropic melt.⁷⁴ Transition of this melt during crystallisation to the solid state usually leads to aggregation of the rigid chain segments.¹⁶³ Heterogeneous nucleation is observed in the crystallisation of many flexible, linear macromolecules from their melts. The overall process of macroscopic crystallisation can be described by an Avrami equation,¹⁸⁸ as presented in Section 3.2.5.1:

$$1 - V_c = \exp [-Kt^n] \quad [7]$$

V_c is the volume fraction of crystallinity, K is temperature dependant nucleation, t is crystallisation time and " n " is Avrami parameter. Kinetic estimations of Avrami

parameter have been reported for polyethylene [PE],^{225,226} polyethylene terephthalate,^{225,227} and poly[aryl ether ketone].²²⁸ Crystallisation kinetics of polymers reveal Avrami parameter "n" to be above 2. The Avrami parameter for flexible random copolyesters of ethylene terephthalate and ethylene sebacate [80:20 in molar ratio], has been found to be close to 3.

Kinetic study of isothermal crystallisations, from mesophasic melts of thermotropic liquid crystalline polymers, has shown the occurrence of transition processes. A fast transition process, characterised as "solidification", due to freezing-in (quenching) of the anisotropic melt. A slow transition process follows, which resembles the normal crystallisation process observable in crystalline thermoplastic polymers but has a low Avrami parameter "n".

4.5.1 Polyesters Investigated

The polyesters investigated for kinetic estimates of isothermal crystallisation from liquid crystalline melts were: PE-103, PE-203, PE-303 and PE-107. Polyesters PE-103, PE-203 and PE-303 were studied to investigate the effect of substitution on the mesogen. These comprised of the three different (methyl, unsubstituted and chloro) triad mesogens coupled through pentamethylene spacer. Here, the effect of differing axial ratios and polarities brought forth by substitution was investigated. The effect of flexible spacer length was examined by comparing polyesters PE-103 (with pentamethylene spacer) and PE-107, with decamethylene spacer. The experimental details of isothermal crystallisation kinetics are presented in Section 3.3.2. The temperatures at which the isothermal studies were conducted are presented in Table 18. The examination of the isothermal crystallisation process was an indirect one. It consisted of annealing the samples for varied times at the selected isothermal temperatures, reheating through the liquid crystal transition temperature and examining the transition temperatures as well as the ensuing enthalpy and entropy changes.

4.5.2 Low Temperature Regime

The two different temperature regimes were chosen for the study. These were arrived at from the crystal to liquid crystal transition temperatures observable in non-isothermal differential scanning calorimetric analysis experiment which is described in Section 3.3.1. Figures 35, 36, 41, 42, 47, 48, 53 and 54 show the occurrence of two different, fast and slow, transition processes in the four polyesters studied here. On the reheating cycle these manifest as two distinguishable endothermic peaks. The first melting peak, at higher temperature, displays linear relationship between heat of transition, ΔH and logarithmic crystallisation time $\log t_c$ represented in equation [10]. The heat of transition corresponding to the second melting peak at lower temperature increases with annealing time.

$$\Delta H_d(h, T_c, t_c) = A(T_c) \log t_c + B \quad [10]$$

Where, the parameter $A(T_c)$ is characterised by the velocity of transition.

The melting peak observable at higher temperature in the reheating cycle arises from melting of crystals formed by very fast crystallisation process which had grown to completion even before the chosen isothermal crystallisation temperature was attained, as seen from Figures. 35, 36, 41, 42, 47, 48, 53 and 54 The melting peak at lower temperature, on the other hand, corresponds to the slow process. Thus, fast transition process generally appeared at higher temperature, while slow transition process appeared at lower temperature. It has been well established that within a given polymeric system, less ordered crystalline forms melt at lower (show lower transition) temperatures while more ordered crystalline forms are displayed at higher transition (melt at higher) temperatures. This arises from the metastability of crystals due to kinetic effects such as crystal size, crystal defects, etc.²¹² From thermodynamic perspective, first order transition is determined by an interplay of $\Delta H/\Delta S$, where ΔH and

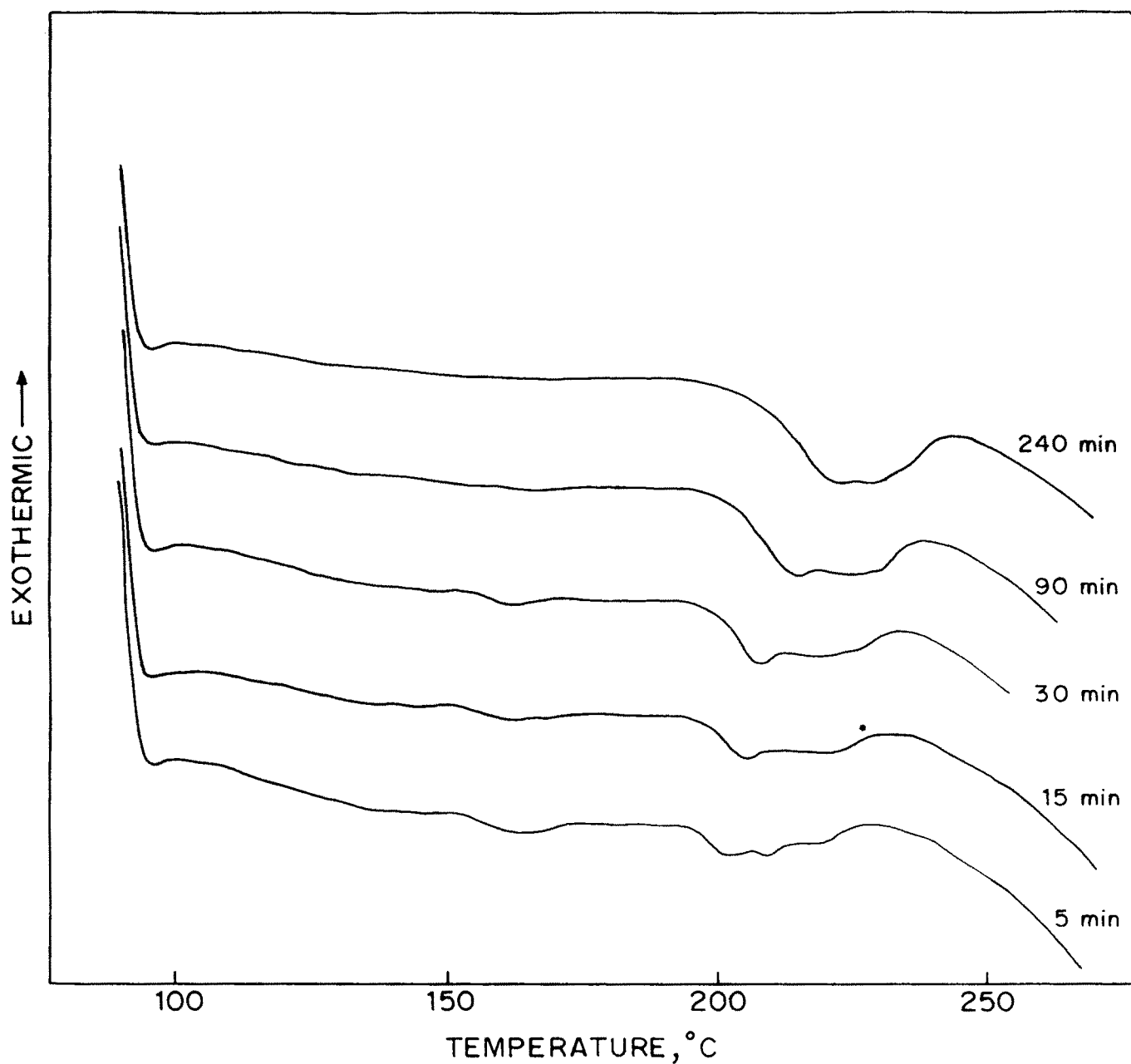


FIG. 35 A SET OF DSC HEATING TRACES IN DIFFERENT TIME PERIODS OF ISOTHERMAL EXPERIMENTS FOR COPOLYESTER PE-203 ($T_c = 191^\circ\text{C}$).

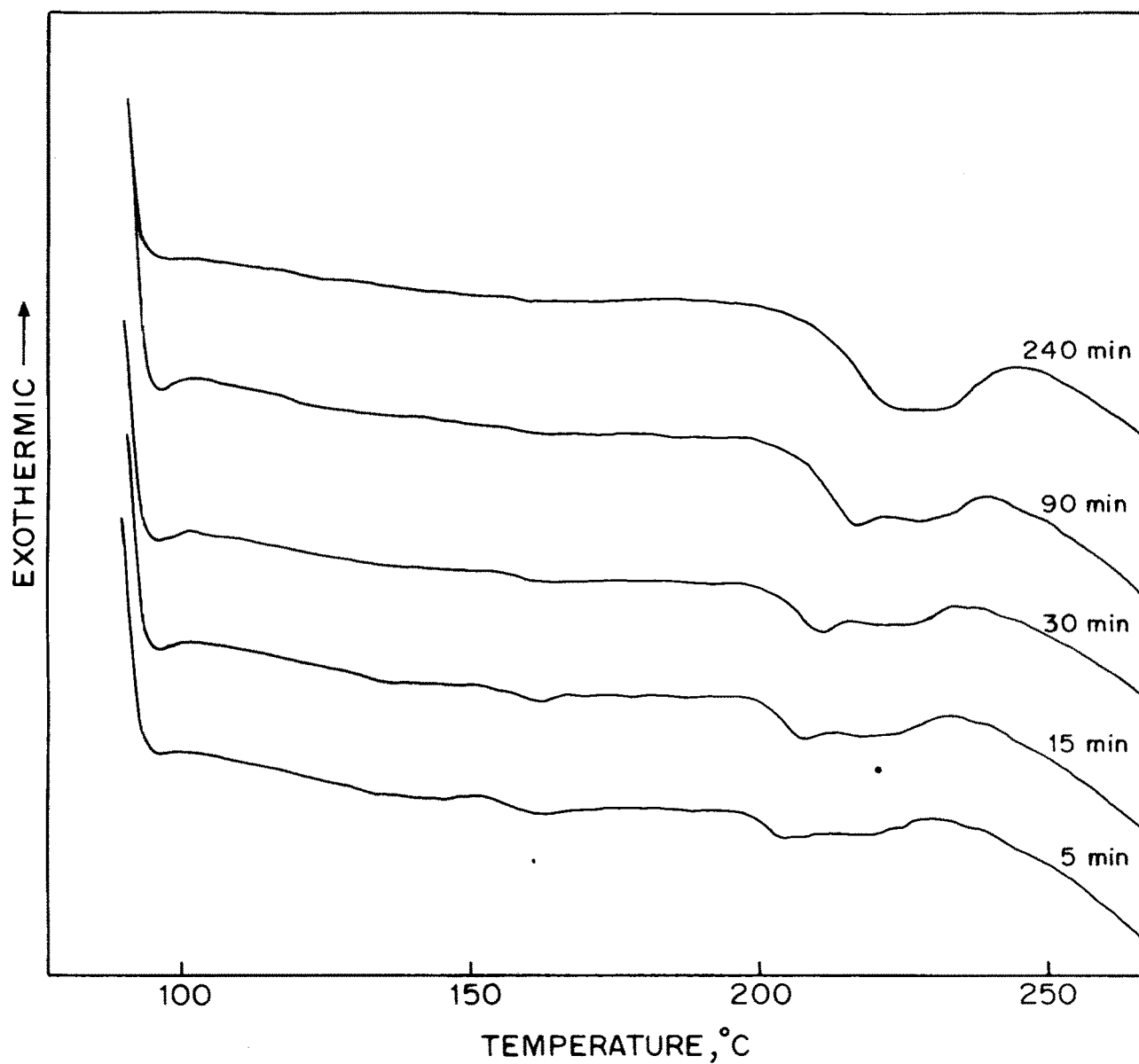


FIG. 36 A SET OF DSC HEATING TRACES IN DIFFERENT TIME PERIODS OF ISOTHERMAL EXPERIMENTS FOR COPOLYESTER PE-203 ($T_c = 194^\circ\text{C}$).

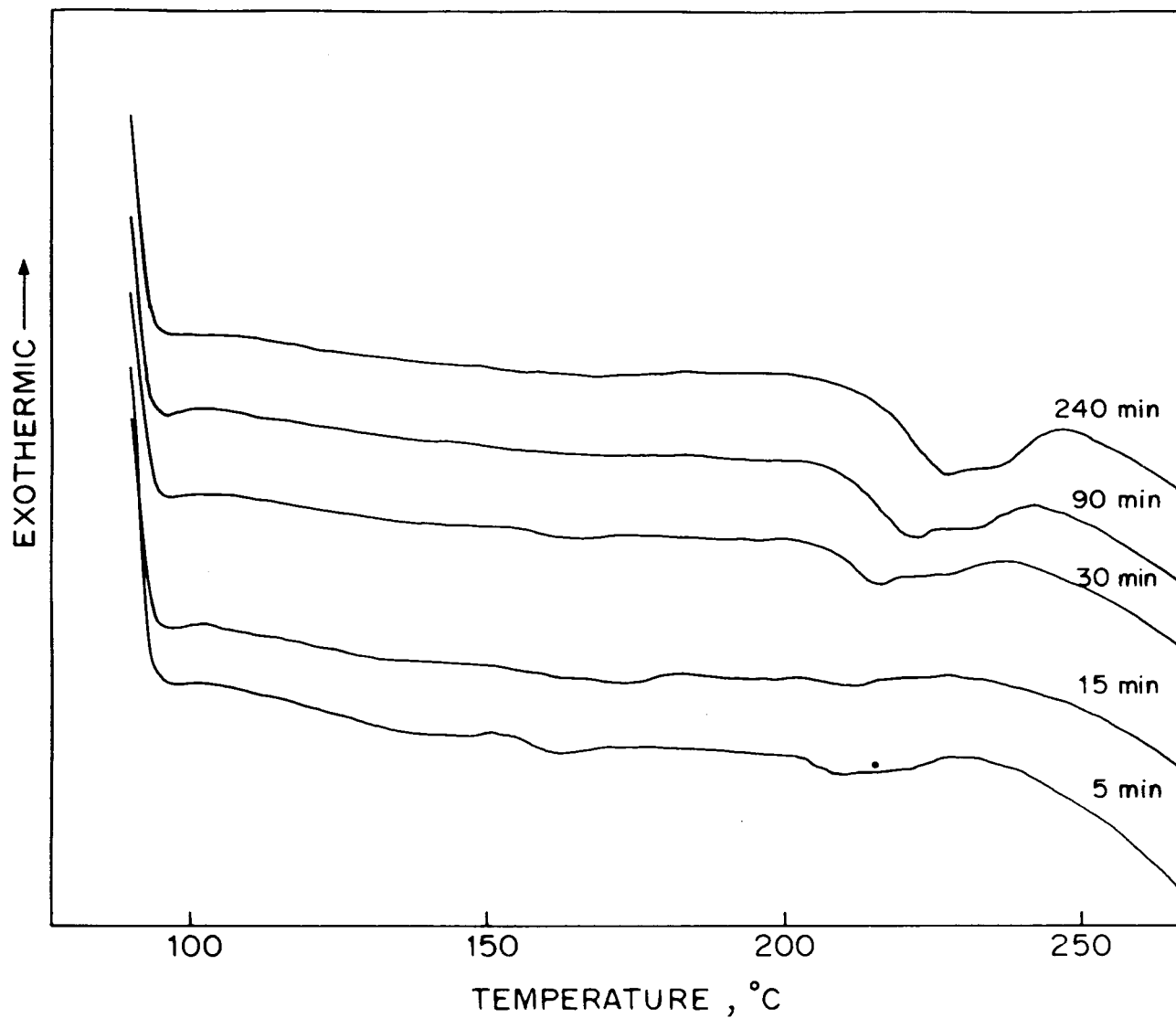


FIG. 37 A SET OF DSC HEATING TRACES IN DIFFERENT TIME PERIODS OF ISOTHERMAL EXPERIMENTS FOR COPOLYESTER PE-203 ($T_c = 198^\circ\text{C}$).

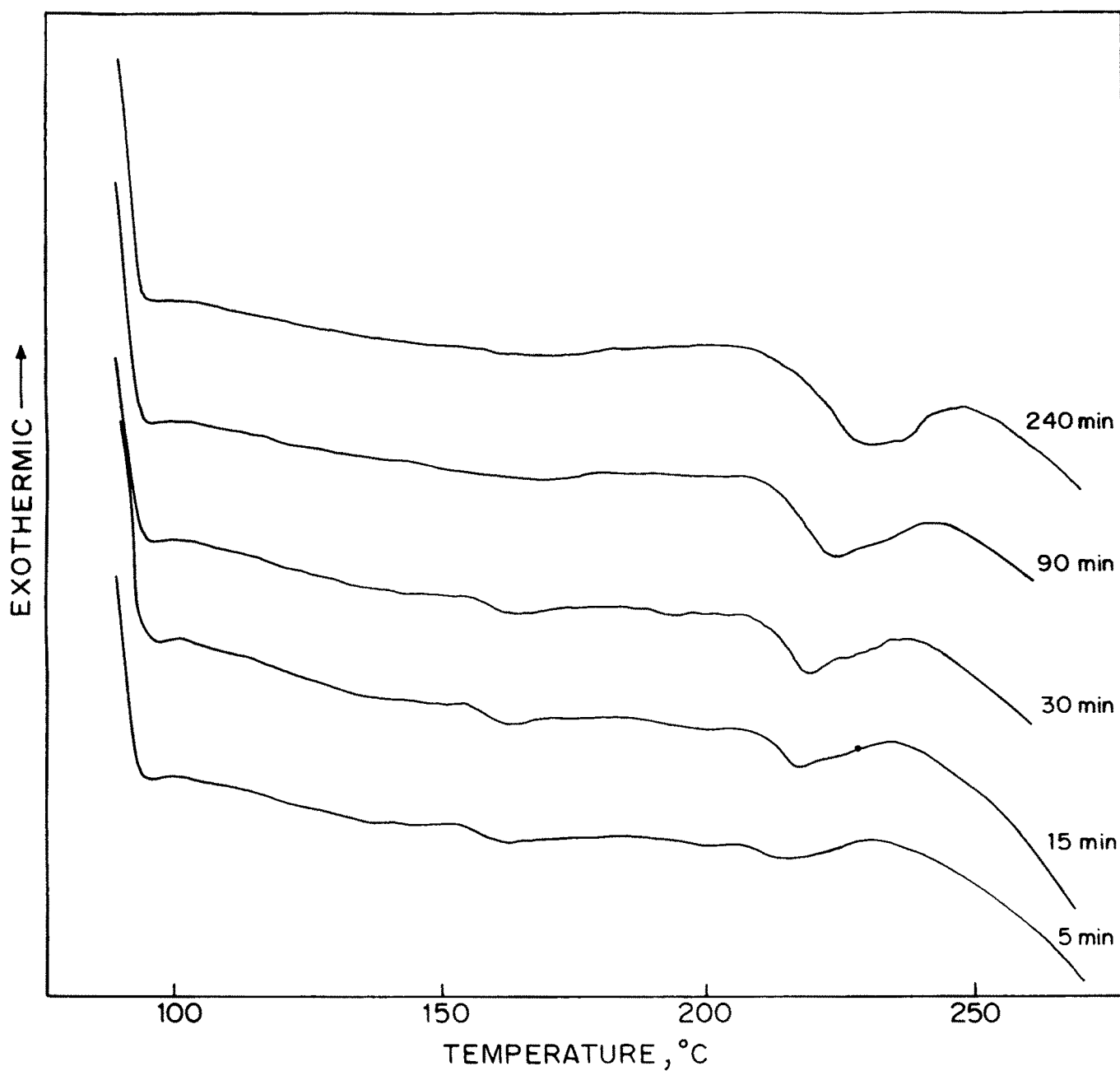


FIG. 38 A SET OF DSC HEATING TRACES IN DIFFERENT TIME PERIODS OF ISOTHERMAL EXPERIMENTS FOR COPOLYESTER PE-203 ($T_c = 202^\circ\text{C}$).

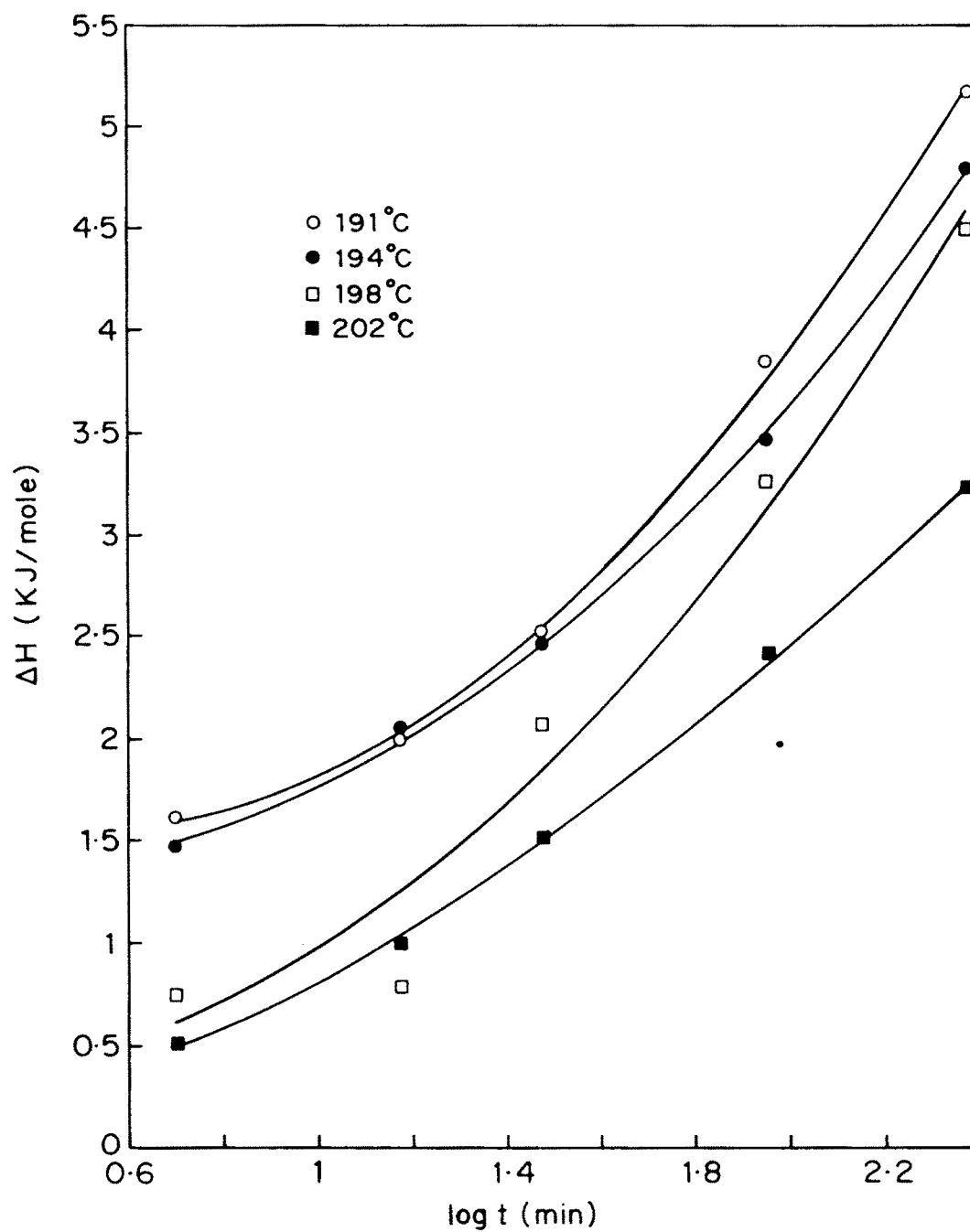


FIG. 39 THE PLOT OF ΔH VERSUS $\log t$ FOR POLYESTER PE-203.

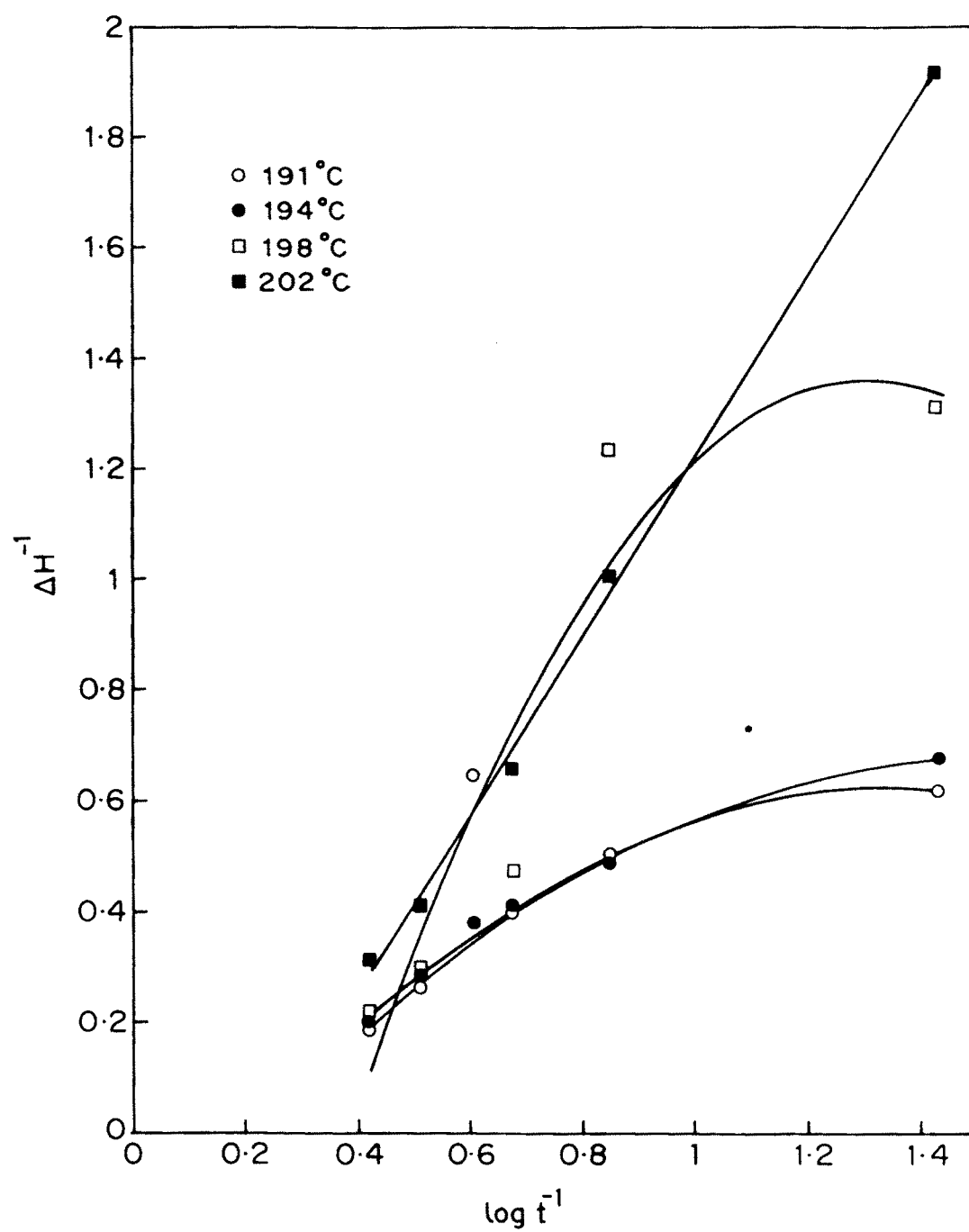


FIG. 40 THE PLOT OF ΔH^{-1} VERSUS $\text{Log } t^{-1}$ FOR POLYESTER PE-203.

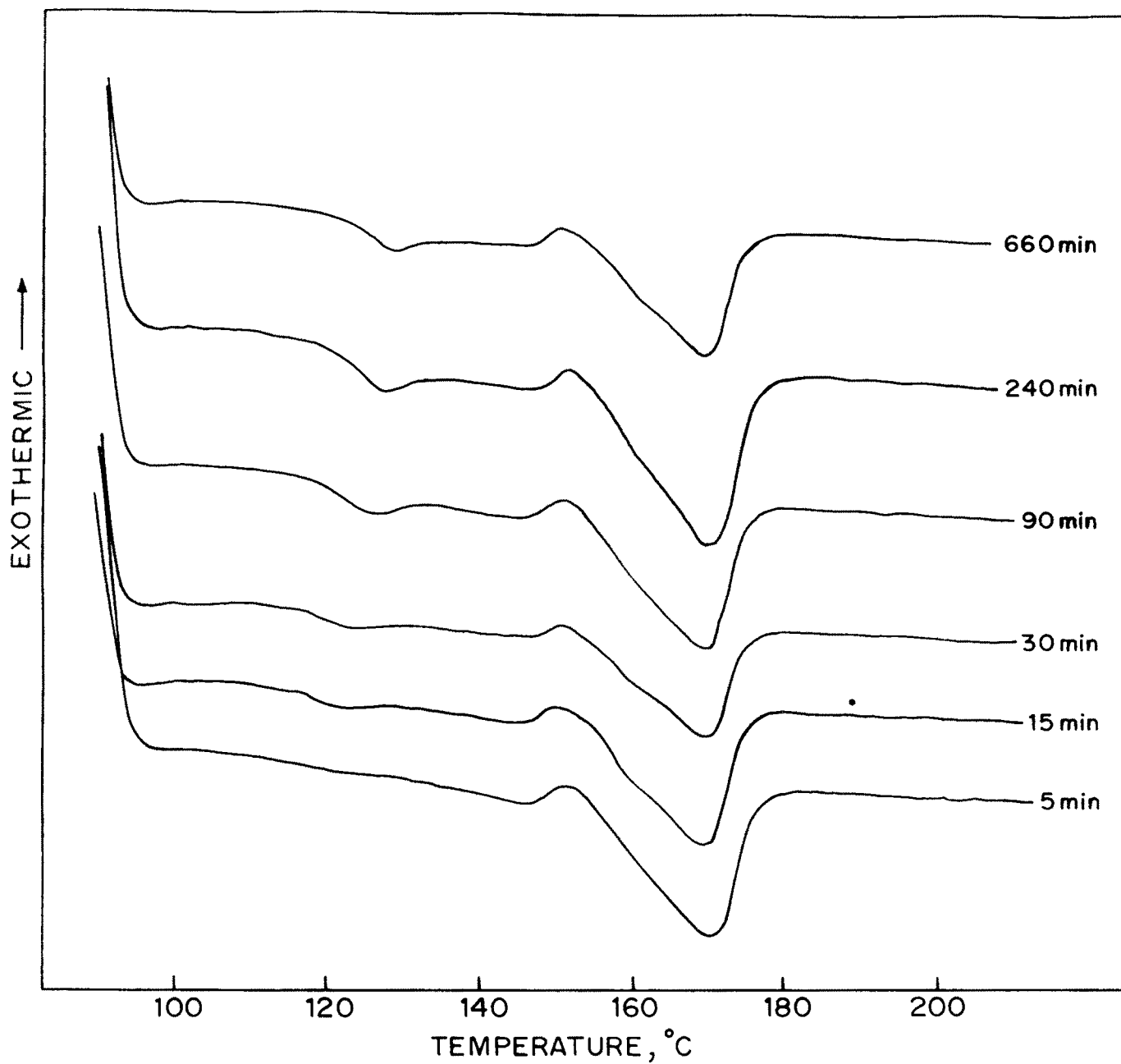


FIG. 41 A SET OF DSC HEATING TRACES IN DIFFERENT TIME PERIODS OF ISOTHERMAL EXPERIMENTS FOR COPOLYESTER PE-103 ($T_c = 110^\circ\text{C}$).

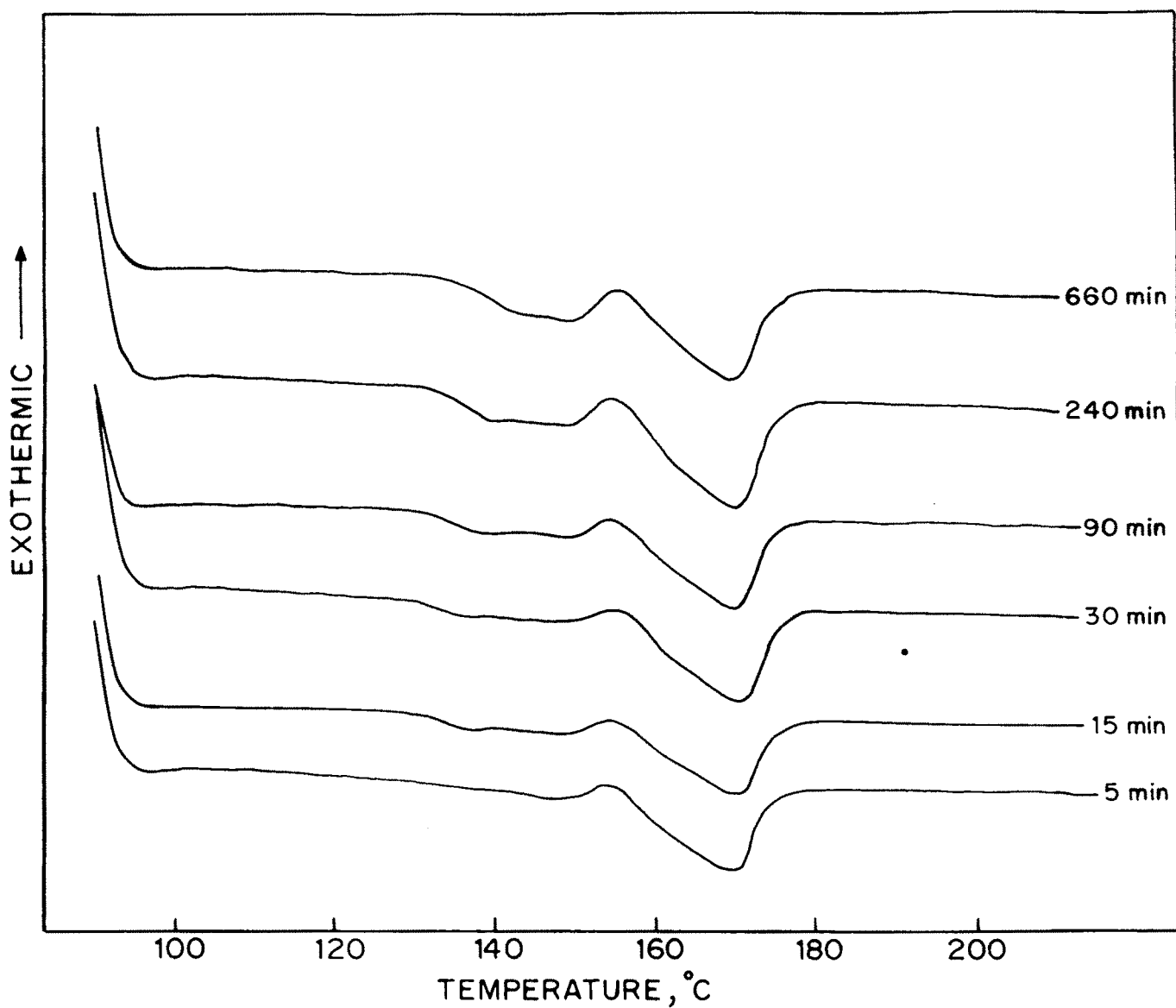


FIG. 42 A SET OF DSC HEATING TRACES IN DIFFERENT TIME PERIODS OF ISOTHERMAL EXPERIMENTS FOR COPOLYESTER PE-103 ($T_c = 125^\circ\text{C}$).

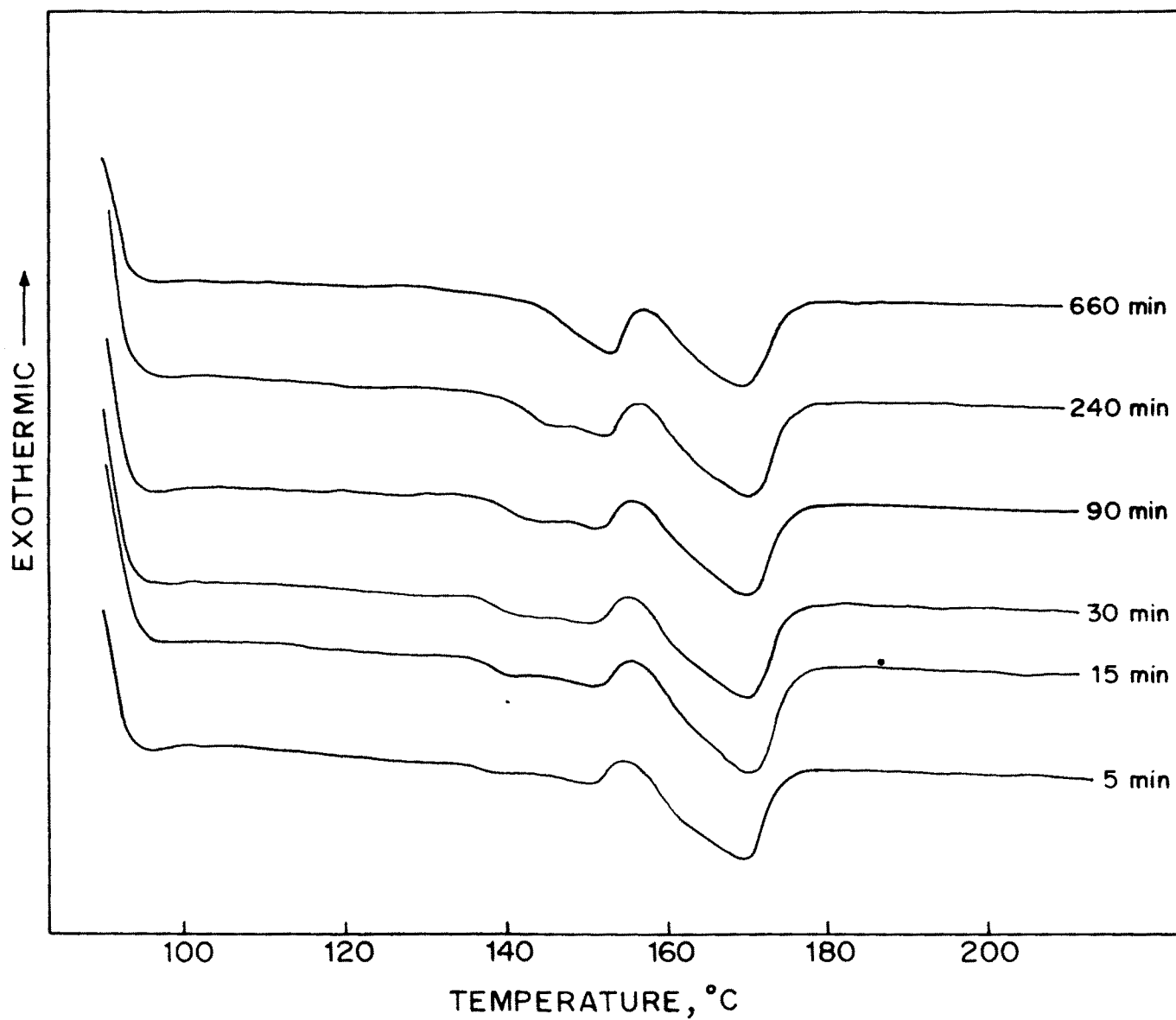


FIG. 43 A SET OF DSC HEATING TRACES IN DIFFERENT TIME PERIODS OF ISOTHERMAL EXPERIMENTS FOR COPOLYESTER PE-103 ($T_c = 131^\circ\text{C}$).

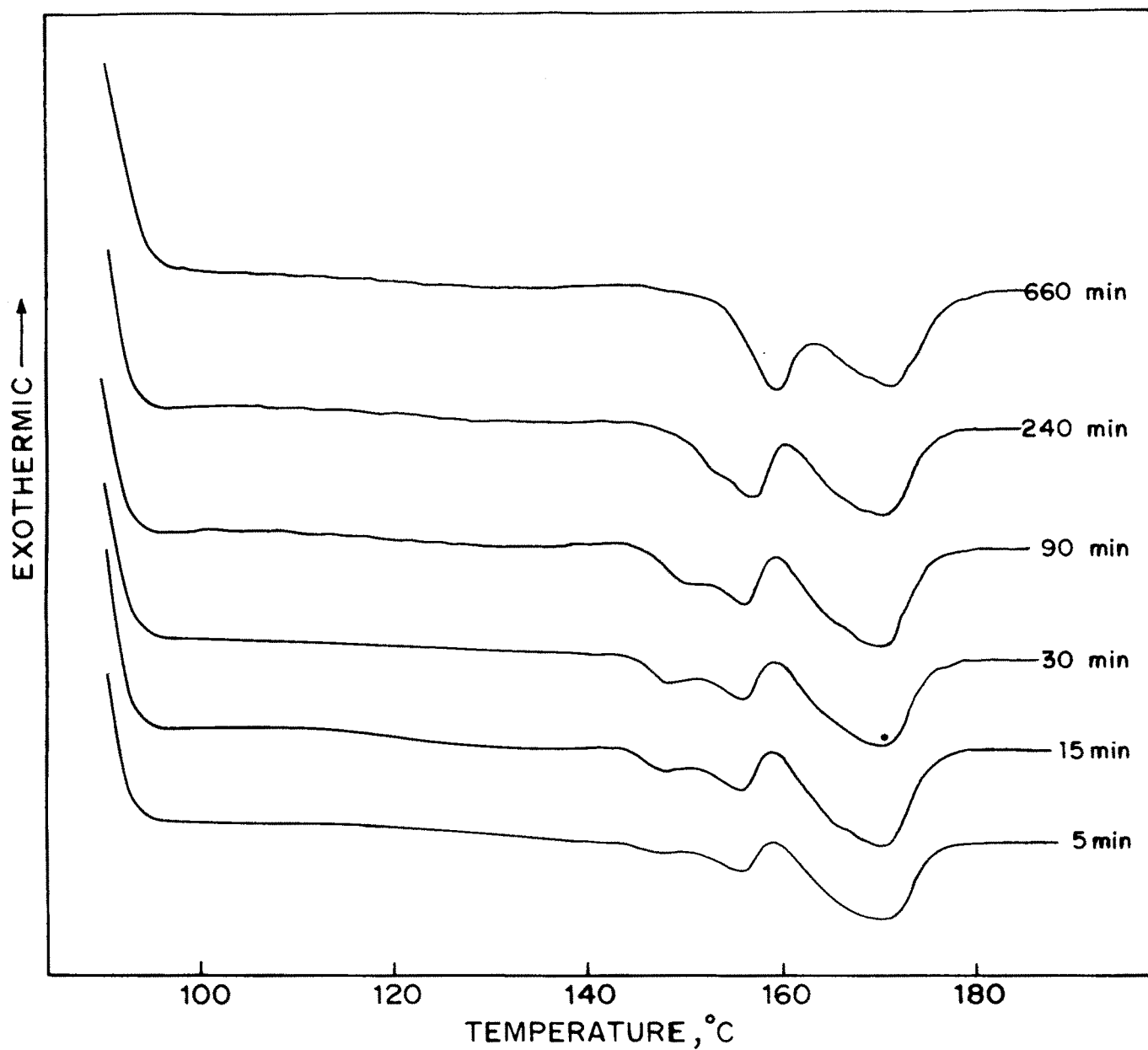


FIG. 44 A SET OF DSC HEATING TRACES IN DIFFERENT TIME PERIODS OF ISOTHERMAL EXPERIMENTS FOR COPOLYESTER PE-103 ($T_c = 140^\circ\text{C}$).

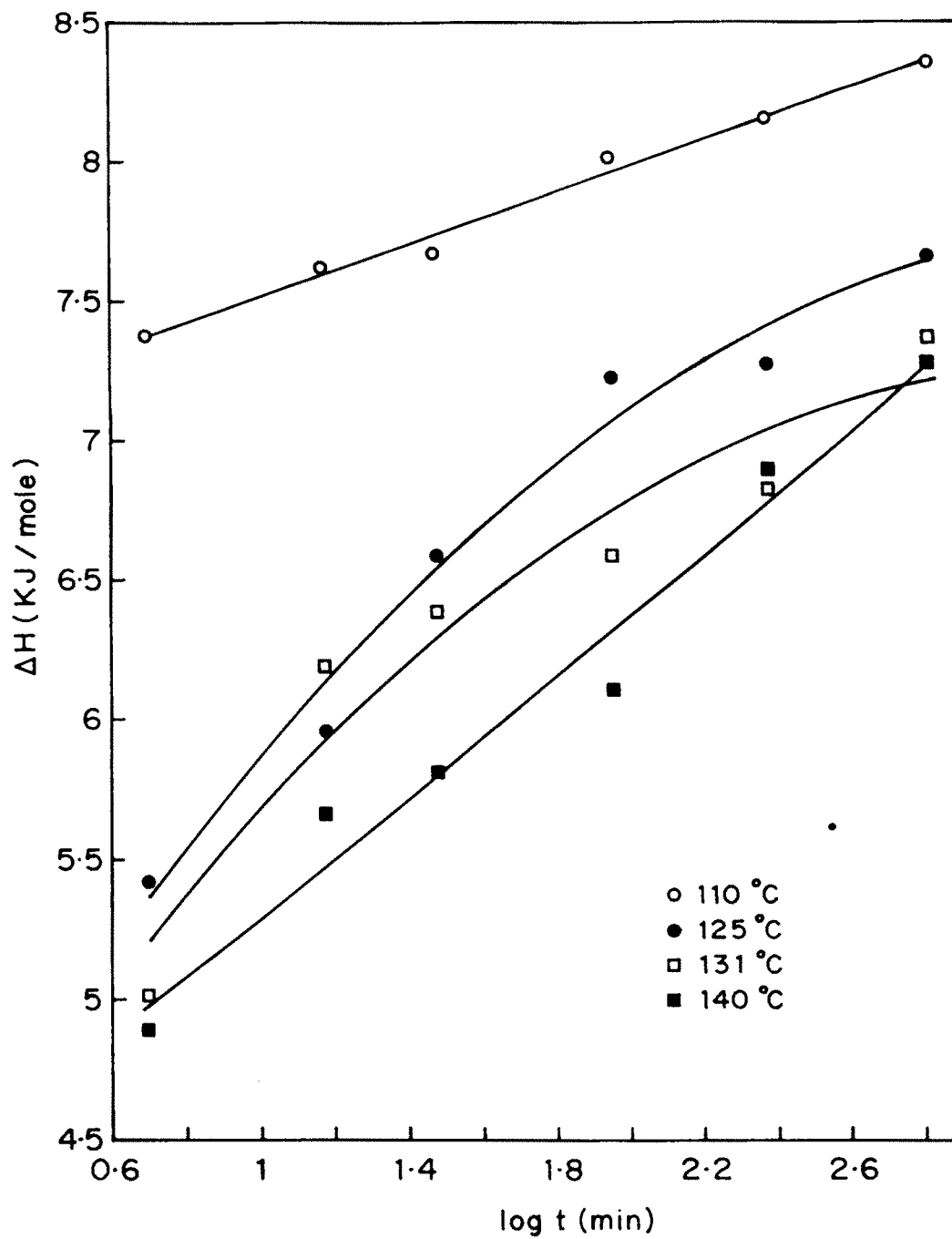


FIG. 45 THE PLOT OF ΔH VERSUS $\log t$ FOR POLYESTER PE-103.

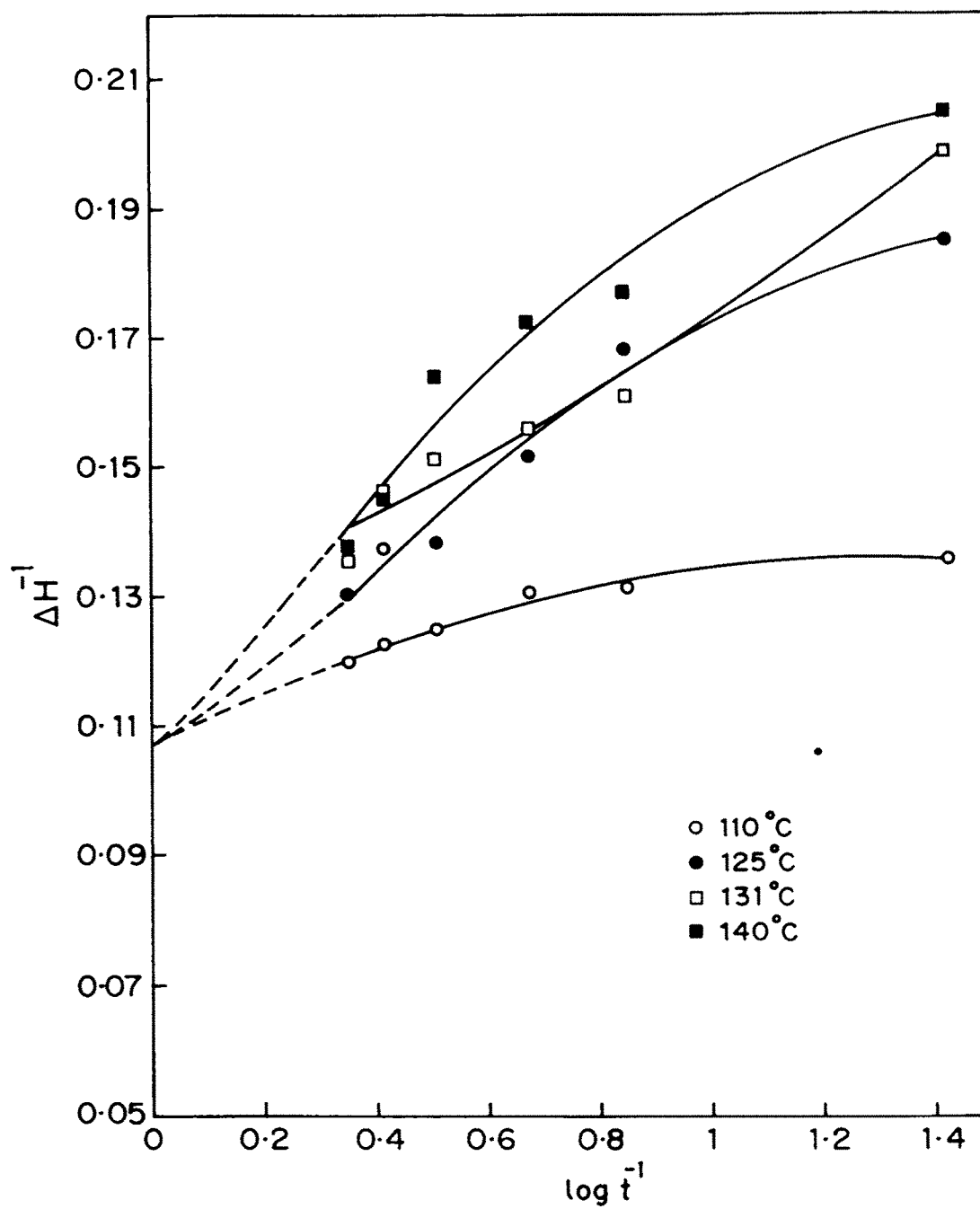


FIG. 46 THE PLOT OF ΔH^{-1} VERSUS $\text{Log } t^{-1}$ FOR POLYESTER PE-103.

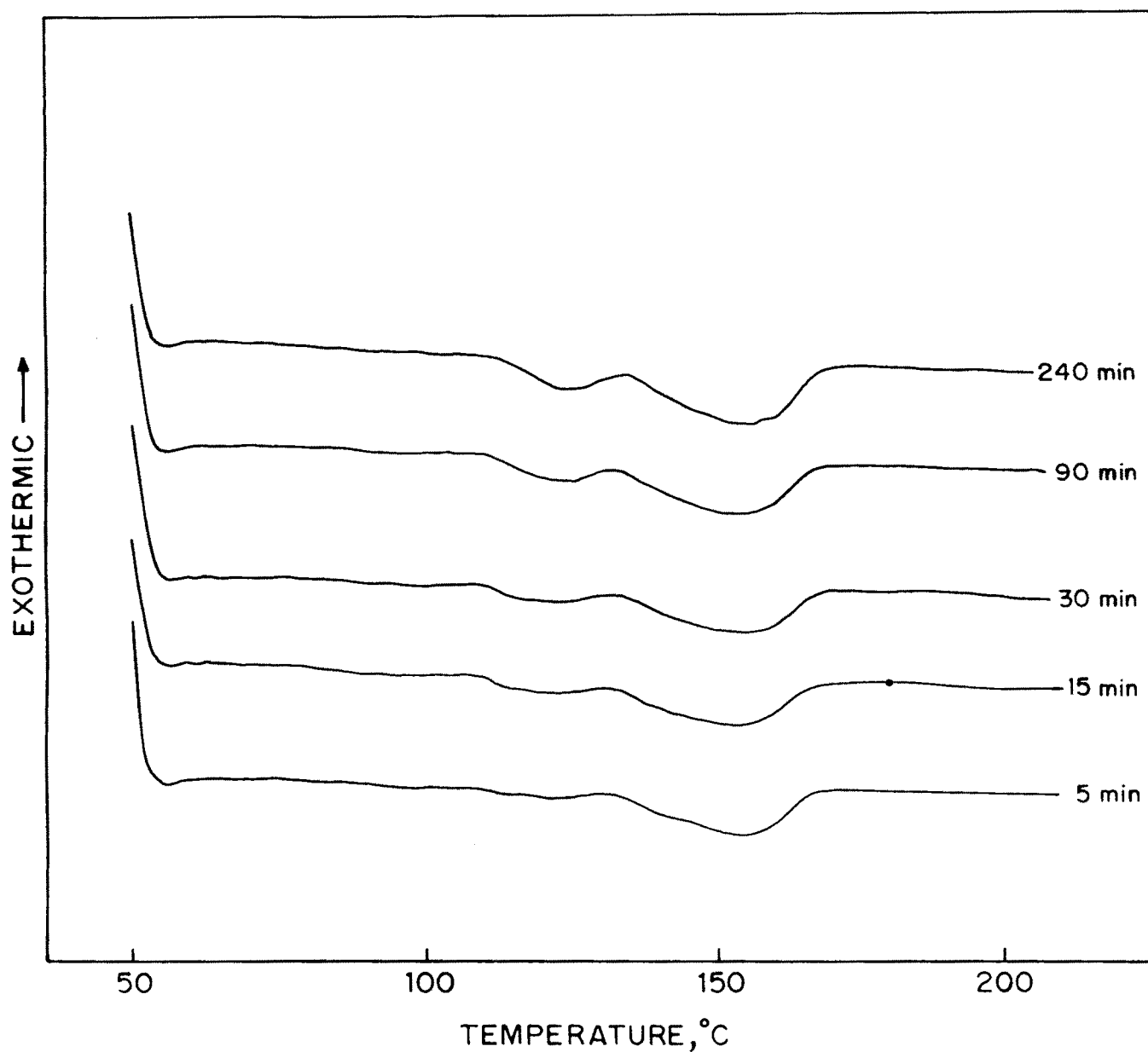


FIG. 47 A SET OF DSC HEATING TRACES IN DIFFERENT TIME PERIODS OF ISOTHERMAL EXPERIMENTS FOR COPOLYESTER PE-303 ($T_c = 108^\circ\text{C}$).

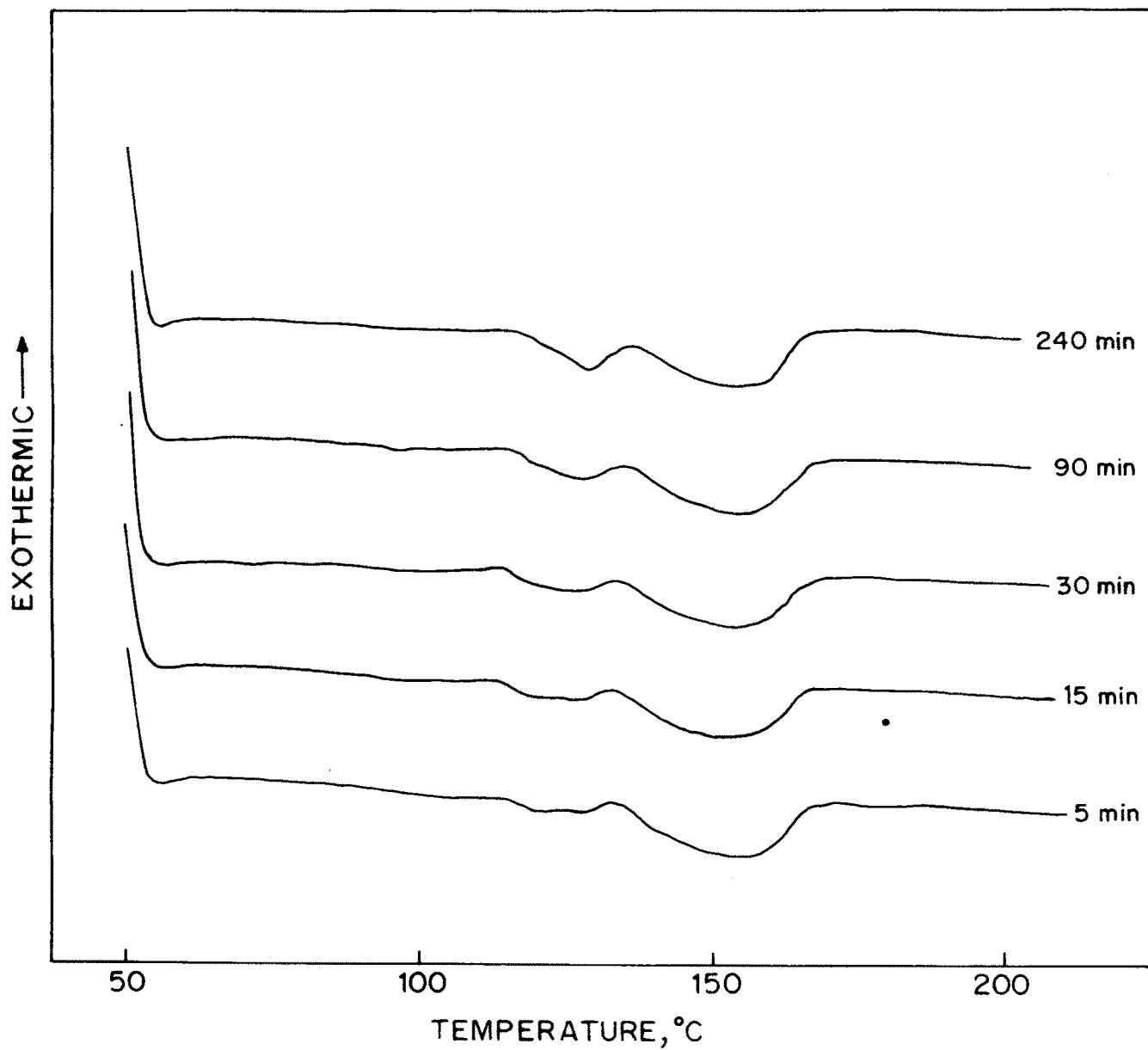


FIG. 48 A SET OF DSC HEATING TRACES IN DIFFERENT TIME PERIODS OF ISOTHERMAL EXPERIMENTS FOR COPOLYESTER PE-303 ($T_c = 113^\circ\text{C}$).

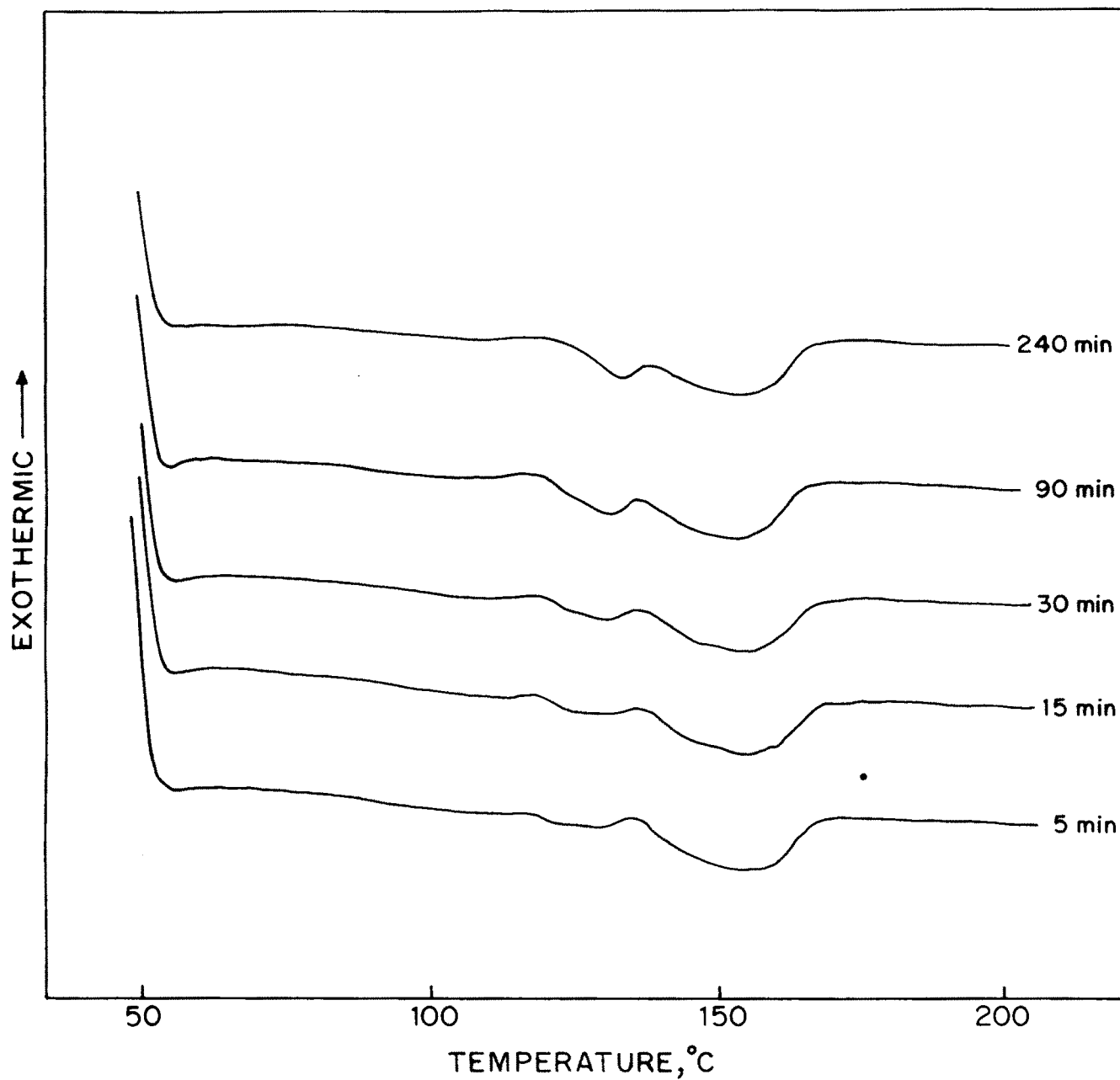


FIG. 49 A SET OF DSC HEATING TRACES IN DIFFERENT TIME PERIODS OF ISOTHERMAL EXPERIMENTS FOR COPOLYESTER PE-303 ($T_c = 118^\circ\text{C}$).

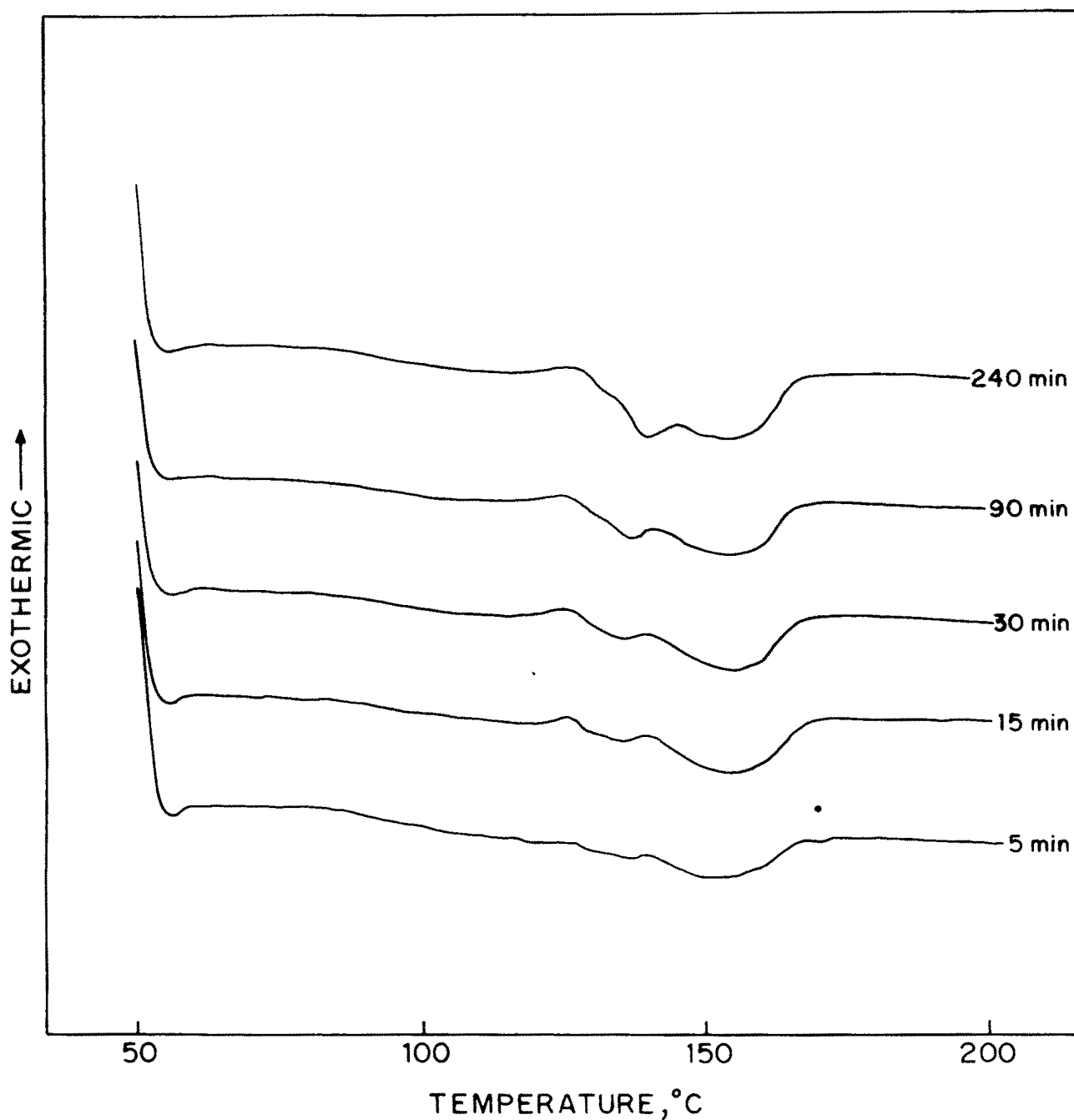


FIG. 50 A SET OF DSC HEATING TRACES IN DIFFERENT TIME PERIODS OF ISOTHERMAL EXPERIMENTS FOR COPOLYESTER PE-303 ($T_c = 125^\circ\text{C}$).

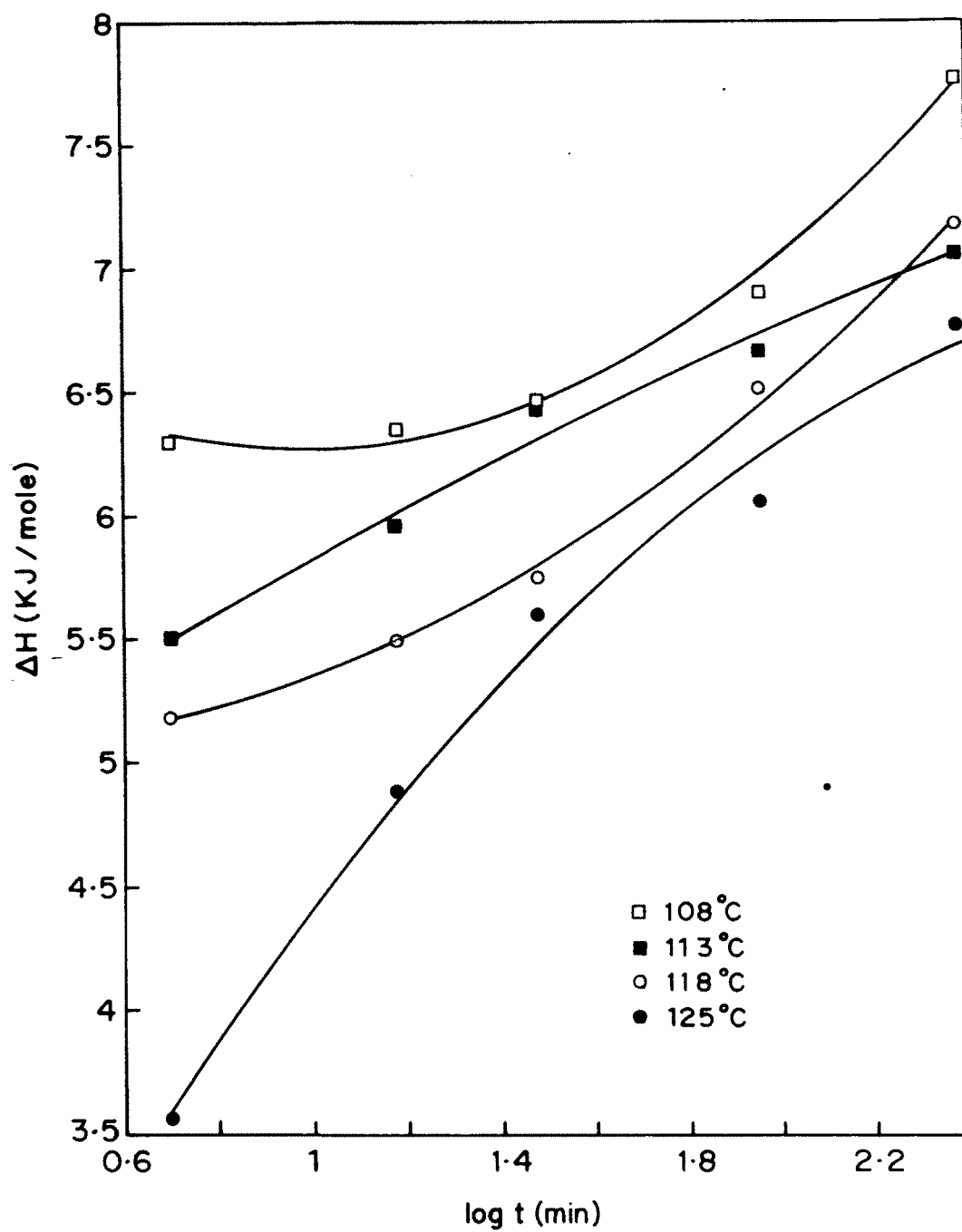


FIG. 51 THE PLOT OF ΔH VERSUS $\log t$ FOR POLYESTER PE-303.

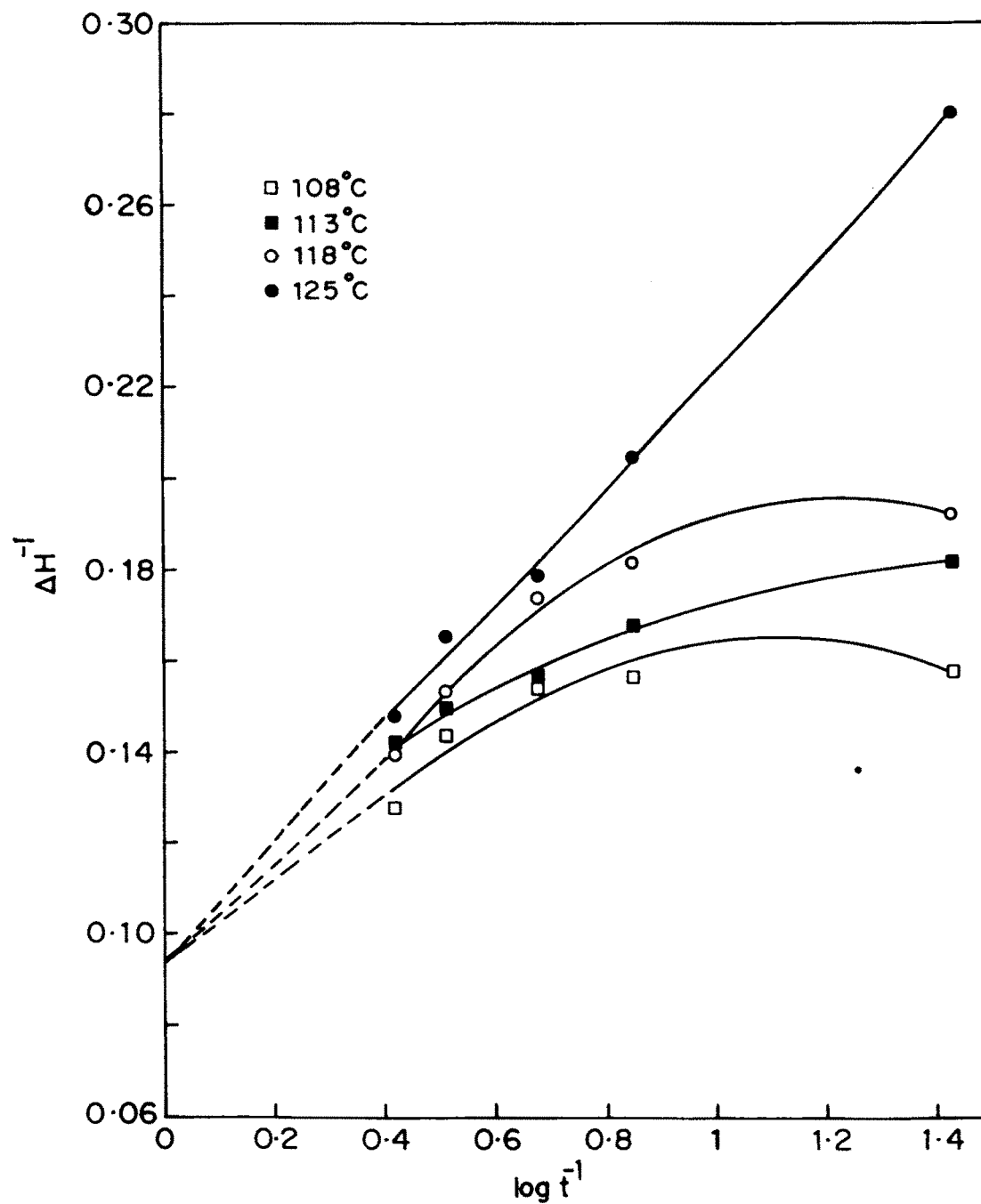


FIG. 52 THE PLOT OF ΔH^{-1} VERSUS $\text{Log } t^{-1}$ FOR POLYESTER PE-303.

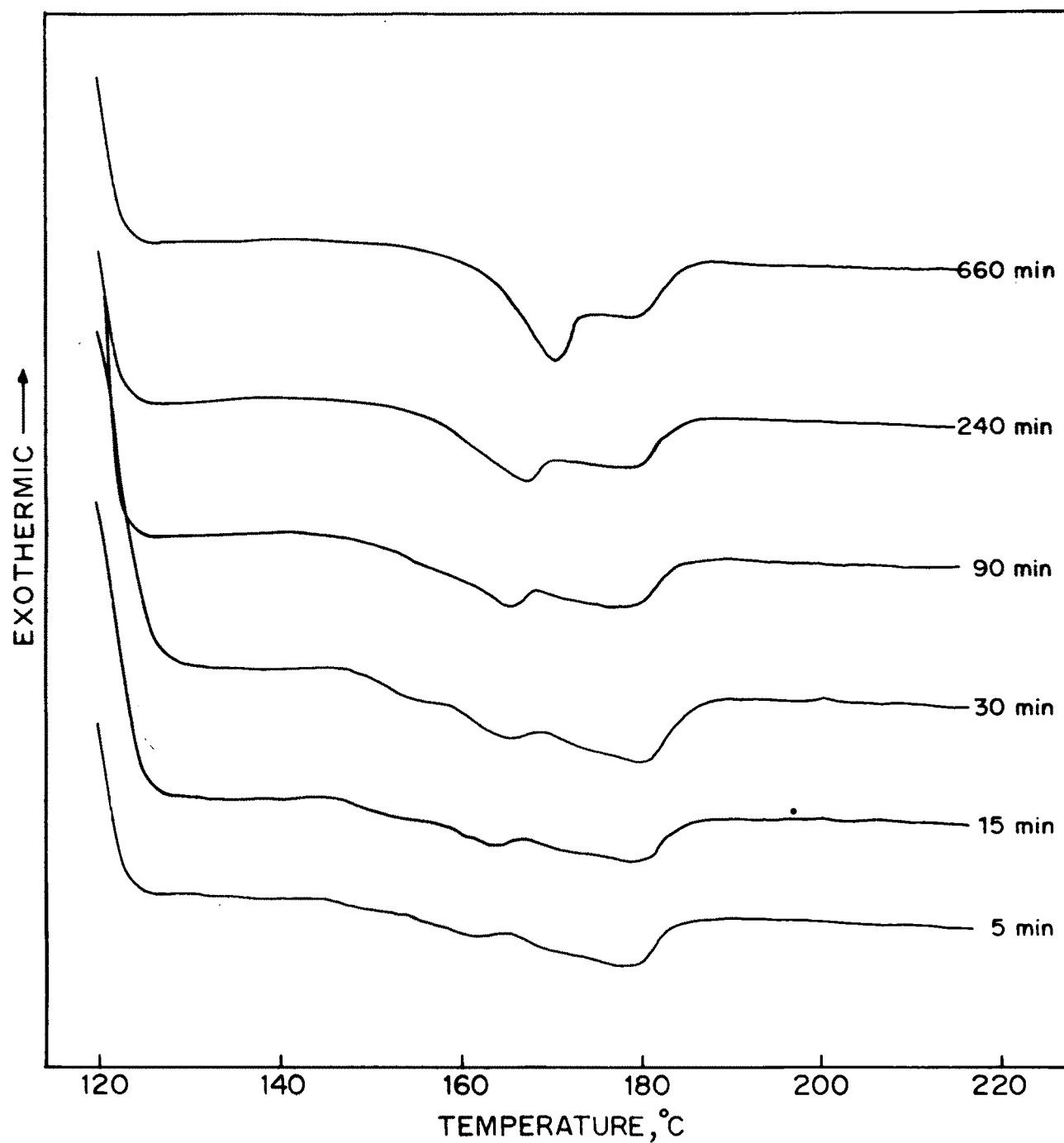


FIG. 53 A SET OF DSC HEATING TRACES IN DIFFERENT TIME PERIODS OF ISOTHERMAL EXPERIMENTS FOR COPOLYESTER PE-107 ($T_c = 143^\circ\text{C}$).

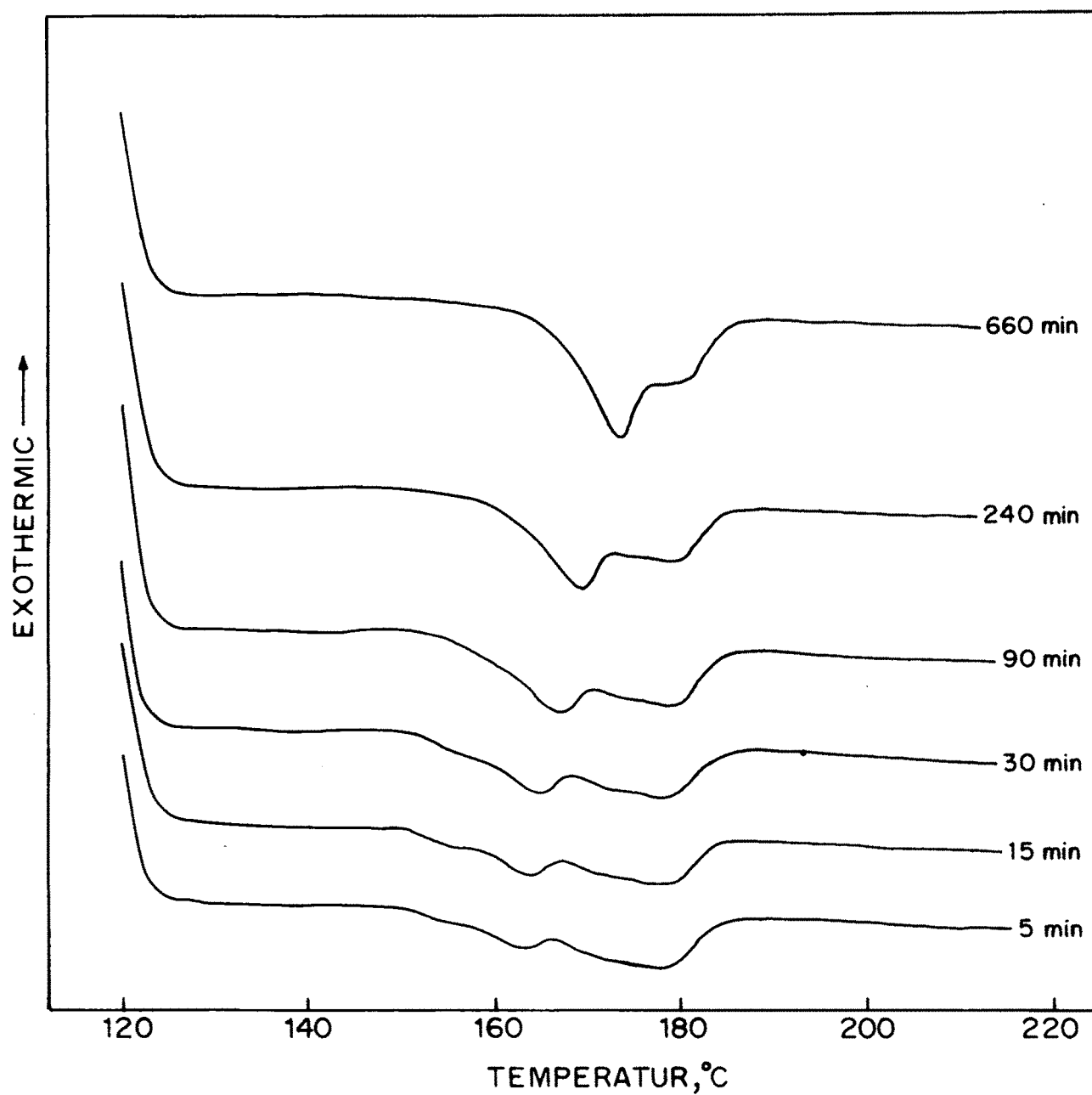


FIG. 54 A SET OF DSC HEATING TRACES IN DIFFERENT TIME PERIODS OF ISOTHERMAL EXPERIMENTS FOR COPOLYESTER PE-107 ($T_c = 148^\circ\text{C}$).

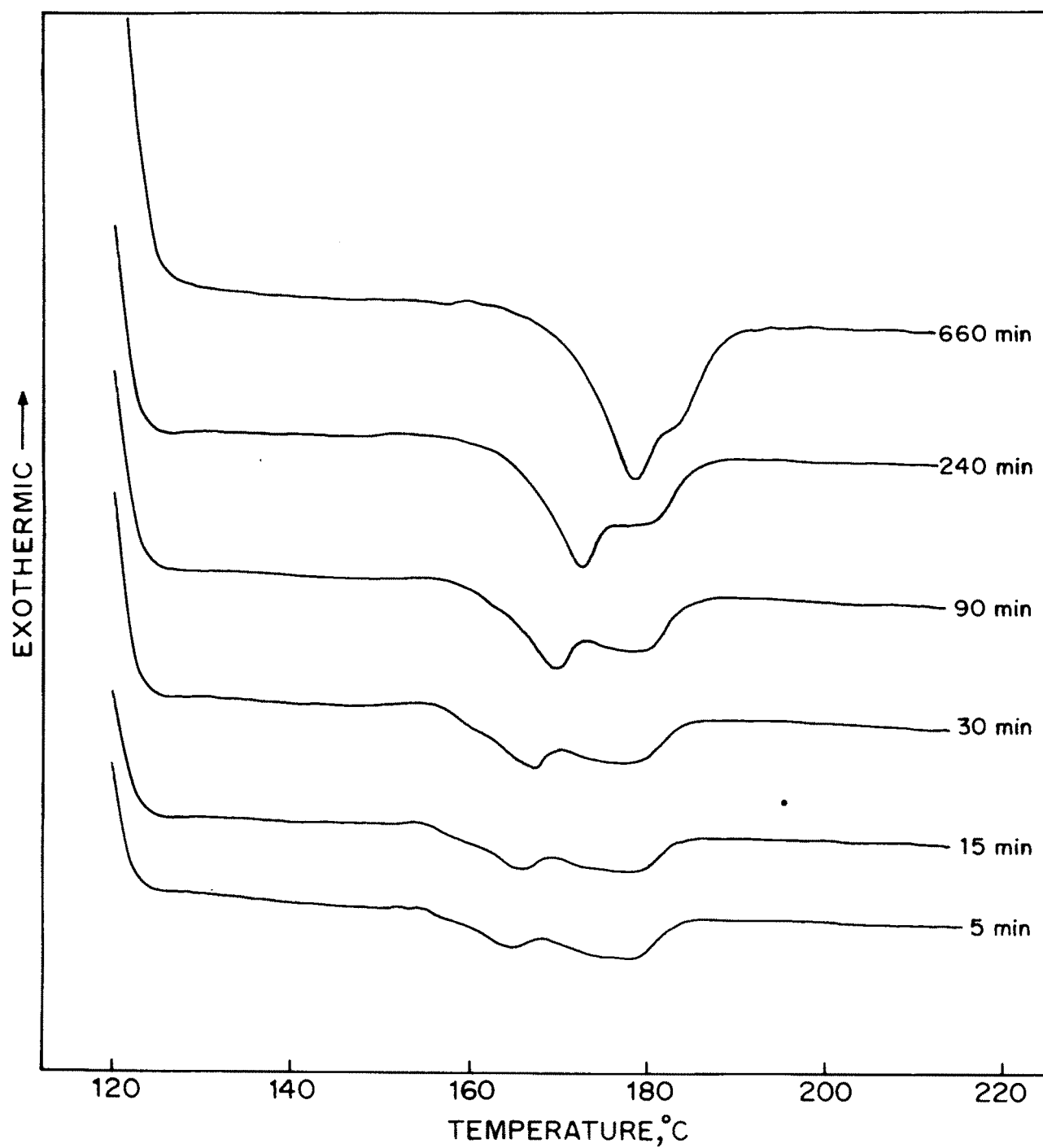


FIG. 55 A SET OF DSC HEATING TRACES IN DIFFERENT TIME PERIODS OF ISOTHERMAL EXPERIMENTS FOR COPOLYESTER PE-107 ($T_c = 153^\circ\text{C}$).

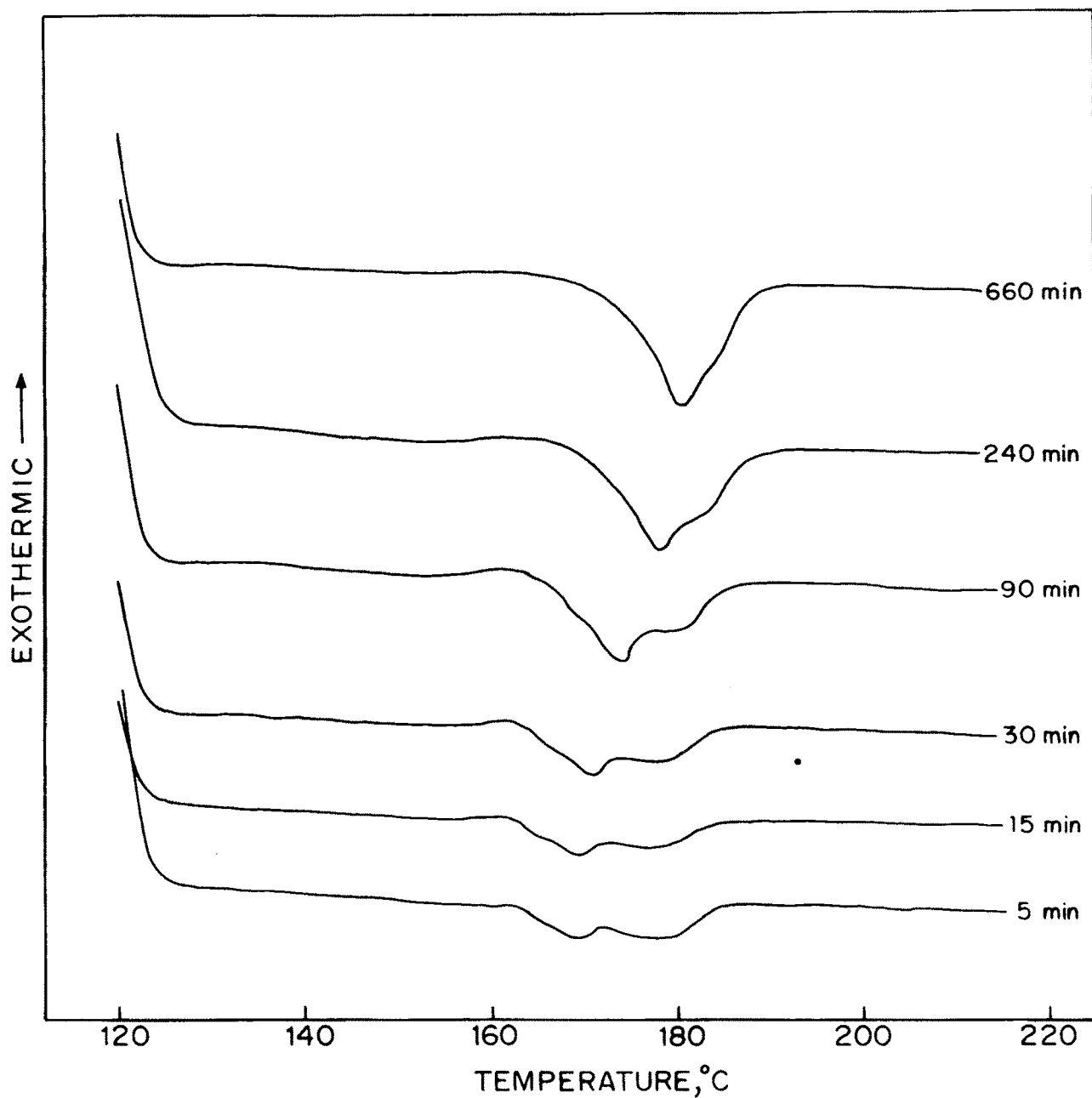


FIG. 56 A SET OF DSC HEATING TRACES IN DIFFERENT TIME PERIODS OF ISOTHERMAL EXPERIMENTS FOR COPOLYESTER PE-107 ($T_c = 160^\circ\text{C}$).

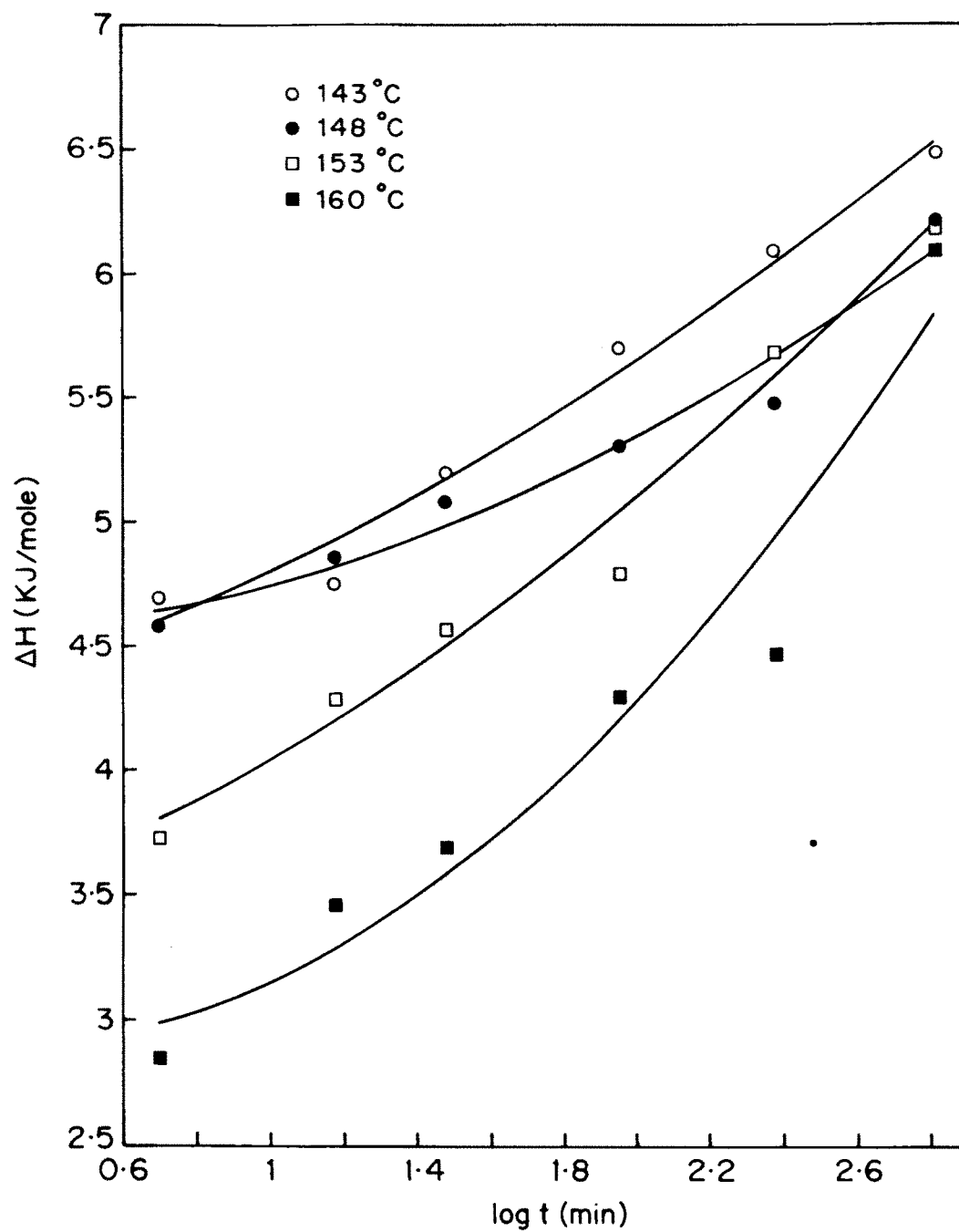


FIG. 57 THE PLOT OF ΔH VERSUS $\text{Log } t$ FOR POLYESTER PE-107.

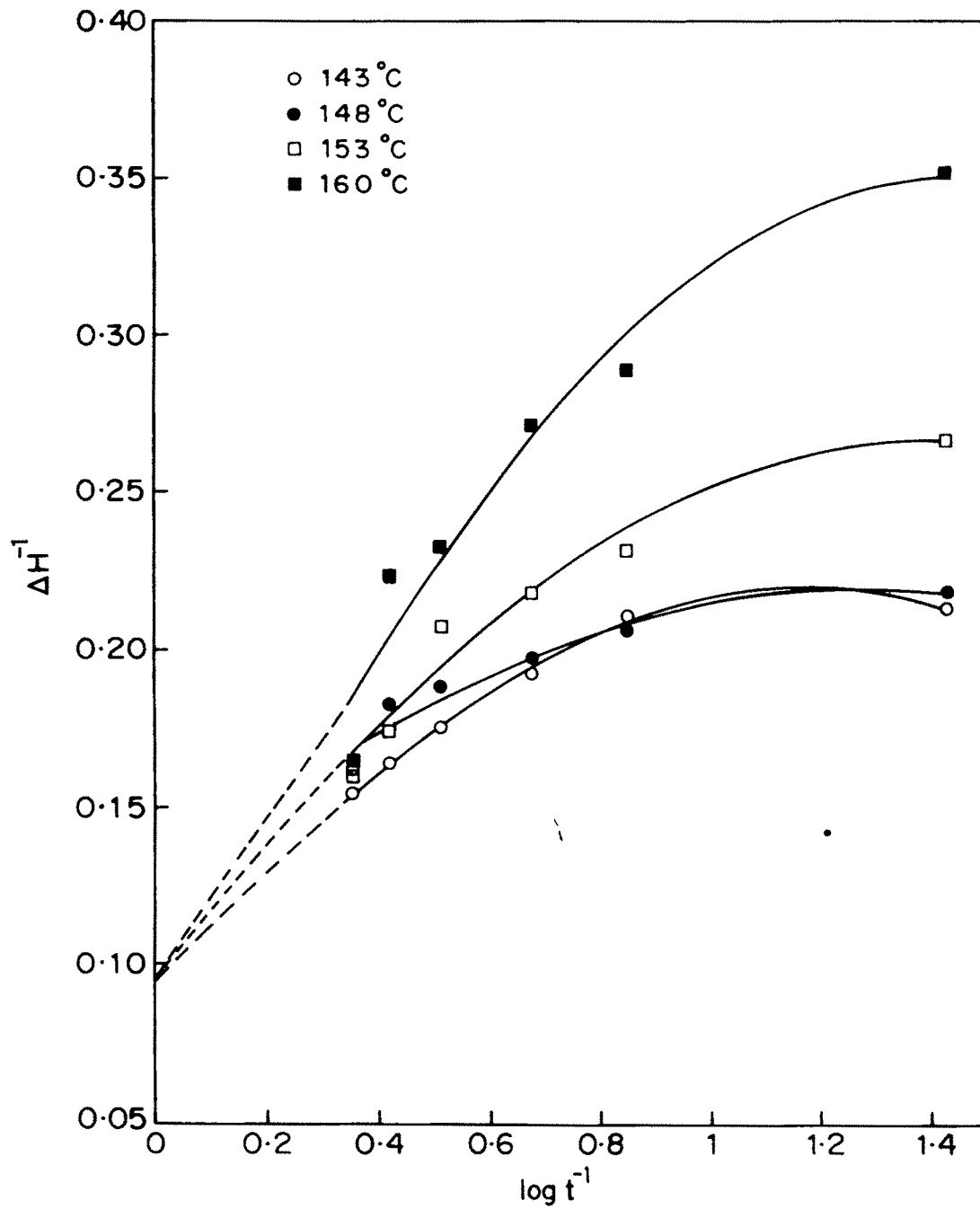


FIG. 58 THE PLOT OF ΔH^{-1} VERSUS $\text{Log } t^{-1}$ FOR POLYESTER PE-107.

ΔS are the enthalpy and entropy changes during the transition respectively. The enthalpy change accompanying isothermal crystallisation at two temperatures in this regime for the four polyesters are presented in Tables 31, 32, 35, 36, 39, 40, 43 and 44 respectively.

It bears out that the heat of transition in the fast process decreases with increasing annealing (crystallisation) times. Simultaneously, heat of transition for the slow process increases with crystallisation time. Also, for these polyesters small entropy changes accompany transformation of quenched forms into their nematic melts. Thus, the quenched forms closely resemble the nematic melt in the structural organisation. In accordance with Wunderlich classification,¹⁸² these polyesters are in the conformational disordered (condis) crystalline state. In crystallisation of polymeric systems such small entropy changes occur when organisation is into a hexagonal packing of cylindrical symmetry which involves many chain conformations and retards molecular motions.²²⁹ On the other hand, the entropy changes between annealed forms of crystals and their nematic melts are relatively large for an orthorhombic packing with a more ordered chain structure. However, enthalpy change accompanying both these transformations are not large. The higher transition temperature for the quenched form has been shown to be due to the small degree of entropy change between the two stages.²²⁹

It turns out from Figures 35, 36, 41, 42, 47, 48, 53 and 54 that the slow transition process tends to gain prominence with increasing annealing time and occurs more effectively. This is due to the gradual change in heat capacity during the transition. It is probable that at sufficiently high annealing times the cooperative molecular motion in the chains increases appreciably and permits chain segments to crossover the phase boundary and aggregate with others.

Table - 31

Isothermal Crystallisation of Polyester PE-203 at 191°C

Time, t [minutes]	log t	ln t	log t ⁻¹	Enthalpy [Δ H]	[Δ H] ⁻¹
5	0.6989	1.6094	1.4308	1.6131	0.6199
15	1.1760	2.7080	0.8503	1.9926	0.5018
30	1.4771	3.4011	0.6770	2.5145	0.3976
90	1.9542	4.4998	0.5117	3.8429	0.2602
240	2.3802	5.4806	0.4201	5.1714	0.1933

Table - 32

Isothermal Crystallisation of Polyester PE-203 at 194°C

Time, t [minutes]	log t	ln t	log t ⁻¹	Enthalpy [Δ H]	[Δ H] ⁻¹
5	0.6989	1.6094	1.4308	1.4707	0.6799
15	1.1760	2.7080	0.8503	2.0401	0.4901
30	1.4771	3.4011	0.6770	2.4671	0.4053
90	1.9542	4.4998	0.5117	3.4634	0.2887
240	2.3802	5.4806	0.4201	4.7918	0.2086

Table - 33

Isothermal Crystallisation of Polyester PE-203 at 198°C

Time, t [minutes]	log t	ln t	log t ⁻¹	Enthalpy [Δ H]	[Δ H] ⁻¹
5	0.6989	1.6094	1.4308	0.7591	1.3173
15	1.1760	2.7080	0.8503	0.8065	1.2399
30	1.4771	3.4011	0.6770	2.0875	0.4790
90	1.9542	4.4998	0.5117	3.2736	0.3054
240	2.3802	5.4806	0.4201	4.5072	0.2218

Table - 34

Isothermal Crystallisation of Polyester PE-203 at 202°C

Time, t [minutes]	log t	ln t	log t ⁻¹	Enthalpy [Δ H]	[Δ H] ⁻¹
5	0.6989	1.6094	1.4308	0.5218	1.9164
15	1.1760	2.7080	0.8503	0.9963	1.0037
30	1.4771	3.4011	0.6770	1.5182	0.6586
90	1.9542	4.4998	0.5117	2.4196	0.4132
240	2.3802	5.4806	0.4201	3.2262	0.3099

Table - 35

Isothermal Crystallisation of Polyester PE-103 at 110°C

Time, t [minutes]	log t	ln t	log t ⁻¹	Enthalpy [Δ H]	[Δ H] ⁻¹
5	0.6989	1.6094	1.4308	7.3758	0.1355
15	1.1760	2.7080	0.8503	7.6200	0.1312
30	1.4771	3.4011	0.6770	7.6688	0.1303
90	1.9542	4.4998	0.5117	8.0108	0.1248
240	2.3802	5.4806	0.4201	8.1573	0.1225
660	2.8195	6.4922	0.3546	8.3527	0.1197

Table - 36

Isothermal Crystallisation of Polyester PE-103 at 125°C

Time, t [minutes]	log t	ln t	log t ⁻¹	Enthalpy [Δ H]	[Δ H] ⁻¹
5	0.6989	1.6094	1.4308	5.4217	0.1844
15	1.1760	2.7080	0.8503	5.9592	0.1678
30	1.4771	3.4011	0.6770	6.5942	0.1516
90	1.9542	4.4998	0.5117	7.2292	0.1383
240	2.3802	5.4806	0.4201	7.2781	0.1373
660	2.8195	6.4922	0.3546	7.6688	0.1303

Table - 37

Isothermal Crystallisation of Polyester PE-103 at 131°C

Time, t [minutes]	log t	ln t	log t ⁻¹	Enthalpy [Δ H]	[Δ H] ⁻¹
5	0.6989	1.6094	1.4308	5.0311	0.1987
15	1.1760	2.7080	0.8503	6.2035	0.1611
30	1.4771	3.4011	0.6770	6.3988	0.1562
90	1.9542	4.4998	0.5117	6.5942	0.1516
240	2.3802	5.4806	0.4201	6.8385	0.1462
660	2.8195	6.4922	0.3546	7.3758	0.1355

Table - 38

Isothermal Crystallisation of Polyester PE-103 at 140°C

Time, t [minutes]	log t	ln t	log t ⁻¹	Enthalpy [Δ H]	[Δ H] ⁻¹
5	0.6989	1.6094	1.4308	4.8868	0.2046
15	1.1760	2.7080	0.8503	5.6661	0.1764
30	1.4771	3.4011	0.6770	5.8127	0.1720
90	1.9542	4.4998	0.5117	6.1058	0.1637
240	2.3802	5.4806	0.4201	6.8873	0.1451
660	2.8195	6.4922	0.3546	7.2781	0.1373

Table - 39

Isothermal Crystallisation of Polyester PE-303 at 108°C

Time, t [minutes]	log t	ln t	log t ⁻¹	Enthalpy [Δ H]	[Δ H] ⁻¹
5	0.6989	1.6094	1.4308	6.3101	0.1584
15	1.1760	2.7080	0.8503	6.3641	0.1571
30	1.4771	3.4011	0.6770	6.4628	0.1547
90	1.9542	4.4998	0.5117	6.9208	0.1444
240	2.3802	5.4806	0.4201	7.7851	0.1284

Table - 40

Isothermal Crystallisation of Polyester PE-303 at 113°C

Time, t [minutes]	log t	ln t	log t ⁻¹	Enthalpy [Δ H]	[Δ H] ⁻¹
5	0.6989	1.6094	1.4308	5.4955	0.1819
15	1.1760	2.7080	0.8503	5.9539	0.1679
30	1.4771	3.4011	0.6770	6.4119	0.1559
90	1.9542	4.4998	0.5117	6.6663	0.1500
240	2.3802	5.4806	0.4201	7.0734	0.1413

Table - 41

Isothermal Crystallisation of Polyester PE-303 at 118°C

Time, t [minutes]	log t	ln t	log t ⁻¹	Enthalpy [Δ H]	[Δ H] ⁻¹
5	0.6989	1.6094	1.4308	5.1906	0.1926
15	1.1760	2.7080	0.8503	5.4959	0.1819
30	1.4771	3.4011	0.6770	5.7503	0.1739
90	1.9542	4.4998	0.5117	6.5147	0.1534
240	2.3802	5.4806	0.4201	7.1778	0.1393

Table - 42

Isothermal Crystallisation of Polyester PE-303 at 125°C

Time, t [minutes]	log t	ln t	log t ⁻¹	Enthalpy [Δ H]	[Δ H] ⁻¹
5	0.6989	1.6094	1.4308	3.5625	0.2806
15	1.1760	2.7080	0.8503	4.8852	0.2046
30	1.4771	3.4011	0.6770	5.5977	0.1786
90	1.9542	4.4998	0.5117	6.0577	0.1651
240	2.3802	5.4806	0.4201	6.7681	0.1477

Table - 43

Isothermal Crystallisation of Polyester PE-107 at 143°C

Time, t [minutes]	log t	ln t	log t ⁻¹	Enthalpy [Δ H]	[Δ H] ⁻¹
5	0.6989	1.6094	1.4308	4.6921	0.2131
15	1.1760	2.7080	0.8503	4.7480	0.2106
30	1.4771	3.4011	0.6770	5.1949	0.1924
90	1.9542	4.4998	0.5117	5.6979	0.1755
240	2.3802	5.4806	0.4201	6.0886	0.1642
660	2.8195	6.4922	0.3546	6.4796	0.1543

Table - 44

Isothermal Crystallisation of Polyester PE-107 at 148°C

Time, t [minutes]	log t	ln t	log t ⁻¹	Enthalpy [Δ H]	[Δ H] ⁻¹
5	0.6989	1.6094	1.4308	4.5804	0.2183
15	1.1760	2.7080	0.8503	4.8597	0.2057
30	1.4771	3.4011	0.6770	5.0832	0.1967
90	1.9542	4.4998	0.5117	5.3066	0.1884
240	2.3802	5.4806	0.4201	5.4742	0.1826
660	2.8195	6.4922	0.3546	6.2003	0.1612

Table - 45

Isothermal Crystallisation of Polyester PE-107 at 153°C

Time, t [minutes]	log t	ln t	log t ⁻¹	Enthalpy [Δ H]	[Δ H] ⁻¹
5	0.6989	1.6094	1.4308	3.7425	0.2672
15	1.1760	2.7080	0.8503	4.3011	0.2324
30	1.4771	3.4011	0.6770	4.5804	0.2183
90	1.9542	4.4998	0.5117	4.8039	0.2081
240	2.3802	5.4806	0.4201	5.6979	0.1755
660	2.8195	6.4922	0.3546	6.2003	0.1612

Table - 46

Isothermal Crystallisation of Polyester PE-107 at 160°C

Time, t [minutes]	log t	ln t	log t ⁻¹	Enthalpy [Δ H]	[Δ H] ⁻¹
5	0.6989	1.6094	1.4308	2.8488	0.3510
15	1.1760	2.7080	0.8503	3.4632	0.2887
30	1.4771	3.4011	0.6770	3.6867	0.2712
90	1.9542	4.4998	0.5117	4.3011	0.2324
240	2.3802	5.4806	0.4201	4.4687	0.2237
660	2.8195	6.4922	0.3546	6.0886	0.1642

It is seen from Figures 39, 45, 51 and 57 that transition temperatures corresponding to the fast process are independent of the crystallisation temperature and remain constant for short annealing times. The transition temperature of the slow process increases linearly with respect to logarithmic time in the same stage. The slope of such linear increase is dependant on crystallisation temperature with increasing temperature and annealing time. The transition temperature of the fast process decreases and simultaneously that for the slow process increases steeply by a factor of 2 to 3.

4.5.3 High Temperature Regime

The data obtained in high temperature regime isothermal crystallisation kinetics for the four polyesters are described in Tables 33, 34, 37, 38, 41, 42, 45 and 46. It is observed from Figures 37, 38, 43, 44, 49, 50, 55 and 56 that two, fast and slow, transition processes operate in the high temperature regime as well. Again, fast transition process is observed at higher temperature while the slow transition process is noted at the lower temperature. However, in the high temperature regime the slow transition process is more effective than in the lower temperature regime.

The enthalpy change in low temperature regime relates the crystallisation and hence crystal formation overwhelmingly to solidification (fast process). Crystallisation through the slow process is only marginal. The opposite is true for the high temperature regime. Here, the fast solidification process is partial, while most crystals are formed during the slow annealing process. There is also a reversal in the linear relationship. Here, the heat of transition for the crystals formed by the slow annealing process follows a linear relationship with logarithmic time, $\log t_c$, as described in equation [10].

4.5.4 Structural Effects

Tables 31 to 42 reveal that in both temperature regimes enthalpy change for polyester based on unsubstituted trimesogen (PE-203) are lower than those for polyesters from substituted mesogens (PE-103 and PE-303). Isothermal crystallisation in Polyester PE-203 proceeds overwhelmingly through the fast transition process which invariably generates lower enthalpy change. This has been shown in wholly aromatic LCPs to be due to the formation of less ordered hexagonal packing. These structures are highly coplanar and rigid.²²⁹ Isothermal crystallisation in polyesters PE-103 and PE-303 predominantly follow through slow transition process which always leads to higher enthalpy changes and only marginally through fast transition process. This process generates a more ordered orthorhombic packing in wholly aromatic LCPs. These structures are less coplanar and rigid.²²⁹

Polyesters PE-103 and PE-107 from methyl substituted trimesogen differ only in the length of flexible spacer. Enthalpy change accompanying isothermal crystallisation of these two polyesters are presented in Tables 43 to 46. The enthalpy of transition for polyester PE-103 with pentamethylene spacer [$n=5$] is larger than that for polyester PE-107 with decamethylene spacer [$n=10$]. Polarising microscopic observations revealed formation of smectic melt in polyester PE-107 which arises from the longer and even decamethylene spacer while polyester PE-103 forms a nematic melt due to a shorter odd pentamethylene spacer. Thus, smectic phases, which encompass greater order in the melt compared to nematic phase, follow fast transition process and result in low enthalpy change.

4.5.5 Avrami Exponent "n"

Plots of $[\Delta H]^{-1}$ against $\log t^{-1}$ are presented in Figures 40, 46, 52 and 58. These show low values of Avrami exponent "n" for polyesters PE-103, PE-107, PE-203 and

PE-303 in isothermal crystallisation. A very simplified rationalisation for the lower values of Avrami exponent "n" is that each individual crystal does not grow with constant radial growth rate. Equation [7] may be expressed in the form:

$$1-V_c = \exp [-gN\gamma^n t^n] \quad [11]$$

Here γ is the radial growth rate, g is geometrical factor ($4\pi/3$ for spheres) and N represents the number of nuclei per unit area.

If γ is attributed to a linear rate of crystal growth, equation [11] becomes equivalent to equation [7] with $K = gN\gamma^n$. However, if γ can not be related to a constant radial growth rate, it can be expressed in terms of:

$$\gamma = \gamma_0 t^m \quad [12]$$

Equation [7] must then be cast into,

$$\begin{aligned} \log [-\ln (1-V_c)] &= \log g + \log N + n \log \gamma_0 + n(m + 1) \log t_c \\ &= \log K^* + n(m + 1) \log t_c \end{aligned} \quad [13]$$

Where, K^* is $gN\gamma_0^n$ and $n(m + 1)$ is an apparent coefficient. According to equation [13], the apparent coefficient becomes $0.5n$, and it would be 0.5, 1 and 1.5 for one-, two- and three-dimensional growths respectively.

A possible reason for very low coefficient "n" in the present kinetics study may arise from the restriction of crystal growth due to previously formed crystals which reduce the molecular mobility.

4.5.6 Conclusion

The isothermal crystallisation process studied had to be an indirect one involving annealing for varied times at the selected isothermal temperatures followed by reheating through the liquid crystal transition temperature and examining the transition temperatures as well as the ensuing enthalpy and entropy changes. Two transition processes are noted. A rapid transition process which occurs almost instantaneously called "solidification" is due to freezing-in (quenching) of the anisotropic melt. A slow transition process resembling normal crystallisation process observable in crystalline thermoplastic polymers then follows but has a low Avrami parameter "n". Two temperature regimes, one on either side of the endothermic maxima in the heating cycle, were chosen for the study. The crystallisation due to the fast transition process results in a melting peak (first order transition in the next heating cycle) at higher temperature. This temperature varies linearly relative with respect to $\log t_c$, where t_c is the crystallisation time. The slow process generates a similar melting peak at lower temperature. The heat of transition corresponding to this peak increases with the crystallisation time t_c . The fast transition process dominates the crystallisation process at lower temperature regime while the slow crystallisation process is more effective in the higher temperature regime. The interplay of structural variables such as substitution on the mesogen and flexible spacer length on the mode of crystallisation are brought out in the study.

4.6 NON-ISOTHERMAL CRYSTALLISATION

Thermotropic liquid crystal polymers (LCPs) display a minimum of two first order transitions on cooling from an isotropic melt. These correspond to a stable liquid crystalline anisotropic melt and then solidification into a crystalline phase. Intrinsic high performance are harnessed only on processing from anisotropic melts. Processing

is usually carried out under dynamic conditions. Therefore, it is advantageous to determine the crystallisation process under non-isothermal conditions. Applications of isothermal crystallisation technique are difficult where-in: (a) material does not crystallise, (b) material does not release sufficient heat of crystallisation per unit time, (c) materials show multiple crystallisation behaviour, or (d) the process begins to occur before the system reaches the desired temperature.

Crystallisation from oriented (nematic) polymer melts differ intrinsically from crystallisation of isotropic melts, observed with flexible thermoplastic crystalline polymers. In isothermal crystallisation study from nematic and smectic melts (Section 4.5), two processes occur which have characteristics indicated above in (b), (c) and (d). Molecules have greater mobility in the nematic phase relative to the corresponding isotropic melt. Heat of fusion of such systems are usually low. These systems could be examined in a more exact manner through non-isothermal procedures. Crystallisation kinetics discussed in this Section were estimated through non-isothermal Ozawa method.

4.6.1 Polyesters Investigated

Avrami exponent for crystallisation from anisotropic melt were estimated for these ordered main chain thermotropic liquid crystalline polyesters comprising of a triad mesogenic unit and flexible spacer. Three different triad mesogenic units were studied to determine the effect of substitution in the mesogenic core on the crystallisation. These mesogens are based on two terminal oxybenzoate units coupled to a central moiety arising from (a) hydroquinone [BHBOB], (b) methyl hydroquinone [BHBOMB] and (c) chloro hydroquinone [BHBOCB]. Six flexible spacers were used to evaluate the effect of spacer length. These were based on aliphatic dicarboxylic acids with 3, 4, 5, 7, 8 and 10 methylene units. Thus, the seven polyesters studied for their crystallisation kinetics were: (1) PE-101, BHBOMB with trimethylene spacer; (2)

PE-102, BHBOMB with tetramethylene spacer; (3) PE-105, BHBOMB with heptamethylene spacer; (4) PE-106, BHBOMB with octamethylene spacer; (5) PE-107, BHBOMB with decamethylene spacer; (6) PE-203, BHBOB with pentamethylene spacer and (7) PE-303, BHBOCB with pentamethylene spacer. Synthesis of these polyesters are presented in Section 2.3. The experimental details of crystallisation kinetics are presented in Section 3.3. These polyesters were heated beyond the mesomorphic (liquid crystalline) transition temperature and cooled at predetermined rates in the range of 4-20°C/minute. The cooling traces (thermograms) were recorded and analysed for estimating crystallisation kinetics.

The enthalpies and peak transition temperatures at various cooling rates for polyesters PE-101, PE-102, PE-105, PE-106, PE-107, PE-203 and PE-303 are presented in Tables 47, 48, 49, 50, 51, 52 and 53 respectively. A reduction in peak (transition) temperature was observable in all polyesters with increase in cooling rates. This primarily arises from the inclusion of non-crystalline counits in the crystalline lattice. These counits produce defects in crystal lattice (comonomer inclusion)²¹² which reduces the crystal perfection and hence peak temperature. Processes occurring during polymer crystallisation have been simulated with particular reference to depression in melting point,²⁰⁷ crystallisation kinetics²⁰⁸ and inclusion of non-crystallisable counits into crystal lattice.²⁰⁷ These point quantitatively to greater incorporation of non-crystallisable counits into the crystalline phase at higher cooling rates. This excessive incorporation of non-crystallisable counits depress crystal perfection and lead to a reduction in peak temperature. This effect is also reflected in enthalpy of transition.

The Ozawa method²³⁰⁻²³² is an extension of Avrami expression to the non-isothermal situation. The equation used for analysis is given below:

$$[1 - \alpha(T)] = -e^{-X_c(T)/a^n} \quad [14]$$

Table - 47

Non-Isothermal Crystallisation of Polyester PE-101 at different cooling rates

Rate, [°C/minute]	Enthalpy, ΔH [KJ/mole]	Peak Temperature [°C]
4.0	5.4327	152.2
5.0	5.3404	148.6
6.0	4.8340	144.2
7.0	4.7880	143.1
10.0	4.6038	141.2
15.0	4.4197	135.6
20.0	3.3147	132.7

Table - 48

Non-Isothermal Crystallisation of Polyester PE-102 at different cooling rates

Rate, [°C/minute]	Enthalpy, ΔH [KJ/mole]	Peak Temperature [°C]
4.0	5.3137	136.1
5.5	4.6369	132.6
6.0	4.2225	130.6
7.0	3.2480	126.7
8.5	3.2261	122.9
10.0	2.7999	121.4
15.0	2.3721	121.3
20.0	0.9963	120.6

Table - 49**Non-Isothermal Crystallisation of Polyester PE-105 at different cooling rates**

Rate, [°C/minute]	Enthalpy, ΔH [KJ/mole]	Peak Temperature [°C]
4.0	4.8522	117.8
5.0	5.3264	116.4
6.0	6.4821	115.1
7.0	6.1303	114.6
10.0	5.6278	112.1
15.0	5.6781	106.6
20.0	5.9293	106.0

Table - 50**Non-Isothermal Crystallisation of Polyester PE-106 at different cooling rates**

Rate, [°C/minute]	Enthalpy, ΔH [KJ/mole]	Peak Temperature [°C]
4.0	4.4035	136.9
5.0	3.9260	135.2
6.0	3.7668	131.4
7.0	3.1301	130.8
8.5	2.8649	128.8
10.0	2.5466	121.1
15.0	1.2733	120.5
20.0	0.9549	119.5

Table - 51

Non-Isothermal Crystallisation of Polyester PE-107 at different cooling rates

Rate, [°C/minute]	Enthalpy, ΔH [KJ/mole]	Peak Temperature [°C]
4.0	2.8488	153.8
5.0	3.0164	152.9
6.0	3.1839	152.1
7.0	3.1839	150.7
10.0	3.4074	147.9
15.0	3.9660	145.8
20.0	4.0770	144.1

Table - 52

Non-Isothermal Crystallisation of Polyester PE-203 at different cooling rates

Rate, [°C/minute]	Enthalpy, ΔH [KJ/mole]	Peak Temperature [°C]
3.0	3.2736	190.9
4.0	3.1713	190.9
5.0	2.3722	190.2
6.0	2.2298	189.6
7.0	2.1824	189.2
10.0	1.9926	188.6
15.0	1.8503	186.5
20.0	1.4233	184.4

Table - 53

Non-Isothermal Crystallisation of Polyester PE-303 at different cooling rates

Rate, [°C/minute]	Enthalpy, ΔH [KJ/mole]	Peak Temperature [°C]
4.0	4.1296	108.1
5.0	3.7148	104.3
6.0	3.4095	103.8
7.0	3.3077	101.3
10.0	3.0533	100.2
15.0	2.7479	99.4
20.0	1.7810	98.5

Table - 54

Avrami exponent "n" observed in non-isothermal Crystallisation of Polyesters

Code No.	-(CH ₂) _n -	T _m °K	Range °K	FM Ratio	["n"]
PE-101	3	414.4	414-419	0.58	2.52±0.2
PE-102	4	401.8	390-405	0.66	1.64±0.1
PE-105	7	384.4	384-394	0.90	2.04±0.2
PE-106	8	399.2	392-401	0.99	1.99±0.3
PE-107	10	420.3	416-423	1.15	1.60±0.2
PE-203	5	461.6	456-465	-	0.80±0.3
PE-303	5	373.2	374-384	-	1.56±0.2

Where, $\alpha(T)$ = fractional crystallisation at temperature (T) , a = cooling crystallisation function at (ΔT) and n = Avrami exponent.

The linear form of the equation [14] is:

$$\log \{-\ln [1 - \alpha(T)]\} = \log X_c(T) - n \log a \quad [15]$$

Thermograms obtained in the present study were analysed to estimate "n". The plot $\log \{-\ln [1 - \alpha(T)]\}$ versus $\log a$ was found to be linear. The value of "n" were evaluated from the slopes observed in thermograms obtained in the 10°C/minute cooling cycle, at temperature range in close proximity to or around the peak temperature. The peak temperature, temperature range over which the value of "n" is estimated and Avrami exponent "n" are tabulated in Table 54.

4.6.2 Effect of Flexible Spacer

The crystalline exotherm were obtained for various cooling rates. DSC scans obtained at various cooling rates for polyester PE-101 is shown in Figure 59. The values of α at different temperatures (T) were obtained by taking the ratio of area resulting from peak integration till temperature T to the total peak area. Plots of these values of $\alpha(T)$ as function of temperature are represented in Figure 60. The Ozawa plot of $\log \{-\ln [1 - \alpha(T)]\}$ versus $\log a$ were obtained using $\alpha(T)$ values. The plot for polyester PE-101 was obtained in the 414-419°K temperature range. Ozawa plot consists of a set of parallel lines. Each straight line represents plot of $\log \{-\ln [1 - \alpha(T)]\}$ versus $\log a$ at the temperature T . Ozawa plot is shown in Figure 61. Avrami exponent "n" of 2.52 ± 0.2 was obtained in polyester PE-101. Figure 62 represents the Time-Temperature-Transformation (T-T-T) diagram of polyester PE-101. As indicated in Section 3.2.4, T-T-T diagram is a familiar non-equilibrium concept used in the study of crystallisation in metal and alloys. It defines the thermal history pathways ideally suited to obtain a

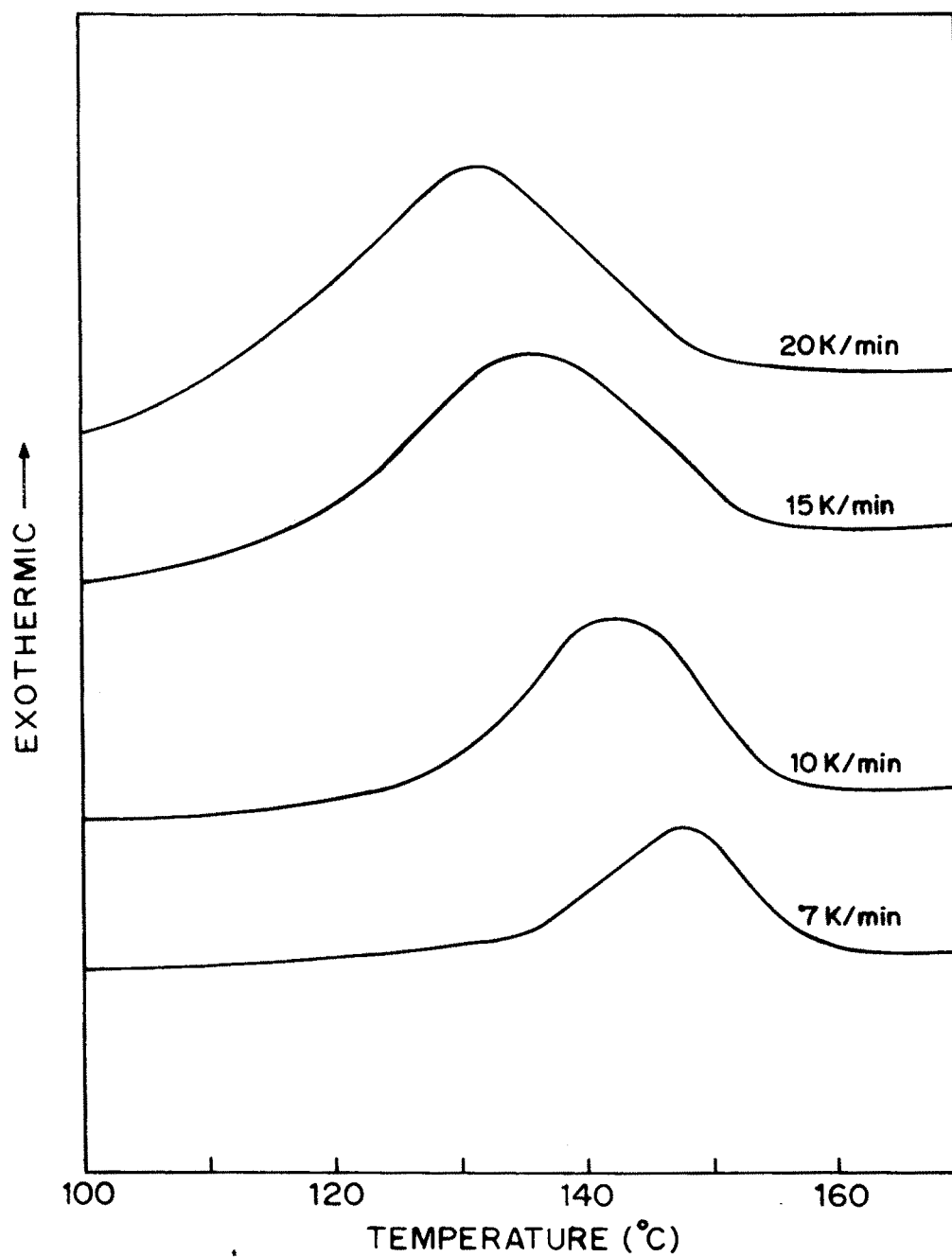


FIG. 59 A SET OF DSC COOLING TRACES FROM THE NEMATIC STATE AT DIFFERENT COOLING RATES (a) FOR HOMOPOLYESTER PE-101.

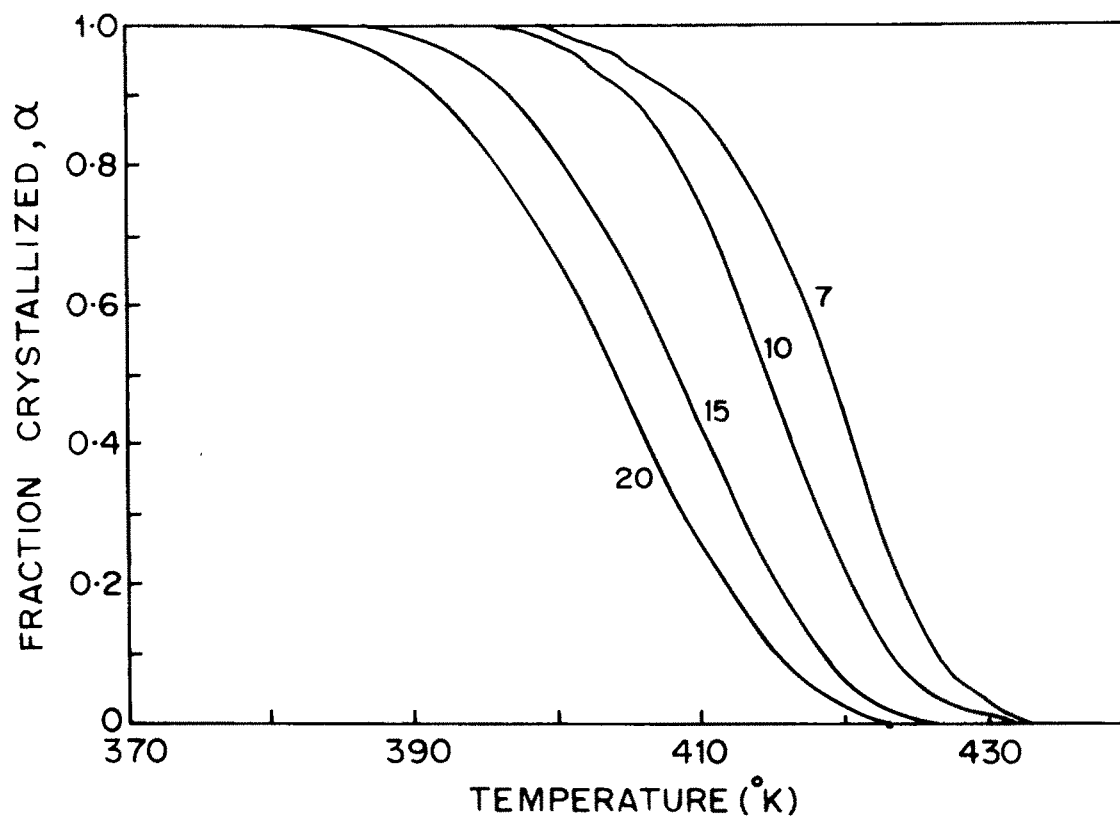


FIG. 60 RELATIONSHIPS BETWEEN α (FRACTION CRYSTALLIZED) AND TEMPERATURE FOR HOMOPOLYESTER PE-101.

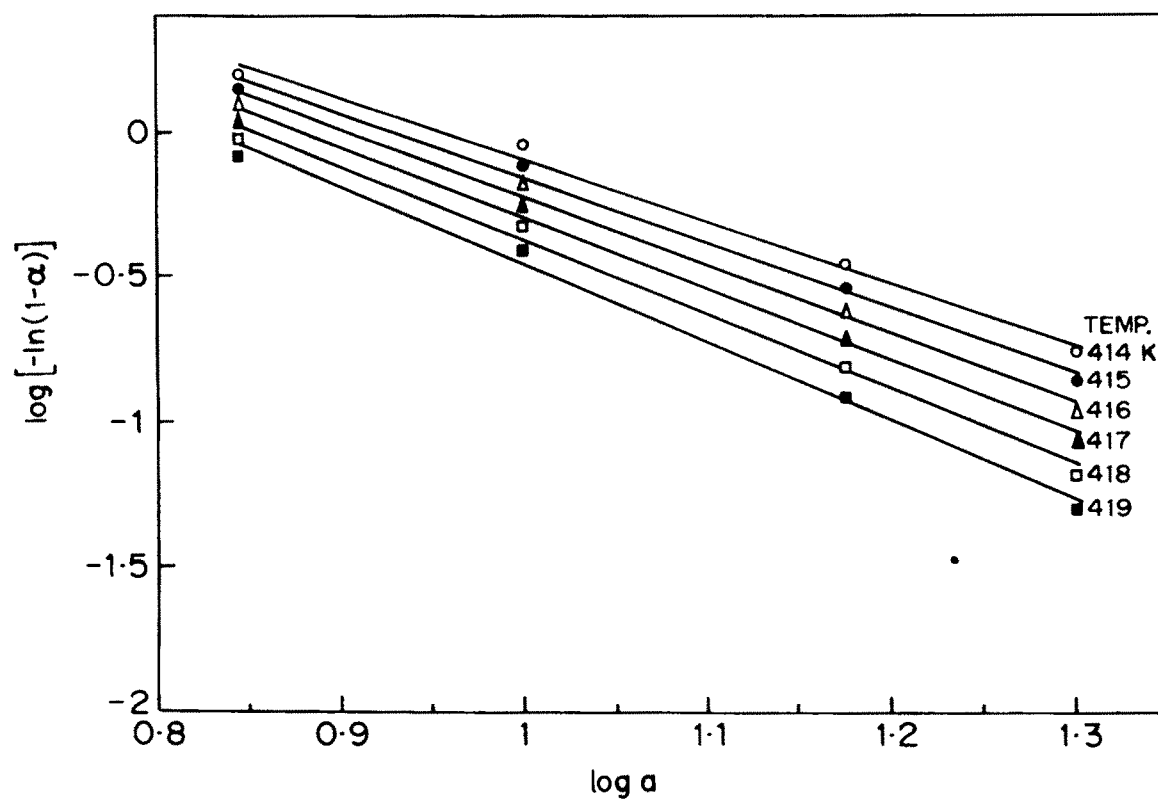


FIG. 61 PLOTS OF $\log [(-\ln(1-\alpha))]$ VERSUS $\log a$ FOR HOMO-POLYESTER PE-101.

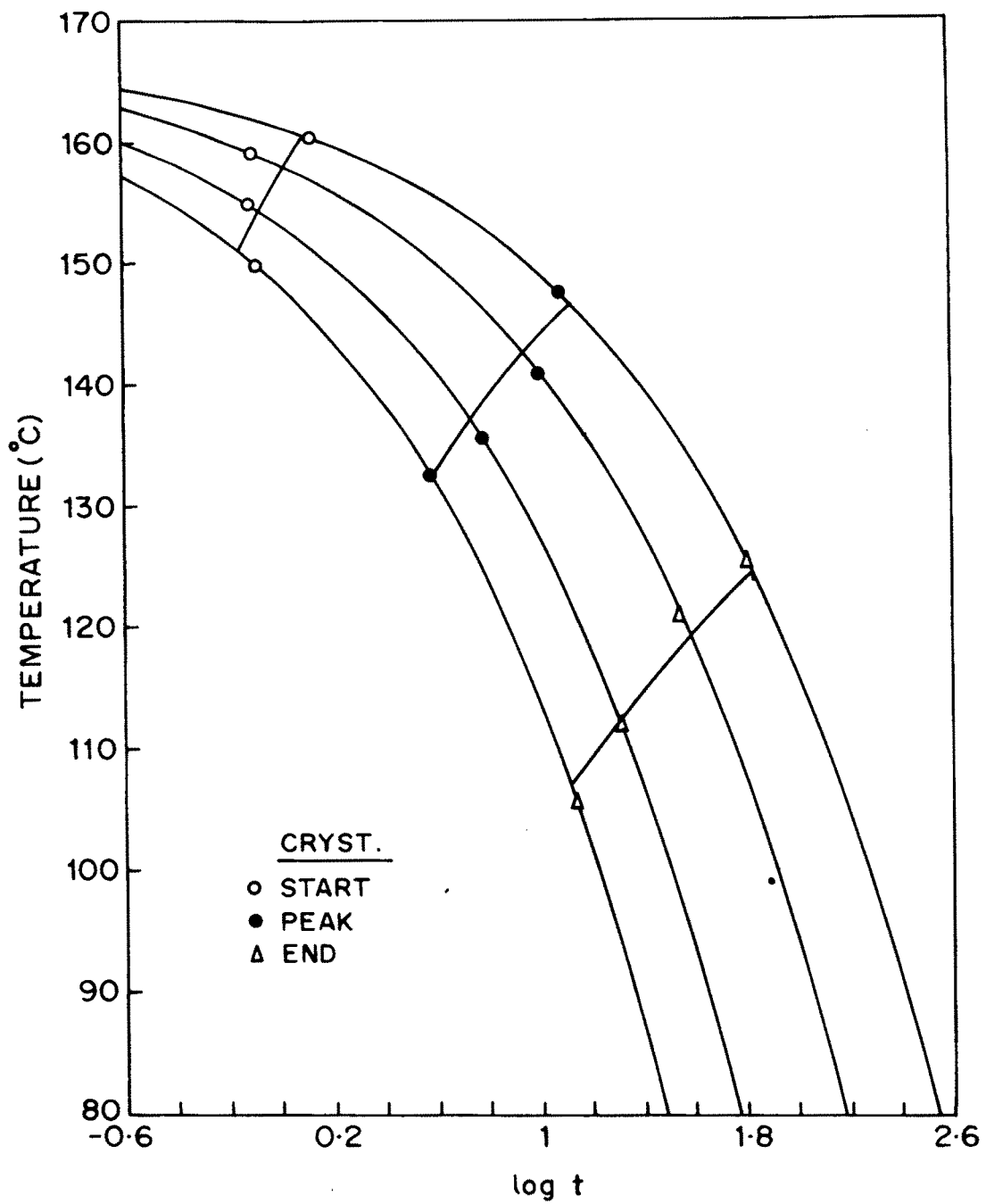


FIG. 62 A PORTION OF THE T-T-T PLOT FOR HOMOPOLYMER PE-101.

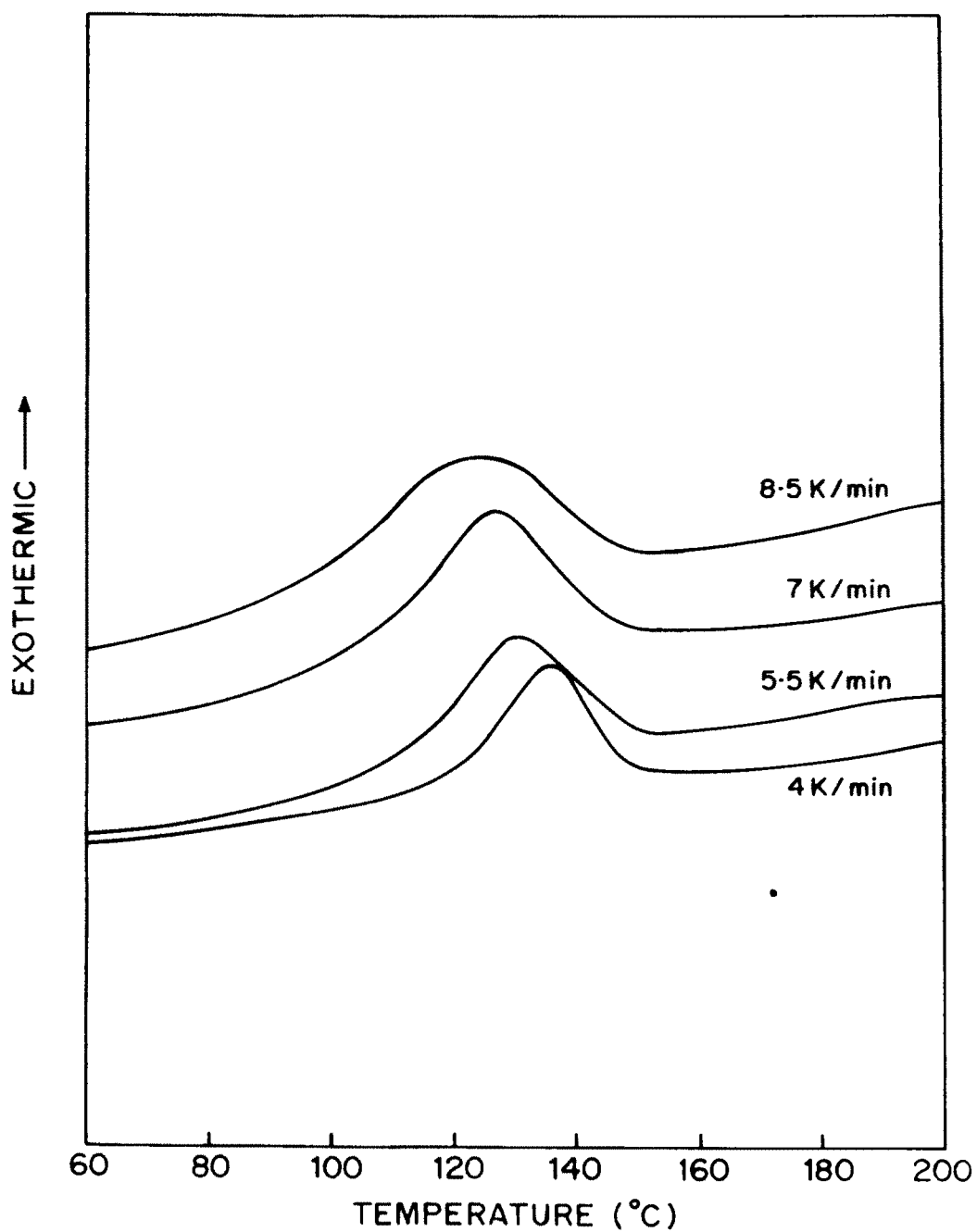


FIG. 63 A SET OF DSC COOLING TRACES FROM THE NEMATIC STATE AT DIFFERENT COOLING RATES (a) FOR HOMOPOLYESTER PE-102.

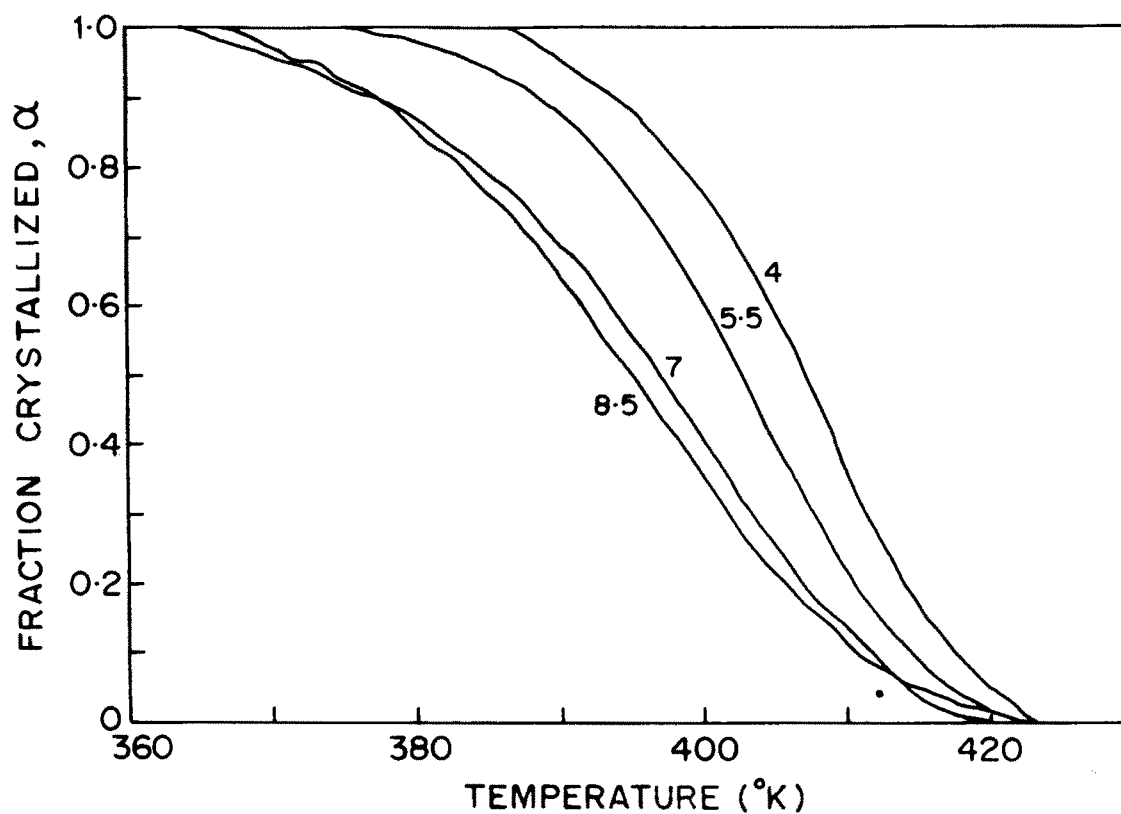


FIG. 64 RELATIONSHIPS BETWEEN α (FRACTION CRYSTALLIZED) AND TEMPERATURE FOR HOMOPOLYESTER PE-102.

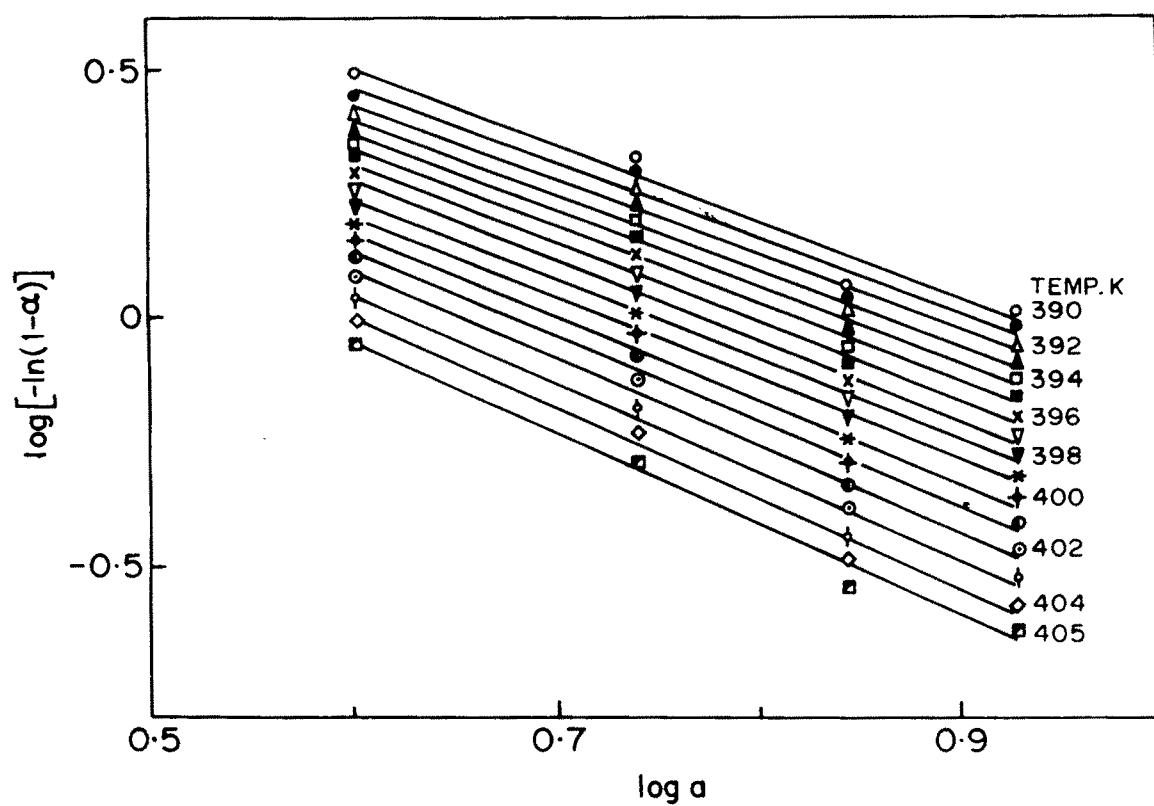


FIG. 65 PLOTS OF $\log [(-\ln(1-\alpha))]$ VERSUS $\log a$ FOR HOMO-POLYESTER PE-102.

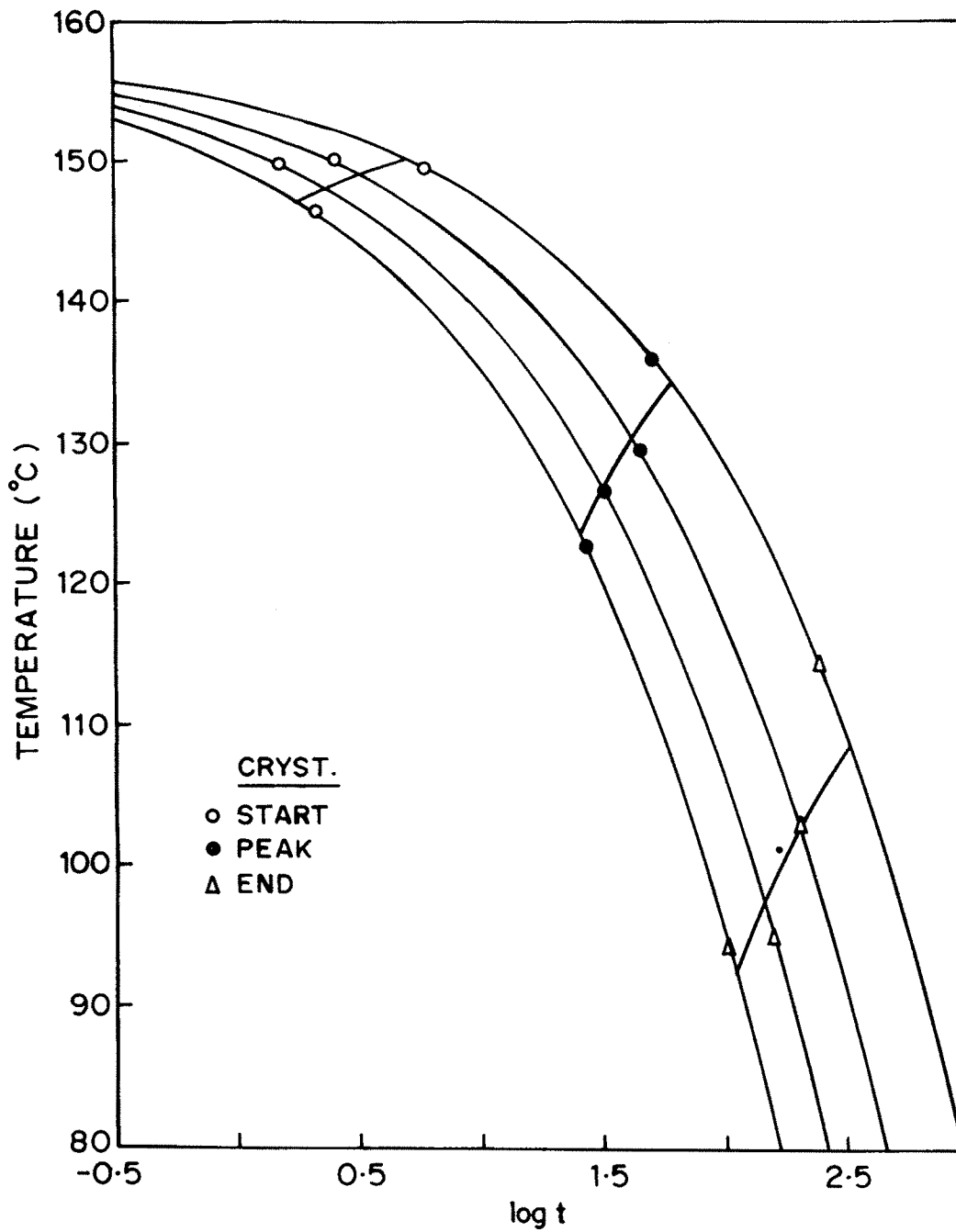


FIG. 66 A PORTION OF THE T-T-T PLOT FOR HOMOPOLYESTER PE-102.

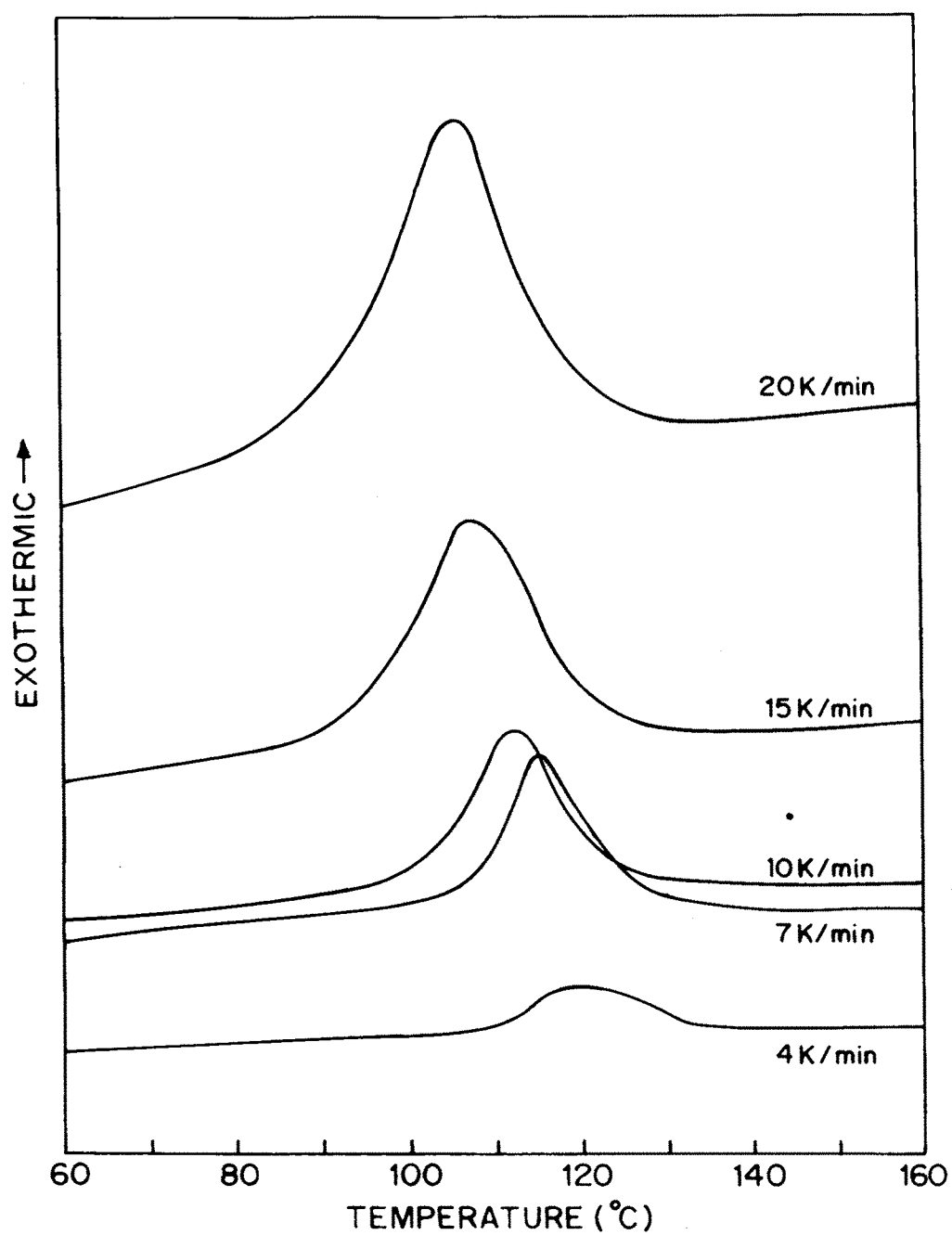


FIG. 67 A SET OF DSC COOLING TRACES FROM THE NEMATIC STATE AT DIFFERENT COOLING RATES (a) FOR HOMOPOLYESTER PE-105.

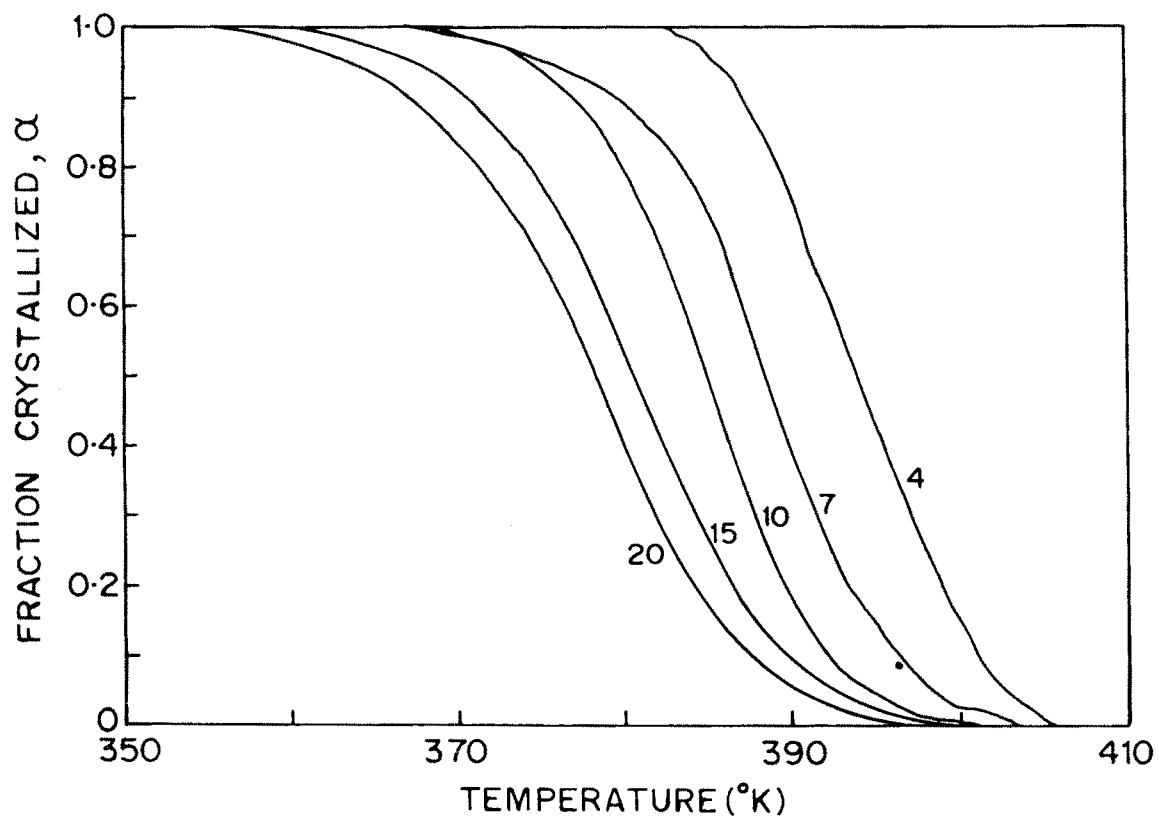


FIG. 68 RELATIONSHIPS BETWEEN α (FRACTION CRYSTALLIZED) AND TEMPERATURE FOR HOMOPOLYESTER PE-105.

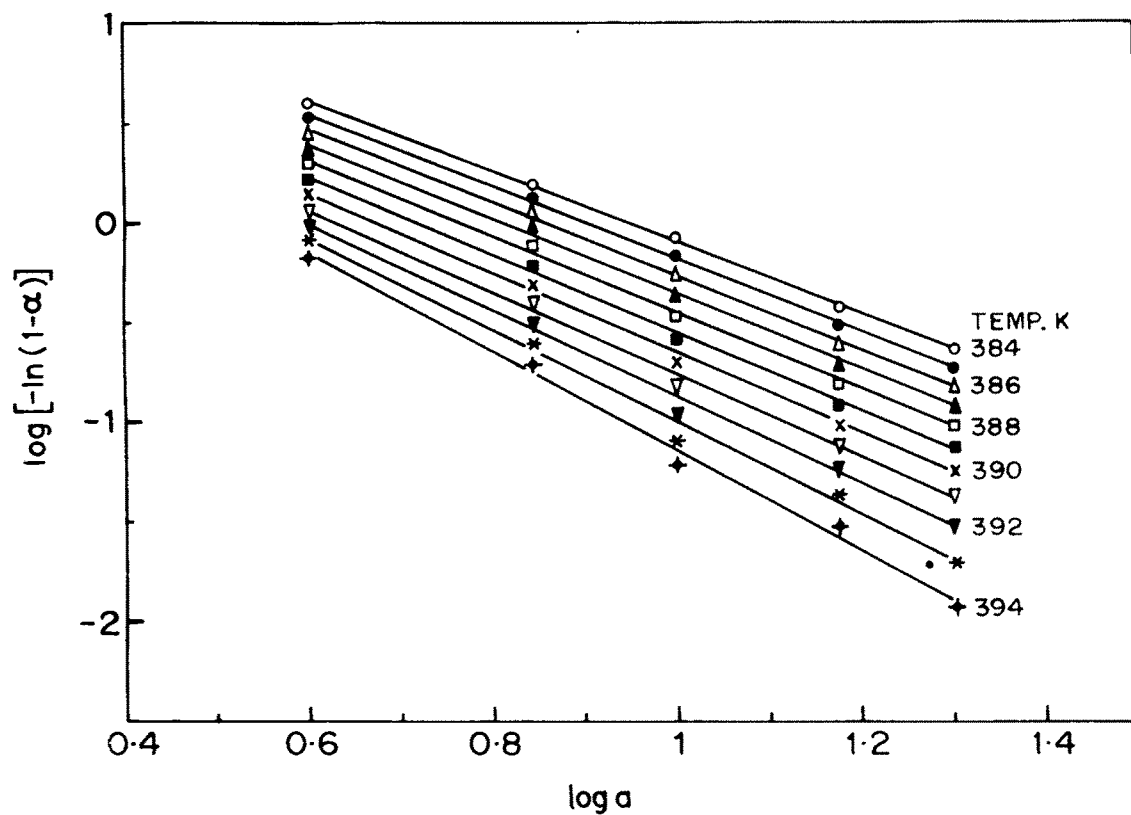


FIG. 69 PLOTS OF $\log[-\ln(1-\alpha)]$ VERSUS $\log a$ FOR HOMO-POLYESTER PE-105.

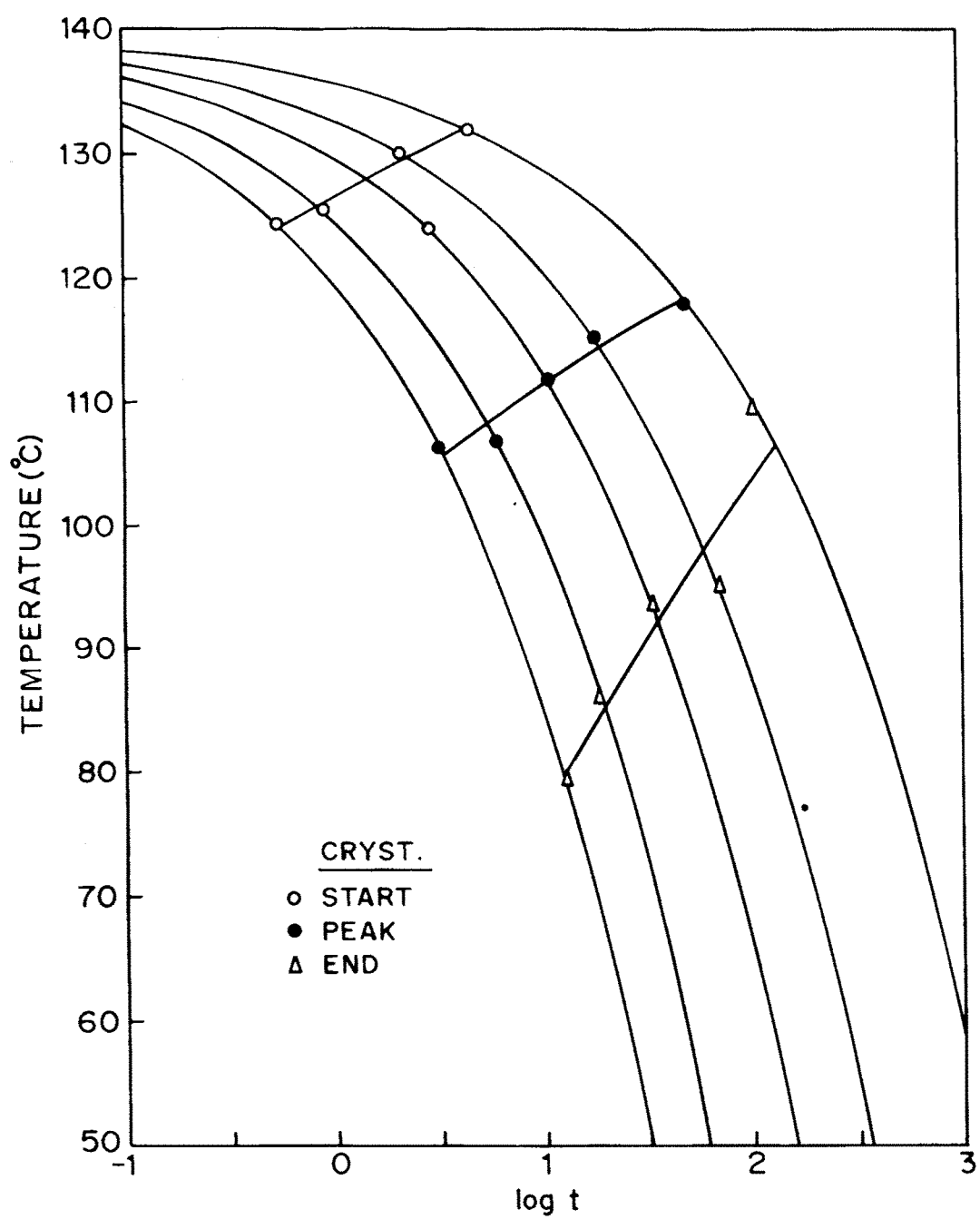


FIG. 70 A PORTION OF THE T-T-T PLOT FOR HOMOPOLYESTER PE-105.

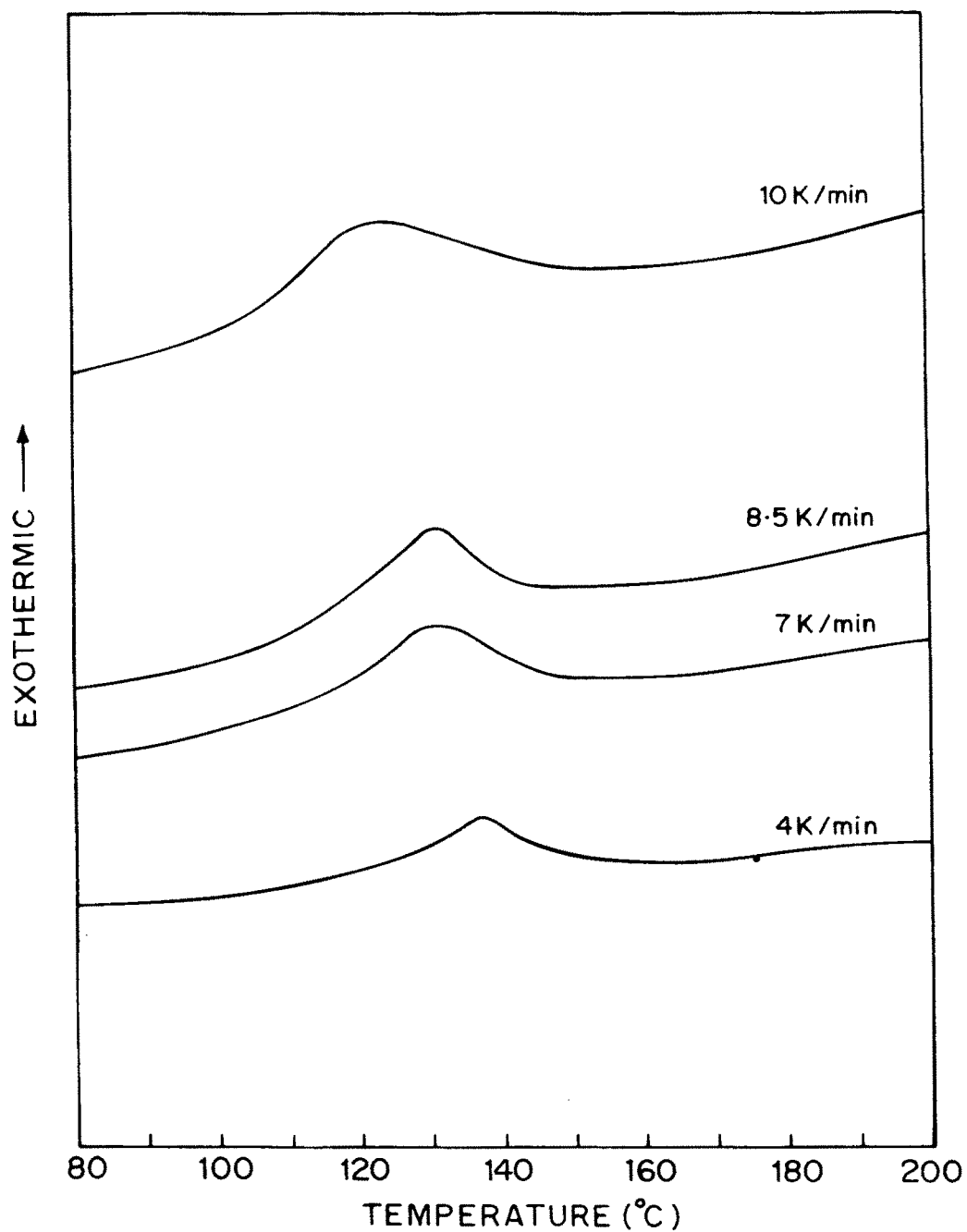


FIG. 71 A SET OF DSC COOLING TRACES FROM THE NEMATIC STATE AT DIFFERENT COOLING RATES (a) FOR HOMOPOLYESTER PE-106.

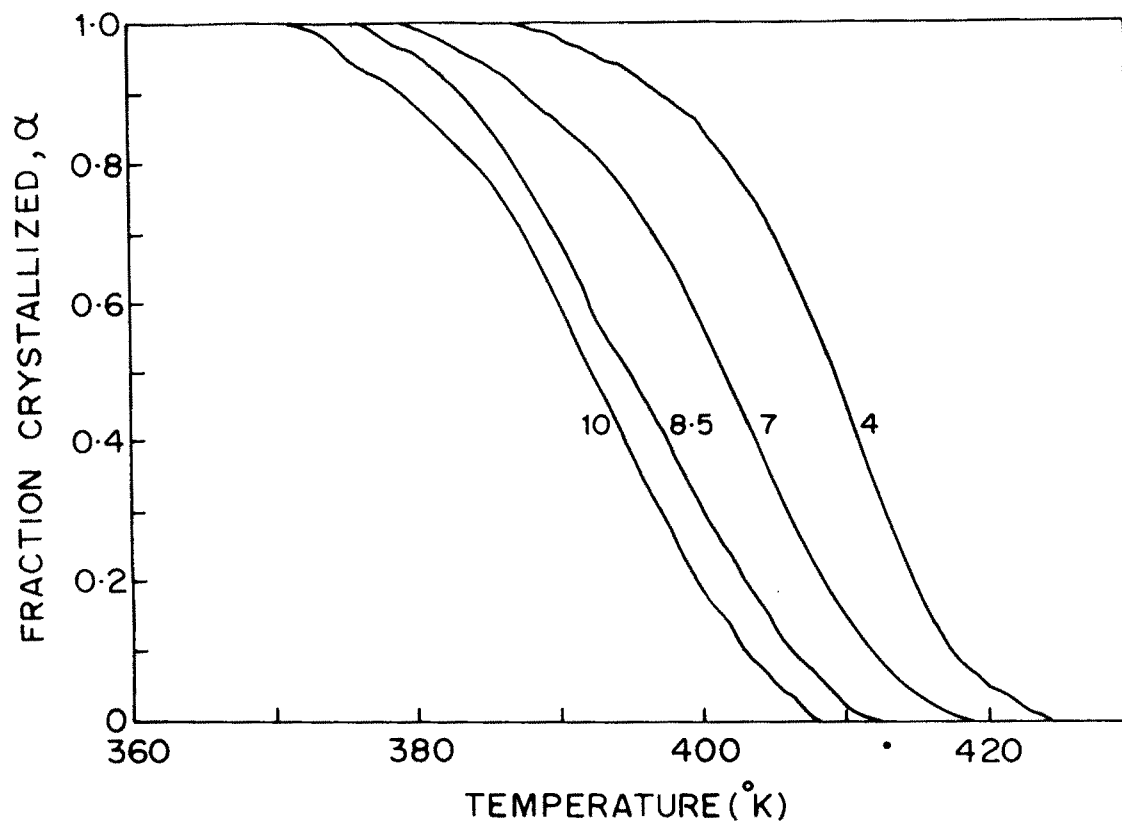


FIG. 72 RELATIONSHIPS BETWEEN α (FRACTION CRYSTALLIZED) AND TEMPERATURE FOR HOMOPOLYESTER PE-106.

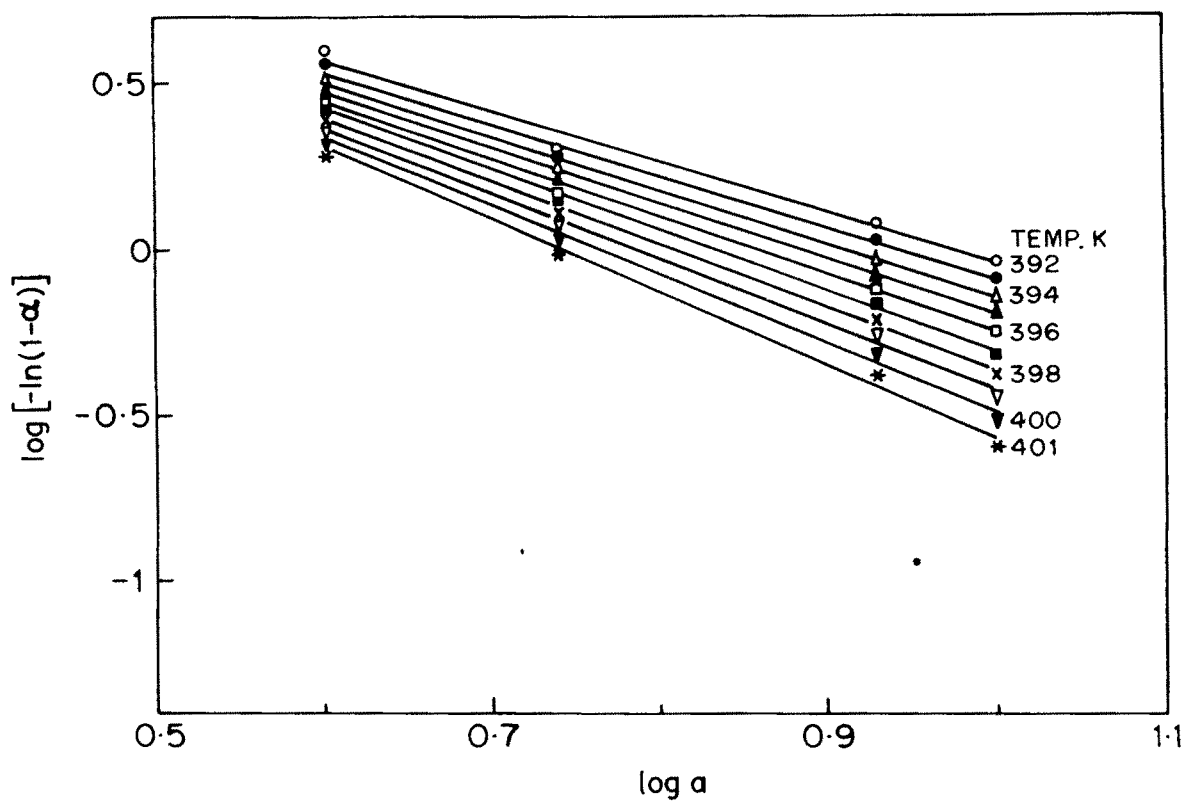


FIG. 73 PLOTS OF $\log [-\ln(1-\alpha)]$ VERSUS $\log a$ FOR HOMO-POLYESTER PE-106.

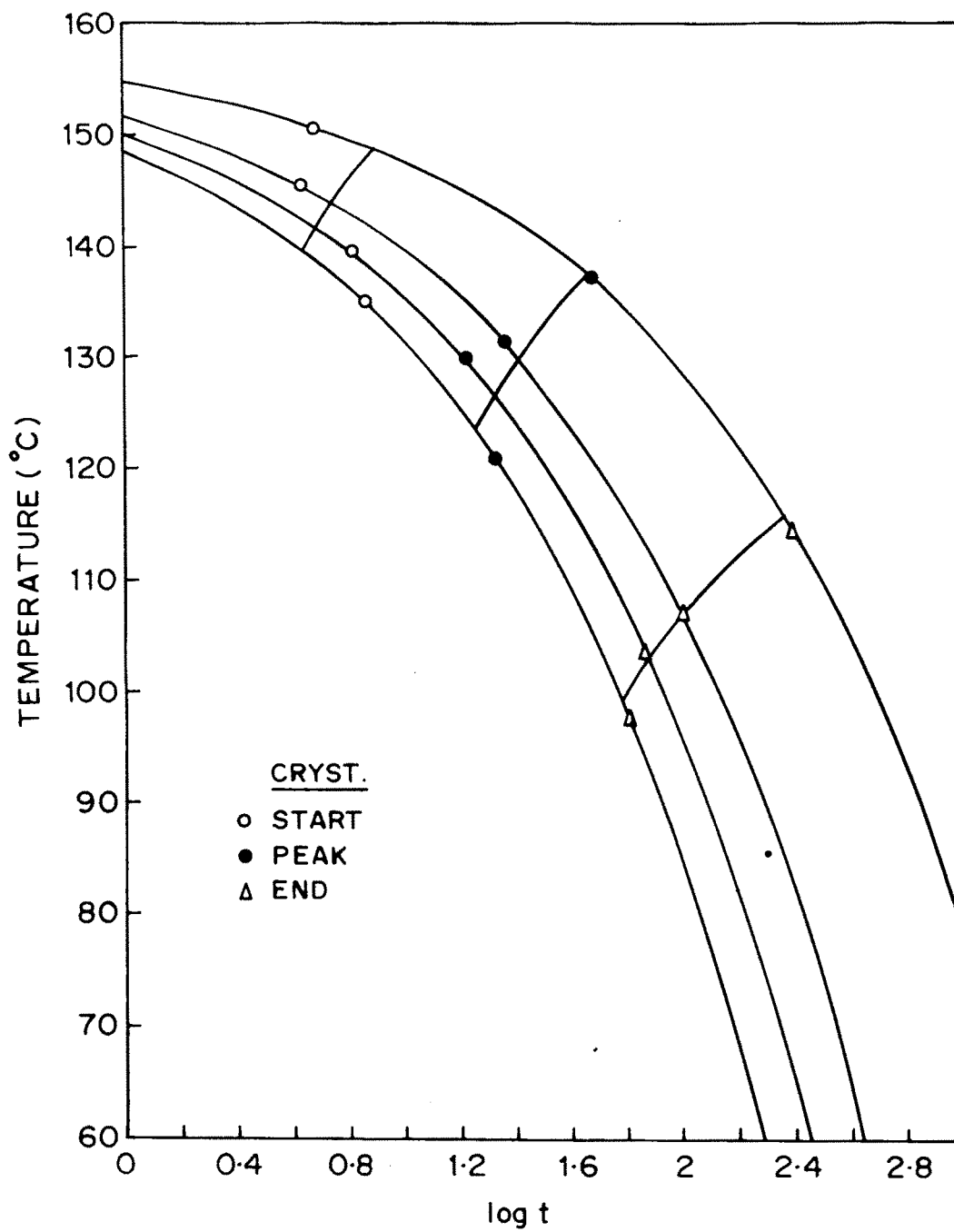


FIG. 74 A PORTION OF THE T-T-T PLOT FOR HOMOPOLYESTER PE-106.

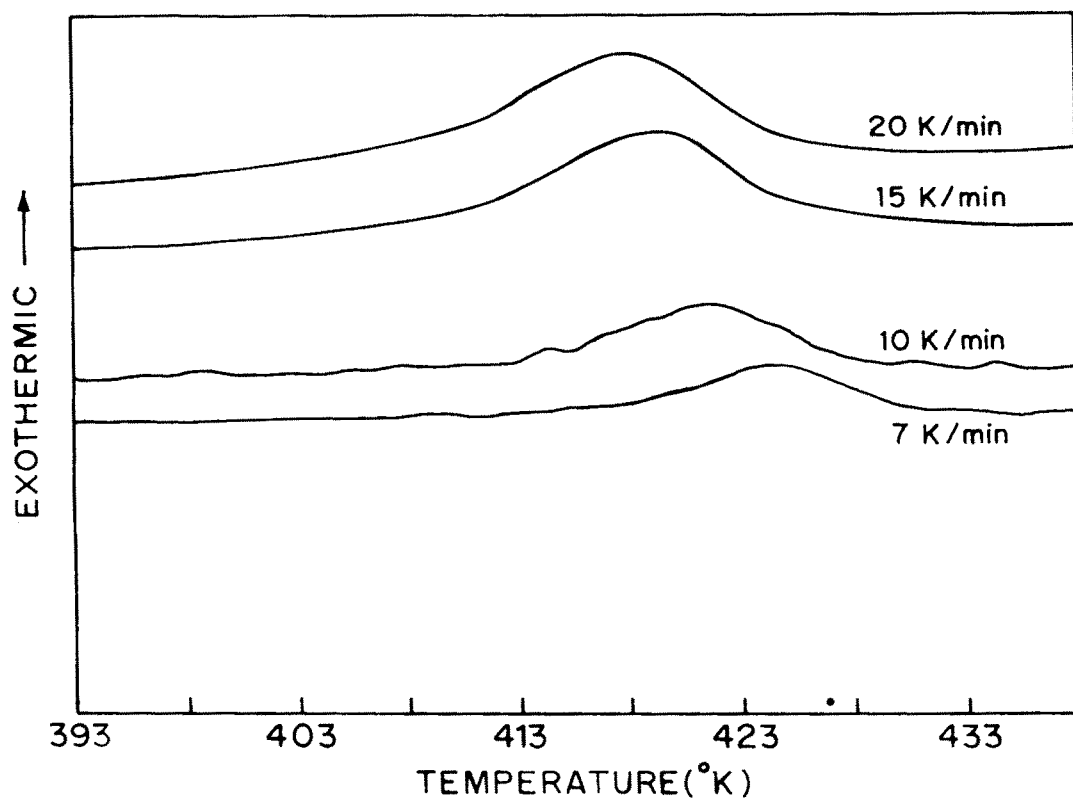


FIG. 75 A SET OF DSC THERMOGRAMS OF THE DYNAMIC COOLING CRYSTALLIZATION OF HOMOPOLYESTER PE-107.

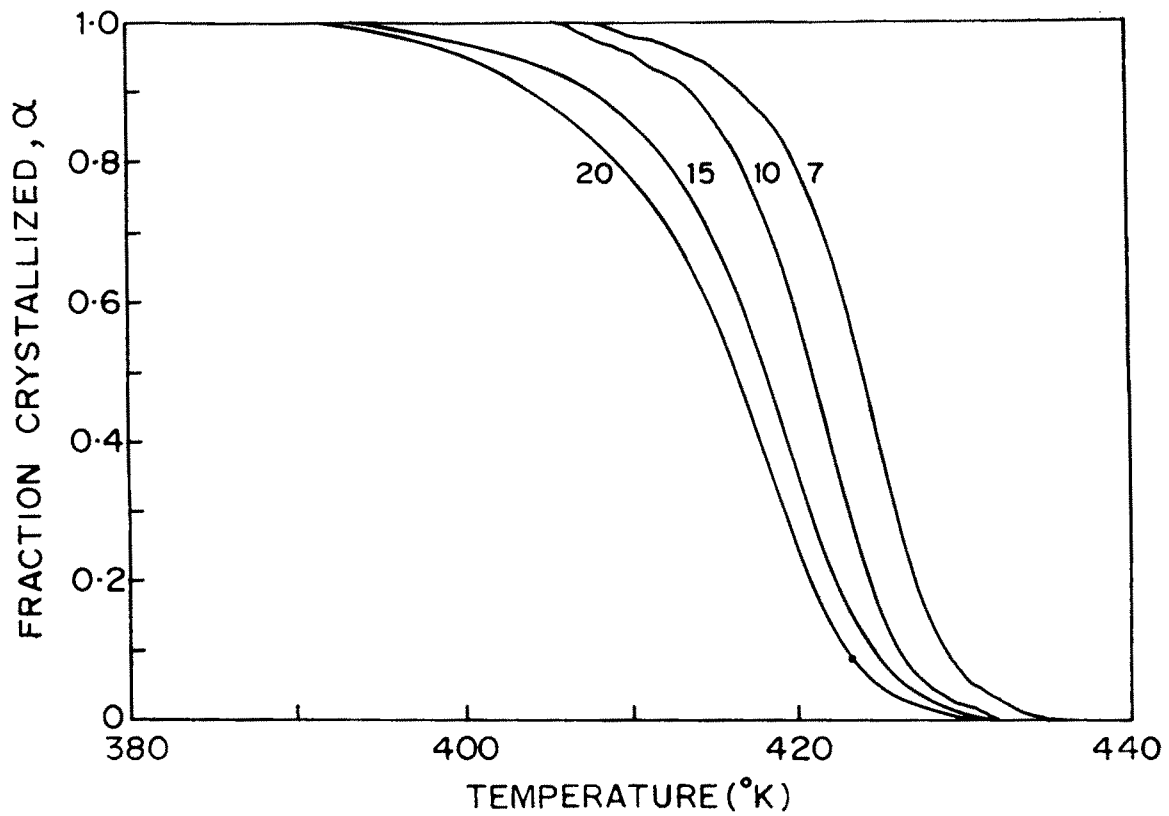


FIG. 76 RELATIONSHIPS BETWEEN α (FRACTION CRYSTALLIZED) AND TEMPERATURE FOR HOMOPOLYESTER PE-107.

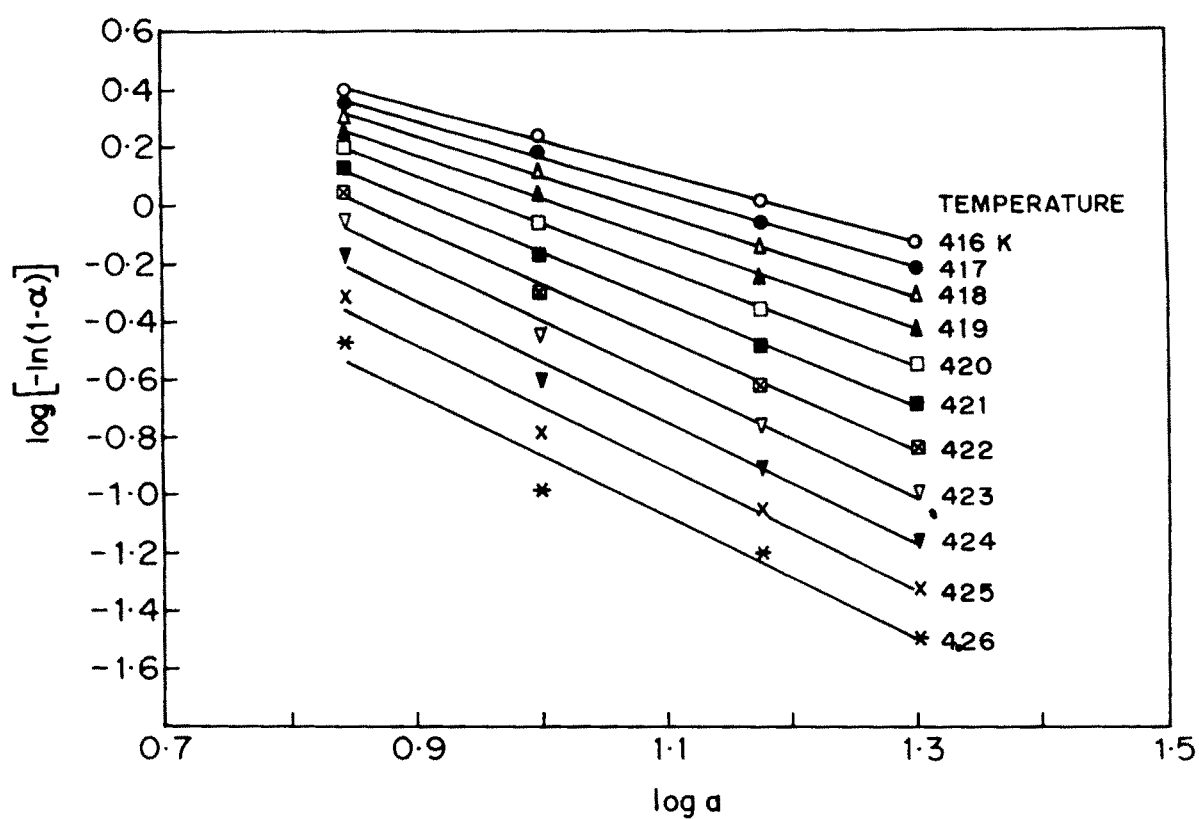


FIG. 77 PLOTS OF $\log [(-\ln(1-\alpha))]$ VERSUS $\log a$ FOR HOMO-POLYESTER PE-107.

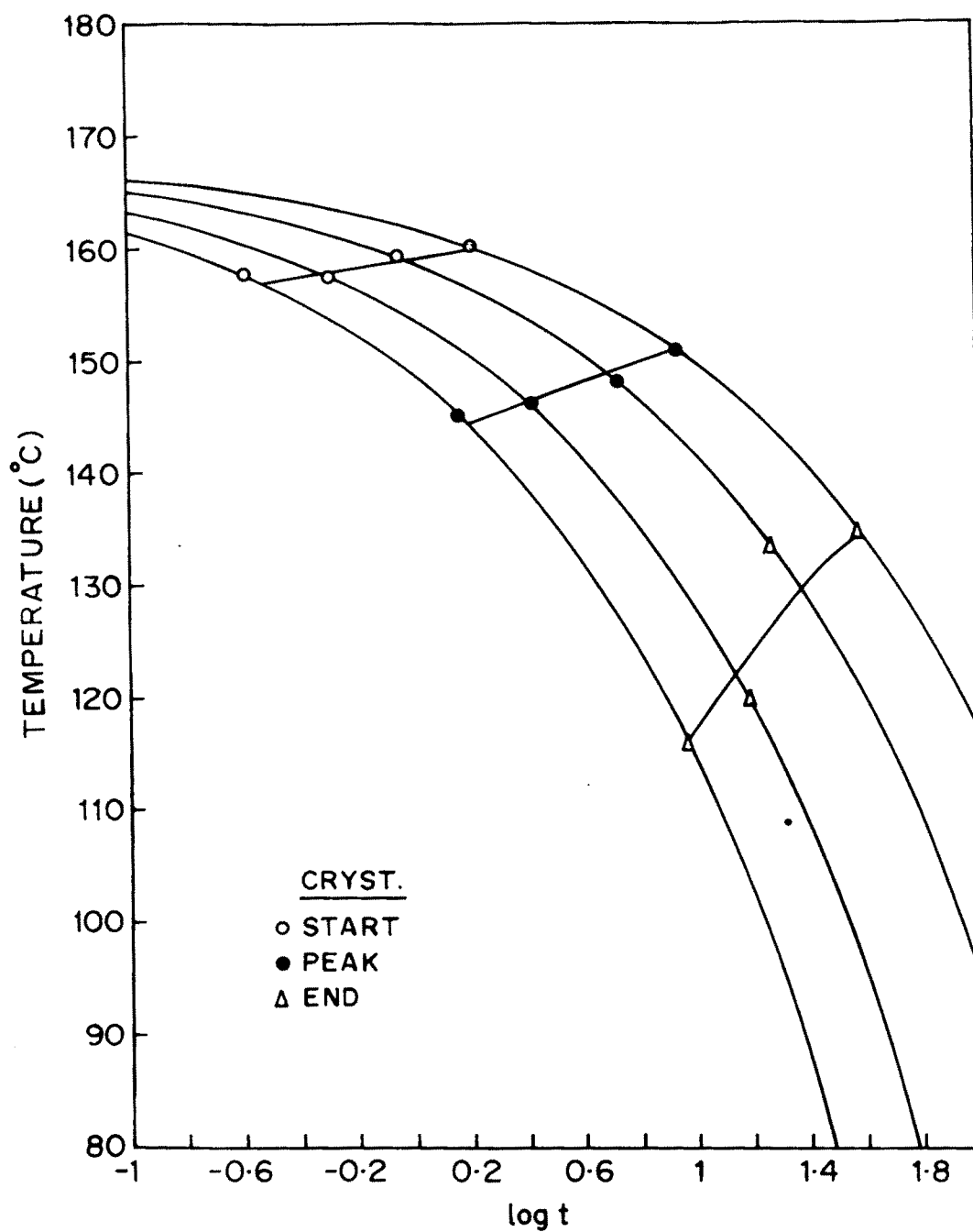


FIG. 78 A PORTION OF THE T-T-T PLOT FOR HOMOPOLYESTER PE-107.

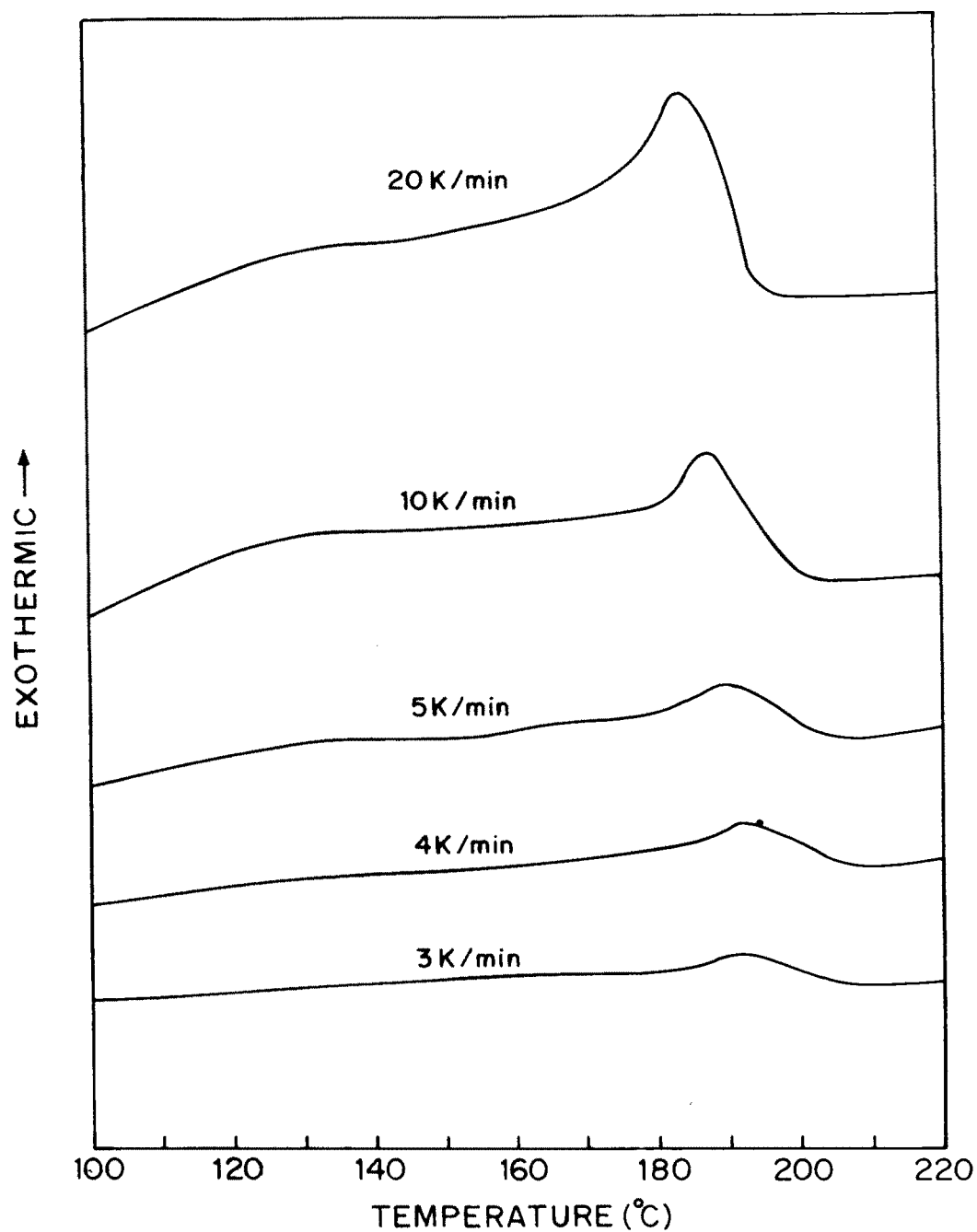


FIG. 79 A SET OF DSC COOLING TRACES FROM THE NEMATIC STATE AT DIFFERENT COOLING RATES (a) FOR HOMOPOLYESTER PE-203.

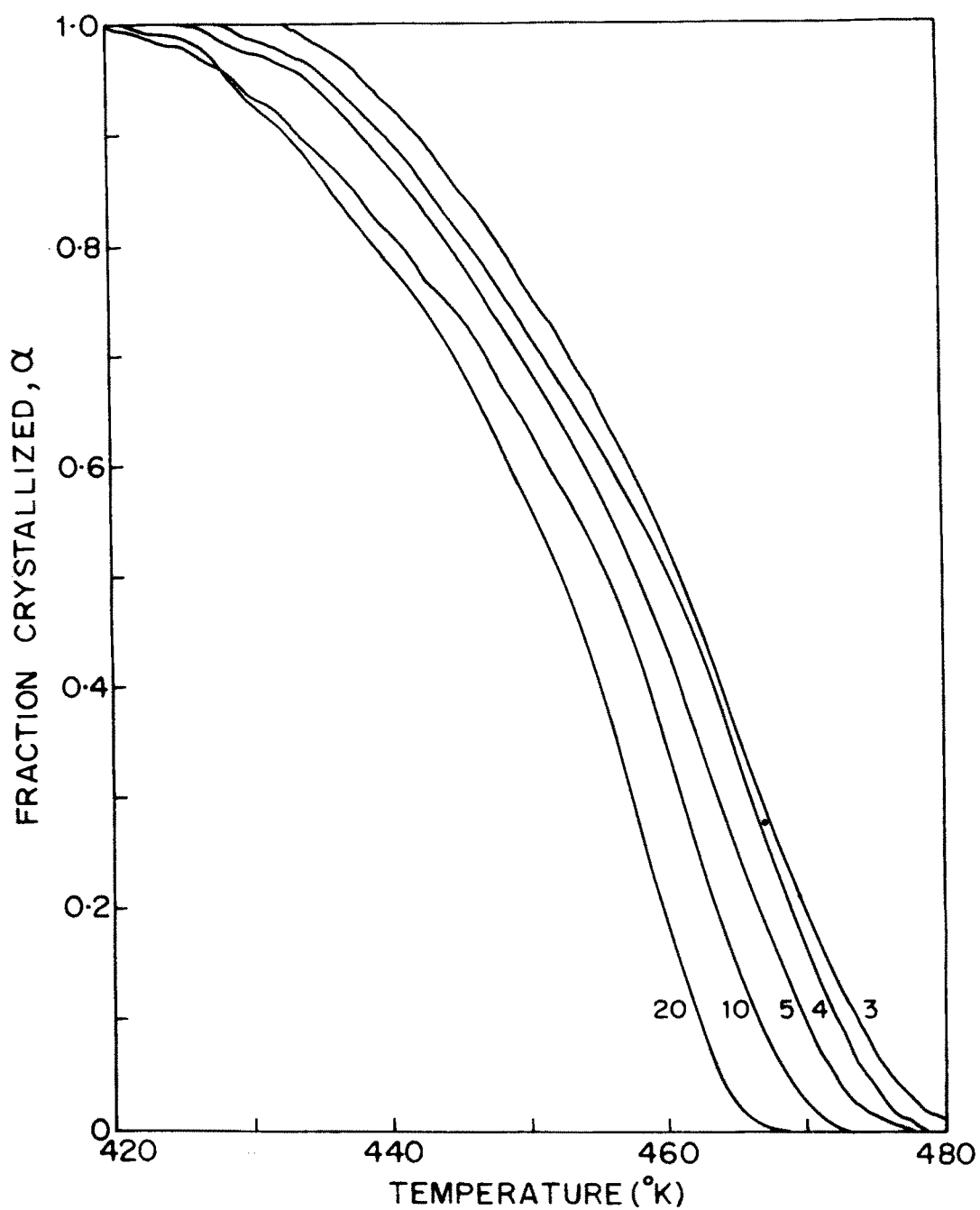


FIG. 80 RELATIONSHIPS BETWEEN α (FRACTION CRYSTALLIZED) AND TEMPERATURE FOR HOMOPOLYESTER PE-203.

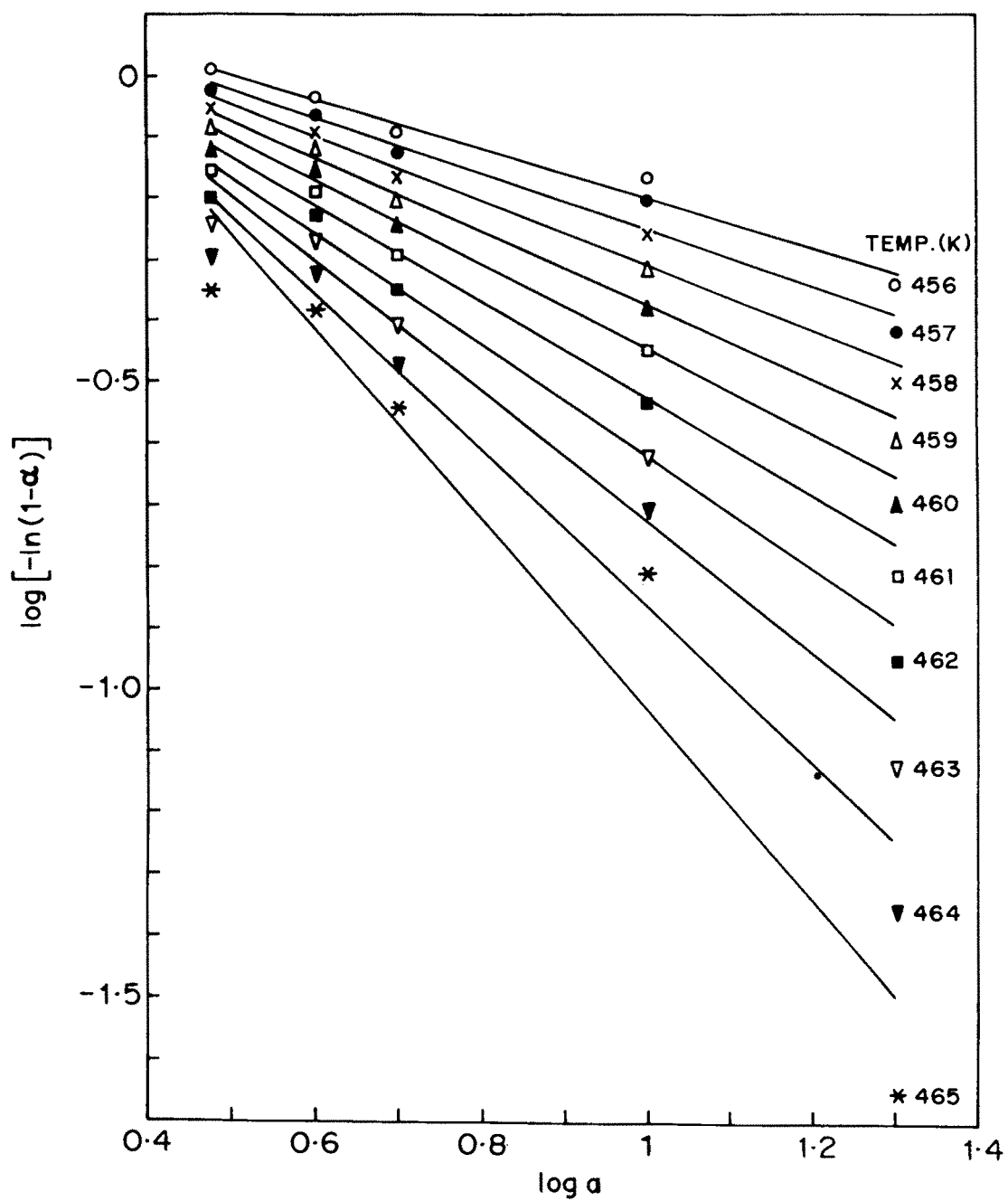


FIG. 81 PLOTS OF $\text{Log} [(-\ln(1-\alpha))]$ VERSUS $\text{Log } a$ FOR HOMO-POLYESTER PE-203.

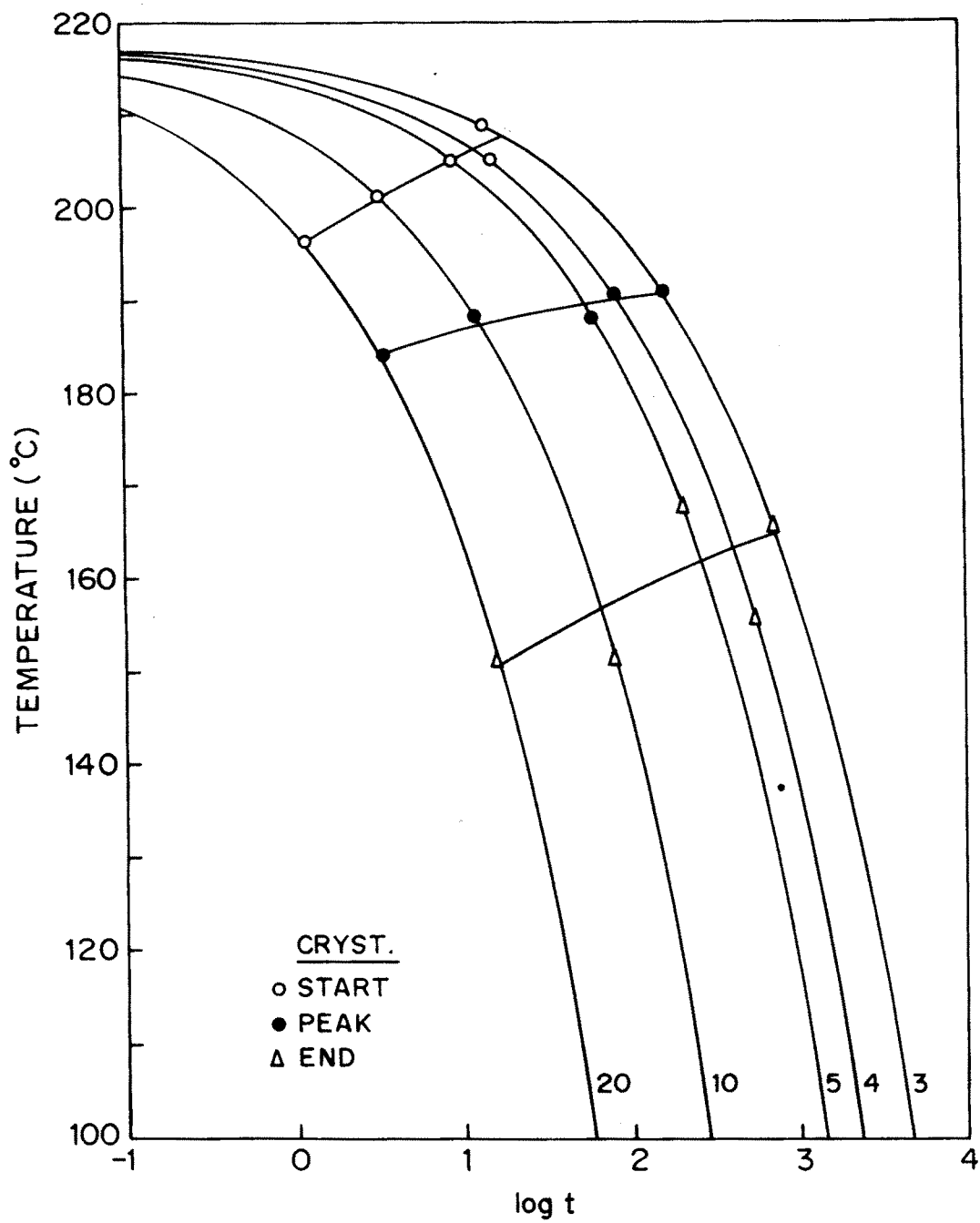


FIG. 82 A PORTION OF THE T-T-T PLOT FOR HOMOPOLYESTER PE-203.

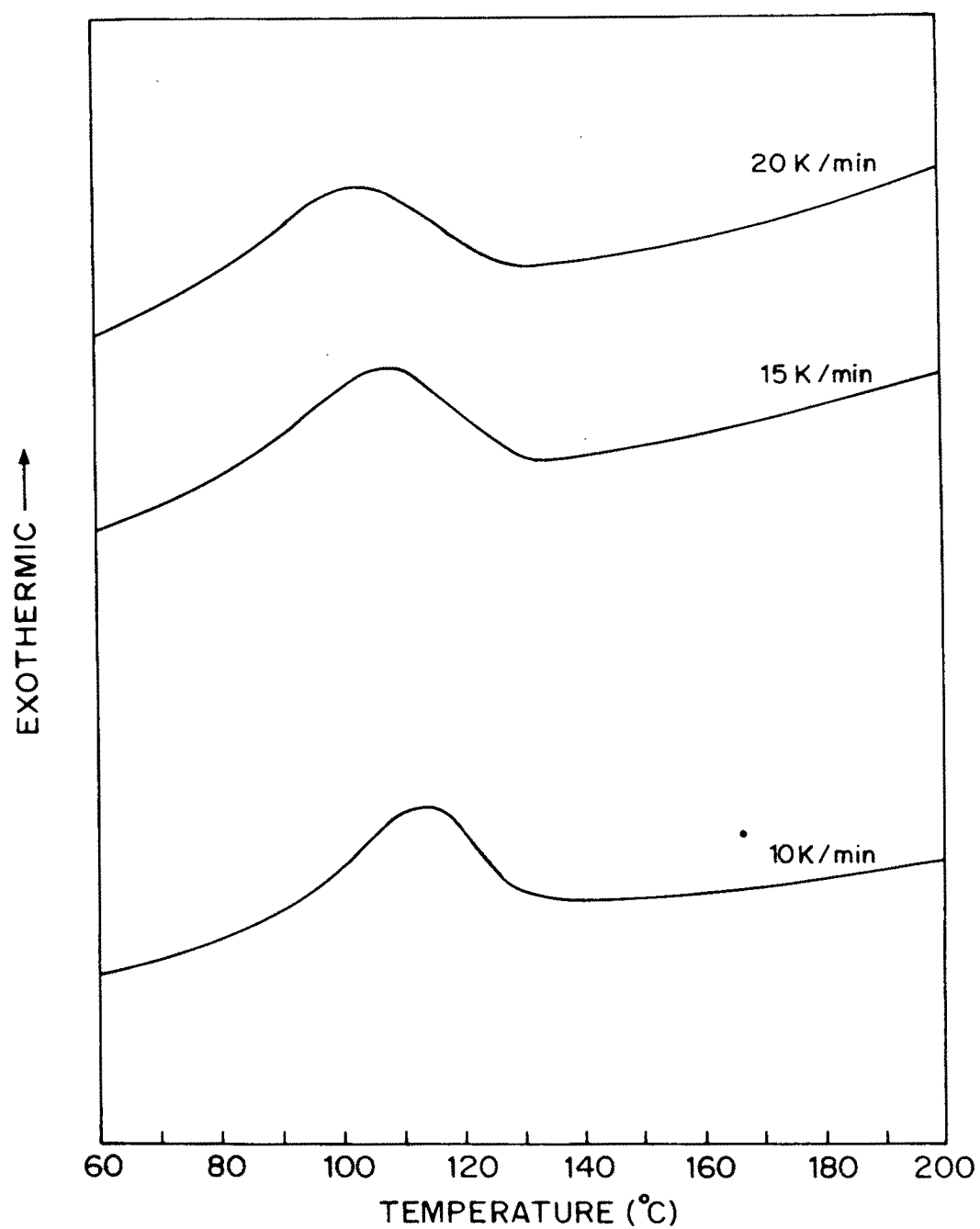


FIG. 83 A SET OF DSC COOLING TRACES FROM THE NEMATIC STATE AT DIFFERENT COOLING RATES (a) FOR HOMOPOLYESTER PE-303.

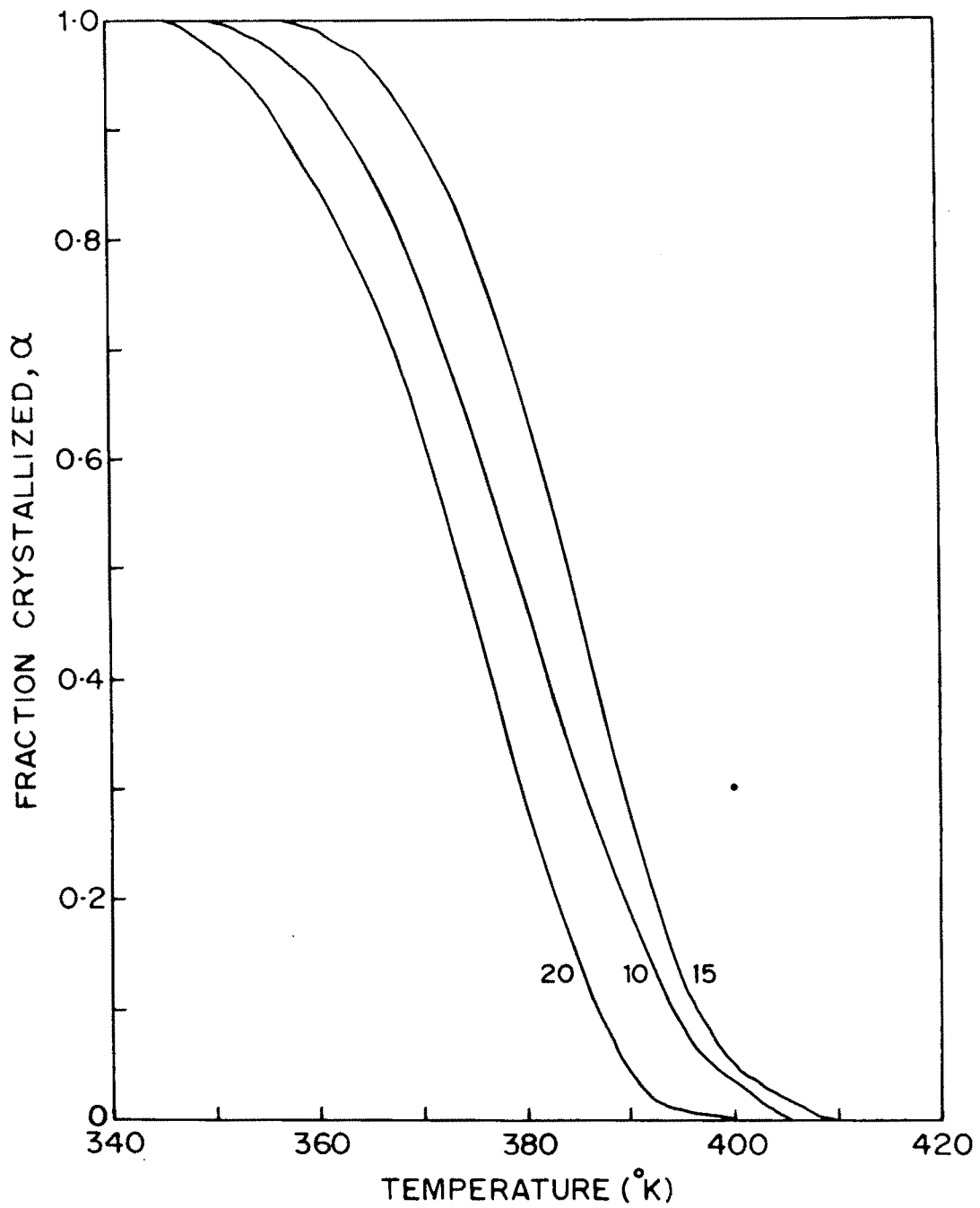


FIG. 84 RELATIONSHIPS BETWEEN α (FRACTION CRYSTALLIZED) AND TEMPERATURE FOR HOMOPOLYESTER PE-303.

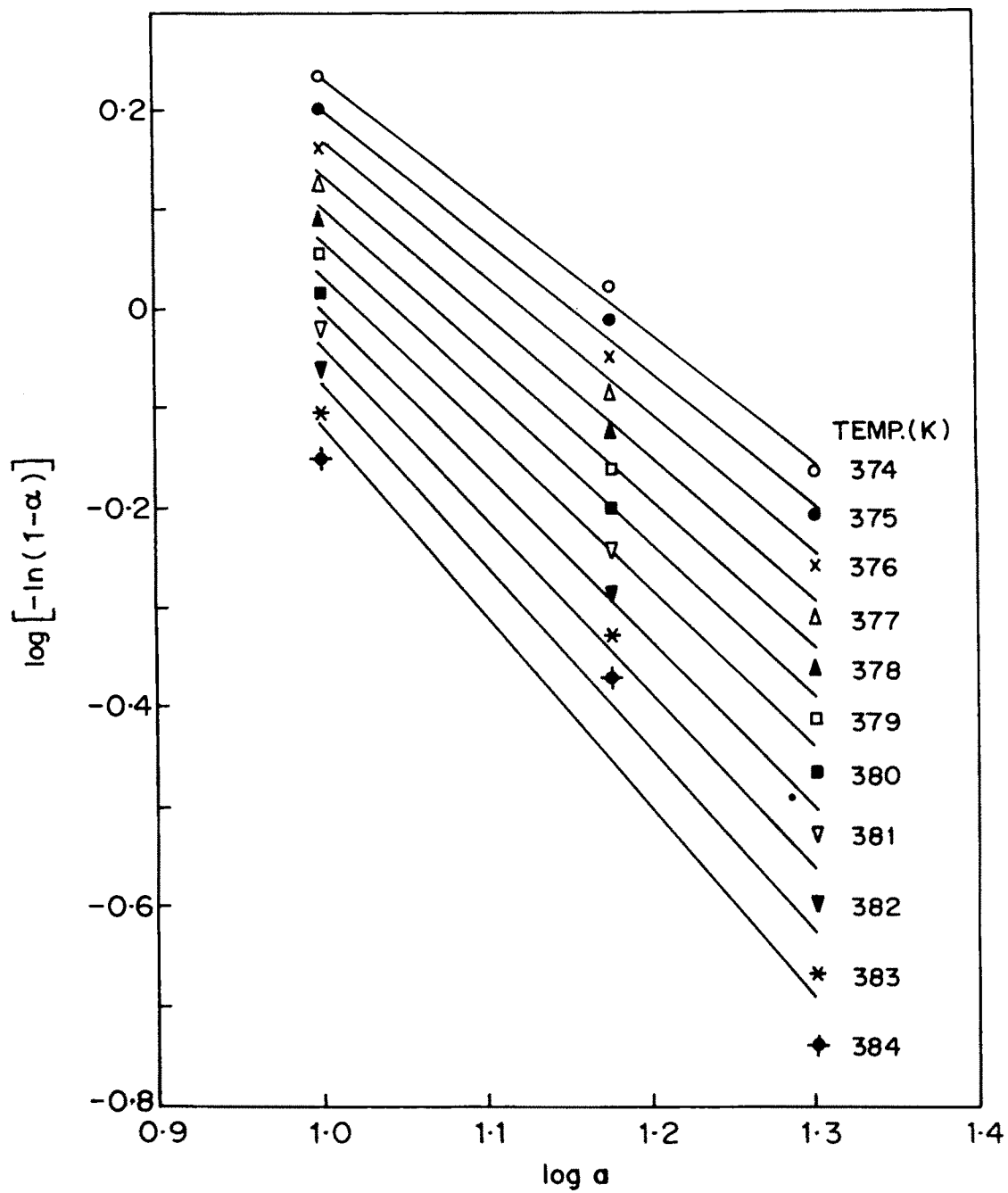


FIG. 85 PLOTS OF $\log [-\ln(1-\alpha)]$ VERSUS $\log a$ FOR HOMO-POLYESTER PE-303.

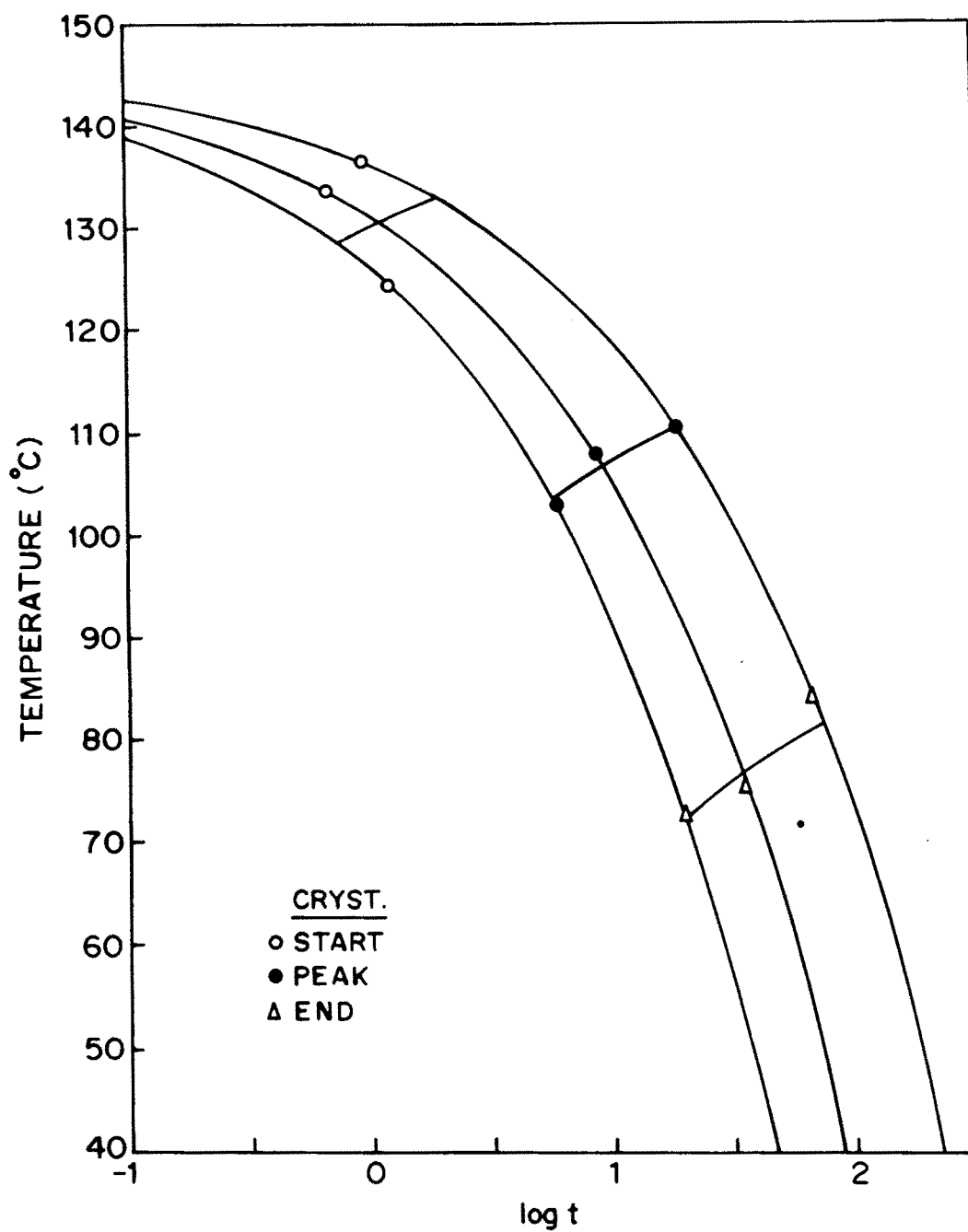


FIG. 86 A PORTION OF THE T-T-T PLOT FOR HOMOPOLYESTER PE-303.

STRUCTURES

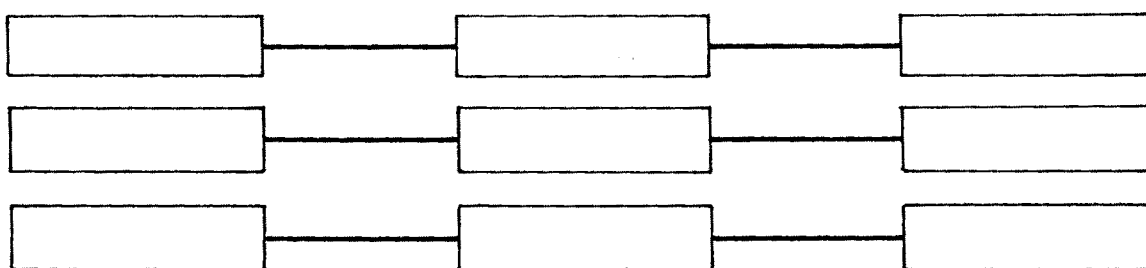
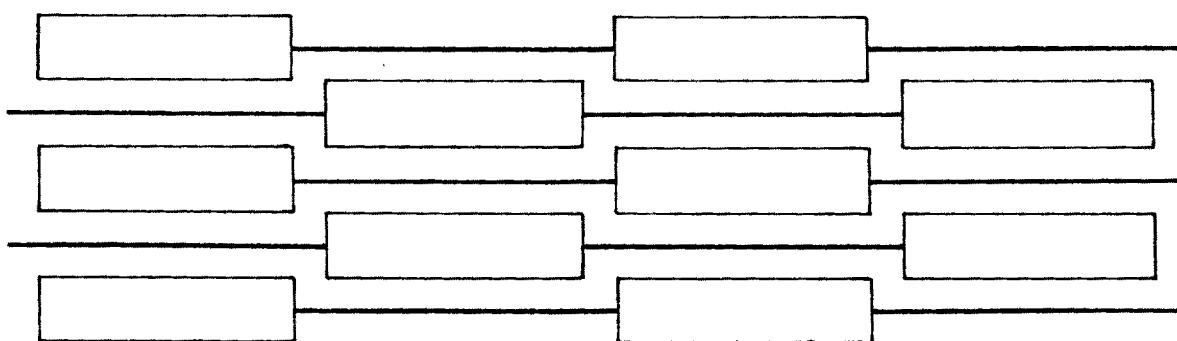
F/M RATIO LESS THAN 1e.g. $m=3,4$ and 7F/M RATIO GREATER THAN 1e.g. $m=10$ 

FIG. 87 NATURE OF PACKING OF FLEXIBLE SPACER RELATIVE TO MESOGEN RATIO LESS OR GREATER THAN ONE.

desired microstructure and crystallinity. The diagram is commercially pertinent in that new polymeric materials available in only small quantities can be screened for their inherent thermal characteristics and the exact thermal pathways needed to harness the potentials of the material can be established without resorting to processing. Here, we could not construct the complete diagram due instrumental limitations arising from a maximum permissible cooling rate of $100^{\circ}/\text{minute}$.

Similar sets of plots were obtained for other polyesters. DSC scan for polyesters PE-102, PE-105, PE-106 and PE-107 are represented in Figures 63, 67, 71 and 75 respectively. Similarly, DSC scan for polyesters PE-203 and PE-303 are represented in Figures 79 and 83. The plots of fractional crystallisation α as a function of temperature for these polyesters are shown in Figures 64, 68, 72, 76, 80 and 84. Avrami exponent " n " were obtained from Ozawa plot. Ozawa plots for polyesters PE-102, PE-105, PE-106 and PE-107 are presented in Figures 65, 69, 73 and 77. The values of " n " for these polyesters are presented in Table 54. Figures 66, 70, 74 and 78 represent the T-T-T diagrams of polyesters PE-102, PE-105, PE-106 and PE-107 respectively.

The higher " n " (2.52) for polyester PE-101, with 3 methylene units, points to a crystallisation behaviour which differs from other systems investigated here. The " n " value points indirectly to the order present in the polymer melt. High " n " values represent higher dimensionality of the crystal growth. The maximum obtainable " n " value for unidirectionally ordered nematic melts equals 3. In two dimensionally ordered smectic melts the maximum value obtainable is 2.

Lower " n " (1.6) was obtained for polyester PE-107 with decamethylene spacer. As previously indicated, optical examination of this polyester in the liquid crystalline state revealed texture typical of smectic phase (Section 4.2.2). Generally, thermotropic rigid rod-flexible spacer type polyesters with spacer lengths exceeding octamethylene

units display smectic phases.⁵³ The lower value of "n" (1.6) obtained for PE-107 corroborates with the optical examination and points to crystallisation from a smectic melt. Similarly, higher "n" (2.52) obtained for PE-101 is attributable to crystallisation from nematic melt. However, it must be stated that detailed high temperature X-ray diffraction analysis are required to quantify these observations. This variation in "n" in these two polyesters can be rationalised from molecular geometry considerations. It is established that the rigid molecules agglomerate into domains for purely geometric reasons.²³³

The FM (flexible spacer to mesogen) ratio for these polyesters,²³⁴ presented in Table 54, were obtained by taking ratios of the lengths of flexible spacer and mesogen. The lengths of mesogen and spacer were calculated by assuming trans conformations for all groups. The FM ratio of polyester PE-107 is greater than 1. This improves the crystal packing by interlocking of mesogen, as shown in the Figure 87, and indicates that this polyester melt is more ordered than the melts of other polyesters in the series and results in lower value of "n".

The Avrami exponent "n" for polyesters with 4, 7, 8 and 10 methylene units are close 2, indicating rodlike growth from sporadic nuclei. The higher value 2.52, is observed for spacer with 3 methylene units, lies between 2 and 3 and suggests diffusion controlled disc-like growth from sporadic nuclei or diffusion controlled spherulitic growth from instantaneous nuclei.¹⁹⁴ However, it is inexact to quantify the growth type and nucleation exclusively from the Avrami exponent "n" alone.

4.6.3 Effect of Substitution

Two polyesters PE-203 and PE-303 were selected to study the effect of substitution on crystallisation behaviour. The length of flexible spacer were the same in these two

polyesters and consisted of pentamethylene units. Polyester PE-203 was based on unsubstituted triad mesogenic unit whereas PE-303 was based on chloro substituted triad mesogenic unit.

DSC scans (thermograms) at various cooling rates, plot of fractional crystallisation versus temperature, Ozawa plots and T-T-T diagrams for polyester PE-203 are presented in Figures 81 and 82 respectively. Similar plots for polyester PE-303 are shown in Figures 85 and 86. The peak temperatures, temperature range of analysis and Avrami exponent "n" are tabulated in Table 54. Lowest value of Avrami exponent "n" (0.8) was obtained for unsubstituted polyester PE-203. The value of Avrami exponent "n" is 1.56 ± 0.2 for chloro substituted polyester PE-303. This is within the range of values obtained for methyl substituted polyesters PE-102, PE-106 and PE-107 respectively. This indicates that the nature of substitution on the central unit of triad mesogen has marginal effect on the Avrami exponent "n" and hence on crystallisation behaviour. The large variation in "n" values between polyesters PE-203 (unsubstituted) and PE-303 (chloro substituted) points to the molecular ordering present in the melt of unsubstituted polyester.

The melt of unsubstituted polyester (PE-203) is probably highly ordered. In chloro substituted polyester (PE-303) the placement of mesogen along the chain is ordered but randomisation still occurs. This arises from head-head, head-tail and tail-tail arrangements between adjacent mesogenic units along the polyester chain generated by the nonsymmetrical mono (chloro) substitution on each mesogenic core.¹³ Therefore, the melts of polyesters synthesised from substituted mesogens are less ordered than highly symmetric polyesters prepared from unsubstituted mesogens.

It must be stated that there is a need to establish order parameters through electron microscopic and high temperature X-ray diffraction studies to arrive at exact and precise mechanisms of crystallisation. However, it is to be added in conclusion

that the study has brought out salient features relating to crystallisation of nematic and smectic melts, the subtle interplay of structural features with the mechanism and the thermodynamics of these transformations. It has also shown that broad processing profiles can be simulated by establishing T-T-T diagrams through a combination of isothermal and non-isothermal crystallisation kinetic estimates.

4.6.4 Conclusion

Effect of substitution on the triad mesogen and type of mesophase (nematic or smectic) on the nonisothermal crystallisation from liquid crystalline phases were examined. Avrami exponents were estimated using Ozawa method. Lower exponent was noted for the polyester forming smectic mesophasic melts with two-dimensional order. Higher exponent was observable in the crystallisation from nematic melts with one-dimensional order. Among nematic melts, the polyester with the lowest trimethylene spacer showed highest Avrami exponent of 2.52, showing the lack of uniform behaviour among nematics and suggested greater disorder in the nematic melts of polyesters with odd number of methylene units. In relation to mesogen type, at constant flexible spacer length, lowest Avrami exponent of 0.8 was noted for the unsubstituted system. At the same spacer length, the chloro substituted system displayed an Avrami exponent of 1.56. This points to greater order in the melts of polyesters synthesised from unsubstituted mesogen. Randomisation due to head-head, head-tail and tail-tail positioning of adjacent monosubstituted mesogens account for this decreased order. Partial T-T-T diagrams were constructed for all polyesters to establish the most suited thermal pathway to process these materials.

REFERENCES

REFERENCES

1. Reinitzer, F.,
Monatsh, **9**, 421 [1888].
2. Lehmann, O.,
Z. Phys. Chem., **4**, 462 [1889].
3. Lehmann, O.,
Z. Krist., **18**, 464 [1890].
4. Reinitzer, F.,
Ann. Physik., **27**, 213 [1908].
5. Lehmann, O.,
Ann. Physik., **25**, 852 [1908].
6. Lehmann, O.,
Ann. Physik., **27**, 1099 [1908].
7. Lehmann, O.,
Ber., **41**, 3774 [1908].
8. a) Smith, G.W., in "Plastic Crystals, Liquid Crystals and the Melting Phenomenon. The Importance of Order. Advances in Liquid Crystals", Vol. 1., G.H. Brown, Ed., Academic Press, NY [1975];
b) Rinne, F.,
Trans Faraday Society, **29**, 1016 [1933].
9. Some general reviews of Liquid Crystals are:
a) Gray, G.W., "Molecular structure and properties of Liquid Crystals", Academic Press, NY [1962];
b) Gray, G.W. and Winsor, P.A., Eds., "Liquid Crystals and Plastic Crystals", Wiley, Chichester [1974];
c) de Gennes, P.G., "The Physics of Liquid Crystals", Clarendon Press, Oxford [1974];
d) Johnson, J.F. and Porter, R.S., Eds., "Liquid Crystals and Ordered Fluids", Vol. 1 and 2, Plenum Press, NY [1970] and [1974];
e) Porter, R.S. and Johnson, J.F., Eds., "Ordered Fluids and Liquid Crystals", Am. Chem. Soc., Washington DC [1967];
f) Symposium of the Faraday Soc. 5. "Liquid Crystals", Faraday Div. Chem. Soc., London [1972];
g) Proc. Int. Conf. Liq. Cryst., Gordon and Breach, London Science [1965].
h) Cifferi, A., Krigbaum, W. and Meyer, R.B., Eds., "Polymer Liquid Crystals", [Material Sci. Tech. Ser.], Academic Press, NY [1983].

10. Some general reviews of Plastic Crystals:
 - a] Sherwood, N., Ed., "The Practically Crystalline State", [Orientationally Disordered Crystals], J. Wiley and Sons, Chichester [1979];
 - b] Aston, J.G., "Plastic Crystals", in Fox, D., Labes, M.M. and Weissberger, A., Eds., "Physics and Chemistry of the Organic Solid State", Vol. 1, Interscience Publ., NY, [1963]; Chapter 9;
 - c] Staveley, L.A.K., "Phase Transitions in Plastic Crystals", Annual Rev. of Phys. Chem., **13**, 351 [1962];
 - d] DuPre, D.B., Samulski, E.T. and Tobolsky, A.V., "The Mesomorphic State: Liquid Crystals and Plastic Crystals", in Tobolsky, A.V., and Mark, H.F., Eds., "Polymer Science and Materials", Wiley-Interscience, NY [1971];
 - e] Proc. of the Symposium on "Plastic Crystals and Rotation in the Solid state", April [1960]; Phys. Chem. Solids., **18** [1], [1961].
11. Brown, G.H.,
Anal. Chem., **41**, 26-A, [1969].
12. Brown, G.H.,
Mol. Cryst., Liq. Cryst., **7**, 127 [1969]
13. Flory, P.J. and Ronco, G.,
Mol. Cryst., Liq. Cryst., **54**, 311 [1979].
14. deVries, A. and Fischel, D.L.,
Mol. Cryst., Liq. Cryst., **16**, 311 [1972].
15. Levelut, A.M. and Lambert, M.,
C. R. Acad. Sci. Ser. B., **B-272**, 1018 [1971].
16. Sackmann, H. and Demus, D.,
Mol. Cryst., Liq. Cryst., **21**, 239 [1973].
17. Gray, G.W. and Lydon, J.E.,
Nature, **252**, 221 [1974].
18. McMillan, W.L.,
Phys. Rev., **A-9**, 1720 [1974].
19. Griffin, A.C. and Johnson, J.F.,
J. Am. Chem. Soc., **99**, 4859 [1977].
20. Taylor, T.R., Arora, S.L. and Ferguson, J.L.,
Phys. Rev. Lett., **25**, 722 [1970].
21. Wise, R.A., Smith, D.H. and Doane, J.W.,
Phys. Rev., **A-7**, 1366 [1973].

22. Leadbetter, A.J., Mazid, M.A., Kelly, B.A., Goodby, J.W. and Gray, G.W.,
Phys. Rev. Lett., **43**, 630 [1979].
23. Moncton, D.E. and Pindak, R.,
Phys. Rev. Lett., **A-43**, 701 [1979].
24. Winsor, P.A.,
Faraday Symposia No. **5**, 89, Chem. IDC, London [1971].
25. Diele, S., Brand, P. and Sackmann, H.,
Mol. Cryst., Liq. Cryst., **17**, 163 [1972].
26. a) Goodby, J.W. and Gray, G.W.,
Mol. Cryst., Liq. Cryst., **49**, 217 [1979].
b) de Vries, A.,
J. Chem. Phys., **70**, 2705 [1979].
27. Arpin, M., Strazielle, C. and Skoulios, A.,
J. Phys., **Part-38**, 307 [1977].
28. Clough, S.B. and Blumstein, A., in Blumstein, A., Ed., "Mesomorphic Order
in Polymers and Polymerization in Liquid Crystal Media", American Chemical
Society, Washington DC [1978].
29. de Vries, A., "Structure and Classification of Thermotropic Liquid Crystals",
in Saeva, F., Ed., "Liquid Crystals: The Fourth State of Matter", Marcel and
Dekker Inc., New York [1979].
30. Helfrich, W.,
Mol. Cryst., **21**, 187 [1973].
31. Ericksen, J.L.,
Kolloid. Z., **173**, 117 [1960].
32. Porter, R.S. and Johnson, J.F., in Eirich, F., Ed., Rheology, **Vol. 4**, Academic
Press, NY [1967].
33. Leslie, F.M., "Theory of flow phenomena in Liquid Crystals", in Brown, G.H.,
Ed., "Advan. in Liquid Crystals", Vol. 4, Academic Press, NY [1979].
34. Dreher, R. and Meier, G.,
Phys. Rev., **A-8**, 1616 [1973].
35. Saeva, F.D.,
Mol. Cryst., Liq. Cryst., **23**, 171 [1973].
36. Demus, D. and Ritcher, L., "Textures of Liquid Crystals", Verlag Chemie, NY,
[1978].

37. Gray, G.W., Hartley, J.B. and Jones, B.,
J. Chem. Soc., 1412 [1955].
38. Gray, G.W. and Jones, B.,
J. Chem. Soc., 3733 [1956].
39. Samulski, E.T. and Tobolsky, A. V.,
Macromolecules, **1**, 555 [1968].
40. Kleinschuster, J.J., Pletcher, T.C. and Schaeffgen, J.R.,
Belg. Pat., 828,935 [1974].
41. Roviello, A. and Sirigu, A.,
J. Polym. Sci., Polym. Lett. Edn., **13**, 455 [1975].
42. McIntyre, J. and Mulburn, A.,
Brit. Polym. J., **13**, 5 [1981].
43. Meurisse, P., Noel, C., Monnerie, L. and Fayolle, B.,
Brit. Polym. J., **13**, 55 [1981].
44. Jackson, W.J. Jr., and Kuhfuss, H.F.,
J. Polym. Sci., Polym. Chem. Edn., **14**, 2043 [1976].
45. Griffin, B.P. and Cox, M.K.,
Brit. Polym. J., **12**, 147 [1980].
46. Wissburn, K.F.,
Brit. Polym. J., **12**, 163 [1980].
47. Polk, M.B., Bota, K.B., Akubuiro, E.C. and Phingobodhipakkiya, M.,
Macromolecules, **14**, 1626 [1982].
48. Jin, J.-I., Antoun, S., Ober, C. and Lenz, R.W.,
Brit. Polym. J., **12**, 132 [1980].
49. Ober, C.K., Jin, J.-I., Zhou, Q. and Lenz, R.W.,
Adv. in Polym. Sci., **59**, 104 [1984].
50. Lenz, R.W.,
Faraday Discuss Chem. Soc., **79**, 21 [1985].
51. Antoun, S., Lenz, R.W. and Jin, J.-I.,
J. Polym. Sci., Polym. Chem. Edn., **19**, 1901 [1981].
52. Zhou, Q.F. and Lenz, R.W.,
J. Polym. Sci., Polym. Chem. Edn., **21**, 3313 [1983].

53. Lenz, R.W.,
Polym. J., **17**, 105 [1985].
54. Zhou, Q.F., Jin, J.-I. and Lenz, R.W.,
Can. J. Chem., **63**, 181 [1985].
55. Galli, G., Chiellini, E., Ober, C.K. and Lenz, R.W.,
Makromol. Chem., **183**, 2693 [1982].
56. Jo, B.W., Jin, J.-I. and Lenz, R.W.,
Eur. Polym. J., **18**, 233 [1982].
57. Ober, C.K., Jin, J.-I. and Lenz, R.W.,
Polymer J., **14**, 9 [1982].
58. Majnusz, J., Catala, J.M. and Lenz, R.W.,
Eur. Polym. J., **19**, 1043 [1983].
59. Jo, B.W., Lenz, R.W. and Jin, J.-I.,
Macromol. Chem., Rap. Commun., **3**, 23 [1982].
60. Ober, C.K., Lenz, R.W., Gallie, G. and Chiellini, E.,
Macromolecules, **16**, 1034 [1984].
61. Chen, G. and Lenz, R.W.,
J. Polym. Sci., Polym. Chem. Edn., **22**, 3189 [1984].
62. Jo, B.W., Jin, J.-I. and Lenz, R.W.,
Polym. J., **14**, 9 [1982].
63. Lenz, R.W. and Jin, J.-I.,
Macromolecules, **14**, 1405 [1981].
64. Lenz, R.W., Jin, J.-I. and Feichtinger, K.,
Polymer, **24**, 327 [1983].
65. Ober, C., Jin, J.-I. and Lenz, R.W.,
Macromol. Chem., Rap. Commun., **4**, 49 [1983].
66. Zhou, Q.F., Jin, J.-I. and Lenz, R.W., in Blumstein, A., Ed., "Polymeric Liquid Crystals", Plenum Press, NY [1985].
67. Kwolek, S.L.,
Brit. Pat., 1,198,081 [1966].
68. Kwolek, S.L.,
Brit. Pat., 1,283,064 [1968].

69. Magat, E.E.,
Phil. Trans. Royal Soc., **A-294**, 463 [1980].
70. Morgan, P.W.,
Macromolecules, **10**, 1381 [1977].
71. Yamazaki, N., Matsumoto, M. and Higashi, F.,
J. Polym. Sci., Polym. Chem. Edn., **13**, 1373 [1975].
72. Akzo, S.R.,
Brit. Pat., 1,547,802 [1975].
73. Shibaev, V.P. and Plate, N.A.,
Polym. Sci., U.S.S.R., **19**, 1065 [1978].
74. Blumstein, A., Ed., "Liquid Crystalline Order in Polymers", Academic Press,
NY [1978].
75. Finkelmann, H., Ringsdorf, H. and Wendorff, J.H.,
Macromol. Chem., **179**, 273 [1978].
76. Krigbaum, W.R. and Meyer, R.B., in Blumstein, A., Ed., "Polymeric Liquid
Crystals", Academic Press, NY [1982].
77. Strzelecki, L. and Liebert, L.,
Eur. Polym. J., **12**, 1271 [1981].
78. Chung, Tai-Shung,
Polym. Engg. Sci., **26**, 901 [1986].
79. Jackson, W.J., Jr.,
Macromolecules, **16**, 1027 [1983].
80. Mcfarlane, F.E., Niceley, V.A. and Davis, T.G.,
Contemp. Topics in Polym. Sci., **2**, 109 [1976].
81. Jackson, W.J., Jr.,
Brit. Polym. J., **12**, 154 [1980].
82. Jackson, W.J. and Morris, J.C.,
U.S. Pat., 4,169,933 [1977].
83. Bhaskar, C., Kops, J., Marcher, B. and Spangard, H., "Liquid Crystal Aromatic
Copolyesters Containing Cycloaliphatic Units", in Chapoy, L.L., Ed., "Recent
Advances in Liquid Crystalline Polymers", Elsevier Applied Science Publ.,
London [1985].
84. Jackson, W.J., Jr.,
I.U.P.A.C. 28th Makromol. Sympo. Proc., 800 [1982].

85. Krigbaum, W.R., Asrar, J., Tanumi, H., Cifferri, A. and Preston, S.J.,
J. Polym. Sci., Polym. Lett. Edn., **20**, 109 [1982].
86. Griffin, A.C. and Havens, S.J.,
Mol. Cryst., Liq. Cryst. [Lett.], **49**, 239 [1979].
87. Griffin, A.C. and Havens, S.J.,
J. Polym. Sci., Polym. Lett. Edn., **18**, 259 [1980].
88. Van Luyen, D. and Strzelecki, L.,
Eur. Polym. J., **16**, 303 [1980].
89. Fayolle, B., Noel, C. and Billard, J.,
J. Phys. [Paris], **40**, 485 [1979].
90. Ringsdorf, H. and Schneller, A.,
Brit. Polym. J., **13**, 43 [1981].
91. Kleinschuster, J.J., Pletcher, T.C., Schaefgen, J.R. and Luise, R.A.,
Ger. Offen., 2,520,819 [1975].
92. Millaud, B., Theiry, A. and Skoulios, A.,
Mol. Cryst., Liq. Cryst. [Lett.], **41**, 263 [1978].
93. McFarlane, F.E. and Davis, T.G.,
U.S. Pat., 4,011,199 [1977].
94. Jackson, W.J. Jr., and Morris, J.C.,
U.S. Pat., 4,156,070 [1979].
95. Morris, J.C. and Jackson, W.J. Jr.,
U.S. Pat. 4,146,702 [1979].
96. Jackson, W.J. Jr., and Morris, J.C.,
U.S. Pat., 4,181,792 [1977].
97. Prerorsek, D.C., in Cifferri, A., Krigbaum, W.R. and Meyer, R.B., Eds.,
"Polymer Liquid Crystals", Academic Press, NY [1982].
98. Roviello, A., Santagata, S. and Sirigu, A.,
Macromol. Chem., Rap. Commn., **4**, 281 [1985].
99. Ghadage, R.S., Ponrathnam, S. and Nadkarni, V.M.,
Polymer Commn., **29**, 116 [1988].
100. Augilera, C. and Luderwald, I.,
Macromol. Chem., **179**, 2817 [1978].

101. Dewar, M.J.S. and Riddle, R.M.,
J. Am. Chem. Soc., **97**, 6658 [1975].
102. Dewar, M.J.S. and Goldberg, R.S.,
J. Am. Chem. Soc., **92**, 1582 [1970].
103. Dewar, M.J.S. and Goldberg, R.S.,
J. Org. Chem., **35**, 2711 [1970].
104. Gray, G.W.,
Molecular Crystals, **1**, 333 [1966].
105. Dave, J.S. and Dewar, M.J.S.,
J. Chem. Soc., 4616 [1954].
106. Dave, J.S. and Dewar, M.J.S.,
J. Chem. Soc., 4305 [1955].
107. Iimura, K., Koide, N. and Ohta, R.,
Rep. Prog. Polym. Phys. Japan, **24**, 231 [1981].
108. Griffin, A.C. and Havens, S.J.,
J. Polym. Sci., Polym. Phys. Edn., **19**, 951 [1981].
109. Strzelecki, L. and Liebert, L.,
Eur. Poly. J., **15**, 1271 [1981].
110. Roviello, A. and Sirigu, A.,
Eur. Poly. J., **15**, 423 [1979].
111. Kuhfuss, H.F. and Jackson, W.J. Jr.,
U.S. Pats., 3, 778,410 [1973] and 3,804,805 [1974].
112. Roviello, A. and Sirigu, A.,
Macromol. Chem., **180**, 2543 [1979].
113. Roviello, A. and Sirigu, A.,
Macromol. Chem., **183**, 8 and 895 [1982].
114. Krigbaum, W.R., Watanabe, J. and Ishikawa, T.,
Macromolecules, **16**, 1271 [1983].
115. Abe, A.,
Macromolecules, **17**, 2280 [1984].
116. Morgan, P.W., Pletcher, T.C. and Kwolek, S.L.,
Polym. Preprint, **24**, 470 [1983].

117. Kalyvas, V. and McIntyre, J.E.,
Mol. Cryst., Liq. Cryst., **80**, 105 [1982].
118. Milland, B. and Strezielle, C.,
Polymer, **20**, 563 [1979].
119. Blumstein, A., Vilasager, S., Ponrathnam, S., Clough, S.B. and Blumstein, R.,
J. Polym. Sci., Polym. Phys. Edn., **20**, 877 [1982].
120. Kapuscinska, M. and Pearce, E.M.,
J. Polym. Sci., Polym. Chem. Edn., **21**, 3989 [1984].
121. Kapuscinska, M., Pearce, E.M., Chung-ching, H.F.M. and Zhou, Q.X.,
J. Polym. Sci., Polym. Chem. Edn., **21**, 3999 [1984].
122. Blumstein, A. and Thomas, O.,
Macromolecules, **15**, 1264 [1982].
123. Cottis, S.G., "Aromatic Polyesters as High Performance Engineering Plastics",
32nd SPE-Conf., 496 [1974].
124. Wooten, W.C. Jr., McFarlane, F.C., Gray, G.W. and Jackson, W.J. Jr.,
"Preparation and Properties of Polyester Exhibiting Liquid-Crystalline Melt",
in Cifferri, A. and Ward, I.M., Eds., "Ultra-High Modulus Polymers", Applied
Sci. Publishers, London [1977].
125. Calundann, G.W. and Jaffe, M., "Anisotropic Polymers: Their Synthesis and
Properties", Proceedings of Robert A. Welch Conference on Chemical
Research, XXVI, Synthetic Polymers, [1982].
126. Calundann, G.W.,
U.S. Pats., 4,067,852 [1978]; 4,161,470 [1979]; 4,185,996 [1980]; and 4,256,624
[1981].
127. East, A.J., Charnonneau, L.F. and Calundann, G.W.,
U.S. Pat., 4,330,475 [1982].
128. Finkelmann, H. and Rehage, G.,
Advan. in Polym. Sci., **60/61**, 99 [1984].
129. Shibaev, V.P. and Plate, N.A.,
Advan. in Polym. Sci., **60/61**, 173 [1984].
130. Chiellini, E. and Galli, G., "Chiral Liquid Crystalline Polyesters", Faraday
Discussn., **79**, 241 [1985].

131. Gray, G.W., "Liquid Crystals and Molecular Structure Nematics and Cholesterics", in Luckhurst, G.R. and Gray, G.W., Eds., "The Molecular Physics of Liquid Crystals", Academic Press, New York [1979].
132. Morgan, P., "Condensation Polymers by Interfacial and Solution Method", Interscience, NY [1965].
133. Blumstein, A. and Vilasagar, S.,
Mol. Cryst., Liq. Cryst. [Lett.], **72**, 1 [1981].
134. Higashi, F., Aklyama, N. and Koyama, T.,
J. Polym. Sci., Polym. Chem. Edn., **21**, 3233 [1983].
135. Higashi, F., Aklyama, N. and Koyama, T.,
J. Polym. Sci., Polym. Chem. Edn., **21**, 3241 [1983].
136. Higashi, F., Aklyama, N. and Koyama, T.,
J. Polym. Sci., Polym. Chem. Edn., **22**, 1653 [1984].
137. Higashi, F., Hoshio, A., Yamada, Y. and Ozawa, M.,
J. Polym. Sci., Polym. Chem. Edn., **23**, 69 [1985].
138. Higashi, F., Kuboto, K., Sekizuka, M. and Higashi, M.,
J. Polym. Sci., Polym. Chem. Edn., **19**, 2681 [1981].
139. Wilfong, R.E.,
J. Polym. Sci., **54**, 385 [1961].
140. Donald, A.M. and Windle, A.H.,
J. Material Sci., **18**, 1143 [1983].
141. Donald, A.M., Viney, C. and Windle, A.H.,
Polymer, **23**, 155 [1983].
142. Viney, C., Donald, A.M. and Windle, A.H.,
J. Material Sci., **18**, 1136 [1983].
143. Donald, A.M.,
J. Material Sci. Lett., **3**, 44 [1984].
144. Donald, A.M. and Windle, A.H.,
J. Material Sci., **19**, 2085 [1984].
145. Mitchell, G.R. and Windle, A.H.,
Polymer, **23**, 1269 [1982].
146. Mitchell, G.R. and Windle, A.H.,
Polymer, **24**, 1513 [1983].

147. Donald, A.M. and Windle, A.H.,
Coll. Polym. Sci., **261**, 6793 [1983].
148. Donald, A.M.,
Phil. Mag., **47-A**, L 13 [1983].
149. Donald, A.M. and Windle, A.H., "Electron Microscopy of Thermotropic Copolyesters", in Chapoy, L.L., Ed., "Recent Advances in Liquid Crystalline Polymers", Elsevier Appl. Sci. Publishers, London [1985].
150. Richardson, J.H., "Optical Microscopy for Material Science", Marcel Dekker, NY, [1971].
151. Mclaughnin, R.B., "Special Methods in Light Microscopy", Microscope Series Vol. 17, Microscope Publ., London [1977].
152. Sawyer, L.C. and Grubb, D.T., "Polymer Microscopy", Chapman and Hall, NY [1987].
153. Hartsharne, N.H., "The Microscopy of Liquid Crystals", Microscope Publ., Chicago [1974].
154. Alexander, L.E., "X-ray Diffraction Polymer Science", John Wiley, NY [1969].
155. Bunn, C.W., "Chemical Crystallography", Oxford University Press, London [1961].
156. Stout, G.H. and Jensen, L.H., "X-ray Structure Determination - A Practical Guide", McMillan, NY [1968].
157. Tanford, C., "Physical Chemistry of Macromolecules", John Wiley, NY [1961].
158. Mandelkarn, L., "Crystallization of Polymers", McGraw Hill Publ. Co., NY [1964].
159. Kavesh, S. and Schultz, J.M.,
Polym. Engg. Sci., **9**, 452 [1969].
160. Jaffey, J.W., "Methods in X-ray Crystallography", Academic Press, NY [1971].
161. Posner, A.S., "X-ray Diffraction", in Kline, G.M., Ed., "Analytical Chemistry of Polymers Part-II", Interscience Division, John Wiley and Sons, NY [1962].
162. Rebak, J.K., "Experimental Methods in Polymer Chemistry", John Wiley and Sons, NY [1984].
163. Wunderlich, B., "Macromolecular Physics", Vol. 1, Academic Press, NY [1976].
164. Wunderlich, B., "Macromolecular Physics", Vol. 3, Academic Press, NY, [1980].

165. Krigbaum, W.R. and Salaris, F.,
J. Polym. Sci., Polym. Phys. Edn., **16**, 883 [1978].
166. Skovby, M.H.B., Lessel, R. and Kops, J.,
J. Polym. Sci., Polym. Chem. Ed., **28**, 75 [1990].
167. Wunderlich, B. and Grebowicz, J.,
Advan. Polym. Sci., Vol. **60/61**, 1 [1984].
168. Richards, J.W.,
Chem. News., **75**, 278 [1987].
169. Walden, P.,
Z. Elektrochem., **14**, 713 [1908].
170. Roviello, A. and Sirigu, A.,
Macromol. Chem., **183**, 895 [1982].
171. Roviello, A. and Sirigu, A.,
Eur. Polym. J., **15**, 61 [1979].
172. Ober, C.K. and Bluhm, T.L., in "Current Topics in Polymer Science" Vol. 1,
Hanser, Munich, [1987]; p. 249.
173. Yoon, D.Y. and Bruckner, S.,
Macromolecules, **18**, 651 [1985].
174. Signaud, G., Yoon, D.Y. and Griffin, A.C.,
Macromolecules, **16**, 875 [1983].
175. Johnson, J.F. and Porter, R.S., "Liquid Crystals and Ordered Fluids", Plenum
Press, NY [1974].
176. Chen, G. and Lenz, R.W.,
J. Polym. Sci., Polym. Chem. Edn., **22**, 3189 [1984].
177. Takeda, M., in Miller, B., Ed., "Thermal Analysis", Vol. 2, Wiley and Sons,
New York [1982]; p. 927.
178. Sun, T. and Porter, R.S.,
Polym. Commn., **31**, 70 [1990].
179. Grebowicz, J. and Wunderlich, B.,
J. Polym. Sci., Polym. Phys. Edn., **21**, 141 [1983].
180. Blumstein, R.B., Stickles, E.M., Gauthier, M.M., Blumstein, A. and
Volino, F.,
Macromolecules, **17**, 177 [1984].

181. Menczel, J. and Wunderlich, B.,
Polymer, **22**, 778 [1981].
182. Wunderlich, B., "Macromolecular Physics", Vol. 1, Academic Press, NY [1973].
183. Wunderlich, B., "Macromolecular Physics", Vol. 2, Academic Press, NY [1976].
184. Boon, J., Challa, G. and van Kravelen, D.W.,
J. Polym. Sci., **A-2**, **6**, 1791 and 1835 [1968].
185. Chadwick, G.A., "Metallography of Phase Transitions", Crane, Russak and
Co., NY [1972].
186. Stachurski, Z.H., "Engineering Science of Polymeric Materials", RACI,
Geelong [1987].
187. Jones, J.B., Barenberg, S. and Geil, P.H.,
Polymer, **20**, 903 [1979].
188. Avrami, M.J.,
Chem. Phys., **7**, 1103 [1939]; **8**, 212 [1940]; **9**, 177 [1941].
189. Evans, U.R.,
Trans. Faraday Soc., **41**, 365 [1945].
190. Meares, P., "Polymer: Structures and Bulk Properties", Van Nostrand, NY
[1965].
191. Hay, J.N.,
Brit. Polym. J., **3**, 74 [1971].
192. Poisson, S.D., "Recearches Sur La Probabilite des Judgements en Matieres
Criminelle et en Matiere Civile.", Bachelier, Paris [1837]; p. 206.
193. Keller, A., in March, N. and Tosi, M., Eds., "Polymers, Liquid Crystals and
Low-dimensional Solids", Plenum Press, NY [1984].
194. Warner, S.B. and Jaffe, M.,
J. Crystal Growth, **48**, 184 [1980].
195. Battacharya, S.K., Misra, A., Stein, R.S., Lenz, R.W. and Hahn, P.E.,
Polymer Bulletin, **16**, 465 [1986].
196. Ozawa, T.,
Polymer, **12**, 150 [1971].
197. Keller, A.,
Philos. Mag., 1171 [1957].

198. Lauritzen, J.I., Jr., and Hoffman, J.D.,
J. Res. Natl. Bur. Stand., **64-A**, 73 [1960].
199. Frank, F.C. and Tosi, M.,
Proc. R. Soc., London, **263-A**, 323 [1961].
200. Hoffman, J.D., Davies, G.T. and Lauritzen, J.I., Jr., in Hannay, N.B., Ed.,
"Treatise on Solid State Chemistry", Vol. 3, Chap. 7, Plenum Press, NY [1976].
201. Hoffman, J.D.,
Polymer, **23**, 656 [1982]; **24**, 3 [1983]; **26**, 803 [1985];
Macromolecules, **19**, 1124 [1986].
202. Point, J.J.,
Macromolecules, **12**, 770 [1979].
203. Cheng, S.Z.D. and Wunderlich, B.,
J. Polym. Sci., Polym. Phys. Edn., **24**, 577 and 595 [1986].
204. Sadler, D.M.,
J. Polym. Sci., Polym. Phys. Edn., **23**, 1533 [1985].
205. Flory, P.J.,
Trans. Faraday Soc., **51**, 848 [1955].
206. Sanchez, I.C. and Eby, R.K.,
J. Res. Natl. Bur. Stand., **77-A**, 353 [1973].
207. Helfand, E. and Lauritzen, J.I., Jr.,
Macromolecules, **6**, 631 [1973].
208. Sanchez, I.C. and Eby, R.K.,
Macromolecules, **8**, 639 [1975].
209. Butzbach, G.D., Wendorff, J.H. and Zimmermann, H.J.,
Macromol. Chem., Rapid Commun., **6**, 821 [1985];
Polymer, **27**, 1337 [1986].
210. Bechtoldt, H., Wendorff, J.H. and Zimmermann, H.J.,
Macromol. Chem., **188**, 651 [1987].
211. Hanna, S. and Windle, A.H.,
Polymer, **29**, 207 [1988].
212. Cheng, S.Z.D.,
Macromolecules, **21**, 2475 [1988].
213. P.G. de Gennes,
C. R. Acad. Sci. Paris, **B-281**, 101 [1975].

214. Blumstein, A., Sivaramkrishnan, K.N. Clough, S.B., and Blumstein, R.B.,
Mol. Cryst., Liq. Cryst. [Lett.], **49**, 255 [1979].
215. Strzelecki, L. and Van Luyen, D.,
Europ. Polym. J., **16**, 299 [1980].
216. Ghadage, R.S., Ponrathnam, S. and Nadkarni, V.M.,
J. Appl. Polym. Sci., **37**, 1579 [1989].
217. Rath, A.K., Selvaraj, L. and Ponrathnam, S.,
Polym. Internatl., **24**, 229 [1991].
218. Krigbaum, W.R., Watanabe, J. and Ishikawa, T.,
Macromolecules, **16**, 1271 [1983].
219. Gray, G.W. and Warrall, B.M.,
J. Chem. Soc., 1545 [1859].
220. Gray, G.W., Johns, B. and Marson, F.,
J. Chem. Soc., 393 [1957].
221. Branch, S.T., Byron, D.J., Gray, G.W., Ibbotson, A. and Warrall, B.M.,
J. Chem. Soc., 3279, [1970].
222. Arora, S.L., Ferguson, J.L. and Taylor, T.R.,
J. Chem. Soc., **35**,(12), 4055 [1970].
223. Young, W.R., Haller, I. and Green, D.C.,
J. Chem. Soc., **37**,(23), 3707 [1972].
224. Rath, A.K. and Ponrathnam, S.,
J. Appl. Polym Sci., [in press].
225. Wunderlich, B., "Macromolecular Physics : Crystal, Nucleation, Growth,
Annealing", Academic Press, NY [1976].
226. Ergoz, E., Fatou, J.G. and Mandelkern, L.,
Macromolecules, **5**, 147 [1972].
227. Villanova, P., Ribas, S. and Guzman, G.,
Polymer, **26**, 423 [1985].
228. Cebe, P. and Hong, S.D.,
Polymer, **27**, 1183 [1986].
229. Cheng, S.Z.D., Janimak, J.J., Zhang, A. and Zhou, Z.,
Macromolecules, **22**, 4240 [1989].

230. Ozawa, T.,
Bull. Chem. Soc. Japan, **38**, 1881 [1965].
231. Ozawa, T.,
J. Thermal Analysis, **5**, 563 [1973].
232. Ozawa, T.,
J. Thermal Analysis, **5**, 499 [1973].
233. Flory, P.J.,
Proc. Royal Soc. [London], **A-234**, 73 [1956].
234. R.S. Ghadge,
Ph.D. Thesis, University of Poona, India [1989].